

ADAPTIVE INTERFERENCE SUPPRESSION IN MULTIUSER DS-CDMA SYSTEMS

A THESIS

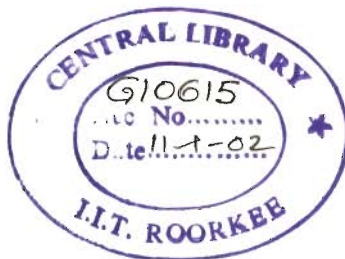
*Submitted in fulfilment of the
requirements for the award of the degree*

of

DOCTOR OF PHILOSOPHY

in

ELECTRONICS AND COMPUTER ENGINEERING



By

ABDULLAH ISMAIL HASSAN KHALIL




**DEPARTMENT OF ELECTRONICS AND COMPUTER ENGINEERING
UNIVERSITY OF ROORKEE
ROORKEE-247 667 (INDIA)**

MAY, 2001

CANDIDATE'S DECLARATION

I hereby certify that the work which is being presented in the thesis entitled **ADAPTIVE INTERFERENCE SUPPRESSION IN MULTIUSER DS-CDMA SYSTEMS** in fulfillment of the requirement for the award of the Degree of **Doctor of Philosophy** and submitted in the Department of **Electronics and Computer Engineering** of the university is an authentic record of my own work carried out during a period from August 1997 to May 2001 under the supervision of Dr. D.K. Mehra.

The matter presented in this thesis has not been submitted by me for the award of any other degree of this or any other university.


(Abdullah Ismail Hassan Khalil)

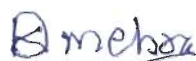
This is to certify that the above statement made by the candidate is correct to the best of my knowledge.

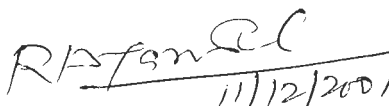
Date: May 24, 2001



(Dr. D.K. Mehra)

Professor
Department of Electronics and
Computer Engineering
University of Roorkee,
Roorkee-247 667,
INDIA

The Ph.D. Viva-Voce examination of **Abdullah Ismail Hassan Khalil**, Research Scholar, has been held on ...11/12/2001.....


Signature of
Supervisor


Signature of
H.O.D.


Signature of the external
Examiner

ABSTRACT

During the last two decades, direct-sequence code-division multiple-access (DS-CDMA) technique has received a considerable interest in mobile and personal communication systems, and will play an important role in future wireless communication systems. In DS-CDMA systems a number of users share a common channel bandwidth, in which the users are distinguished from one another by superimposing a distinct pseudo-random code sequence. The code sequence, which is known at the receiver, spreads the bandwidth of the data signal and also provides the multiple access capability. All users can transmit at the same time and are allocated the entire frequency spectrum for transmission, in contrast to frequency-division multiple-access (FDMA) and time-division multiple-access (TDMA) techniques. Hence, the detector receives signal composed of the sum of the signals of all users, which overlap in time and frequency. In practice, the interfering signals are not truly orthogonal to the desired signal, due to the random time offsets of the received signals. Hence the orthogonality property of the codes will not be achieved at the receiver, which results in the production of the multiple access interference (MAI). The MAI is a factor which limits the capacity and performance of DS-CDMA systems. Additionally, due to the propagation mechanism, the received signal from a user close to the base station will be stronger than that received from another user located far from the base station. Hence, a close user will dominate the distant users and reliable reception in this situation is not possible. This is called the near far problem and a possible solution to this is to use power control: such that all users will achieve the same power at the base station. The conventional matched-filter receiver output contains contributions from the MAI. Thus, even if the receiver thermal noise level goes to zero, the error probability of the conventional receiver

exhibits a non-zero floor because of the MAI. Moreover, under the near-far situation, the weak signal will be overwhelmed by the MAI.

The MAI and the near-far problem can be overcome by the use of multiuser detection (MUD) techniques. In MUD, the receiver jointly detects all signals in order to mitigate the non-orthogonal properties of the received signals. MUD has been a topic of extensive research interest since 1986 when Verdu formulated an optimum MUD based on the maximum likelihood sequence detection (MLSD). However, the complexity of the optimal detector is exponential in the number of active users, which has motivated the design of a number of suboptimal multiuser detectors with lower computational complexity.

Amongst the linear suboptimal detectors, which apply a linear transform to the output of the matched filters to remove the MAI, is the linear minimum mean square error (MMSE) detector. It minimizes the mean square error between the actual and the estimated data bit, and possesses a linear computational complexity in the number of users. Adaptive interference suppression techniques are analogous to adaptive equalization of dispersive channels by virtue of the analogy between MAI and intersymbol interference (ISI). The adaptive MMSE receiver eliminates the use of the matched filter bank and can be implemented using a tapped delay line filter. It directly processes samples of the received signal at the chip interval without the explicit knowledge of the MAI. However, it requires the knowledge of the timing of the desired user as well as the knowledge of the training sequence of symbols transmitted by the desired user.

In this work, adaptive multiuser detection techniques based on the MMSE error criterion have been considered for the adaptation and demodulation of DS-CDMA signals to solve the problems inherited in both conventional and non-adaptive detection techniques. The main issues considered in this work are to develop adaptive algorithms with low computational

complexity which are near-far resistant. They may be adapted blindly and without the knowledge of the timing of the desired user (i.e. with lower requirement for side information).

A comparative study of the adaptation techniques using the least mean square (LMS), normalized LMS (NLMS) and recursive least squares (RLS) algorithms based on the MMSE criterion has been considered for the interference suppression in DS-CDMA systems. Different performance measures (such as the probability of error, convergence rate, near-far resistance, capacity, computational complexity and signal to interference ratio) have been used for the assessment of the performance of the various algorithms. A number of examples have been simulated to illustrate the performance comparison of these algorithms. It is well known, that the RLS algorithm possesses much faster convergence rate as compared to LMS algorithm, however the RLS algorithm requires larger number of computations, ($O[N^2]$), as compared to LMS, ($O[N]$). To reduce the computational complexity, we have proposed and implemented a novel block algorithm for the adaptation and demodulation of DS-CDMA signals. The block algorithm possesses fast convergence rate which is comparable to the RLS algorithm, while requiring computational complexity comparable to that of the LMS algorithm. Simulation has been performed to compare the performance of the proposed block algorithm with the LMS and RLS algorithms for interference suppression and demodulation of DS-CDMA signals.

We have next proposed the use of the Kalman filter (KF) for the adaptation and interference suppression of DS-CDMA signals. A motivation for using the KF is that it is the best linear unbiased estimator and is optimal in the MMSE sense. Moreover, the KF is usually formulated using the state-space approach, which contains the necessary information about the system. A number of examples have been simulated which show its improved

performance compared to the algorithms mentioned above. A drawback of the KF algorithm is that it requires the knowledge of the noise variance and like RLS, is prone to numerical instability due to the use of finite word-length arithmetic for calculating the Riccati difference equation. To solve this problem, the state-error correlation matrix is factorized into two square-root matrices and unitary transformations are used to update the matrix at each iteration. We have considered the use of the square-root KF (SQRT-KF) algorithm for the interference suppression and demodulation of DS-CDMA signals and implemented the system using both Givens rotations and Householder transformations. Simulations have been performed, to compare its performance with the conventional KF algorithm, which show better numerical stability but at the expense of increased computational complexity.

To deal with the problems of instability in the RLS algorithm periodic re-initialization has been proposed in the literature. However, this requires the use of a training sequence periodically, which will result in decrease in the rate of transmission of the system. To remedy this problem, algorithms based on matrix factorization of the input auto-correlation matrix using orthogonal transformations have been derived and investigated. The resulting algorithms are less sensitive to round off errors, and, moreover can be efficiently mapped into systolic array structure for parallel implementation. Also, the computation of the least-squares weight vector of the adaptive filtering algorithm may be accomplished by working directly with the incoming data matrix via the matrix factorization and decomposition rather than working with the (time-averaged) correlation matrix of the input data as in the RLS algorithm. Therefore, we have proposed the use of the QR-decomposition technique based on the recursive modified Gram-Schmidt (RMGS) algorithm for the adaptation and interference suppression of DS-CDMA signals. It requires lower computational complexity as compared to RLS, KF, SQRT-KF and other QR-RLS algorithms based on Givens rotations or

Householder transformations. An attractive feature of the RMGS algorithm is that it can be set for parallel implementation, realized in a highly modular structure using systolic arrays such that using N -parallel processors will reduce the computational complexity to $O[N]$ per processor. It is worth mentioning that the RMGS-based algorithm does not involve the computationally expensive square roots as in the QR-RLS algorithms. An improved error feedback version of the RMGS algorithm (RMGSEF) is more efficient and has even better numerical properties as compared to the RMGS algorithm. Results show that the RMGSEF algorithm is near-far resistant, possesses the same convergence as the RLS algorithm and has improved numerical stability. The performance of the DS-CDMA receiver based on the RMGS algorithm has also been studied in a multipath fading dispersive environment. Simulations show that the proposed RMGS algorithm performs much better compared to LMS algorithm in a multipath fading dispersive environment and possesses lower error floor.

The implementation of the adaptive MMSE receiver, considered so far, requires the knowledge of training sequence of the desired user during initial adaptation, and then switching to the decision directed mode during actual data transmission. Moreover, a fresh training sequence may also be required when the receiver loses synchronization due to deep fades or due to the interference from a strong interferer entering the network. However, in some applications, the use of training sequences may be impractical. Therefore, there is a need for adaptive receivers which do not require training sequence during the adaptation mode (i.e. blind). Blind algorithms using subspace estimation approach through either eigenvalue or singular-value decomposition of the data matrix are either computationally expensive, for adaptive applications, or suffer from relatively slow convergence rate. Blind equalization based on the Bussgang technique uses a soft decision (non-linear function) at the output of the detector in contrast to the MMSE detector. The constant modulus algorithm

(CMA) is considered as the most successful and the simplest higher-order statistics (HOS) based algorithm among the Bussgang family of blind equalization algorithms. It chooses a linear receiver that minimizes the deviation of the receiver output from a constant modulus. However, its cost function includes a number of local minima. The constrained blind minimum output energy (MOE) detector for the interference suppression in DS-CDMA systems minimizes the mean output energy of the detector. It requires the knowledge of the spreading sequence of the desired user and its cost function does not include any local minima, which ensures global convergence. Based on the attractive features of the RMGS algorithm, we have derived and implemented a novel blind adaptive RMGS-based MOE algorithm for the adaptation and interference suppression in DS-CDMA systems. A number of numerical examples have been simulated which show that the convergence rate of the blind RMGS algorithm is much faster than that of the CMA and blind MOE-based LMS algorithm. Parallel implementation of the blind RMGS algorithm via systolic arrays, using N -parallel processors, will reduce the computational complexity to $O[N]$ per processor.

The implementation of the MMSE receiver in DS-CDMA systems, considered so far, requires the knowledge of the timing of the desired user. This knowledge is used to successfully suppress MAI as well as to demodulate the desired user data bits. Therefore, in the literature there has been considerable effort devoted towards the development of time delay estimators for DS-CDMA systems. The commonly used sliding correlator technique for time delay estimation (TDE) fails in a near far environment. Delay acquisition using the MUSIC estimator based on subspace decomposition, in DS-CDMA systems, is shown to be near far resistant, however, its complexity is $O[N^3]$. Moreover, a poor performance is achieved when the number of users is unknown and large. Joint data detection and parameter estimation using the extended KF (EKF) has also been proposed earlier. Although, the

algorithm is near far resistant and could be used in the tracking mode, it requires the initial parameter estimates of all users to be known and is computationally expensive. In this work, we have considered two techniques for TDE in DS-CDMA systems, which can be used during both the initialization and tracking modes. The first method is based on cross-correlating the MMSE weights vector, obtained by the RMGS algorithm, with the desired user spreading sequence. The estimated delay is specified by the location of the maximum value of the cross-correlation peak. This method is shown to be near far resistant but it requires an all one training sequence, or alternatively, the adaptive filter has to be of length $2N$ taps. In the second technique, estimate of the time delay is obtained by running N -parallel adaptive MMSE algorithms at N -hypothetical values of the delay (equal to multiples of the chip period). This technique is near far resistant and it can also be used for both the initialization and tracking modes. A number of examples have been simulated to evaluate the performance of these techniques in both initialization and tracking modes. Lastly a novel blind adaptive DS-CDMA receiver for interference suppression, which does not require any side information except the desired user's spreading sequence, has been implemented.

ACKNOWLEDGEMENTS

The author wishes to express his deep sense of gratitude to Dr. D.K. Mehra for his keen interest, painstaking supervision and invaluable help through out the course of this work. He has been generous in undertaking comprehensive discussions and meticulous reading and reviewing of the text, without which the work could not have come to its shape. His supporting directives and patronizing affection showered on the author are cherished in the memory of the author.

The facilities and working conditions provided by the Head, Department of Electronics and Computer Engineering are gratefully acknowledged. The author is also grateful to University of Mosul for providing the study leave. I sincerely acknowledge the ICCR, Government of India, for sponsoring the research.

The author wishes to express his respectful tribute to his mother K.O. Mohammed who passed away before two years during the course of his work.

Task of undertaking research involves sacrifice on the part of many. Words do not suffice to express the author's feeling towards his wife B.M. Jasim and his son Omar, who suffered too much through out the period of this study because of the author's pre-occupation.

My deep regards and thanks are due to my brothers and sisters and their families for their encouragement and help, which deserves a special mention.

The author is also thankful to his fellow research scholars who helped in a way or another during this course of study.

Abdullah Ismail Hassan Khalil

TABLE OF CONTENTS

	Page no.
CANDIDATE'S DECLARATION	
ABSTRACT	i
ACKNOWLEDGEMENTS	viii
TABLE OF CONTENTS	ix
LIST OF TABLES	xii
LIST OF FIGURES	xiii
LIST OF ACRONYMS	xx
LIST OF NOTATIONS	xxiii
CHAPTER 1 INTRODUCTION	
1.1 Review of the earlier work	2
1.2 Statement of the problem	14
1.3 Organization of the thesis	15
CHAPTER 2 ADAPTIVE ALGORITHMS FOR INTERFERENCE SUPPRESSION IN DS-CDMA SYSTEMS	18
2.1 Introduction	19
2.2 MMSE receiver for DS-CDMA systems	24
2.3 Adaptive MMSE receiver	31
2.3.1 The Least-Mean-Square (LMS) algorithm	32
2.3.1.1 Fixed step-size LMS algorithm	33
2.3.1.2 The normalized LMS algorithm	34
2.3.1.3 Modified variable step-size LMS algorithm	35
2.3.2 The Recursive Least Squares (RLS) algorithm	37
2.3.3 The block adaptation algorithm	40
2.4 Performance measures	44
2.5 Simulation results and discussion	47
CHAPTER 3 ADAPTIVE DS-CDMA RECEIVER USING KALMAN FILTERING	
3.1 Introduction	79

3.2 The Kalman filter	81
3.3 Square-Root Kalman Filter (SQRT-KF)	85
3.3.1 SQRT-KF Algorithm	85
3.3.2 Givens rotations	88
3.3.3 Householder transformation	91
3.4 Simulation results and discussion	93

CHAPTER 4 RMGS-BASED ADAPTIVE INTERFERENCE

SUPPRESSION IN DS-CDMA SYSTEMS

4.1 Introduction	106
4.2 The QR-RLS algorithm	108
4.3 Inverse QR-RLS algorithm	111
4.4 The RMGS algorithm	113
4.4.1 Parallel implementation on systolic arrays	116
4.4.2 Computational complexity	119
4.5 Simulation Results and Discussion	120

CHAPTER 5 BLIND ADAPTIVE INTERFERENCE SUPPRESSION

ALGORITHMS FOR DS-CDMA SYSTEMS

5.1 Introduction	143
5.2 Blind equalization based on Bussgang technique	147
5.3 Blind MOE multiuser detector	151
5.3.1 LMS-based blind MOE detector	151
5.3.2 RLS-based blind MOE detector	153
5.3.3 QR-RLS Blind adaptive multiuser detector	155
5.3.4 RMGS-based blind adaptive algorithm	156
5.4 Simulation Results and Discussion	158

CHAPTER 6 ADAPTIVE TIME-DELAY ESTIMATION USING

RMGS ALGORITHM

6.1 Introduction	170
6.2 TDE by processing the MMSE weights vector	174
6.3 Parallel adaptive MMSE TDE scheme	178

6.4 Blind TDE	181
6.5 Computational complexity	182
6.6 Simulation results and discussion	184
CHAPTER 7 CONCLUSIONS	211
7.1 Suggestions for further work	215
APPENDIX A MULTIPATH FADING DISPERSIVE CHANNEL MODEL	218
APPENDIX B SOLUTION OF THE CONSTRAINED OPTIMIZATION	
PROBLEM (Eqs. 5.26 & 5.27)	221
REFERENCES	224

LIST OF TABLES

		<i>Page no.</i>
Table 2.1	The LMS algorithm.	33
Table 2.2	The NLMS algorithm.	35
Table 2.3	The MVSS-LMS algorithm.	37
Table 2.4	The RLS algorithm.	40
Table 2.5	The block algorithm.	43
Table 2.6	The MVSS-block algorithm.	43
Table 2.7	Comparison of the computational complexity per output point required for the LMS, RLS and the block algorithms.	44
Table 3.1	Summary of the Kalman filter algorithm.	84
Table 3.2	Summary of the Givens rotation algorithm.	90
Table 3.3	Summary of the SQRT-KF algorithm.	92
Table 4.1	Summary of the QR-RLS algorithm.	111
Table 4.2	Summary of the inverse QR-RLS algorithm.	112
Table 4.3	Modified Gram-Schmidt (MGS) algorithm.	114
Table 4.4	Recursive Modified Gram-Schmidt (RMGS) algorithm.	116
Table 4.5	The RMGS algorithm using the error feedback formula.	117
Table 4.6	Computational complexity of various adaptive algorithms.	120
Table 5.1	CMA-based algorithm for DS-CDMA systems.	151
Table 5.2	Blind LMS-based MOE algorithm.	153
Table 5.3	The blind RLS algorithm.	154
Table 5.4	The blind QR-RLS algorithm.	156
Table 5.5	Summary of the Blind RMGS algorithm.	157
Table 5.6	Computational complexity for the blind adaptive algorithms.	158
Table 6.1	Computational complexity of the implemented TDE methods in the acquisition mode (The observation interval equal $2N$).	183

LIST OF FIGURES

Page no.

Fig.2.1	Block diagram of K CDMA transmitters.	26
Fig.2.2	Illustration of the contribution to the channel output from the desired user and kth interferer.	26
Fig.2.3	Block diagram of the adaptive DS-CDMA receiver.	27
Fig.2.4a	Convergence characteristics of the adaptive DS-CDMA receiver using the block algorithm with 4 interferers (each interferer has 10dB power advantage over the desired user), for different values of step size (μ_b).	49
Fig.2.4b&c	Convergence characteristics of the adaptive DS-CDMA receiver using the block algorithm with 4 interferers (each interferer has 10dB power advantage over the desired user), for different values of block length (L).	50
Fig.2.5	Convergence characteristics of the adaptive DS-CDMA receiver with different number of interferers (each interferer has 10dB power advantage over the desired user) for a)LMS b)block and c) RLS algorithms.	53
Fig.2.6	Comparison of the convergence characteristics for the adaptive DS-CDMA receiver using NLMS, RLS, Block, MVSS-LMS and MVSS-Block algorithms with a) 4-interferers b) 8-interferers (each interferer has 10dB power advantage over the desired user).	57
Fig.2.7	Comparison of the convergence characteristics for the adaptive DS-CDMA receiver with PN, Gold and Random sequences with 4 interferers (each interferer has 10dB power advantage over the desired user) using a) NLMS, b) Block and c) RLS algorithms.	60
Fig.2.8	Effect of entry of interferers on the performance of the adaptive DS-CDMA receiver using NLMS algorithm (each interferer has 10dB power advantage over the desired user).	63
Fig.2.9	Probability of error performance for the adaptive DS-CDMA receiver using NLMS, RLS and block algorithms with a) 4-interferers, b) 10-interferers (each interferer has 10dB power advantage).	65

Fig.2.10	Convergence characteristics for the adaptive DS-CDMA receiver Using the RLS algorithm for both synchronous and asynchronous systems with a)4 interferers b)8 interferers (each interferer has 10dB power advantage over the desired user).	67
Fig.2.11	Probability of error performance for the adaptive DS-CDMA receiver using the RLS algorithm for synchronous and asynchronous systems with a)4 interferers b)8 interferers (each having 10dB power advantage over the desired user).	70
Fig.2.12	Comparison of the output SNR of the adaptive DS-CDMA receiver using NLMS, RLS and block algorithms as a function of the number of interferers (each interferer has 10dB power advantage over the desired user) at a) input SNR=10dB b) input SNR=30dB c) input SNR=50dB.	72
Fig.2.13	Probability of error performance for the desired user as a function of the second user power relative to the desired user at input SNR 10dB and 12dB using the NLMS, RLS and block algorithms.	76
Fig.2.14	Probability of error performance for the adaptive DS-CDMA receiver as a function of the number of interferers at input SNR of 10dB and 12dB using the NLMS, RLS and block algorithms.	78
Fig.3.1	Convergence characteristics for the adaptive DS-CDMA receiver using the KF algorithm with different number of interferers (each interferer has 10dB power advantage over the desired user).	94
Fig.3.2	Comparison of the convergence characteristics for the adaptive DS-CDMA receiver using the NLMS, RLS, KF and block algorithms with a)4 interferers b)8 interferers (each interferer has 10dB power advantage over the desired user).	96
Fig.3.3	Probability of error performance for the adaptive DS-CDMA receiver using the NLMS and SQRT-KF algorithms with a)4 interferers b)8 interferers (each interferer has 10dB power advantage over the desired user).	98

Fig3.4a	Probability of error performance for the desired user as a function of the second user's power relative to the desired user at input SNR of 10dB and 12dB using the NLMS and SQRT-KF algorithms.	101
Fig.3.4b	Probability of error performance for the desired user as a function of the interferer's power relative to the desired user at input SNR of 10dB and 12dB using the SQRT-KF algorithm.	102
Fig.3.5	Probability of error performance for the adaptive DS-CDMA receiver as a function of the number of interferers (each interferer has 10dB power advantage over the desired user) using the NLMS and SQRT-KF algorithms at input SNR of 10dB and 12dB.	103
Fig.4.1	Systolic array implementation of the RMGS algorithm.	118
Fig.4.2a	Convergence characteristic for the adaptive Ds-CDMA receiver using the RMGS algorithm with different number of interferers (each interferer has 10dB power advantage over the desired user).	122
Fig..4.2b	Comparison of the convergence characteristics for the adaptive DS-CDMA receiver using NLMS, RLS and RMGS algorithms with 4 and 8 interferers (each interferer has 10dB power advantage over the desired user).	123
Fig.4.3	Convergence characteristics for the adaptive DS-CDMA receiver using RLS and RMGS algorithms, in both training mode (up to 800 bits) and decision modes. The system includes 4 interferers (each interferer has 10dB power advantage).	125
Fig.4.4a	Theoretical and simulated weight vector at the end of the training cycle for the adaptive DS-CDMA receiver using the RMGS algorithm with 4 interferers (each interferer has 10dB power advantage over the desired user).	126
Fig.4.4b	The trajectory of a single weight (w_{17}) of the TDL filter for the adaptive DS-CDMA receiver using the RMGS algorithm with 4 interferers (each interferer has 10dB power advantage over	

	the desired user).	128
Fig.4.5	Probability of error performance for the adaptive DS-CDMA receiver using the RMGS algorithm with a)8 interferers b)10 interferers (each interferer has 10dB power advantage over the desired user).	129
Fig.4.6	Comparison of the output SNR for the adaptive DS-CDMA receiver using NLMS and RMGS algorithms with different number of interferers (each interferer has 10dB power advantage over the desired user).	132
Fig.4.7	Probability of error performance for the desired user as a function of the second user's power relative to the desired user, at input SNR 10dB and 12dB for NLMS and RMGS algorithms.	133
Fig.4.8	Probability of error performance for the desired user as a function of the number of interferers (each interferer has 10dB power advantage) using the NLMS and RMGS algorithms at input SNR 10dB and 12dB.	135
Fig.4.9	The equivalent discrete-time channel model for fading dispersive channel.	136
Fig.4.10	Probability of error for the adaptive DS-CDMA receiver using the NLMS and RMGS algorithms in a fading multipath environment for a)8 interferers b)10 interferers (each interferer has 10dB power advantage over the desired user).	137
Fig.4.11	Probability of error for the adaptive DS-CDMA receiver using the NLMS and RMGS algorithms in a fading multipath environment for different values of maximum delay spread (T_d) with a)8 interferers b)10 interferers (each interferer has 10dB power advantage).	140
Fig.5.1	Block diagram of blind equalizer using nonlinear estimator.	148
Fig.5.2	Convergence characteristics for the adaptive DS-CDMA receiver using the CMA, LMS, RLS and RMGS blind algorithms with nine synchronous interferers (each interferer has 10 dB power advantage over the desired user).	160
Fig.5.3	The behavior of the adaptive Ds-CDMA receiver based on blind RMGS algorithm in a dynamic environment as given by <i>example 5.2</i> .	162

Fig.5.4	Effect of changing the forgetting factor (λ) on the time-averaged SIR versus number of bits in the blind adaptation mode for the adaptive DS-CDMA receiver using the RMGS algorithm with 4 interferers (each interferer has 10dB power advantage over the desired user).	163
Fig.5.5	Time averaged SIR versus number of bits for the RMGS algorithm using the blind adaptation rule and the decision directed mode, with 4 interferers (each interferer has 10dB power advantage over the desired user).	165
Fig.5.6	Probability of error performance versus interferer's power for the RMGS-based blind adaptive DS-CDMA receiver at different input SNRs for one and four interferers cases.	166
Fig.5.7	Probability of error performance for the adaptive DS-CDMA receiver with blind-adaptation and training sequence adaptation using the RMGS algorithm for a)8 interferers and b)10 interferers (each interferer has 10dB power advantage over the desired user).	168
Fig.6.1	Code timing estimation algorithm block diagram.	175
Fig.6.2	The observation interval includes three consecutive bits.	179
Fig.6.3	Performance of the two TDE methods based on the a)RMGS b)LMS algorithms for the adaptive DS-CDMA receiver with 4-interferers (each interferer has 10dB power advantage over the desired user).	186
Fig.6.4a	Average number of training bits required for correct acquisition as a function of number of users using the TDE methods based on LMS and RMGS algorithms (each interferer has 10dB power advantage over the desired user).	188
Fig.6.4b	Average number of training bits required for correct acquisition as a function of MAI from each user based on the parallel TDE method for 3 and 11 users, using both LMS and RMGS algorithms.	190
Fig.6.4c	Average number of training bits required for correct acquisition as a function of MAI from each user based on the weights processing TDE	

	method for 3 and 11 users, using LMS and RMGS algorithms.	191
Fig.6.4d	Average number of training bits required for correct acquisition as a function of the MAI for 3 and 11 users using on the two TDE methods based on RMGS algorithms.	192
Fig.6.5a	Probability of correct acquisition as a function of the average number of training bits of the two TDE methods based on the LMS and RMGS algorithms with 4-interferers (each interferer has 10dB power advantage over the desired user).	194
Fig.6.5b	Probability of correct acquisition as a number of users using the two TDE methods based on the RMGS algorithm (each interferer has 10dB power advantage over the desired user).	195
Fig.6.5c	Probability of correct acquisition as a function of the MAI from each user for the two TDE methods using the RMGS algorithm with 10-interferers.	196
Fig.6.6a	RMSE of the timing estimate in chips as a function of the average number of training bits for the two TDE methods based on LMS and RMGS algorithms with 10-interferers (each interferer has 10dB power advantage over the desired user).	198
Fig.6.6b	RMSE of the timing estimate in chips as a function of the MAI from each interferer for the two TDE methods based on the RMGS algorithm with 3 and 11 users.	199
Fig.6.6c	RMSE of the timing estimate in chips as a function of the number of users for the two TDE methods based on the RMGS algorithm (each interferer has 10dB power advantage over the desired user).	201
Fig.6.7	Performance of the two TDE methods in the tracking mode using a)RMGS b)LMS algorithms with 4 interferers (each having 10dB power advantage over the desired user).	202
Fig 6.8a	Probability of correct acquisition for the parallel TDE method based on the RMGS algorithm as a function of the number of users using	

	training sequence based adaptation and blind adaptation modes (each interferer has 10dB power advantage over the desired user).	205
Fig 6.8b	Probability of correct acquisition for the parallel TDE method based on the RMGS algorithm as a function of the MAI from each user using training sequence based adaptation and blind adaptation modes with 3-users.	206
Fig.6.9a	RMSE of the timing estimate in chips for the parallel TDE method as a function of number of users using training sequence based adaptation and blind adaptation modes based on the RMGS algorithm, (each interferer has 10dB power advantage over the desired user).	207
Fig.6.9b	RMSE of the timing estimate in chips for the parallel TDE method as a function of the MAI from each user using training sequence based adaptation and blind adaptation modes based on the RMGS algorithm with two interferers.	208
Fig 6.10	Probability of error performance for the adaptive DS-CDMA receiver For the synchronous, training sequence based TDE and blind based TDE cases with 4-interferers (each interferer has 10dB power advantage).	210

LIST OF ACRONYMS

3G	Third Generation
AWGN	Additive White Gaussian Noise.
BER	Bit Error Rate.
BLMS	Block LMS.
BLUE	Best Linear Unbiased Estimator.
BRLS	Block RLS.
CCI	Cochannel Interference.
CMA	Constant Modulus Algorithm.
CSFB	Cyclically Shifted Filter Bank.
DFE	Decision Feedback Equalizer.
DMMT	Discrete Matrix Multitone.
DS-CDMA	Direct-Sequence Code-Division Multiple-Access.
EDT	Equivalent Discrete Time model.
EKF	Extended Kalman Filter.
FDMA	Frequency Division Multiple Access.
FIR	Finite Impulse Response.
FTF	Fast-Transversal Filter.
FFT	Fast Fourier Transform.
FSS	Fixed Step Size.
GM	Gram-Schmidt procedure.
HOS	Higher-Order Statistics.
iid	independent and identically distributed.
IIR	Infinite Impulse response.

ISI	Inter Symbol Interference.
KF	Kalman Filter.
LDC	Lower-triangular Diagonal Correction.
LE	Linear Equalizer.
LMMSE	Linear Minimum Mean Square Error.
LMS	Least Mean Square.
LPF	Low-Pass Filter.
MAI	Multiple Access Interference.
MF	Matched-Filter.
MGS	Modified Gram-Schmidt procedure.
ML	Maximum Likelihood.
MLSD	Maximum Likelihood Sequence Detection.
MLSE	Maximum Likelihood Sequence Estimation.
MMSE	Minimum Mean-Square Error.
MOE	Minimum Output Energy.
MSE	Mean Square Error.
MUD	Multiuser Detection.
MVSS	Modified Variable Step Size.
NBI	Narrow Band Interference.
NLMS	Normalized LMS algorithm.
PE	Polynomial Expansion.
PN	Pseudo-Random sequence.
PSK	Phase-Shift Keying.
QR-RLS	QR-Decomposition based Recursive Least Squares.

RBF	Radial Basis Function.
RLS	Recursive Least Squares.
RMGS	Recursive Modified Gram-Schmidt algorithm.
RMGSEF	Recursive Modified Gram-Schmidt Error-Feedback algorithm.
RMSE	Root Mean Square estimation Error.
SINR	Signal-to-Interference Plus Noise Ratio.
SNR	Signal-to-Noise Ratio.
SSMF	Spreading Sequence Matched Filter.
STVC	Spatio-Temporal Vector Coding.
SVD	Singular-Value Decomposition.
TCB	Time Complexity per Bit.
TDE	Time-Delay Estimation.
TDL	Tapped-Delay Line.
TDMA	Time division Multiple Access.
VA	Viterbi Algorithm.
VLSI	Very Large Scale Integration.
VSS	Variable Step Size.
ZF-DF	Zero-Forcing Decision-Feedback.
WCDMA	Wideband CDMA.
WSSUS	Wide Sense Stationary Uncorrelated Scattering.

List of Notations

$\hat{\mathbf{V}}(n)$	gradient vector of the estimated MSE.
$\eta(n)$	random gaussian noise vector of zero mean and unit variance.
$\xi(n)$	MSE.
ξ_{ex}	excess MSE
ξ_{min}	minimum MSE
$\psi(t)$	Chip waveform.
σ^2	noise variance.
ω_c	carrier frequency.
τ_k	delay of the kth user.
δ_k	fractional chip delay lies in the interval $[0, T_c)$.
ρ_k	number of delayed chips, which is integer between 0 and N-1.
θ_k	Phase shift of the kth user.
λ	forgetting factor.
λ_{max}	maximum eigen value of \mathbf{R} .
μ	adaptation scalar constant.
$c_k(t)$	Spreading waveform of the kth user.
$c_{k,j}$	jth element of the kth user spreading sequence.
$d(n)$	Data bit at instant n.
f_d	Doppler frequency.
$e(n)$	the estimation error signal.
\mathbf{I}	identity matrix.
K	No. of active users in the channel.

N	Processing gain (or TDL filter length).
$n(t)$	additive white Gaussian noise.
$\mathbf{P}(n)$	crosscorrelation vector.
P_k	Received power of the k th user.
$\mathbf{R}(n)$	autocorrelation matrix of the input vector.
$r(n)$	TDL contents (discrete received vector).
$r(t)$	baseband received signal.
$s_k(t)$	the k th user transmitted signal.
T	Bit interval
T_c	Chip interval.
$\mathbf{w}(n)$	The TDL filter weights.
$y(t)$	received signal.

INTRODUCTION

Direct-sequence code-division multiple-access (DS-CDMA) technique has received considerable interest in mobile and personal communication systems, and it will play an important role in future wireless communication systems. In CDMA, users are assigned distinct spreading sequences and can transmit at the same time using the entire frequency spectrum for transmission, in contrast to both frequency division multiple access (FDMA) and time division multiple access (TDMA) techniques. CDMA techniques have been investigated widely during the 1980's, which finally led to the commercialization of cellular spread spectrum communications in the form of the narrowband CDMA (IS-95 standard). CDMA has also been the selected approach for the third generation (3G) wireless communication systems.

A significant amount of interference is inherent in CDMA systems due to the multiple access operation. Because of the non-orthogonality of spreading sequences, the conventional correlator integrator receiver suffers from the near-far problem, in which the interference from strong users can be much larger than the power of the desired user, and hence detection is rendered unreliable. Multiuser detection (MUD) techniques are used to overcome the multiple-access interference (MAI) and the near-far problem. In MUD techniques, the receiver jointly detects all signals in order to mitigate the non-orthogonal properties of the spreading codes. There has been an extensive research interest in MUD since 1986 when Verdu [116] formulated an optimum MUD based on the maximum likelihood sequence detection (MLSD). However, the complexity of the optimal detector is exponential in the number of users, and moreover, it requires the knowledge of the interferer's parameters. This

has motivated the design of suboptimal detectors with computational complexity which is linear in the number of users. These detectors can be classified in one of two categories; linear multiuser detectors and subtractive interference cancellation detectors. One of the linear multiuser detectors is the MMSE receiver which implements a linear mapping to minimize the MSE between the actual and the estimated data bits. Adaptive signal processing algorithms have been proposed to suppress, partially or completely, the MAI without the knowledge of the interferer's parameters. In this thesis we have considered the adaptive multiuser DS-CDMA receivers based on the MMSE criterion for the interference suppression.

In the following sections, we present a brief summary of the earlier work carried out in the related areas, followed by the statement of the problem and the organization of the material embodied in this thesis.

1.1 Review of the earlier work

The conventional receiver for DS-CDMA uses a matched filter corresponding to each user and demodulates each user independently. Due to the non-orthogonality of the spreading codes, the output of the conventional matched filter for the desired user contains contributions from other users, which is known as multiple access interference (MAI). If the power of interferers is much stronger than that of the desired user, then the weak signal of the desired user is overwhelmed by the MAI and reliable reception is impossible. This is known as the near-far problem. The classical way to deal with this problem is to use power control, in which it is ensured that the transmitted powers of all users are controlled such that the received signals have equal power levels. In IS-95 system, the mobiles adjust their power such that the transmitted power is inversely proportional to the power level it receives from

the base station. Alternatively the base station sends power control to the mobiles based on the power level of the signal it receives [23].

The main reason why multiuser detection did not develop until relatively recently was the belief by many workers in spread spectrum that multiuser interference is accurately modeled as a white Gaussian random process, and thus the conventional detector is essentially optimum [118]. However, the number of transmitters, signature waveforms, and power levels encountered in many practical situations render the Gaussian approximation completely useless.

Verdu in [116] proposed and analyzed the optimum multiuser detector for asynchronous CDMA signals. Similar work also appeared in [49]. The detector consists of a bank of matched filters followed by a Viterbi algorithm. It outperforms the conventional single user detector at the expense of marked increase in the computational complexity: exponential in the number of users. Another disadvantage of this detector is that it requires the knowledge of the received amplitudes and phases of all the users. The aim of reducing the complexity has motivated the design of a number of suboptimal multiuser detectors with lower complexity.

Lupas and Verdu [65, 66] describe a linear suboptimal detector, the decorrelating detector, which possesses the ideal near-far resistance but results in noise enhancement similar to the zero-forcing equalizer [95]. Moreover, it requires the knowledge of the interference parameters and the inverse of the crosscorrelation matrix. The successive interference cancellation has been proposed in [119] and [50], where one interferer is cancelled at each stage from the received signal. These detectors require a minimal amount of additional hardware, however, the disadvantage of this detector is that, one additional bit delay is required for each stage of cancellation. Moreover, there is a need to reorder the

signals whenever the power profile changes. Varanasi and Aazhang [113, 114, 115] have studied different suboptimal multiuser detectors called the multistage detectors, which achieve considerable improvements over linear detectors, but they require accurate knowledge of the channel parameters, which may incur excessive complexity.

Duel-Hallen [19, 20] has introduced the multiuser zero-forcing decision-feedback (ZF-DF) receivers. It performs linear preprocessing (partially decorrelates the users) followed by a SIC detection. Interference from stronger users is removed by the use of decision feedback leading to significant performance improvement compared to the decorrelating detector. The ZF-DF detector can be implemented by computing the Cholesky decomposition and the matrix inversion. It also requires the estimate of the received signal amplitudes.

Xie et. al. [124] had developed, for the first time, the centralized MMSE receiver for DS-CDMA systems, which minimizes the MSE between the actual data and the soft output of the matched filter. It has been shown to perform better than the decorrelating detector in terms of probability of error performance. However, the receiver is non-adaptive and requires the knowledge of the users parameters and the knowledge of the inverse of the correlation matrix. Klien et al. [47] had presented four suboptimal detectors based on MMSE and zero-forcing criterion with and without decision feedback to combat both ISI and MAI.

Moshavi [83] had proposed the polynomial expansion (PE) detector, which applies a polynomial expansion in R (autocorrelation matrix) to the matched filter bank output. The weights of the polynomial are chosen to optimize the performance of the detector. It can be used to approximate the decorrelating and MMSE detectors in which, neither the correlation matrix nor its inverse need to be calculated.

It is also worth mentioning that there have been attempts to use the neural networks in the adaptation of multiuser DS-CDMA detectors. Aazhang et al. [1] had first proposed the

use of a multiuser perceptron. It outperforms the linear interference suppression technique only if training sequences of all users are available. Mitra et al. [79] has considered a nonlinear perceptron-based multiuser receiver that exploit a linear MMSE and a simple neural network in the adaptation process. It has been shown that the LMS filter and neural network have similar performance. In [78] the radial basis functions (RBF's) networks have been considered to adaptively determine unknown system parameters. The output of the RBF is a linear combination of non-linear functions, each of which is applied to the vector input data. This detector is a single user detector in multiuser communications scenario and performs as a one shot or Bayesian receiver. Least squares algorithms for adapting MMSE receivers perform better than a neural network implementation when training sequences for interfering users are not available.

The Kalman filter, which is the best linear unbiased estimator (BLUE), has been proposed in the literature for equalization and interference excision. In [54] a discrete Kalman filter has been considered for the equalization of digital binary transmission in the presence of noise and intersymbol interference. The Kalman filter has also been used in the channel estimation and demodulation of binary signals. Kozminchuk and Sheikh [51] present a Kalman filtering approach for the suppression of narrowband interference in DS-CDMA communication systems. This approach is based on the digital phase-locked loop Kalman filter. The application of the KF concept to CDMA detection is also described in [60] in which an extended KF (EKF) based detector is used for the joint symbol and time delay estimation of all users in the tracking mode. In [61] a multiuser receiver for asynchronous DS-CDMA signals based on the KF is introduced in which improved performance of this detector over the MMSE detector is demonstrated. In [62] it has been shown that the use of the KF produces symbol estimates with the lowest possible MSE among all linear filters in

long- or short-code systems for a given detection delay, and with a complexity that is fixed for a given detection delay unlike the case of the MMSE detector.

A major limitation of non-adaptive detectors is that they require the knowledge of the spreading codes, timings and amplitudes of all the users, which may not be available to single-user receiver. Moreover, the use of non-adaptive receivers will result in a wasted resource of unnecessary computations if only a subset of possible users is active. An important subject in MUD, is the design of adaptive detectors that self-tune the detector parameters from the observation of the received waveform. Adaptive multiuser DS-CDMA receivers based on the MMSE criterion have been proposed by many researchers [2, 70, 74, 75, and 97]. These detectors have been implemented without requiring any knowledge about the user parameters except the timing information of the desired user and the use of training sequence. The typical operation of these adaptive multiuser detectors requires each transmitter to send a training sequence at start up, which the receiver uses for initial adaptation. After the training phase ends, the adaptation during actual data transmission occur in the decision directed mode. In [2] a single user fractionally-spaced decision-feedback equalizer for MAI rejection has been proposed in an indoor wireless Rayleigh fading environment. In [70] an N-tap MMSE receiver is proposed, where N is the processing gain. Two MAI suppression schemes, to reduce the complexity, have also been considered, namely; the cyclically shifted filter bank (CSFB) and the oversampling schemes. In [74] an adaptive MMSE structure is introduced, and the performance of the receiver is analyzed. In [97] the authors consider a centralized MMSE detector, where in addition to a fractionally spaced feed-forward filter that processes the chip-matched filter output, a feedback filter processes previous decision from all users to cancel both ISI and MAI. The receiver is able to remove the effect of slow multipath propagation and the narrowband interference.

Chen and Roy [16] proposed a real-time adaptive form of the decorrelating detector to combat MAI in CDMA systems. The adaptive receiver combines the matched filtering followed by the decorrelation operation in one unified step and thus providing an efficient structure. The incorporation of decision feedback in this structure yields an improved multiuser receiver. Mitra et al. [80] had developed the adaptive decorrelating detector by placing constraint on the set of spreading codes to be used by the active users. It has two modules: it first decorrelates the existing user, and then it determines the spreading code of a new user entering the network with or without the use of a training sequence. The maximum likelihood detector has been proposed to determine the new user's spreading code, which outperforms the LMS algorithm. However, it is assumed that the receiver knows the existence of a new user.

Halford, K.W. et al. [32] have proposed three detectors/estimators (DE), which are able to detect a new user and estimate its parameters, which can be incorporated in multiuser detector. These are the maximum likelihood DE (MLDE), the generalized MLDE and the cyclic DE (CDE). The first two detectors produce the ML estimates of the new user's signature sequence, delay and amplitude, while the CDE detects a new user by testing for cyclostationarity and then uses suboptimal schemes to estimates the new user's signature sequence, delay and amplitude. A disadvantage of these detectors is that they are computationally expensive. Moreover, they cannot detect and estimate the parameters of more than one new user at a time, and the DE's do not perform well at small values of SNR. Rapajic and Borah [96] have proposed an adaptive MMSE-ML receiver structure for CDMA in multipath fading channels. The proposed receiver has the ability to perform joint synchronization, channel parameter estimation, and signal detection. Moreover, an improved information capacity and BER performance is achieved as compared to the MF-ML receiver.

However, the receiver requires the knowledge of the spreading sequences of all the users and also, its computational complexity increases as the number of users grows. A number of techniques for spatial filtering in CDMA receivers using antenna array have been proposed in [108]. Results are presented to compare the performance of both the MF and interference suppression algorithms in a CDMA cellular system. A method for trading convergence performance with complexity for algorithms using the maximum SINR approach is also discussed.

Efforts have been directed, in the literature, towards the performance evaluation of the DS-CDMA receiver in a fading multipath dispersive environment [12, 102]. Zvonar and Brady [128] have derived an expression for the probability of error of linear multipath-decorrelating receivers with coherent and differentially coherent reception. Both receivers have superior performance compared to the RAKE receiver and eliminate error probability floor caused by MAI on a CDMA reverse link. Sung et al. [107] have generalized the multiuser communication systems to fading environments. A LMMSE unbiased estimator is proposed to efficiently estimate the received signal strength of each user in fading environments which has lower complexity than the optimum receiver. Letaief et al. [58] have evaluated the error rate performance of an asynchronous DS-CDMA receiver in a wireless radio communications environment that is characterized by Rayleigh multipath fading channels.

Hui and Letaief [41] have proposed and analyzed a cochannel interference cancellation detector for demodulating asynchronous DS-CDMA signals over wireless channel that are characterized by multipath fading links. Results show that the proposed multistage detector can significantly improve the system performance over fading channels that are modeled as slowly varying Rayleigh-fading discrete multipath channels. Kansal et al. [46] have

combined the RAKE principles with the linear maximum SINR processing criteria and investigated DS-CDMA transmission over frequency-selective fading channels. Sayeed et al. [103] have introduced a new approach, for achieving diversity in spread spectrum communications over fast-fading multipath channels using a framework that exploits joint multipath-Doppler diversity in an optimal fashion.

Miller et al. [76] have evaluated the performance of the MMSE receiver for DS-CDMA in frequency selective fading channels. It is demonstrated through analytical means the inability of adaptive implementations of MMSE receivers to perform up to the potential promised by the ideal MMSE receiver in fast frequency selective fading channels. A method to achieve the performance of the ideal MMSE is to explicitly track the channel parameter of all users and then forming the correlation matrix and steering vectors directly, however, this leads to a computationally costly multiuser receiver.

The optimal solution for the adaptive filtering problems using the least squares criterion is given by the Wiener-Hopf equations, in which the weight vector is calculated using direct matrix inversion of the autocorrelation matrix and thus requiring $O[N^3]$ computational complexity. However, adaptive algorithms such as LMS or RLS are used to approximate this solution. The LMS algorithm requires $O[N]$ computations but it converges slowly, while, the RLS algorithm, on the other hand, converges much faster but requires large number of computations $O[N^2]$.

It is well known that the RLS algorithm suffers from numerical instability, which has motivated the development of numerically stable QR-RLS algorithms [83, 36] and the inverse QR-RLS algorithm [4], which are used in DS-CDMA receivers [93].

To improve the convergence speed of the adaptive digital filters, various algorithms have been proposed in the literature; the self-orthogonalization algorithm [26],

implementation of the LMS algorithm in the frequency domain [56, 71] and self-orthogonalization of the LMS algorithm in the frequency domain proposed in [85]. Generally, frequency-domain adaptive digital filters have advantages over time-domain implementations [104] by providing faster convergence rate, comparable to RLS but with lower computational complexity. However, frequency domain adaptive filtering is not directly applicable to DS-CDMA receivers, since the input signal is sampled at the chip rate while its output is sampled at the bit rate, i.e. the shifting property of the input data does not exist. For exactly the same reason, fast versions of the RLS algorithm (such as fast transversal filter (FTF) and fast Kalman algorithms) are also not applicable in this case. Complexity reduction can be achieved using block adaptive filtering algorithms such as block LMS (BLMS) [17], in which the filter coefficients are adjusted once per output block, while maintaining equivalent convergence properties. In [81] a set of algorithms linking normalized LMS (NLMS) and block RLS (BRLS) have been proposed. These algorithms converge much faster than the NLMS algorithm (comparable to that of RLS algorithm) while requiring lower number of operations than the LMS algorithm.

Adaptive MMSE receivers assume the availability of a known sequence in the training mode, which requires extra coordination between the receiver and transmitter. In the decision-directed mode, adaptation may fail due to fading or interference transients which necessitates the transmission of fresh training sequence in order to recover from failure. This has motivated the development of blind adaptive interference suppression algorithms, which do not require the knowledge of a training sequence of the desired user.

Honig, Madhow and Verdu [38] have proposed a blind adaptive multiuser detector based on the stochastic gradient minimum output energy (MOE) criterion, which requires the knowledge of the desired user sequence and its timing only. The proposed algorithm

possesses low computational complexity but it suffers from switching back and forth between blind and decision directed modes during the access of new user to the network. The MOE criterion idea has been extended for the joint acquisition and demodulation of DS-CDMA signals in a near-far resistant situation [67, 69]. Fathallah et al. [22] have used the blind MOE based receiver of [38] to suppress narrow-band interference (NBI). A constrained MOE (CMOE) approach has been used in [111] to derive a blind adaptive CDMA receiver for obtaining the receiver parameters directly without estimating the system/channel in a multipath environment. Huang and Wei [42] have presented a blind adaptive algorithm for the near-far resistant DS-CDMA demodulation to mitigate the effects of mismatch caused by the timing error on the MOE algorithm. The timing error is also estimated adaptively, and the estimation can be used for further improving the accuracy in synchronization.

Liu and Xu [64] have proposed a subspace based approach for blind signature estimation in synchronous CDMA systems. The estimation is accomplished by exploiting the fact that the user's signature waveform is confined to a subspace defined by its associated code. The principal advantage of this approach is that it is highly data efficient and is most suitable for a rapidly changing environment. However, the computation cost is relatively high due to the complicated matrix manipulation. De Gaudenzi et al. [18] have introduced a generalized structure of the blind adaptive interference-mitigating detector [38], in which few modifications to the original algorithm has been performed to make it more suitable for practical implementations. It is shown that the proposed detector is particularly robust in the presence of strong asynchronous MAI, and attains the MMSE performance over a large range of SNR without the need to resort to any additional decision-directed scheme.

In [52] an accelerated-convergence stochastic gradient algorithms have been derived and analyzed for blind MUD and joint suppression of MAI and NBI. The method of

accelerating the convergence is a second round of averaging in the stochastic gradient algorithm. Simulation results show that this algorithm and the blind RLS have the same asymptotic convergence rate and tracking properties. However, for short data lengths and high NBI, blind RLS appears to have better transient tracking properties than the blind adaptive gradient detector.

Poor and Wang [93] have considered an RLS blind adaptive version of the MMSE multiuser detection algorithm for the simultaneous suppression of NBI and MAI of a DS-CDMA communication systems. Two QR-RLS based blind algorithms have been derived, which can be considered for efficient parallel implementation via systolic arrays.

Wang and Poor [121] have also proposed a multiuser detection scheme based on signal subspace approach, which can blindly adapt both the decorrelating and the linear MMSE detector. In [120] the authors have extended the work of [121] by developing subspace-based techniques to combat both MAI and ISI blindly in the high-rate dispersive CDMA system. Furthermore, initial delay estimation within the framework of subspace approach has also been considered. In [99] a new efficient blind adaptive MOE-based detector is proposed, by exploiting the property that the optimal weight of the MOE filter lies in the signal subspace. The receiver requires fewer filter coefficients and has improved detector characteristics (superior convergence rates and steady-state SINR) as indicated by analysis and by simulation results in comparison to the blind adaptive detector of [38]. Ulukus and Yates [112] have presented a blind adaptive multiuser decorrelating detector for CDMA systems which uses observables that are readily available at the receiver. The detector is constructed via a distributed iterative algorithm, which updates the receiver filter coefficients of a desired user by using the previous output of the filter under construction. Since the filter output is random, the algorithm evolves stochastically.

Iltis [43] has described a code-tracking algorithm for a DS-CDMA receiver based on the extended Kalman filter (EKF), which provides both code synchronization and joint estimates of interferer and channel parameters. Iltis et al. [44] have developed a multiuser DS-CDMA detector without the knowledge of the delays and amplitudes of the signals. The algorithm is made adaptive and the likelihood function in the symbol-by-symbol metric is updated using a set of extended Kalman filters (EKF) innovations. Lim et al. [60] has introduced adaptive multiuser detector structures using the EKF and RLS formulation to jointly estimate the transmitted bits of each user and individual amplitudes and time delays. The proposed detector works in the tracking mode, assuming that initial delay estimate is already available. However, the detector possesses high computational complexity and, moreover, requires the knowledge of the noise variance.

Algorithms based on the maximum likelihood (ML) rule, for the time delay estimation (TDE) of CDMA systems have been developed in [10]. The estimator includes a whitening filter to suppress MAI, thus yielding a near-far resistant estimator. However, it requires the knowledge of the transmitted symbols, which can be accomplished by feedback decisions from the detector. Strom et al. [106] have proposed algorithms based on the ML, MUSIC and the sliding correlator to deal with the propagation delay, phase and amplitude estimation of all users in DS-CDMA systems. Parkvall, S. et al. [89] proposed a CDMA receiver using the modified MUSIC estimator in conjunction with the MMSE interference suppression to obtain a near-far resistant receiver.

Smith et al. [105] have presented a single user code timing estimation algorithm that is based on processing the weight vector of an adaptive DS-CDMA receiver. The only side information required is the spreading sequence of the desired user. The performance of this

detector is found to be near-far resistant when the RLS adaptive filter is used. An all one training sequence or double the filter length is required to provide correct estimates.

Madhow [68] has suggested a near-far resistant TDE method. The delay is estimated by running N-parallel adaptive algorithms, and then finding the delay, which provides the lowest MSE. The only requirements are a training sequence for the desired user and a finite uncertainty regarding the symbol timing.

1.2 Statement of the problem

The present work encompasses a study of adaptive multiuser detection (MUD) techniques based on the MMSE criterion for the interference suppression and demodulation of DS-CDMA signals. The aim of the work is to develop techniques and algorithms, which possess fast convergence rate, require low computational complexity, and moreover, they may require minimum side information about the users (i.e. without the knowledge of the training sequence or the knowledge of the timing of the desired user).

The problem, as treated in this study, may be divided into five main parts as follows:

- i) A comparative study of the adaptive algorithms based on LMS, NLMS, RLS and the modified variable step-size LMS (MVSS-LMS) for interference suppression in DS-CDMA systems. The development of a block algorithm for the interference suppression in DS-CDMA systems, which possesses fast convergence rate with low computational complexity.
- ii) A study of the implementation of the KF algorithm, which is optimum in the MMSE sense, for the interference suppression in DS-CDMA systems. To deal with the instability problem of the KF, the implementation of the SQRT-KF algorithm, which exhibits better numerical stability, for the interference suppression in DS-CDMA systems is considered.

- iii) The implementation of the RMGS algorithm and its error feedback form for the interference suppression and demodulation of DS-CDMA signals, in the presence of both AWGN and ISI. Parallel implementation via systolic arrays is also studied to reduce the complexity.
- iv) A study of blind adaptation techniques based on constant modulus algorithm (CMA), LMS, RLS and QR-RLS for adaptation and interference suppression in DS-CDMA systems.
- v) A study of time-delay estimation (TDE) techniques for DS-CDMA signals in both initialization and tracking modes.

1.3 Organization of the thesis

The work embodied in this thesis has been arranged in seven chapters as detailed below:

Chapter 2: Adaptive algorithms for interference suppression in DS-CDMA systems.

In this chapter, we first introduce the asynchronous DS-CDMA system model, and then we present its MMSE solution, which can be implemented using a TDL filter receiver. Next we present adaptive algorithms for interference suppression of DS-CDMA systems based on the LMS, NLMS, RLS, MVSS-LMS and RLS algorithms. The performance measures, which are used to assess the performance of the receiver, are considered next. A novel block algorithm for interference suppression in DS-CDMA systems is introduced, which possesses comparable convergence rate as RLS while requiring less computations. Several numerical examples have been simulated to evaluate the performance of the various algorithms for different sets of parameters.

Chapter 3: Adaptive DS-CDMA receiver using Kalman filtering.

In this chapter, we consider the application of KF algorithm for the adaptation and demodulation of DS-CDMA signals. We briefly review the use of the KF in the adaptive

filtering problem. Then we formulate the state-space representation of the DS-CDMA signals. To deal with the numerical instability of the KF, we have used the SQRT-KF algorithm for the interference suppression in DS-CDMA signals, which shows better numerical stability. Several numerical examples have been simulated to evaluate the performance of these algorithms.

Chapter 4: RMGS-based adaptive interference suppression in DS-CDMA signal.

In this chapter, we first review the QR-RLS algorithms, which are used to deal with the least squares problem in an effort to enhance its stability. We then present the QR-RLS and inverse QR-RLS algorithms for the adaptation and demodulation of DS-CDMA signals. Next we have proposed the implementation of the RMGS algorithm for the interference suppression in DS-CDMA signals. The parallel implementation of the RMGS algorithm via systolic arrays is presented in detail. We then present the results of the simulations using the RMGS algorithm and compare its performance with other adaptive algorithms. Also we present the performance of the adaptive DS-CDMA receiver based on NLMS and RMGS algorithms in a multipath fading dispersive environment.

Chapter 5: Blind adaptive interference suppression algorithms.

In this chapter, we remove the requirement for the knowledge of a training sequence and present several blind adaptive algorithms. First we present the CMA algorithm for the adaptation and interference suppression of DS-CDMA signals. Then we focus on the blind MOE algorithms for the adaptation and interference suppression in DS-CDMA systems, namely blind LMS, blind RLS and blind QR-RLS algorithms. A novel blind RMGS-based algorithm is derived and implemented for the demodulation of DS-CDMA systems. The performance of the various blind adaptive algorithms is presented by simulating a number of numerical examples.

Chapter 6: Adaptive time-delay estimation Using RMGS algorithm.

In this chapter, we consider the TDE problem in DS-CDMA systems. We first review the adaptive TDE techniques, and then we present two TDE methods; the first method is based on cross-correlating the MMSE weight vector, obtained by implementing the RMGS algorithm, with the desired user spreading sequence. The second method is based on running N-parallel MMSE adaptive algorithms, based on the RMGS algorithm. The two methods are implemented for both the initialization and tracking modes. A blind version of the parallel TDE algorithm is also presented. Several numerical examples have been simulated to evaluate the performance of these TDE methods in a near-far environment.

Chapter 7: Conclusions

We conclude the thesis with a summary of the important results and the suggestions for future work.

Also included are two appendices. Appendix (A) presents the derivation of the multipath fading dispersive channel model, which is used to study the performance of the adaptive DS-CDMA receiver in multipath fading environments. Appendix (B) presents the solution of the constrained optimization problem (equations 5.26 & 5.27) which is used in the derivation of the blind MOE-based RLS algorithm.

ADAPTIVE ALGORITHMS FOR INTERFERENCE SUPPRESSION IN DS-CDMA SYSTEMS

Over the last two decades DS-CDMA has become a feasible alternative to both frequency-division multiple-access (FDMA) and time-division multiple-access (TDMA) in cellular, personal and wireless communications. The primary advantage of spread spectrum technology, the basis of CDMA, is its ability to reject interference whether it be an unintentional interference by another user simultaneously attempting to transmit over the channel, or an intentional interference by a hostile transmitter attempting to jam the transmission. The inherent processing gain of the spread spectrum provides the system with the interference rejection capability. A single-user receiver treats the received signals due to other active users as stationary interference, but suffers from near-far effect in the absence of power control. In multiuser detection, the receiver jointly detects those signals in order to mitigate the effect of non-orthogonal properties of received signals. Adaptive multiuser detection has been proposed to solve the problems inherited in the conventional detection techniques and has become an active area of research in recent years.

In this chapter, we first briefly review the interference rejection techniques in DS-CDMA systems in section 2.1. This is followed by the introduction of the DS-CDMA signal model in section 2.2. In section 2.3, we next consider the use of the LMS, normalized LMS, modified variable step-size LMS and RLS algorithms based on the MMSE criterion, for the adaptation and demodulation of DS-CDMA signals. Then a novel block adaptive filtering algorithm is introduced which possesses a fast convergence rate as compared to LMS

algorithm, while simultaneously requiring much lower computations as compared to RLS algorithm. The performance measures, which are used to assess the various adaptation algorithms, are presented in section 2.4. Finally, simulation results are presented in section 2.5 to compare and assess the performance of different adaptive algorithms.

2.1 Introduction

In DS-CDMA systems a number of users share a common channel bandwidth in which the users are distinguished from one another by superimposing a distinct pseudo-random code, which is known at the receiver to recover the transmitted information. All users can transmit at the same time and are allocated the entire frequency spectrum for transmission. Hence, the detector receives a signal composed of the sum of the signals of all the users, which overlap in time and frequency. Earlier demodulation schemes were restricted to single-user detection strategy which makes use of the cross-correlation properties of the signal constellation. The conventional receiver consists of a bank of K matched filters, one corresponding to each user. By correlating the received signal with the signature sequence of the desired user, the data bits are demodulated. This receiver exploits the orthogonality property of the spreading waveform and ignores MAI in the receiver design. Since, in practice the interfering signals are not truly orthogonal to the desired signal, the output of the conventional matched filter for the desired user contains contributions from the MAI. Thus, even if the receiver's thermal noise level goes to zero, the error probability of the conventional receiver exhibits a non-zero floor because of the MAI. The MAI caused by any one of the users is generally small, but as the number of interferers or their power increases, MAI becomes substantial. Moreover, if the power of the interferers is much stronger than that of the desired signal, then the weak signal of the desired user is overwhelmed by the MAI and reliable reception is impossible. This is known as the near-far problem (which may

also occurs due to fading). The performance of the conventional single-user detector is acceptable, provided the energies of the received signals are not too dissimilar and that the signature waveforms are designed so that their crosscorrelations are low enough [118]. The MAI and the near-far problem encountered by conventional reception technique can be eliminated by the use of multiuser detection (MUD) [116,117] in which the information about multiple users is used to detect each individual user. The optimum multiuser detector [116] uses a bank of matched filters followed by the use of a Viterbi maximum likelihood algorithm. However, it requires the knowledge of the interfering user's power, timing and spreading sequence. Furthermore, the complexity of the receiver grows exponentially with the number of active users.

To reduce the complexity, a number of suboptimal detectors have been proposed in the literature, such as the linear decorrelating detector [65, 66], the successive interference cancellation detector [119, 50, 113, 114, 115], and the zero-forcing decision-feedback (ZF-DF) detectors [19, 20]. These detectors are near-far resistant thus eliminating the need for strict power control. The drawback of these detectors is that their computational complexity increases linearly with the number of users, and the users parameters are required to be known at the receiver.

Xie et al [124] had developed the centralized MMSE detector, which minimizes the error between the actual data and the soft output of the receiver. This detector can be implemented using a tapped delay line filter having a linear complexity in the number of users. The MMSE detector possesses better probability of error than the decorrelating detector. As the background noise goes to zero the MMSE detector converges in performance to the decorrelating detector. However, the disadvantage of this detector is that it requires the knowledge of the received amplitudes of all users and, moreover, the knowledge of the

inverse of the correlation matrix is also required. It may be noted that it possesses lower near-far resistance compared to the decorrelating detector.

Adaptive interference suppression techniques have been used in the multiuser detection schemes, which do not require explicit knowledge of the MAI. It is analogous to adaptive equalization of dispersive channels by virtue of the analogy between MAI and intersymbol-interference (ISI). These receivers require the knowledge of sequence of symbols transmitted by the desired user during training period, and the knowledge of the timing of the desired user.

Madhow and Honig [70] have considered a single-user MMSE receiver for interference suppression in DS-CDMA systems, and have proposed three schemes for interference suppression in DS-CDMA detectors with finite-complexity. The output of the chip matched filter is sampled at the chip rate and then an N -tap FIR filter is used to minimize the mean-squared error between the transmitted and detected symbols, where N is the processing gain. It is demonstrated that the MMSE-based receiver can offer a dramatic performance improvement relative to the matched filter detector.

Rapajic and Vucetic [97] have considered the adaptive MMSE linear and centralized DF receivers. The timing, signatures and carrier phase information from other users are not needed. Moreover, its complexity is independent of the number of users and is slightly higher than the complexity of the matched filter receiver. It is also shown that the adaptive linear receiver is able to completely remove the effect of narrowband interference and multipath propagation, provided that the variation in multipath parameters is slow. The centralized DF-receiver is shown to have the same timing recovery, near-far resistance, and multipath suppression properties as the linear receiver, whereas MAI cancellation is significantly

improved as compared with the linear receiver. However, the complexity of the adaptive centralized DF receiver increases linearly with the number of users.

Abdulrahman et al [2] have presented an adaptive fractionally spaced DFE for a CDMA system in an indoor wireless Rayleigh fading environment. The system only uses information about the desired user's spreading code and the training sequence. The optimum performance, convergence time, and BER results show the capabilities of this receiver in minimizing the effects of interference, multipath, fading, and AWGN in a slow acting power control environment. Two receiver configurations were considered: one that has knowledge of desired user spreading code (spreading sequence MF {SSMF} receiver) and the other has no information about all spreading codes (LPF receiver). A study of the performance showed that the LPF receiver gives better MSE performance than that obtained by the SSMF receivers.

Miller [74] has considered an adaptive DS-CDMA receiver for interference rejection. It uses a chip-matched filter followed by an adaptive equalizer structure to perform the despreading operation. This receiver has been analyzed to determine the equalizers tap gains and the steady state residual MSE, from which the capacity of the system can be calculated. It is shown that the receiver is near-far resistant and provides a two-fold increase in capacity compared to a conventional receiver with perfect power control. Klien et al [47] have presented four suboptimal detectors-based on MMSE and zero-forcing detectors with and without decision feedback to combat both ISI and MAI. The performance of these detectors is shown to be better than that of the conventional detector. The MMSE detector performs better than the corresponding ZF detector and the performance of the equalizers with DF is better than the corresponding equalizers without feedback.

Based on the MMSE criterion, in this chapter, we first consider the use of the LMS and RLS algorithms [36] for the adaptation of the TDL-filter weights for the DS-CDMA receiver. It is well-known that the RLS algorithm possesses faster convergence but requires a large number of computations, $O[N^2]$. On the other hand, the LMS algorithm requires much lower computations $O[N]$, but it converges slowly.

One approach to improve the performance of the LMS algorithm is to employ a time-varying step-size in the weights update recursion. A large step-size is used when the receiver is far from convergence, thus speeding up the convergence speed. On the other hand, a small step size is used when the algorithm is nearing convergence, thus a low value of misadjustment is achieved, thus improving the overall performance [53, 72, 34]. However, the performance is sensitive to the noise disturbance, and performs well only in a high SNR environment. A robust MVSS-LMS algorithm is proposed in [3], where the step size is adjusted according to the square of the time-averaged estimate of the autocorrelation of the instantaneous error $e(n)$ with pervious error $e(n-1)$. Simulation results indicate it superior performance compared to other VSS-LMS algorithms in a stationary environments, whereas for a nonstationary environments it performs as well as other VSS algorithms.

Various structures combined with adaptation algorithms have been proposed, in the signal processing literature, to improve the convergence speed of the adaptive filters. The self-orthogonalization algorithm [26] is used to increase the convergence speed of the LMS adaptive algorithm using a variable step-size. This step size is obtained by multiplying the inverse of the correlation matrix by a constant. The resultant matrix, which controls the convergence speed, is the identity matrix and hence all its eigenvalues are equal. Therefore, the convergence rate will become faster but with a large increase in the computational complexity. Another method of increasing the convergence speed of the adaptive filters is to

realize the LMS algorithm in the frequency domain, using the discrete Fourier transform [56, 71]. By transforming the input signal to the frequency domain, a set of uncorrelated (orthogonal) signals are generated, and then by using a variable step-size in the weights update equation (i.e. by dividing the same constant by the power estimates of each frequency bin), an improved convergence characteristics is achieved. This is called the self-orthogonalization of the adaptive digital filters in the frequency domain proposed first in [85], which is reported to have significantly improved stability performance over the LMS adaptive digital filter [56]. However, frequency domain adaptive filtering is not directly applicable to DS-CDMA receivers, since the input signal is sampled at the chip rate while its output is sampled at the bit rate, i.e. the shifting property of the input data does not exist. For exactly the same reason, fast versions of the RLS algorithm (such as fast transversal filter FTF and fast Kalman algorithms) are also not applicable in this case.

Complexity reduction can be achieved using block adaptive filtering algorithms such as block LMS (BLMS) [17], in which the filter coefficients are adjusted once per output block, while maintaining equivalent convergence properties. A set of algorithms linking normalized LMS (NLMS) and block RLS (BRLS), which allow a trade off between arithmetic complexity and convergence rate, have been proposed in [81]. These algorithms require a lower number of operations than the classical LMS algorithm, while converging much faster (comparable to that of RLS algorithm). Based on these algorithms, in this chapter, a novel block adaptive algorithm (with low computational complexity) has been adopted to DS-CDMA systems to increase the convergence speed in comparison to the LMS algorithm.

2.2 MMSE receiver for DS-CDMA systems

In CDMA systems, the channel is shared by K users, where each user is assigned a spreading waveform $c_k(t)$, which is zero outside the interval $[0, T]$, defined by:

$$c_k(t) = \sum_{j=0}^{N-1} c_{k,j} \psi(t - jT_c) \quad (2.1)$$

where T is the signaling bit interval, $N=T/T_c$ is the processing gain, $\psi(t)$ is the chip waveform of rectangular shape and duration T_c , and $c_{k,j} \in \{-1,1\}$ is the j th element of the spreading code of the k th user. The spreading codes (signature sequences) are typically chosen to have crosscorrelation properties that reduce multiple access interference between users. This type of signaling will spread the bandwidth of the data signal by a factor of N . The non-orthogonality of these spreading codes increases the MAI to the desired user data bits, and thus affects the detectability. However, the effect of this interference can be suppressed through proper signal processing algorithms and multiuser detection techniques [39, 40] as mentioned earlier.

The k th user transmits a signal, in the interval $0 \leq t \leq T$ corresponding to first bit, of the form

$$s_k(t) = d_k(t) c_k(t) \cos(\omega_c t + \theta_k) \quad 0 \leq t \leq T \quad (2.2)$$

where $d_k(t)$ is the k th user data bit, ω_c is the carrier frequency and θ_k is its phase. The input data is antipodal randomly generated zero mean signal. The received signal (Fig.2.1) is of the form:

$$y(t) = \sum_{k=1}^K \sqrt{P_k} s_k(t - \tau_k) + n(t) \quad (2.3)$$

where P_k is the received power of the k th user and τ_k is its delay which is assumed to be uniformly distributed over $[0, T]$, and $n(t)$ is additive white Gaussian noise. It is assumed that the receiver is synchronized with the desired user (user 1). The contribution of the k th user within the interval $(n-1)T$ to nT , associated with user's one data bit $d_1(n)$, is due to two data bits $d_1(n-1)$ and $d_1(n)$, as shown in Fig.2.2.

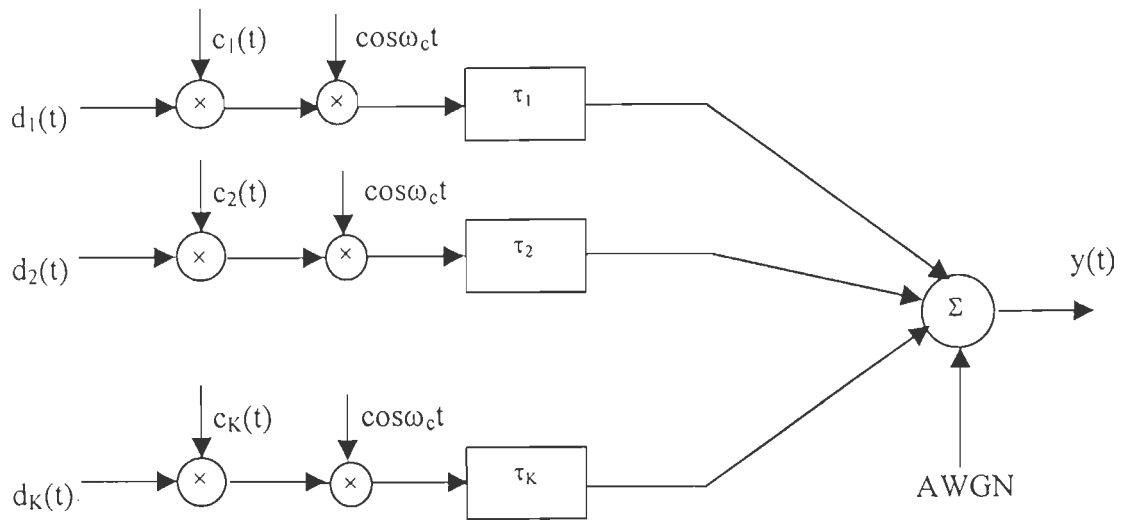


Fig.2.1 Block diagram of K CDMA transmitters.

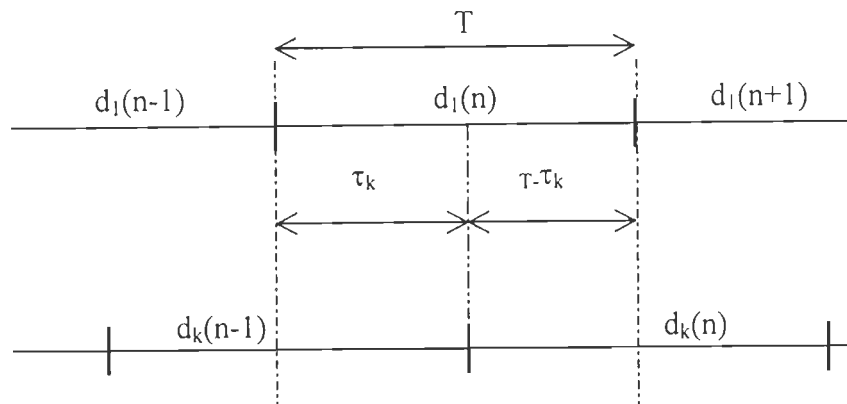


Fig.2.2 Illustration of the contribution to the channel output from the desired user and kth interferer.

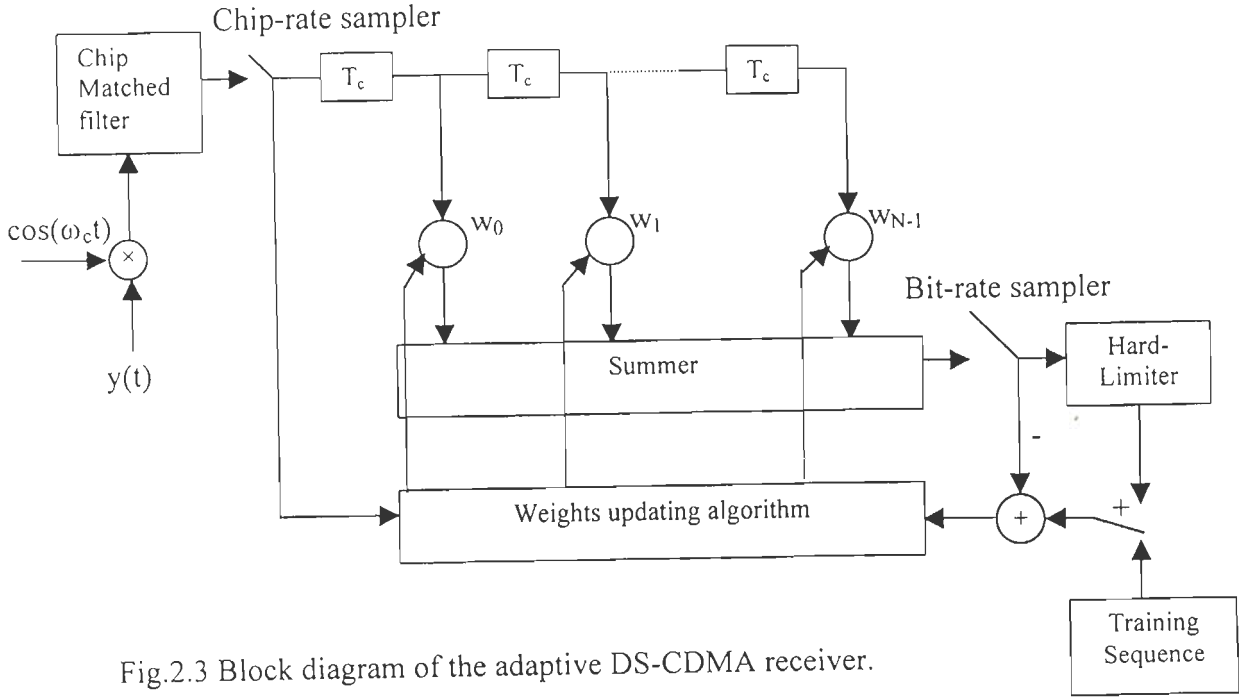


Fig.2.3 Block diagram of the adaptive DS-CDMA receiver.

The block diagram of a DS-CDMA receiver is shown in Fig.2.3. The receiver converts the received signal $y(t)$ to a baseband signal. After the baseband conversion, the received signal is passed through a chip-matched filter and sampled at the end of each interval. The output of the chip-matched filter at the m th sample of the n th bit is then

$$r_m(n) = \int_{mT_c + \tau_1}^{(m+1)T_c + \tau_1} y(t) \psi(t - mT_c) \cos(\omega_c t + \theta_1) dt \quad (2.4)$$

Substituting Eq.(2.3) into Eq.(2.4) yields:

$$r_m(n) = \int_{mT_c + \tau_1}^{(m+1)T_c + \tau_1} \left[\sum_{k=1}^K \sqrt{P_k} s_k(t - \tau_k) + n(t) \right] \psi(t - mT_c) \cos(\omega_c t + \theta_1) dt$$

$$r_m(n) = \int_{mT_c + \tau_1}^{(m+1)T_c + \tau_1} \left[\sum_{k=1}^K \sqrt{P_k} s_k(t - \tau_k) \right] \psi(t - mT_c) \cos(\omega_c t + \theta_1) dt$$

$$+ \int_{mT_c + \tau_1}^{(m+1)T_c + \tau_1} n(t) \psi(t - mT_c) \cos(\omega_c t + \theta_1) dt \quad (2.5)$$

Substituting Eqs. (2.1) and (2.2) in the first term (F) of Eq.(2.5) yields:

$$F = \int_{mT_c + \tau_i}^{(m+1)T_c + \tau_i} \left[\sum_{k=1}^K \sqrt{P_k} d_k(t - \tau_k) c_k(t - \tau_k) \cos\{\omega_c(t - \tau_k) + \theta_k\} \right] \psi(t - mT_c) \cos(\omega_c t + \theta_1) dt$$

$$F = \int_{mT_c + \tau_i}^{(m+1)T_c + \tau_i} \left[\sum_{k=1}^K \sqrt{P_k} d_k(t - \tau_k) \sum_{j=0}^{N-1} \{c_{k,j} \psi(t - jT_c - \tau_k)\} \cos\{\omega_c(t - \tau_k) + \theta_k\} \right] \psi(t - mT_c) \cos(\omega_c t + \theta_1) dt \quad (2.6)$$

During the estimation of the desired signal $d_1(n)$, the interference of the k th user are from two adjacent data bits: $d_k(n-1)$ contributes in the interval $(n-1)T < t \leq (n-1)T + \tau_k$ and $d_k(n)$ contributes in the interval $(n-1)T + \tau_k \leq t < nT$. Therefore, Eq.(2.6) can be written as:

$$F = \left\{ \int_{mT_c + \tau_i}^{(m+1)T_c + \tau_i} \left[\sum_{k=1}^K \sqrt{P_k} d_k(n-1) \sum_{j=0}^{N-1} \{c_{k,j} \psi(t + NT_c - jT_c - \tau_k)\} \cos\{\omega_c(t - \tau_k) + \theta_k\} \right]_{(n-1)T \leq t < (n-1)T + \tau_k} \right. \\ \left. + \int_{mT_c + \tau_i}^{(m+1)T_c + \tau_i} \left[\sum_{k=1}^K \sqrt{P_k} d_k(n) \sum_{j=0}^{N-1} \{c_{k,j} \psi(t - jT_c - \tau_k)\} \cos\{\omega_c(t - \tau_k) + \theta_k\} \right]_{(n-1)T + \tau_k \leq t < nT} \right\} \psi(t - mT_c) \cos(\omega_c t + \theta_1) dt \quad (2.7)$$

Assuming that $P_1=1$ and $\tau_1=0$ for the desired user, and that $\theta_j=0$, although it can be easily modified to take non-zero values into account. The high-frequency term of $\cos^2 \omega_c t$ will be filtered out since we are integrating in the interval $(0$ to $T_c)$, then the last integral will be simplified to:

$$F = d_1(n) \sum_{j=0}^{N-1} c_{1,j} \int_{mT_c}^{(m+1)T_c} \psi(t - mT_c) \psi(t - jT_c) dt \\ + \sum_{k=2}^K \sqrt{2P_k} \left\{ d_k(n-1) \sum_{j=0}^{N-1} c_{k,j} \int_{mT_c}^{(m+1)T_c} \psi(t - mT_c) \psi(t + NT_c - jT_c - \tau_k) dt \right\}_{(n-1)T \leq t < (n-1)T + \tau_k} \\ + d_k(n) \sum_{j=0}^{N-1} c_{k,j} \int_{mT_c}^{(m+1)T_c} \psi(t - mT_c) \psi(t - jT_c - \tau_k) dt \left. \right\}_{(n-1)T + \tau_k \leq t < nT} \quad (2.8)$$

Integration on chip intervals!

Good how on partial bit intervals

Let the delay of the kth user be expressed as: $\tau_k = \rho_k T_c + \delta_k$, where ρ_k is an integer between 0 and N-1, and δ_k lies in the interval $[0, T_c)$, then the last integral will be:

$$\begin{aligned}
 F = & d_1(n) \sum_{j=0}^{N-1} c_{1,j} \int_0^{T_c} \psi(t) \psi(t - jT_c + mT_c) dt \\
 & + \sum_{k=2}^K \sqrt{P_k} \left\{ d_k(n-1) \sum_{j=0}^{N-1} c_{k,j} \int_0^{T_c} \psi(t) \psi(t + NT_c - jT_c + mT_c - \rho_k T_c - \delta_k T_c) dt \Big|_{(n-1)T \leq t < (n-1)T + \tau_k} \right. \\
 & \left. + d_k(n) \sum_{j=0}^{N-1} c_{k,j} \int_0^{T_c} \psi(t) \psi(t - jT_c + mT_c - \rho_k T_c - \delta_k T_c) dt \Big|_{(n-1)T + \tau_k \leq t < nT} \right\} \quad (2.9)
 \end{aligned}$$

Since $\sum_{j=0}^{N-1} c_{1,j} \int_0^{T_c} \psi(t) \psi(t - jT_c + mT_c) dt$ is always zero except when $j=m$, then the first term

of Eq.(2.9) is equal to $d_1(n) c_{1,m}$. In a similar manner, the last terms of Eq.(2.9) will reduce to

$$\sum_{k=2}^K \sqrt{2P_k} \left\{ d_k(n-1) c_{k, N+m+\rho_k} \delta_k + d_k(n) c_{k, m+\rho_k} (1-\delta_k) \right\}.$$

Let $\mathbf{c}_k = [c_{0,k} \ c_{1,k} \ \dots \ c_{N-1,k}]^T$ be the spreading sequence for the kth user and let $\mathbf{r}(n) = [r_0(n) \ r_1(n) \ \dots \ r_{N-1}(n)]^T$ be the contents of the TDL at the nth data sample time. The normalized contents of the TDL filter can be written as in [74]:

$$\mathbf{r}(n) = d_1(n) \mathbf{c}_1 + \sum_{k=2}^K \sqrt{P_k} d_k(n) \mathbf{I}_k(n) \cos(\theta_k) + \eta(n) \quad (2.10)$$

$$\mathbf{I}_k(n) = z_{2k-1}(n) \mathbf{a}_{2k-1}(\rho_k, \delta_k) + z_{2k}(n) \mathbf{a}_{2k}(\rho_k, \delta_k) \quad (2.11)$$

$$z_{2k-1}(n) = [d_k(n) + d_k(n-1)]/2$$

$$z_{2k}(n) = [d_k(n) - d_k(n-1)]/2 \quad (2.12)$$

where:

$$\mathbf{a}_{2k-1}(\rho_k, \delta_k) = \left\{ \delta_k \mathbf{c}_k^{(\rho_k+1)} + (1-\delta_k) \mathbf{c}_k^{(\rho_k)} \right\} \quad (2.13)$$

$$\mathbf{a}_{2k}(\rho_k, \delta_k) = \left\{ \delta_k \hat{\mathbf{c}}_k^{(\rho_k+1)} + (1-\delta_k) \hat{\mathbf{c}}_k^{(\rho_k)} \right\} \quad (2.14)$$

$$\mathbf{c}_k^{(m)} = [c_{k,N-m} \ c_{k,N-m+1} \ \dots \ c_{k,N-1} \ c_{k,0} \ c_{k,1} \ \dots \ c_{k,N-m-1}]^T \quad (2.15)$$

$$\hat{\mathbf{c}}_k^{(m)} = [-c_{k,N-m} \ -c_{k,N-m+1} \ \dots \ -c_{k,N-1} \ c_{k,0} \ c_{k,1} \ \dots \ c_{k,N-m-1}]^T \quad (2.16)$$

$\eta(n)$ is a vector of random Gaussian noise variables with zero mean and variance of σ^2 .

The process of adjusting the TDL weights vector, $\mathbf{w}(n)$, is called weight adaptation, where $\mathbf{w}(n)=[w_0(n), w_1(n), \dots, w_{N-1}(n)]^T$ is the TDL filter weights during interval $(n-1)T < t < nT$. The output of the TDL filter is given by [122]:

$$\hat{d}_1(n) = \sum_{k=0}^{N-1} w_k(n) r_k(n) \quad (2.17)$$

or, using vector notation

$$\hat{d}_1(n) = \mathbf{r}^T(n)\mathbf{w}(n) = \mathbf{w}^T(n)\mathbf{r}(n) \quad (2.18)$$

The error signal is obtained by subtracting the error signal from the desired response, i.e.:

$$e(n) = d_1(n) - \hat{d}_1(n) = d_1(n) - \mathbf{w}^T(n)\mathbf{r}(n) \quad (2.19)$$

The instantaneous squared error is ^{given} by:

$$e^2(n) = d_1^2(n) + \mathbf{w}^T(n)\mathbf{r}(n)\mathbf{r}^T(n)\mathbf{w}(n) - 2d_1(n)\mathbf{r}^T(n)\mathbf{w}(n) \quad (2.20)$$

Assuming, that $e(n)$, $d_1(n)$ and $\mathbf{r}(n)$ are statistically stationary and taking the expected value of $e^2(n)$ over n ;

$$E[e^2(n)] = E[d_1^2(n)] + \mathbf{w}^T(n)E[\mathbf{r}(n)\mathbf{r}^T(n)]\mathbf{w}(n) - 2E[d_1(n)\mathbf{r}^T(n)]\mathbf{w}(n) \quad (2.21)$$

Let $\mathbf{R}(n) = E[\mathbf{r}(n)\mathbf{r}^T(n)]$, be designated as the input autocorrelation matrix. Similarly, define $\mathbf{P}(n) = E[d_1(n)\mathbf{r}(n)]$ as the crosscorrelation vector between the desired response and the input components. Thus the MSE designated by ξ , is given as:

$$\xi = E[e^2(n)] = E[d_1^2(n)] + \mathbf{w}^T(n)\mathbf{R}(n)\mathbf{w}(n) - 2\mathbf{P}^T(n)\mathbf{w}(n) \quad (2.22)$$

The gradient of the MSE may be written as:

$$\nabla(\xi) = \frac{\partial \xi}{\partial \mathbf{w}} = \left[\frac{\partial \xi}{\partial w_0} \ \frac{\partial \xi}{\partial w_1} \ \dots \ \frac{\partial \xi}{\partial w_{N-1}} \right]^T \quad (2.23)$$

$$= 2 \mathbf{R}(n) \mathbf{w}(n) - 2 \mathbf{P}(n)$$

To obtain the minimum MSE, the weight vector $\mathbf{w}(n)$ is set at its optimal value \mathbf{w}_o ,

where the gradient is zero:

$$\nabla(\xi) = 0 = 2 \mathbf{R} \mathbf{w}_o - 2 \mathbf{P} \quad (2.24)$$

Assuming \mathbf{R} is non-singular, the optimal weight vector \mathbf{w}_o called the Wiener weight vector, is given by:

$$\mathbf{w}_o = \mathbf{R}^{-1} \mathbf{P} \quad (2.25)$$

which is an expression of the Wiener-Hopf equation in matrix form. Also, the minimum MSE is given by:

$$\begin{aligned} \xi_{\min} &= E[d_1^2(n)] + \mathbf{w}_o^T \mathbf{R} \mathbf{w}_o - 2 \mathbf{P}^T \mathbf{w}_o \\ &= E[d_1^2(n)] - \mathbf{P}^T \mathbf{w}_o \end{aligned} \quad (2.26)$$

2.3 Adaptive MMSE receiver

After chip-matched filtering and chip-rate sampling of the received signal, the output samples are fed into a tapped delay line (TDL) filter of length N . The output of the TDL filter is sampled at the bit interval, and hard-limited to form an estimate of the desired data bit $\hat{d}_1(n)$. The receiver requires the knowledge of the training sequence at the beginning of the learning phase and then it switches to the decision directed mode during actual data transmission.

The optimal weights vector for the MMSE receiver, given by $\mathbf{w}_o = \mathbf{R}^{-1} \mathbf{P}$, minimizes the MSE (ξ), where $\mathbf{R}(n)$ is the autocorrelation matrix of the vector $\mathbf{r}(n)$ defined as:

$$\mathbf{R}(n) = \mathbf{c}_1 \mathbf{c}_1^T + \sum_{k=2}^K P_k \cos^2 \theta_k E [\mathbf{I}_k(n) \mathbf{I}_k^T(n)] + \sigma^2 \mathbf{I}_{N \times N} \quad (2.27)$$

where $\mathbf{I}_{N \times N}$ is the identity matrix, σ^2 is the noise variance and $\mathbf{P}(n)$ is the crosscorrelation vector defined as $\mathbf{P}(n) = E[d_1(n) \mathbf{r}(n)]$, which using Eq.(2.10) reduces to:

$$\mathbf{P}(n) = \mathbf{c}_1 \quad (2.28)$$

It is clear from Eq.(2.22) that in order to calculate the weights vector, the inverse of $\mathbf{R}(n)$ is required, which requires $O[N^3]$ operations. To reduce the complexity, adaptive signal processing algorithms, such as LMS and RLS, have been proposed in the literature to calculate the weight vector $\mathbf{w}(n)$.

2.3.1 The Least-Mean-Square (LMS) algorithm

The LMS algorithm is based on the method of steepest descent [122]. It is developed to update the weights vector $\mathbf{w}(n)$ by estimating the gradient vector of the MSE $\xi = E[e^2(n)]$, where $e(n)$ is the estimation error calculated using the current estimate of the weight vector $\mathbf{w}(n)$ as defined by Eq.(2.19). However, in the LMS algorithm, $e^2(n)$ itself is taken as an estimate of ξ . The gradient of the estimate is then given by:

$$\hat{\nabla}(n) = -2 e(n) \mathbf{r}(n) \quad (2.29)$$

According to this method the value of the weight vector at instant $(n+1)$ is computed using the simple recursive relation [122]:

$$\begin{aligned} \mathbf{w}(n+1) &= \mathbf{w}(n) - \mu(n) \hat{\nabla}(n) \\ &= \mathbf{w}(n) + 2 \mu(n) e(n) \mathbf{r}(n) \end{aligned} \quad (2.30)$$

where $\mu(n)$ is a scalar gain factor that controls the rate of convergence and stability of the algorithm. According to the value of the step-size, in the following two algorithms have been considered; namely the fixed step-size and variable step-size LMS algorithms.

2.3.1.1 Fixed step-size LMS algorithm

In this algorithm the step-size is fixed to a certain value μ . For convergence to occur and to ensure stability of the algorithm, μ should be chosen such that $0 < \mu < 2/\lambda_{\max}$ where λ_{\max} is the largest eigenvalue of the input correlation matrix. The recursive procedure is started with the initial guess $\mathbf{w}(0)$, where a convenient guess is a null vector.

From Eq.(2.30) it is clear that the LMS algorithm can be implemented without squaring, averaging or differentiation and is elegant in its simplicity and efficiency. It requires $2N+1$ multiplications per iteration. However, its disadvantage is that it needs large data samples to guarantee convergence (i.e. slow convergence-rate) and it is sensitive to the input signal statistics. The LMS algorithm is summarized in Table 2.1.

Table 2.1 The LMS algorithm

<i>Initialization</i> $\mathbf{w}(0)=0.$, $0 < \mu < 2/\lambda_{\max}$	
<i>Algorithm</i>	<i>Complexity</i>
$e(n)=d(n)-\mathbf{w}^T(n)\mathbf{r}(n)$	N Mult.
For $n=1, 2, \dots$, do	
$\mathbf{w}(n+1) = \mathbf{w}(n) + 2\mu(n)e(n)$	(N+1) Mult.
<i>Total</i>	(2N+1) Mult.

Note that in complexity evaluation, only multiplications have been taken into account.

The excess MSE due to estimation noise (ξ_{ex}) of the LMS adaptive algorithm is given by [122] :

$$\xi_{\text{ex}} = \mu \text{tr}(\mathbf{R}) \xi_{\text{min}} \tag{2.31}$$

where $\text{tr}(\cdot)$ stands for trace of the matrix in the brackets and ξ_{\min} is the minimum value of the MSE. The misadjustment of the adaptive algorithm is defined as the ratio of the excess MSE to the minimum MSE, and is thus a measure of how closely the adaptive process tracks the true Wiener solution. Therefore, the misadjustment of the LMS algorithm is given by:

$$M = \frac{\xi_{ex}}{\xi_{\min}} = \mu \text{tr}(\mathbf{R}) \quad (2.32)$$

The efficiency of the LMS algorithm has been shown to approach the theoretical limit for adaptive algorithms, when the eigenvalues of the correlation matrix \mathbf{R} are equal or nearly equal. With disparate eigenvalues, however, the misadjustment is primarily determined by the fastest mode of adaptation, while the settling time is limited by the slowest mode [122].

2.3.1.2 The normalized LMS algorithm

In the LMS algorithm to adapt the weights vector $\mathbf{w}(n)$ in Eq.(2.30), a correction factor proportional to the input vector $\mathbf{r}(n)$ is directly applied. Therefore, when $\mathbf{r}(n)$ is large, the LMS algorithm experiences a gradient noise amplification [36]. To solve this problem and to ensure the stability of the algorithm, the normalized LMS algorithm is used, in which, the correction factor is normalized with respect to the instantaneous input power.

Therefore, the weights update equation is written as:

$$\mathbf{w}(n+1) = \mathbf{w}(n) + \frac{\tilde{\mu}}{\|\mathbf{r}(n)\|} e(n) \mathbf{r}(n) \quad (2.33)$$

where $\tilde{\mu}$ is the adaptation constant, which should satisfy the following relation to ensure convergence and stability: $0 < \tilde{\mu} < 2$, and $\|\mathbf{r}(n)\|$ is the norm of vector $\mathbf{r}(n)$ defined as $\mathbf{r}^T(n)\mathbf{r}(n)$. The NLMS algorithm is summarized in Table 2.2.

Table 2.2 The NLMS algorithm.

Initialization $\mathbf{w}(0)=0.$, $0 < \tilde{\mu} < 2$ (adaptation constant)	
Algorithm	Complexity
$E(n)=d(n)-\mathbf{w}^T(n)\mathbf{r}(n)$ For $n=1, 2, \dots$ do	N Mult.
$\mathbf{w}(n+1) = \mathbf{w}(n) + \frac{\tilde{\mu}}{\ \mathbf{r}(n)\ } e(n)\mathbf{r}(n)$	2N+1 Mult.
TOTAL	(3N+1) Mult.

2.3.1.3 Modified variable step-size LMS algorithm

To overcome the inherent limitations of the fixed step-size LMS algorithm, a time-varying step-size LMS algorithm may be employed. The algorithm is based on using large step-size values when the algorithm is far from the optimal solution, thus speeding up the convergence rate. On the other hand, when the algorithm is near optimum, small step-size is used to achieve a low level of residual MSE, thus improving the overall performance. The step-size adjustment follows some criterion that can provide an approximate measure of the adaptation state.

In this section, we introduce the Modified Variable Step-Size (MVSS) LMS algorithm proposed in [3] for the adaptation of DS-CDMA systems. In MVSS algorithm the step-size is adjusted according to the time-averaged estimate of the autocorrelation of $e(n)$ and $e(n-1)$. The weight update recursion follows Eq.(2.30). The step-size recursion update uses an estimate of the autocorrelation between $e(n)$ and $e(n-1)$ which is described as:

$$p(n) = p(n-1) + (1-\beta) e(n) e(n-1) \quad (2.34)$$

where $p(n)$ is introduced in the update since the autocorrelation is a good measure of the proximity to the optimum and also because it rejects the effect of the uncorrelated noise sequence on the step-size [3]. In the early stage of adaptation the error autocorrelation estimate $p^2(n)$ is large, resulting in a large step-size $\mu(n)$. As we approach the optimum, the error autocorrelation approaches zero, resulting in a smaller step-size. Therefore, this provides the fast convergence due to large initial value of $\mu(n)$ while maintaining low residual MSE due to the small final value of $\mu(n)$. The proposed step-size update given by [3] is:

$$\mu(n+1) = \alpha \mu(n) + \gamma p^2(n) \quad (2.35)$$

where $0 < \alpha < 1$, $\gamma > 0$ and $\mu(n+1)$ is set to μ_{\min} or μ_{\max} when it falls below or above these lower and upper bounds, respectively. The constant μ_{\max} is normally selected near the point of instability of the conventional LMS to provide the maximum possible convergence speed. The value of μ_{\min} is chosen as a compromise between the desired level of steady-state MSE and the required tracking capabilities of the algorithm. The parameter γ controls the convergence time as well as the level of residual MSE of the algorithm. The positive constant β is an exponential weighting factor. The choice of α , β and γ is important, and practically, their values are selected to provide the same MSE attained by the FSS-LMS algorithm while improving the convergence speed. The MVSS algorithm is summarized in Table 2.3, and it is clear that it involves two additional update equations as compared to the conventional LMS, thus, the added complexity is six multiplications per iteration.

To ensure the convergence of the weight vector mean, the value of the step-size should satisfy the:

$$0 < E[\mu(n)] < 2/\lambda_{\max} \quad (2.36)$$

Table 2.3 The MVSS-LMS algorithm.

<i>Initialization</i> $\mathbf{w}(0)=\mathbf{0}$.	
<i>Algorithm</i>	<i>Complexity</i>
For $n=1, 2, \dots$, do	
$e(n)=d(n)-\mathbf{w}^T(n)\mathbf{r}(n)$	N Mult.
$\mathbf{w}(n+1)=\mathbf{w}(n)+2\mu(n)\mathbf{r}(n)e(n)$	(N+1) Mult.
$p(n)=p(n-1)+(1-\beta)e(n)e(n-1)$	3 Mult.
$\mu(n+1)=\alpha\mu(n)+\gamma p^2(n)$	3 Mult.
<i>TOTAL</i>	(2N+7) Mult.

However, a sufficient condition that ensures convergence of the MSE is

$$0 < \frac{E[\mu^2(\infty)]}{E[\mu(\infty)]} < \frac{2}{3 \text{tr}(\mathbf{R})} \quad (2.37)$$

where $E[\mu(\infty)]$ and $E[\mu^2(\infty)]$ are the steady-state values of the $E[\mu(n)]$ and $E[\mu^2(n)]$ respectively. The misadjustment of the MVSS-LMS algorithm can be approximated by [3]:

$$M = \frac{\gamma \alpha \xi_{\min}^2 (1-\beta)}{(1-\alpha^2)(1+\beta)} \text{tr}(\mathbf{R}) \quad (2.38)$$

2.3.2 The Recursive Least Squares (RLS) algorithm

The method of least squares can be adopted recursively to update the filter weights by minimizing the exponentially weighted sum of squared errors defined as:

$$\begin{aligned} \epsilon(n) &= \sum_{i=1}^n \lambda^{n-i} e^2(n) \\ &= \sum_{i=1}^n \lambda^{n-i} [d_i(i) - \mathbf{w}^T(i)\mathbf{r}(i)]^2 \end{aligned} \quad (2.39)$$

where λ is the forgetting factor less than but close to unity. The inverse of $(1-\lambda)$ is a measure of the memory of the algorithm.

The optimum value of the weight vector for which the cost function $\epsilon(n)$ is minimized is given by the set of equations:

$$\mathbf{R}(n) \mathbf{w}_o(n) = \mathbf{P}(n) \quad (2.40)$$

where $\mathbf{R}(n)$ is an N-by-N correlation matrix defined by:

$$\mathbf{R}(n) = \sum_{i=1}^n \lambda^{n-i} \mathbf{r}(i) \mathbf{r}^T(i) \quad (2.41)$$

and $\mathbf{P}(n)$ is the crosscorrelation vector defined by

$$\mathbf{P}(n) = \sum_{i=1}^n \lambda^{n-i} \mathbf{r}(i) d_1(i) \quad (2.42)$$

The solution of Eq.(2.40) requires $O[N^3]$ computations at each iteration. This can be reduced to $O[N^2]$ by using a recursive approach to compute $\mathbf{R}^{-1}(n)$ rather than computing the inverse of $\mathbf{R}(n)$ at each iteration.

The correlation matrix $\mathbf{R}(n)$ and the crosscorrelation vector $\mathbf{P}(n)$ can be recursively updated as:

$$\mathbf{R}(n) = \lambda \mathbf{R}(n-1) + \mathbf{r}(n) \mathbf{r}^T(n) \quad (2.43)$$

and

$$\mathbf{P}(n) = \lambda \mathbf{P}(n-1) + \mathbf{r}(n) d_1(n) \quad (2.44)$$

Applying the matrix inversion lemma [36] to Eq.(2.43) enables the computation of $\mathbf{R}^{-1}(n)$ as follows:

$$\mathbf{R}^{-1}(n) = \lambda^{-1} \mathbf{R}^{-1}(n-1) - \lambda^{-1} \mathbf{k}(n) \mathbf{r}^T(n) \mathbf{R}^{-1}(n-1) \quad (2.45)$$

which is the Riccati equation for RLS, where:

$$\mathbf{k}(n) = \frac{\lambda^{-1} \mathbf{R}^{-1}(n-1) \mathbf{r}(n)}{1 + \lambda^{-1} \mathbf{r}^T(n) \mathbf{R}^{-1}(n-1) \mathbf{r}(n)} \quad (2.46)$$

is known as the Kalman gain vector. By rearranging Eq.(2.46) the Kalman gain vector can be written as:

$$\begin{aligned}\mathbf{k}(n) &= [\lambda^{-1} \mathbf{R}^{-1}(n-1) - \lambda^{-1} \mathbf{k}(n) \mathbf{r}^T(n) \mathbf{R}^{-1}(n-1)] \mathbf{r}(n) \\ &= \mathbf{R}^{-1}(n) \mathbf{r}(n)\end{aligned}\tag{2.47}$$

The recursive equation for updating the weight vector in accordance with the least-square error criterion can be shown to be [36]:

$$\mathbf{w}(n) = \mathbf{w}(n-1) + \mathbf{k}(n) \varepsilon(n)\tag{2.48}$$

where $\varepsilon(n)$ is the a priori estimation error defined by:

$$\varepsilon(n) = d_1(n) - \mathbf{w}^T(n-1) \mathbf{r}(n)\tag{2.49}$$

The excess MSE due to estimation noise is given by [21]:

$$\xi_{\text{ex}} = \frac{1 - \lambda}{1 + \lambda} N \xi_{\text{min}}\tag{2.50}$$

The misadjustment will be

$$M = \frac{1 - \lambda}{1 + \lambda} N\tag{2.51}$$

The RLS algorithm is summarized in Table 2.4.

An important feature of the RLS algorithm is that the tap-weight vector changes with time by an amount proportional to the Kalman gain vector $\mathbf{k}(n)$, and each tap-weight in effect is controlled by one of the elements of $\mathbf{k}(n)$. Correspondingly, the rapid convergence is achieved. The convergence speed of the RLS algorithm is much superior to that of LMS algorithm, but at the expense of a large increase in the computational complexity, $O[N^2]$ per iteration, in contrast to LMS algorithm in which $O[N]$ computations per iteration are required.

It has been shown that the RLS algorithm attains the optimum solution in just N iterations if the uncorrelated thermal noise is small. Moreover, the solution is less sensitive to the eigenvalue disparity in the input autocorrelation matrix than the LMS solution.

Table 2.4 The RLS algorithm

<i>Initialization</i> $\mathbf{P}(0)=\mathbf{I}/\delta$ (δ is small positive constant), $\mathbf{w}(0)=\mathbf{0}$.	
<i>Algorithm</i>	<i>Complexity</i>
For $n=1, 2, \dots$ do	
$\mathbf{k}(n) = \frac{\lambda^{-1} \mathbf{R}^{-1}(n-1) \mathbf{r}(n)}{1 + \lambda^{-1} \mathbf{r}^T(n) \mathbf{R}^{-1}(n-1) \mathbf{r}(n)}$	$2N^2 + N$ Mult. N Div.
$\varepsilon(n) = d_1(n) - \mathbf{w}^T(n-1) \mathbf{r}(n)$	N Mult.
$\mathbf{w}(n) = \mathbf{w}(n-1) + \mathbf{k}(n) \varepsilon(n)$	N Mult.
$\mathbf{R}^{-1}(n) = \lambda^{-1} \mathbf{R}^{-1}(n-1) - \lambda^{-1} \mathbf{k}(n) \mathbf{r}^T(n) \mathbf{R}^{-1}(n-1)$	N^2 Mult.
<i>TOTAL</i>	$(3N^2 + 3N)$ Mult. $+ N$ Div.

2.3.3 The block adaptation algorithm

As has been stated earlier, the LMS algorithm allows simple implementation and requires $O[N]$ operations per iteration, but suffers from slow convergence. The RLS algorithm, on the other hand, has much faster convergence rate as compared to LMS, but requires more computations per iteration. In this section, we present the implementation of a modified version of the block algorithm introduced in [81], which links NLMS and block RLS [BRLS] algorithms, for the demodulation of DS-CDMA signals. This algorithm allows a trade-off between arithmetic complexity and convergence rate.

The implemented algorithm processes blocks of data each of size L bits. Let the contents of the TDL filter at the interval $(n-1)T \leq t \leq nT$ be defined as $\mathbf{r}(n) = [r_0(n), r_1(n), \dots, r_{N-1}(n)]^T$. Also, define $\mathbf{X}(n) = [\mathbf{r}(n-L+1), \dots, \mathbf{r}(n-1), \mathbf{r}(n)]$ with N -by- L dimension as the input data matrix constructed from the last L input vectors to the TDL, $\mathbf{w}(n) = [w_0(n), w_1(n), \dots, w_{(N-1)}(n)]^T$ as the TDL filter weights at interval n which is assumed to be fixed during

a block interval and $\mathbf{D}(n)=[d_{n-L+1}, \dots, d_{n-1}, d_n]^T$ as the vector of last L data bits of the desired signal. The adaptation algorithm for a block size of L data bits, and filter of length N is given by [81]:

$$\mathbf{w}(n+1) = \mathbf{w}(n-L+1) + \mathbf{X}(n) \mathbf{E}^\mu(n) \quad (2.52)$$

$$\mathbf{E}^f(n) = \mathbf{D}(n) - \mathbf{X}^T(n) \mathbf{w}(n-L+1) \quad (2.53)$$

$$\mathbf{E}^\mu(n) = [\mathbf{X}^T(n) \mathbf{X}(n)]^{-1} \mathbf{E}^f(n) \quad (2.54)$$

where: $\mathbf{E}^f(n)$ is the error vector resulting from filtering the input sequence by the previous set of coefficients $\mathbf{w}(n-L+1)$ (or is the a priori error vector), and $\mathbf{E}^\mu(n)$ is the vector of the N last weighted errors. This algorithm is easily seen to reduce to an NLMS algorithm (if $L=1$), and to a BRLS algorithm (if $L=N$). To ensure the stability of the algorithm the adaptation gain factor μ_b (step size) in the weights update equation ($0 < \mu_b < 1$) is used, thus:

$$\mathbf{w}(n+1) = \mathbf{w}(n-L+1) + \mu_b \mathbf{X}(n) \mathbf{E}^\mu(n) \quad (2.55)$$

It is clear from the above algorithm that the filter weights are updated only once per each block. However, it requires the inversion of the system matrix $\mathbf{G}(n) = \mathbf{X}^T(n) \mathbf{X}(n)$. This matrix is symmetrical but not Toeplitz, since in this case the TDL filter contents come as block of samples (and not sample by sample), i.e., the shifting property of the input samples does not occur (in contrast with [81]). Therefore, the Levinson algorithm, with complexity of $O(N^2)$, is not applicable in this case.

The QR decomposition has been used, to find the inverse of the system matrix $\mathbf{G}(n)$, due to its numerical stability and lower sensitivity to round off errors compared to direct matrix inversion algorithms [30]. The system matrix $\mathbf{G}(n)$ is factorized as $\mathbf{G}(n) = \mathbf{Q}\mathbf{R}$ where \mathbf{R} is an invertible upper triangular matrix, while \mathbf{Q} is orthogonal matrix, that is $\mathbf{Q}^T \mathbf{Q} = \mathbf{I}$ (where \mathbf{I} is the identity matrix). The decomposition is constructed by applying successive Householder

transformations to annihilate successive columns of $\mathbf{G}(n)$ below the diagonal. Using $\mathbf{G}(n)=\mathbf{QR}$, it is easy to find the inverse of $\mathbf{G}(n)$ by solving the equations:

$$\mathbf{G}(n)\mathbf{S}_k=\mathbf{B}_k \quad k=1, 2, \dots, L \quad (2.56)$$

$$\text{or } \mathbf{S}_k=\mathbf{G}^{-1}(n)\mathbf{B}_k = \mathbf{R}^{-1} \mathbf{Q}^T \mathbf{B}_k$$

where \mathbf{S}_k is the k th column vector of $\mathbf{G}^{-1}(n)$, while \mathbf{B}_k is the k th column vector of the identity matrix \mathbf{I} . Hence, the computation of \mathbf{S}_k requires only the computation of the matrix-vector product, $\mathbf{Q}^T \mathbf{B}_k$, followed by back substitution in the triangular system $\mathbf{RS}_k=\mathbf{Q}^T \mathbf{B}_k$.

Therefore, by using QRD and back substitution it is straightforward to find the inverse of the matrix $\mathbf{G}(n)$ column by column.

The total MSE for a block of size L is defined by, using the estimation error vector $\mathbf{E}^f(n)$, [81]:

$$\xi_{\text{block}}^l = E[\|\mathbf{E}^f(n)\|^2] \quad (2.57)$$

which can be approximated as follows:

$$\begin{aligned} \xi_{\text{block}}^l &\approx L \sigma^2 + \mu^2 \sigma^2 \text{tr}[\mathbf{X}^T(n) \mathbf{X}(n-L) \{\mathbf{X}^T(n-L) \mathbf{X}(n-L)\}^{-1} \cdot \{\mathbf{X}^T(n-L) \mathbf{X}(n-L)\}^{-1} \mathbf{X}^T(n-L) \mathbf{X}(n)] \\ &= L \sigma^2 + \xi_n^{\text{ex}} \end{aligned} \quad (2.58)$$

i.e. the total MSE error approaches a final value equal to $L \sigma^2$ plus excess MSE (ξ_n^{ex}). To decrease the excess MSE, the adaptation gain constant (μ_b) may be decreased, however this results in slower convergence. This is the same tradeoff as in NLMS algorithm.

The block algorithm and its computational complexity, measured in terms of the number of multiplications required per output point, is summarized in Table 2.5.

The MVSS algorithm discussed in section 2.3.1.3 can be implemented for the block algorithm using the following modifications for the update equations:

$$\mathbf{p}(n) = \mathbf{p}(n-1) + (1-\beta) [\mathbf{E}^f(n)]^T \mathbf{E}^f(n-1) \quad (2.59)$$

and the step-size $\mu_b(n)$ can be updated using Eq.(2.35). The MVSS-block algorithm is summarized in Table 2.6.

Table 2.5 The block algorithm.

<i>Initialization</i> $\mathbf{w}(0) = \mathbf{0}$., $0 < \mu_b < 1$	
<i>Algorithm</i>	<i>Complexity</i> (per bit)
For $n=1, 2, \dots$ do $\mathbf{E}^f(n) = \mathbf{D}(n) - \mathbf{X}^T(n) \mathbf{w}(n-L+1)$ $\mathbf{G}(n) = \mathbf{X}^T(n) \mathbf{X}(n)$ $\mathbf{E}^\mu(n) = \mathbf{G}(n)^{-1} \mathbf{E}^f(n)$ $\mathbf{w}(n+1) = \mathbf{w}(n-L+1) + \mu_b \mathbf{X}(n) \mathbf{E}^\mu(n)$	N Mult. $N(L+1)/2$ Mult. $(4/3)L^2 + N$ Mult. $(N+1)$ Mult.
TOTAL	$(2N+1) + N(L+1)/2 + 4/3 L^2 + N$ Mult.

Table 2.6 The MVSS-block algorithm.

<i>Initialization</i> $\mathbf{w}(0) = \mathbf{0}$., $0 < \mu_b < 1$	
<i>Algorithm</i>	<i>Complexity</i> (per bit)
For $n=1, 2, \dots$ do $\mathbf{E}^f(n) = \mathbf{D}(n) - \mathbf{X}^T(n) \mathbf{w}(n-L+1)$ $\mathbf{G}(n) = \mathbf{X}^T(n) \mathbf{X}(n)$ $\mathbf{E}^\mu(n) = \mathbf{G}(n)^{-1} \mathbf{E}^f(n)$ $\mathbf{w}(n+1) = \mathbf{w}(n-L+1) + \mu_b(n) \mathbf{X}(n) \mathbf{E}^\mu(n)$ $p(n) = P(n-1) + (1-\beta) [\mathbf{E}^f(n)]^T \mathbf{E}^f(n-1)$ $\mu_b(n+1) = \alpha \mu_b(n) + \gamma p^2(n)$	N Mult. $N(L+1)/2$ Mult. $(4/3)L^2 + N$ Mult. $(N+1)$ Mult. $(L+1)/L$ Mult. $3/L$ Mult.
TOTAL	$(2N+1) + N(L+1)/2 + 4/3 L^2 + N + (L+4)/L$ Mult.

Table 2.7 lists the number of multiplications required per output point using the LMS, RLS [35] and the implemented block algorithm for different filter lengths and block sizes. It is clear that the implemented block algorithm requires much lower number of multiplications than that of the RLS algorithm.

Table 2.7 Comparison of the computational complexity per output point for the LMS, RLS and the block algorithms.

Filter Length (N)	LMS			RLS		Block Length (L)	Block	MVSS Block
	FSS	NLMS	MVSS	Mult.	Div.		Mult.	Mult.
	Mult.	Mult.	Mult.					
31	63	94	69	2976	31	4	193	141
						8	319	321
63	127	190	133	12096	63	8	559	561
127	255	382	261	48768	127	16	1802	1083
255	511	766	517	195840	255	32	6339	6340

2.4 Performance measures

The main performance measure of the multiuser detection receiver for DS-CDMA systems is the bit error rate. Using Gaussian approximation for the interference and noise in the received signal, the analytical (theoretical) probability of bit error for the receiver is given by [74]:

$$P_e = Q\left(\frac{1}{\sqrt{\xi_{\min}}}\right) \quad (2.60)$$

where:

$$Q(x) = \frac{1}{\sqrt{2\pi}} \int_x^{\infty} \exp\left(-\frac{t^2}{2}\right) dt \quad (2.61)$$

and

$$\xi_{\min} = 1 - \mathbf{c}_1^T \mathbf{R}^{-1}(n) \mathbf{c}_1 \quad (2.62)$$

where \mathbf{c}_1 is the spreading sequence of the desired user.

Bounds for the probability of error performance are generally used, namely, single-user (lower) bound and matched filter (upper) bound. The single-user probability of error bound is evaluated using only the thermal noise in the calculations, i.e.,

$$Pe^{SU} = Q\left(\frac{1}{\sqrt{\sigma^2}}\right) \quad (2.63)$$

On the other hand, to calculate the matched filter probability of error (upper) bound, the interference from other users is considered as Gaussian noise and will be added directly to the thermal noise, thus the probability of error is evaluated as follows:

$$Pe^{MF} = \left(\frac{1}{\sqrt{\sigma^2 + MAI_{MF}}}\right) \quad (2.64)$$

The MAI_{MF} has been calculated in this work by correlating the spreading sequence of the desired user \mathbf{c}_1 with the received signal $\mathbf{r}(n)$ and then taking the average over hundred independent trials.

In cases where interference cannot be modeled as Gaussian noise, then the probability of error performance is generally obtained by simulation. However, for large values of the input SNR, it would be difficult to obtain respective bit error rates using simulation. In such cases, the performance of adaptive receivers is typically measured by the output signal MSE as a function of the input SNR. Since the output SNR directly depends on the MSE and is closely related to the bit error rate, the results can also be presented in the form of the output SNR as a function of the input SNR. The input signal to noise ratio (SNR_{in}) is defined as:

$$SNR_{in} = 10 \log_{10} \frac{\sigma_d^2}{\sigma^2} \quad (2.65)$$

where σ^2 is the AWGN variance and σ_d^2 is the power of the desired user symbol (equal to 1). The output signal to noise ratio (SNR_{out}) is defined by:

$$\text{SNR}_{\text{out}} = 10 \log_{10} \frac{\sigma_d^2}{\xi_{\min}} \quad (2.66)$$

where ξ_{\min} is the minimum MSE.

The number of users, i.e. the capacity, which an adaptive DS-CDMA system can support, is limited by the residual MSE [97]. As the number of users increases the residual MSE increases, resulting in degradation of the bit-error rate (BER) performance. The limit of the MSE is defined in terms of the acceptable probability of error for a fixed number of users. The capacity of the DS-CDMA receiver is thus determined by plotting the output SNR as a function of the number of users with the input SNR as a parameter, and can be determined in terms of the number of users which will provide the acceptable output SNR at a certain value of the input SNR.

The rate of convergence of the adaptive DS-CDMA receiver is measured in terms of the number of bits required to achieve the steady-state residual MSE error. It may be noted that when the convergence occurs, the TDL filter weights will approach the optimal weights [$\mathbf{w}_o = \mathbf{R}^{-1}(n) \mathbf{P}(n)$]. The computational complexity of the various detectors can be quantified by their time complexity per bit (TCB). The TCB is defined as the number of operations required for demodulating one data bit.

Two additional performance measures related to the asymptotic behavior of the MMSE receiver are the asymptotic efficiency and the near-far resistance [116, 118]. The efficiency is defined as the ratio between the effective and actual energies $E_k^f(\sigma)/E_k^c$ (where E_k^c is the energy of the k th bit). It quantifies the performance loss due to existence of other users in the

channel. The asymptotic efficiency is defined as the ratio between the SNR required to achieve the same unloaded bit rate in the absence of interfering users and the actual SNR:

$$\eta_k = \sup \left\{ 0 \leq r \leq 1; \lim_{\sigma \rightarrow 0} [\text{Pe}(\sigma) / Q(\sqrt{rE_k^c} / \sigma)] < \infty \right\} \quad (2.67)$$

The near-far resistance is the minimum asymptotic efficiency over relative energies of all the users:

$$\bar{\eta}_k = \inf_{E_k^c > 0} \eta_k \quad (j \neq 0) \quad (2.68)$$

In this case, to show the near-far resistance of the adaptive receivers, the probability of error for the desired user has been plotted for various levels of MAI.

2.5 Simulation results and discussion

In order to provide a basis for comparing the various adaptive algorithms discussed in this chapter, extensive simulation results are presented. In all simulation results, an asynchronous system is assumed, in which the delays, τ_k , of interferers are chosen from a uniform distribution. However, without loss of generality, it is assumed that the receiver is synchronized with the desired user (user number one). The receiver does not require the knowledge of the spreading sequence for the desired user; however, it requires the knowledge of training sequence in the training mode, before switching to the decision-directed mode. The performance of the previously mentioned adaptive algorithms is studied under various situations. Different types of spreading sequences have been used and the number of users and their power levels has also been varied. AWGN channel is assumed with different values of SNR. The TDL filter length is assumed fixed at $N=31$, unless stated otherwise. Ensemble averaging over 100 independent trials is performed when the convergence characteristics are evaluated.

Example 2.1

In this example the performance of the block adaptation algorithm in DS-CDMA receiver is examined using different values of block length and step-size. The simulated receiver consists of four interferers each having a 10dB power advantage over the desired user with input SNR=20 dB, and the filter length is set to $N=31$ taps.

Fig.2.4a shows the convergence characteristics of the block algorithm with block length $L=4$ for different values of step-size (μ_b) (in the range $0 < \mu_b < 1$). It is noticed that fast convergence but with high residual MSE is obtained when $\mu_b=0.99$, while slow convergence with low residual MSE is achieved when $\mu_b=0.05$. Therefore, it is concluded that by changing the step-size either faster convergence (when μ_b is large) or a lower residual MSE error (when μ_b is small) is obtained. Fig.2.4b&c show the effect of changing the block length (L) on the convergence characteristics of the adaptive DS-CDMA receiver using the block algorithm. Different values of the block length are used while the step-size is fixed at $\mu_b=0.4$. It is clear that faster convergence occur when $L=4$ and $L=8$. However, it is preferred to use $L=4$ since it requires lower computational complexity (table 2.7), and it possesses lower residual MSE with small delay. Therefore, it is concluded that this algorithm performs better using moderate block lengths, such that a faster convergence rate will be achieved with low computational complexity and small delay.

Example 2.2

In this example, an asynchronous MMSE DS-CDMA receiver (based on LMS, block and RLS adaptive algorithms) has been simulated having a desired user with variable number of interferers. Each interferer has 10 dB power advantage over the desired user with input SNR=20dB.

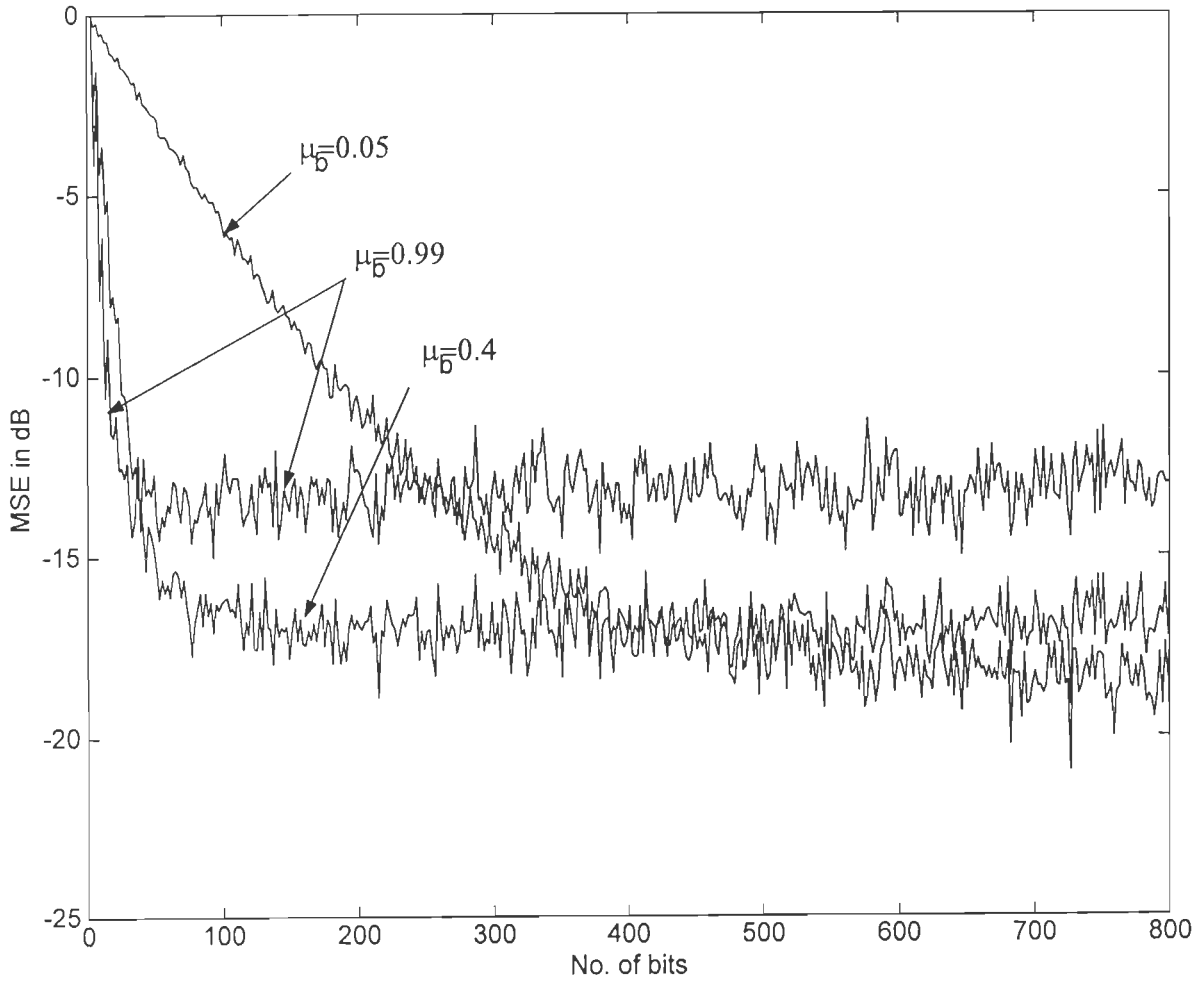


Fig.2.4a Convergence characteristics of the adaptive DS-CDMA receiver using the block algorithm with 4 interferers (each interferer has 10dB power advantage over the desired user), for different values of step size (μ_b).

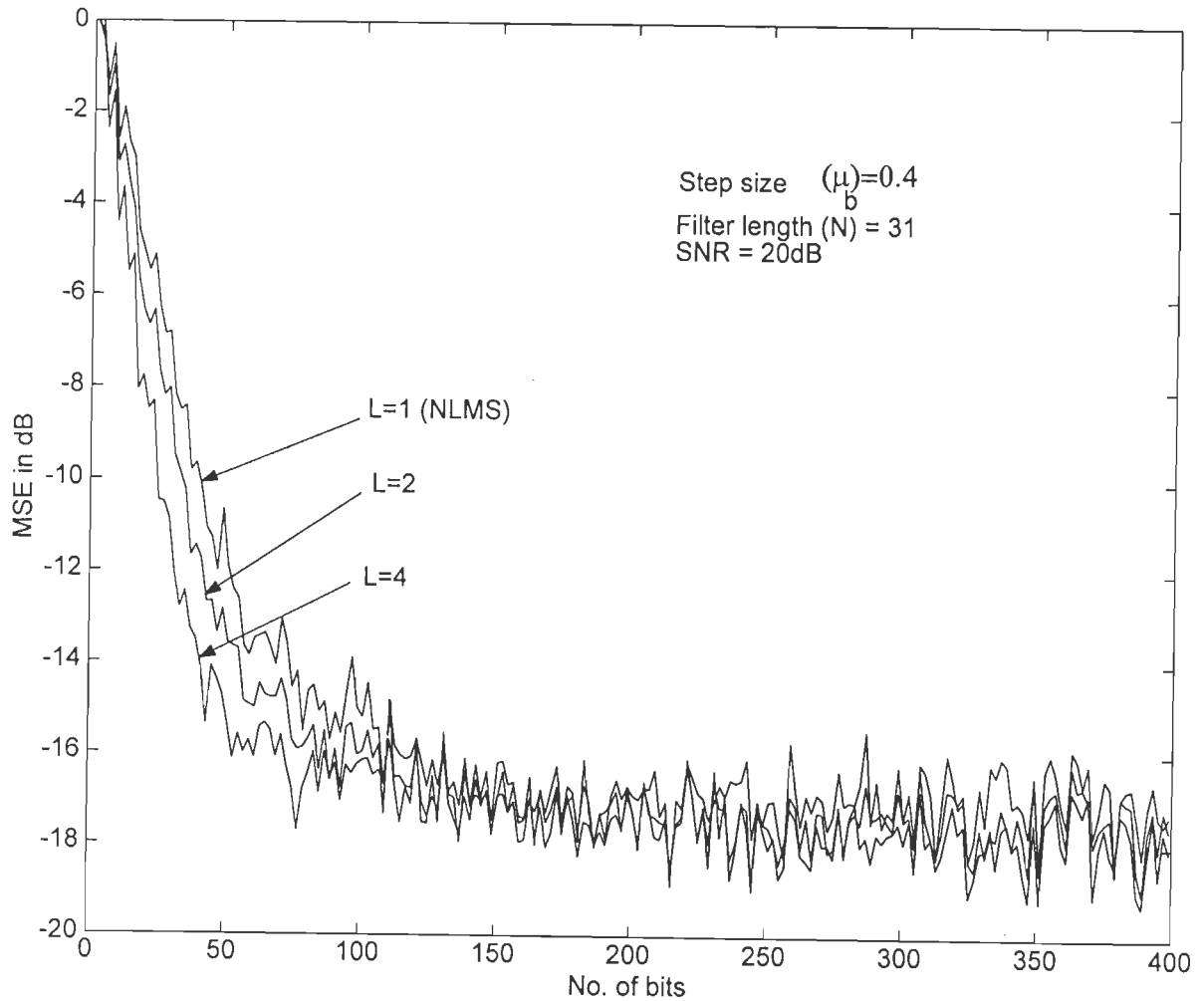
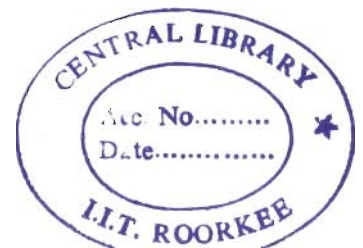


Fig.2.4.b Convergence characteristics of the adaptive DS-CDMA receiver using the block algorithm, with 4 interferers (each interferer has 10dB power advantage over the desired user) for different values of block length (L).

G10615



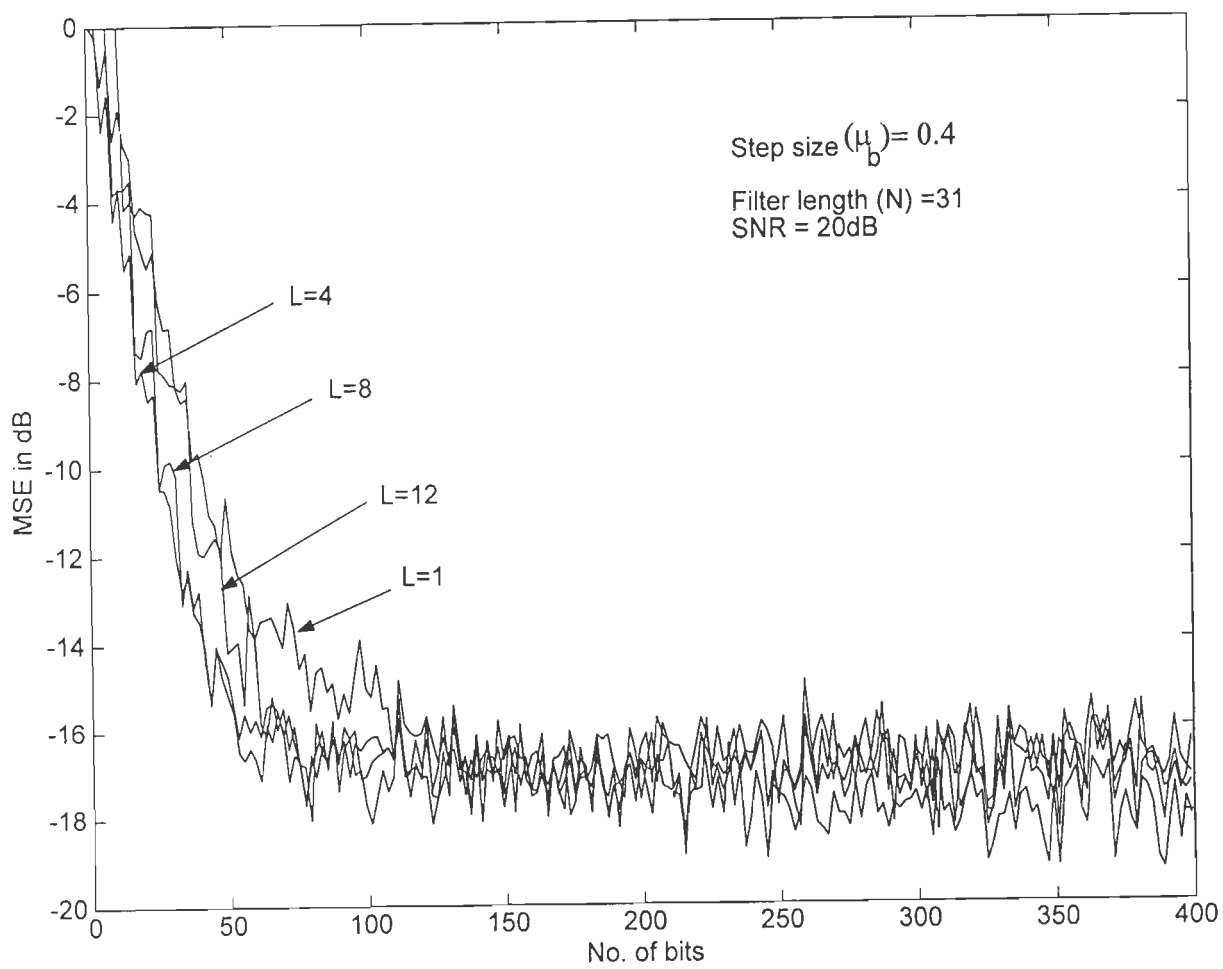


Fig.2.4.c

Fig.2.5a shows the convergence characteristics, i.e. the residual MSE as a function of the number of adaptation bits, using the LMS algorithm with step-size $\mu=0.0002$. From inspection of this figure, we infer that as the number of interferers increase the convergence rate becomes slower and the residual MSE increases. For example, for a single-user (no MAI) case, the receiver converges within 250 bits to a residual MSE of -20dB , while for the four interferers case, the receiver converges within 500 bits to about -16dB residual MSE. Fig.2.5b shows the convergence characteristics for the adaptive DS-CDMA receiver based on the block adaptive algorithm with $L=4$ and $\mu=0.4$. It is clear that when the number of interferers increases the residual MSE will increase and the convergence will be slower. For example, for a single-user case, the receiver converges within about 40 bits to about a -19dB residual MSE, while for the four interferers case, the receiver converges in about 80 bits to about -17 dB residual MSE. Fig.2.5c shows the convergence characteristics for the adaptive DS-CDMA receiver based on the RLS adaptive algorithm. It is clear that when the number of interferers increases the convergence rate and the residual MSE will increase slightly. For example, for a single-user case, the receiver converges within 40 bits to about a -20dB residual MSE, while for the four interferers case, the receiver converges within 80 bits to nearly -19dB residual MSE.

A comparison between the previous three figures shows that as the number of interferers increases, the convergence will be slower and the residual MSE will be larger. However, increasing the number of interferers will have less influence on the convergence rate and residual MSE using the RLS algorithm as compared with the LMS algorithm. It may be noticed that the block algorithm performs better than the LMS algorithm in terms of the convergence speed and residual MSE.

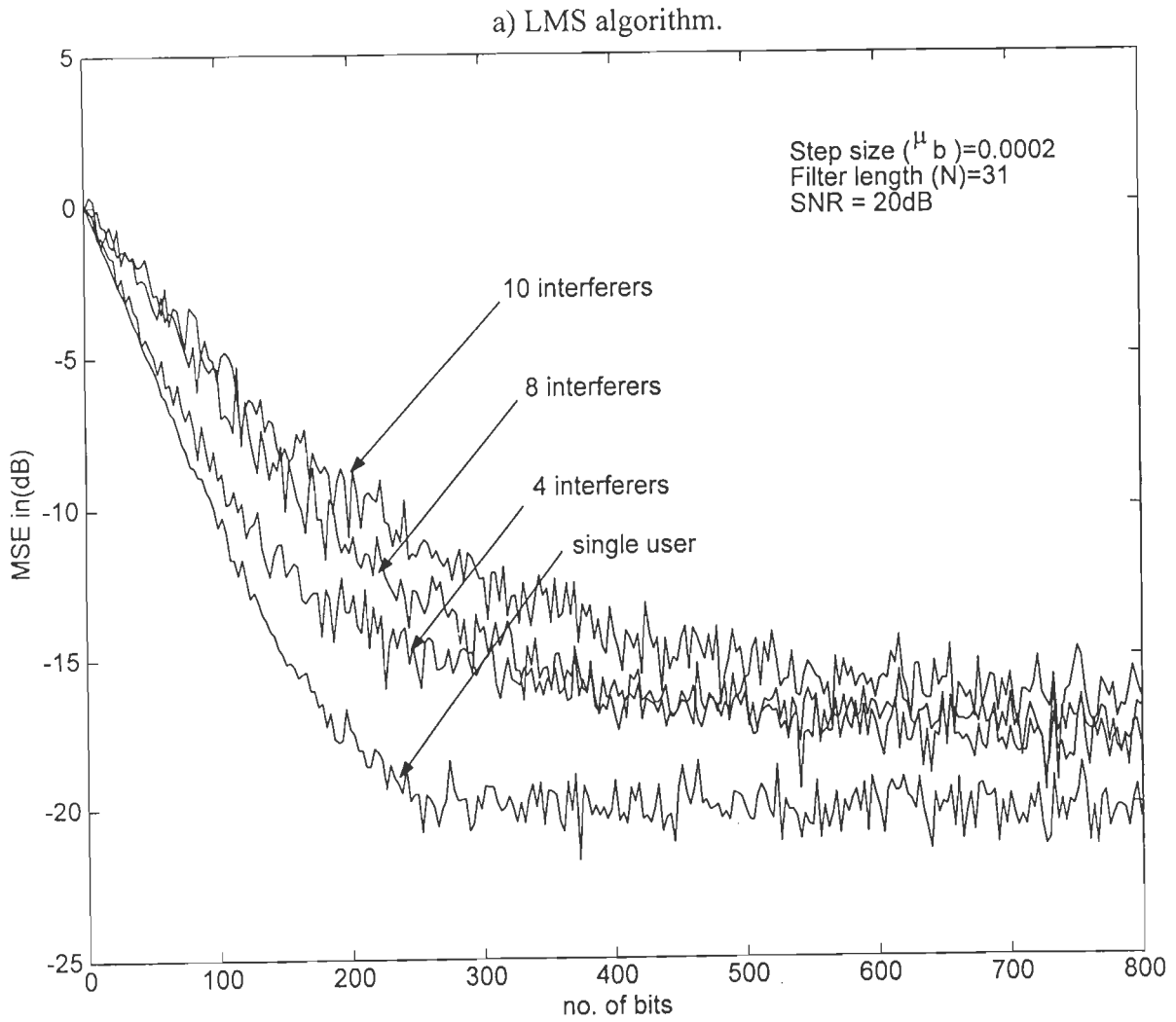


Fig.2.5 Convergence characteristics of the adaptive DS-CDMA receiver with different number of interferers (each having 10dB power advantage over the desired user) for a) LMS b)block c) RLS algorithms.

b) Block algorithm.

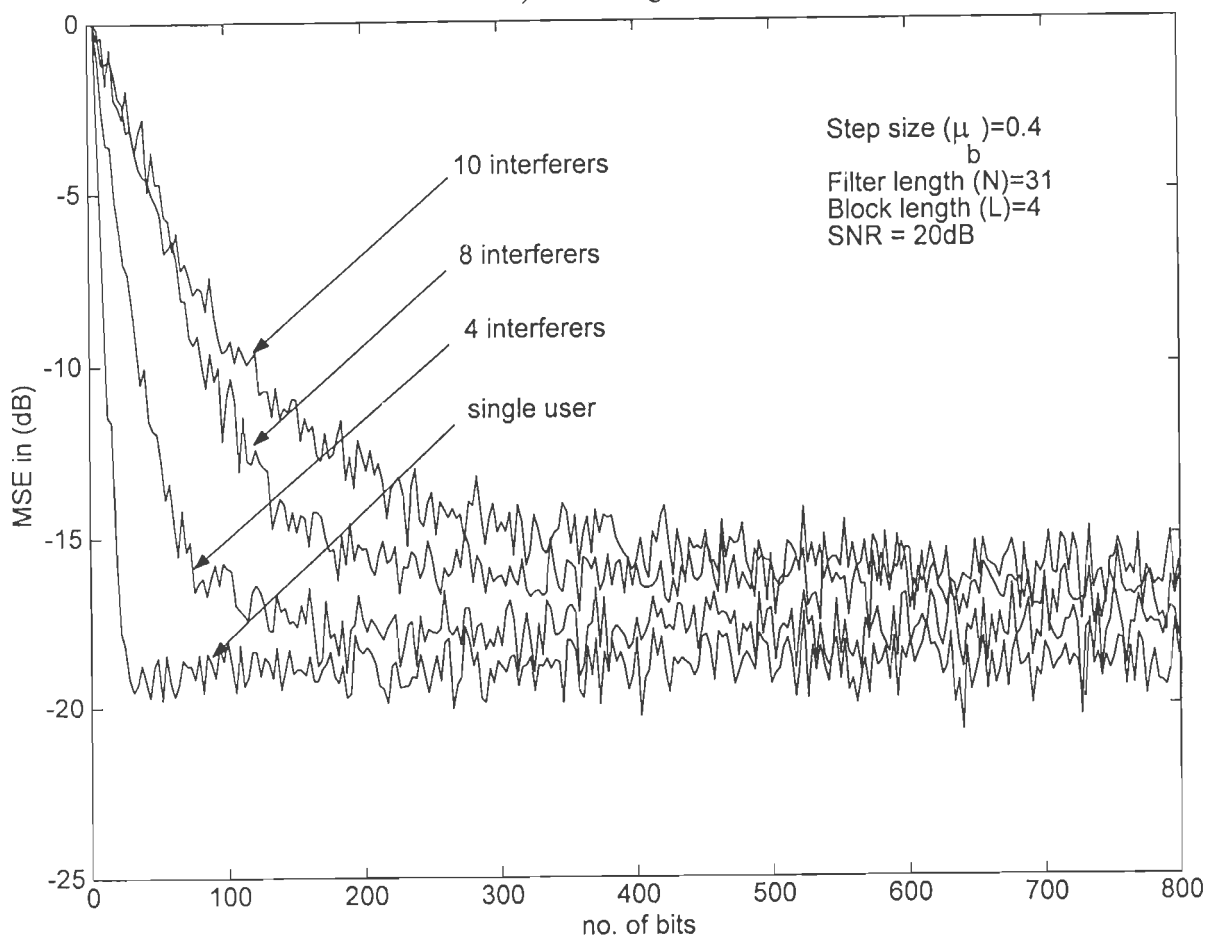


Fig.2.5b

c) RLS algorithm.

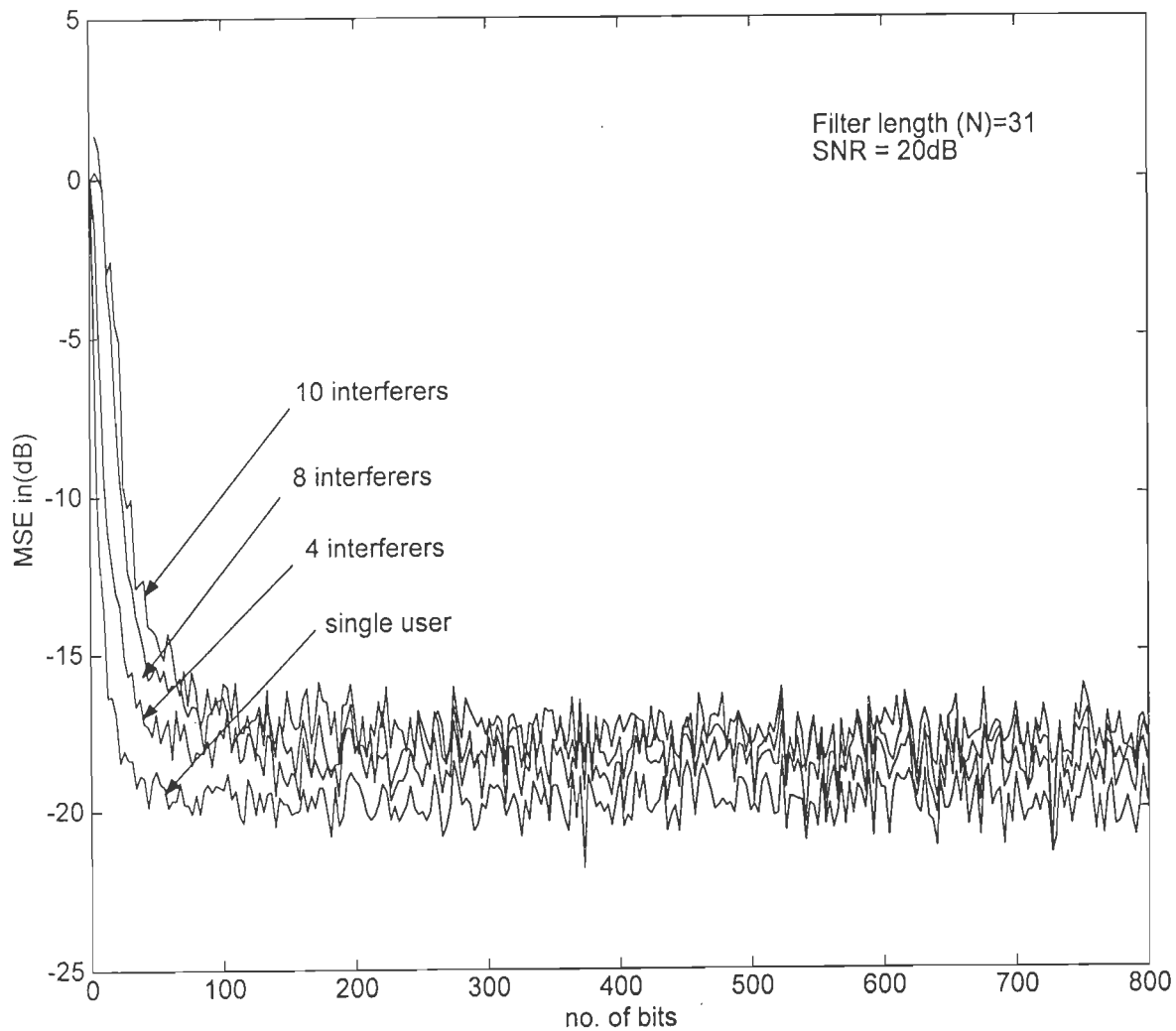


Fig.2.5c

Example 2.3

In this example, RLS, NLMS and the block adaptive algorithms are used to adapt the weights vector of the DS-CDMA receiver and for comparison the MVSS method for both LMS and block algorithms have been used. Four and eight interferers have been considered, where each interferer has a 10dB power advantage over the desired user, and the input SNR has been assumed to be equal to 20dB. The block length is chosen to be $L=4$. The step-size of both the NLMS and the block algorithm has been tuned such that, in all the cases, the residual MSE will approximately be the same, and, hence a fair comparison will be achieved.

It is clear from Fig.2.6 that the block algorithm provides a much faster convergence as compared to NLMS algorithm but is slightly slower than that of the RLS algorithm. Also, it may be noted that the variable step-size (VSS) algorithms perform much better than that of the fixed step-size (FSS) algorithms for both LMS and block algorithms. For example, for the 4-interferers case, the NLMS algorithm converges in about 500 bits compared to about 50 bits for the RLS algorithm and about 80 bits for the block algorithm. For 8-interferers case, the NLMS algorithm converges in about 600 bits compared to about 75 bits for the RLS algorithm and about 180 bits for the block algorithm. It is also noticed that the use of the MVSS algorithm will fasten the convergence rate for both the LMS and block algorithms, while maintaining the residual MSE at the same value. It is concluded that the block algorithm provides a much faster convergence rate as compared to NLMS algorithm, but its convergence is slightly slower than that of the RLS algorithm. Moreover, the computational complexity of the modified block algorithm is much lower than that of the RLS algorithm (Table 2.7).

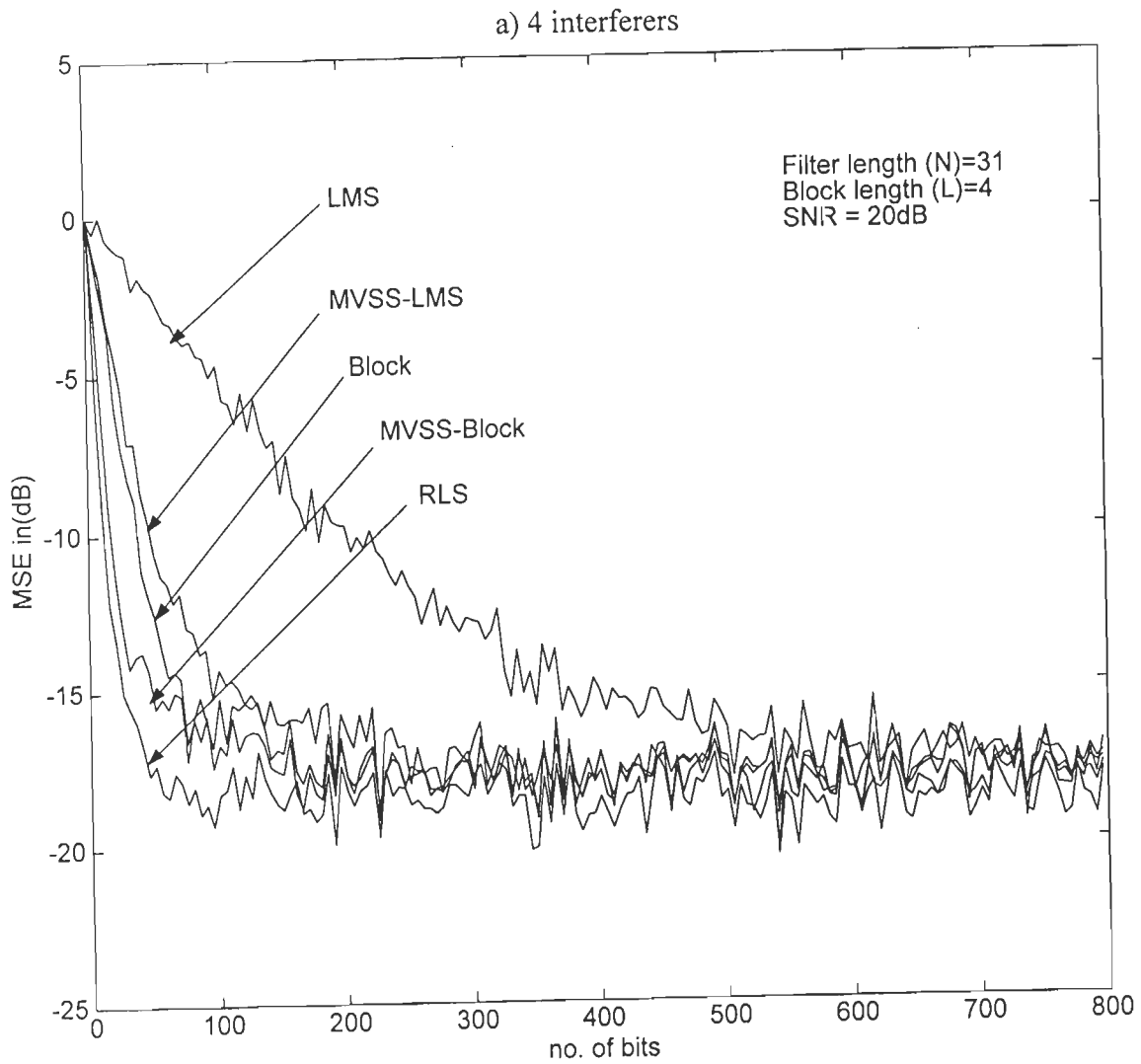


Fig.2.6 Comparison of the convergence characteristics for the adaptive DS-CDMA receiver using NLMS, RLS, block, MVSS-LMS and MVSS-block algorithms with a) 4 interferers b) 8 interferers (each interferer has 10dB power advantage over the desired user).

b) 8 interferers.

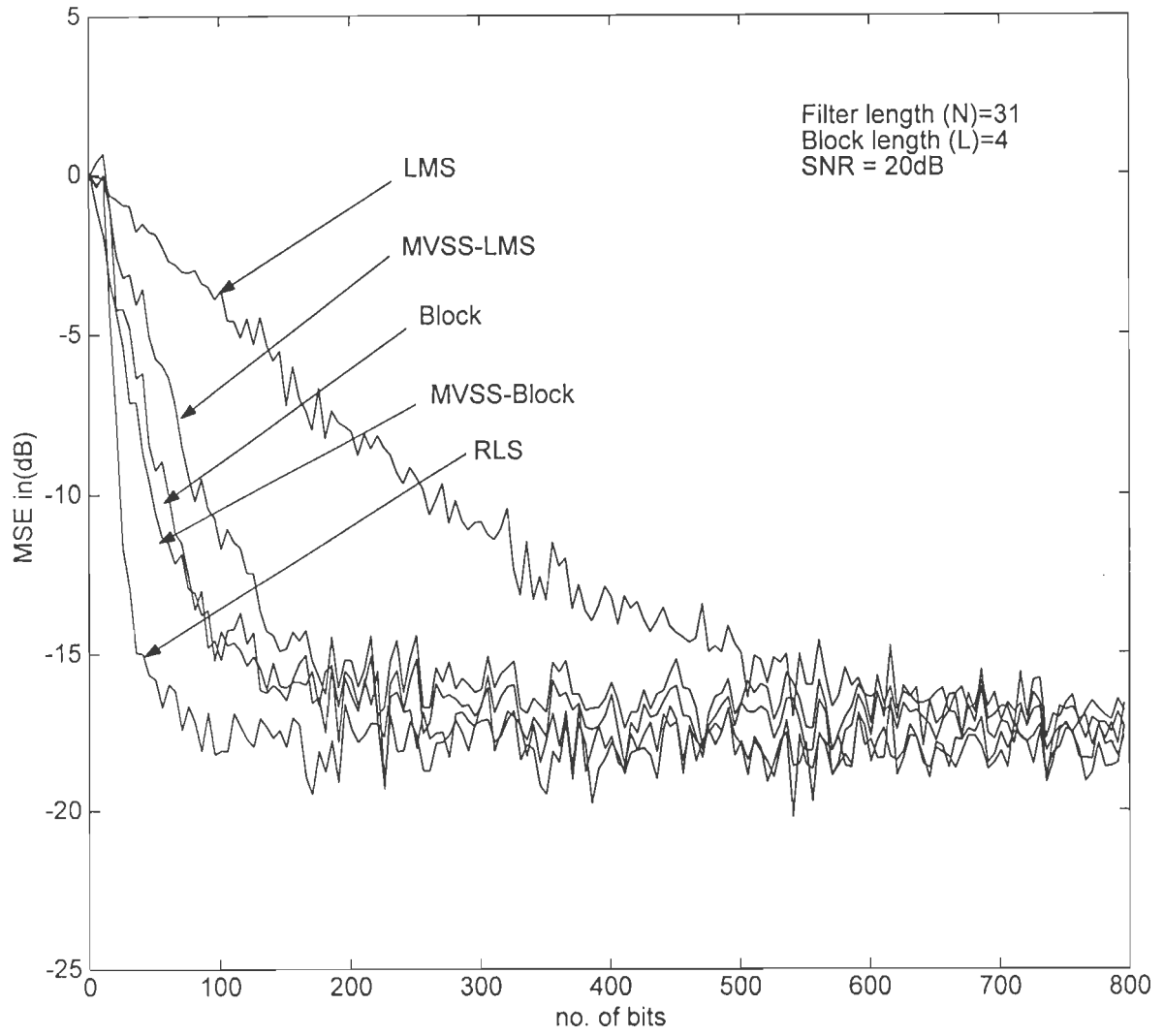


Fig.2.6b

Example 2.4

In this example, an asynchronous DS-CDMA receiver has been simulated with four interferers each having a 10 dB power advantage over the desired user at 20dB input SNR. The effect of changing the type of the spreading sequence has been studied. Fig.2.7 shows the convergence characteristics of the adaptive DS-CDMA receiver using three different types of spreading sequences of length 31, viz., Gold [31], PN and random sequences using NLMS, RLS and block algorithms. It is quite clear that the type of the spreading sequence only mildly affect the convergence characteristics, when using RLS and block algorithms. However, Fig.2.7 shows that for the NLMS algorithm some performance degradation occurs when using random and PN sequences as compared to Gold sequence. Also it is noticed that the PN sequence provides improved performance as compared to that of the random sequence.

The maximum number of users in a CDMA system is equal to the spreading gain. However, due to the limited number of combinations in the Gold and PN sequences, random sequences are used whenever the number of users is comparatively high.

Example 2.5

In this example, simulation of a sudden access (birth) of interferers in the DS-CDMA receiver is performed. The system initially starts with 4-interferers each having 10-dB power advantage over the desired user, then after the end of the training phase, a new interferer enters the system after every 1000 bits up to a maximum of ten users. Fig.2.8 shows that the residual MSE increases with the access of every new interferer. Moreover, it is shown that the sudden access of interferers with full power creates a jump (click) in the MSE of nearly -7dB which might be beyond the acceptable MSE of the receiver. Therefore, a possible solution to this problem [2] is to suggest the use of low power access scheme, where a new interferer increases his power linearly within a short period of time.

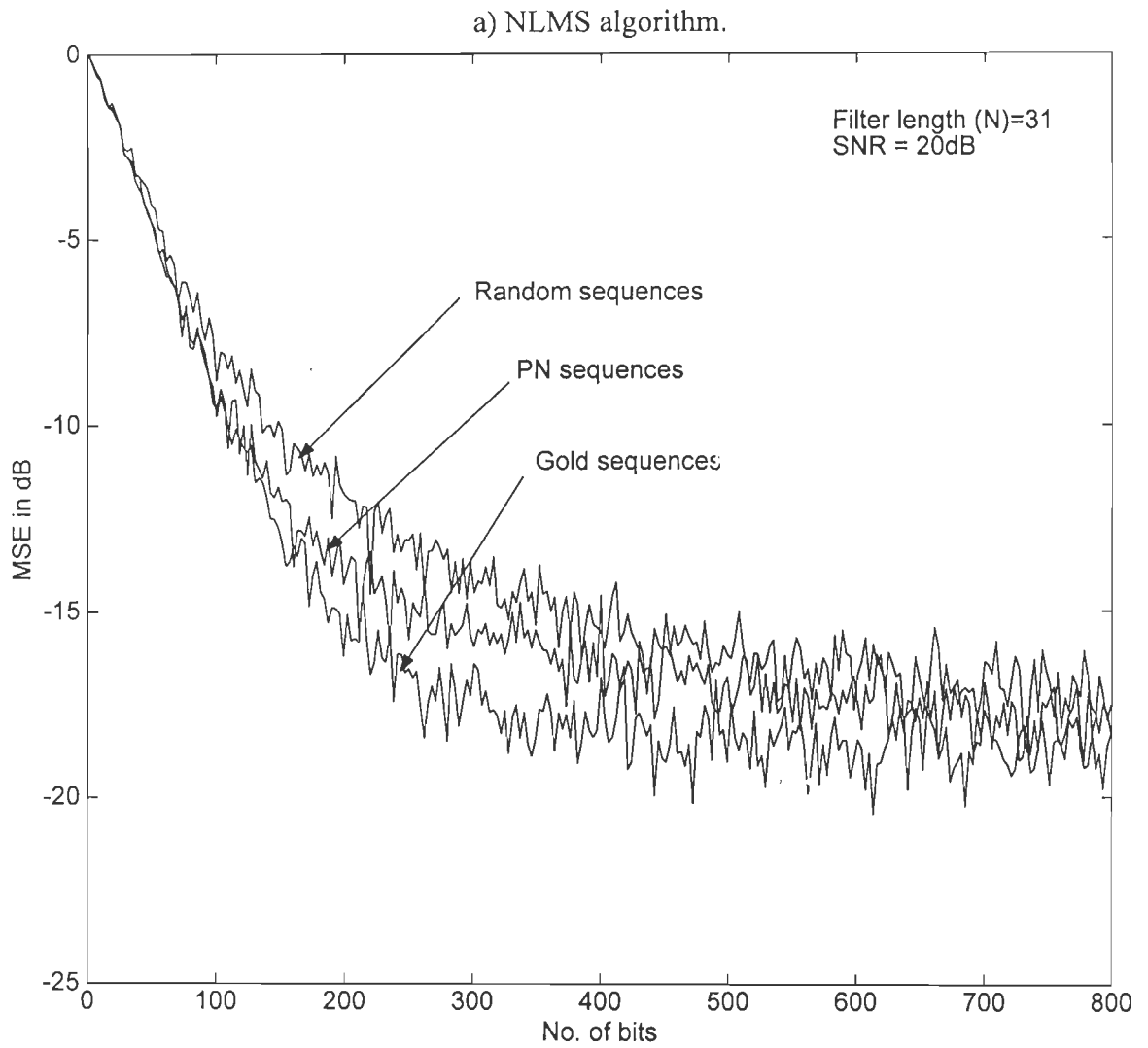


Fig.2.7 Comparison of the convergence characteristics for the adaptive DS-CDMA receiver with PN, Gold and random sequences with 4-interferers (each interferers has 10dB power advantage) using a) NLMS b) Block c) RLS algorithms.

b) Block algorithm.

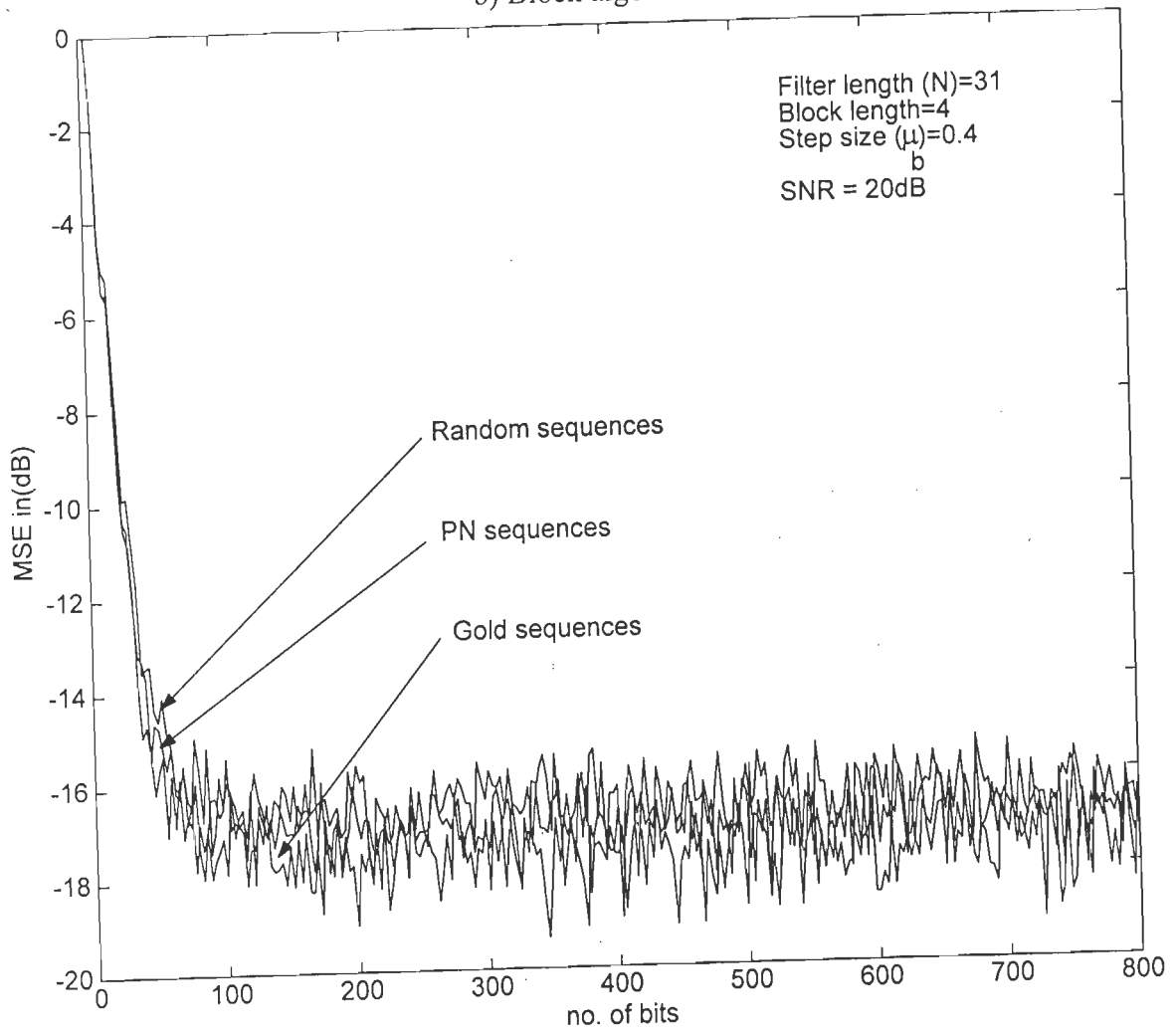


Fig.2.7b

c) RLS algorithm.

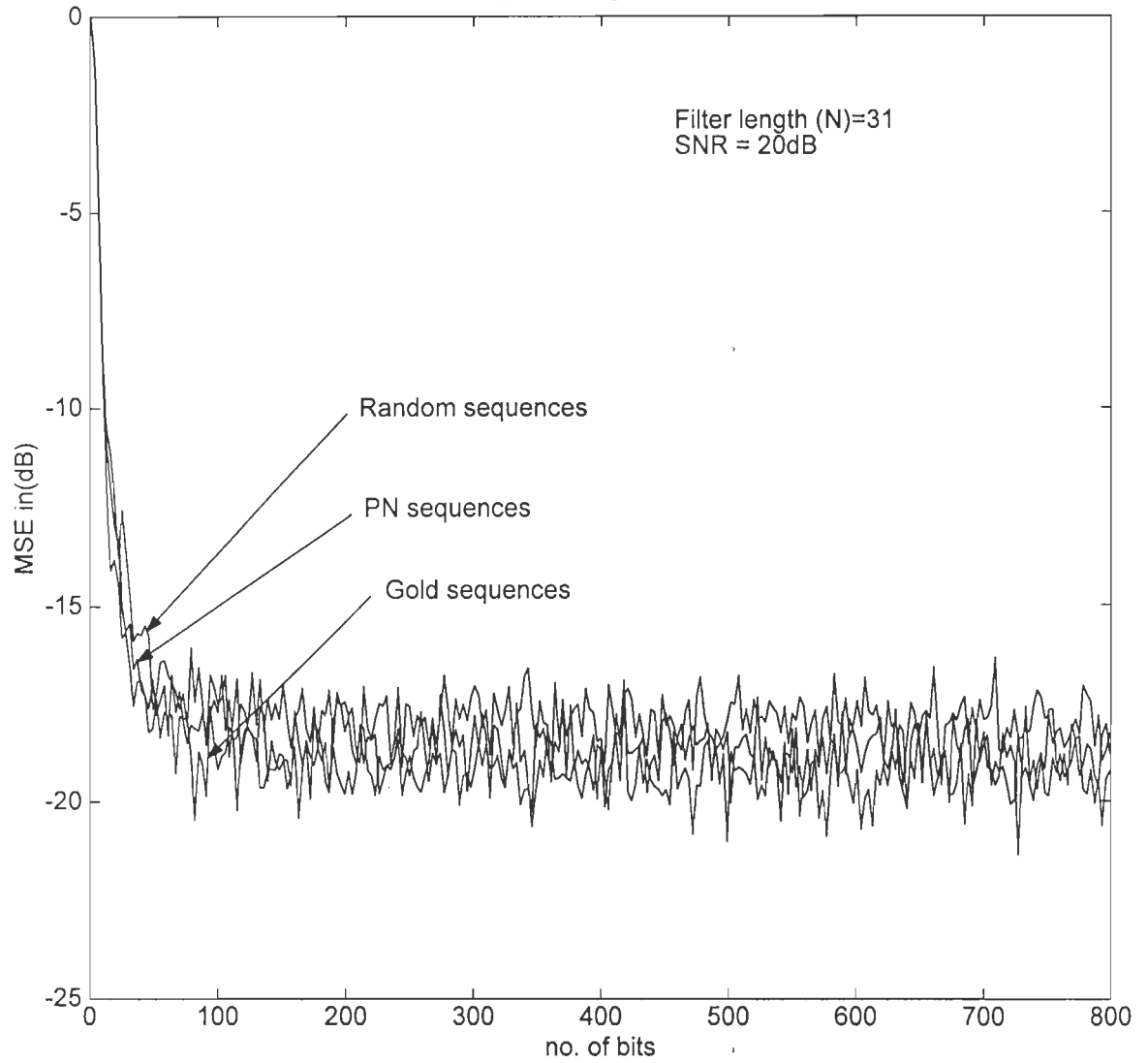


Fig.2.7c

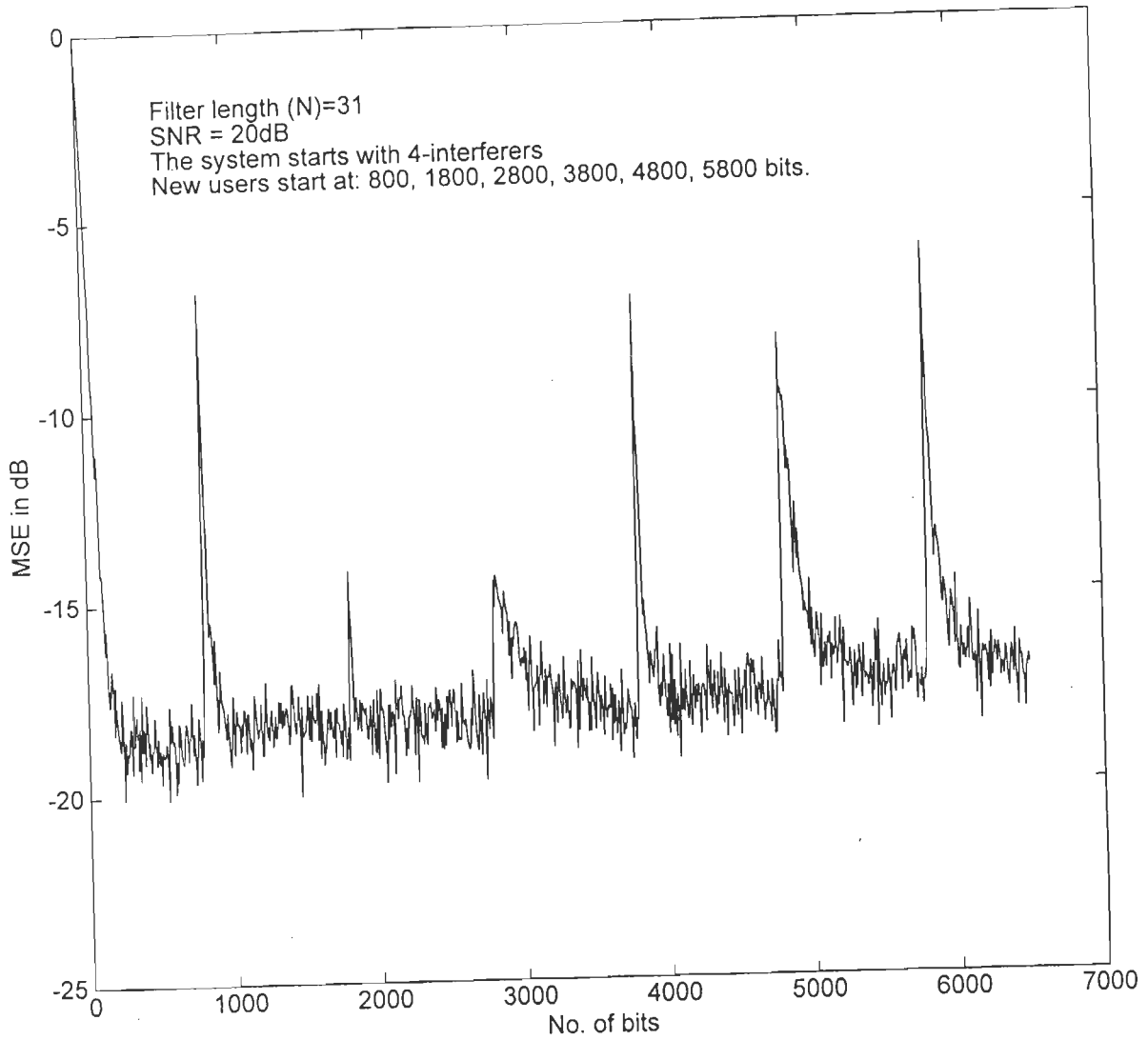


Fig.2.8 Effect of entry of interferers on the performance of the adaptive DS-CDMA receiver using NLMS algorithm (each interferer has 10dB power advantage over the desired user).

Example 2.6

In this example, the bit-error rate performance of the adaptive DS-CDMA receiver is examined using RLS, NLMS and the block algorithms. Two cases are simulated, one with 8-interferers, while the other with 10-interferers, each having a 10 dB power advantage over the desired user. The step-size of both the NLMS and the block algorithm were adjusted such that the three adaptive algorithms will possess approximately the same residual MSE in the single-user case. Due to the instability of the RLS algorithm, periodic re-initialization is performed every 1000 bits, in the decision-directed mode. It is quite clear from Fig.2.9 that the bit-error rate performance of the three algorithms is almost comparable and matches the theoretical values. Also provided in Fig.2.9 are the lower (single-user) and upper (matched filter) bounds. The performance degradation in terms of input SNR is about 2dB as compared to the single user case for the 8-interferers case, while the degradation is about 3dB for the 10-interferers case.

Example 2.7

In this example, the asynchronous operation of the adaptive DS-CDMA receiver based on the RLS algorithm is compared with the synchronous case in terms of the convergence characteristics and the probability of error performance. Random spreading codes of length 31 are used, and the interferers delay is assumed to be uniformly distributed in the interval $[0, T)$ for the asynchronous case, while for the synchronous case it is assumed that all the user are synchronized with the receiver. The system includes 4 or 8 interferers each having 10dB power advantage over the desired user.

Fig.2.10 shows the convergence characteristics for the adaptive DS-CDMA receiver for both synchronous and asynchronous cases operated at input SNR=20dB. It is observed that there is performance degradation when using the asynchronous system as compared to the

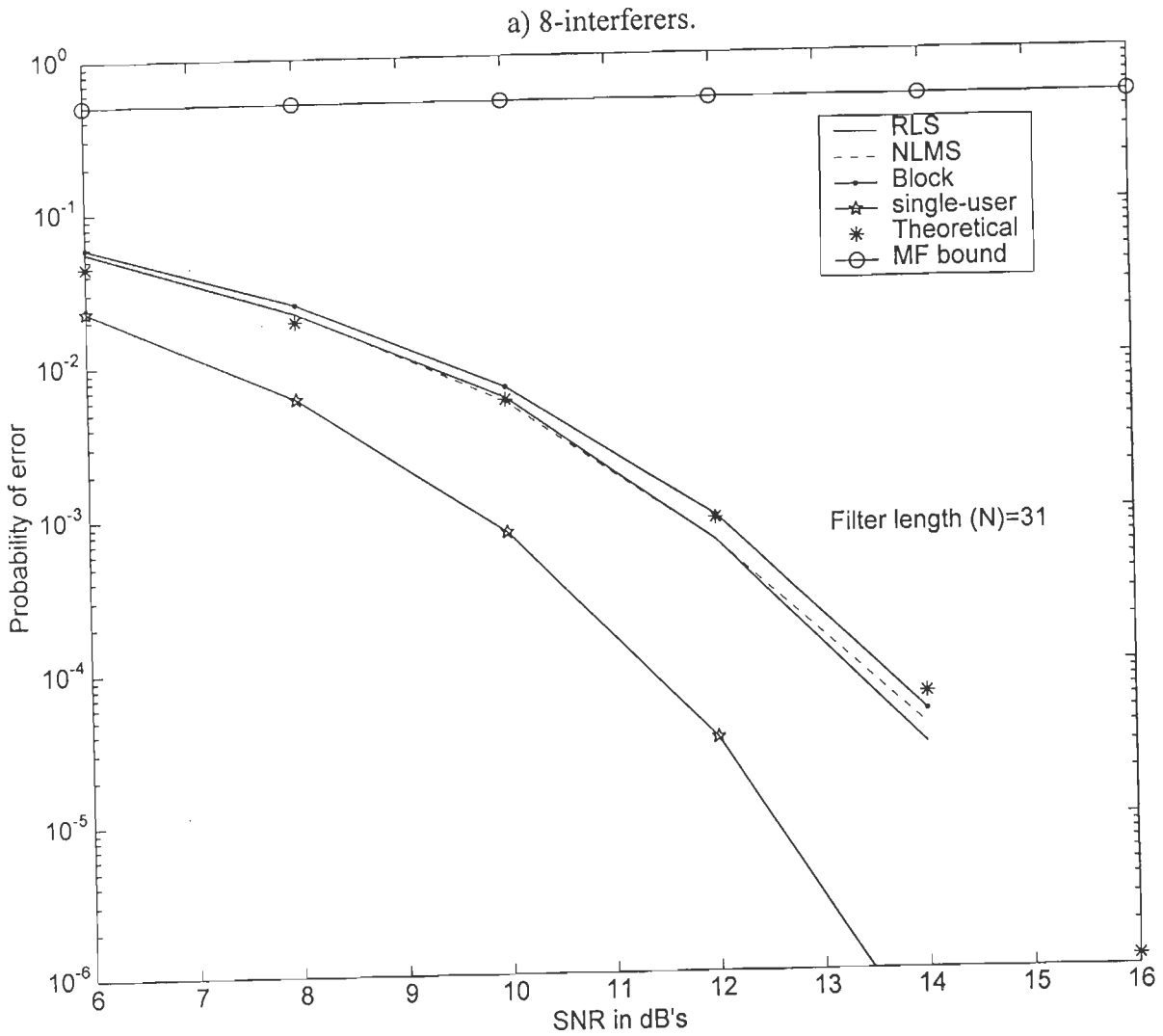


Fig.2.9 Probability of error performance for the adaptive DS-CDMA receiver using NLMS, RLS and block algorithms with a) 8-interferers b) 10-interferers (each interferer has 10dB power advantage over the desired user)

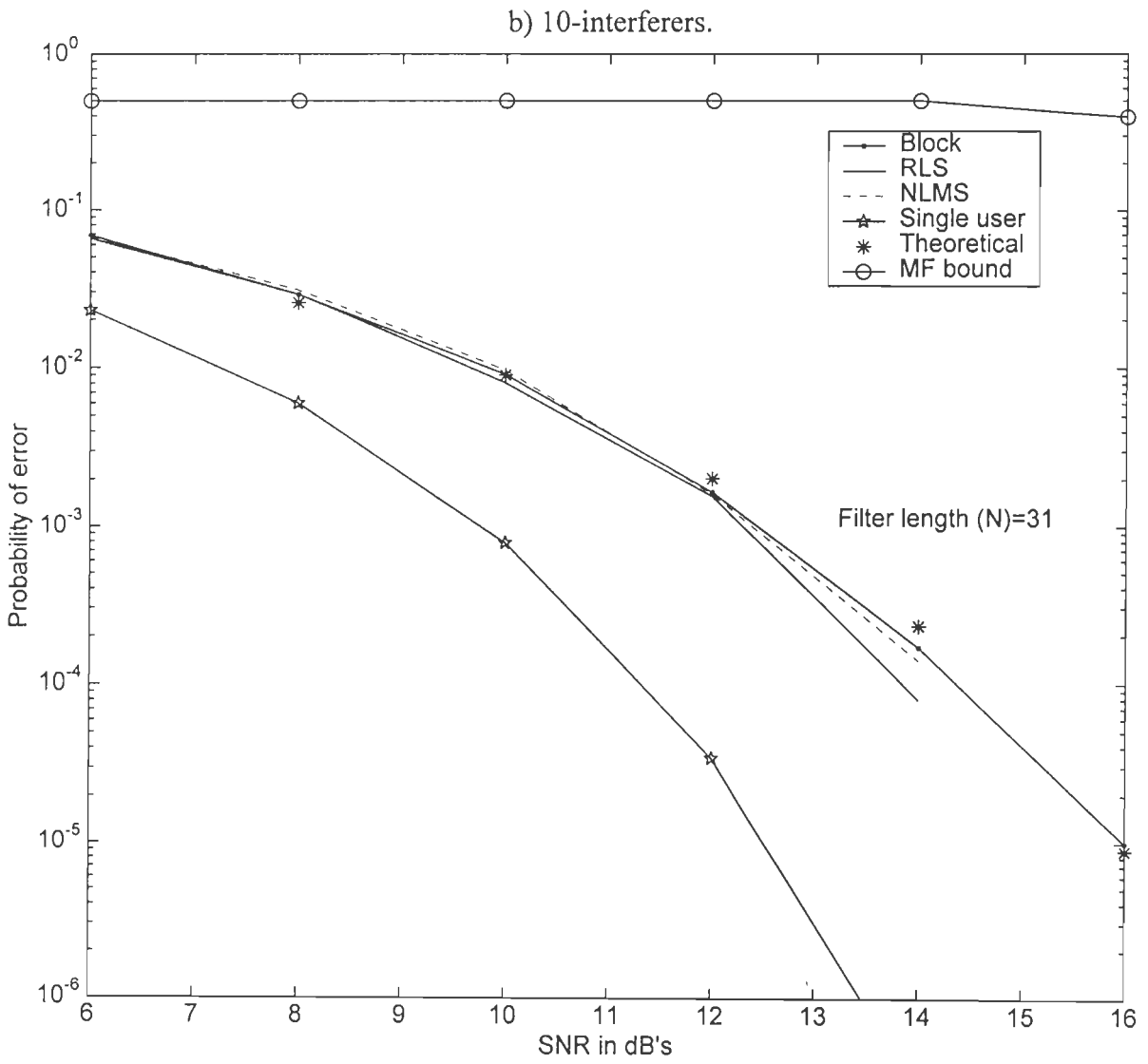


Fig.2.9b

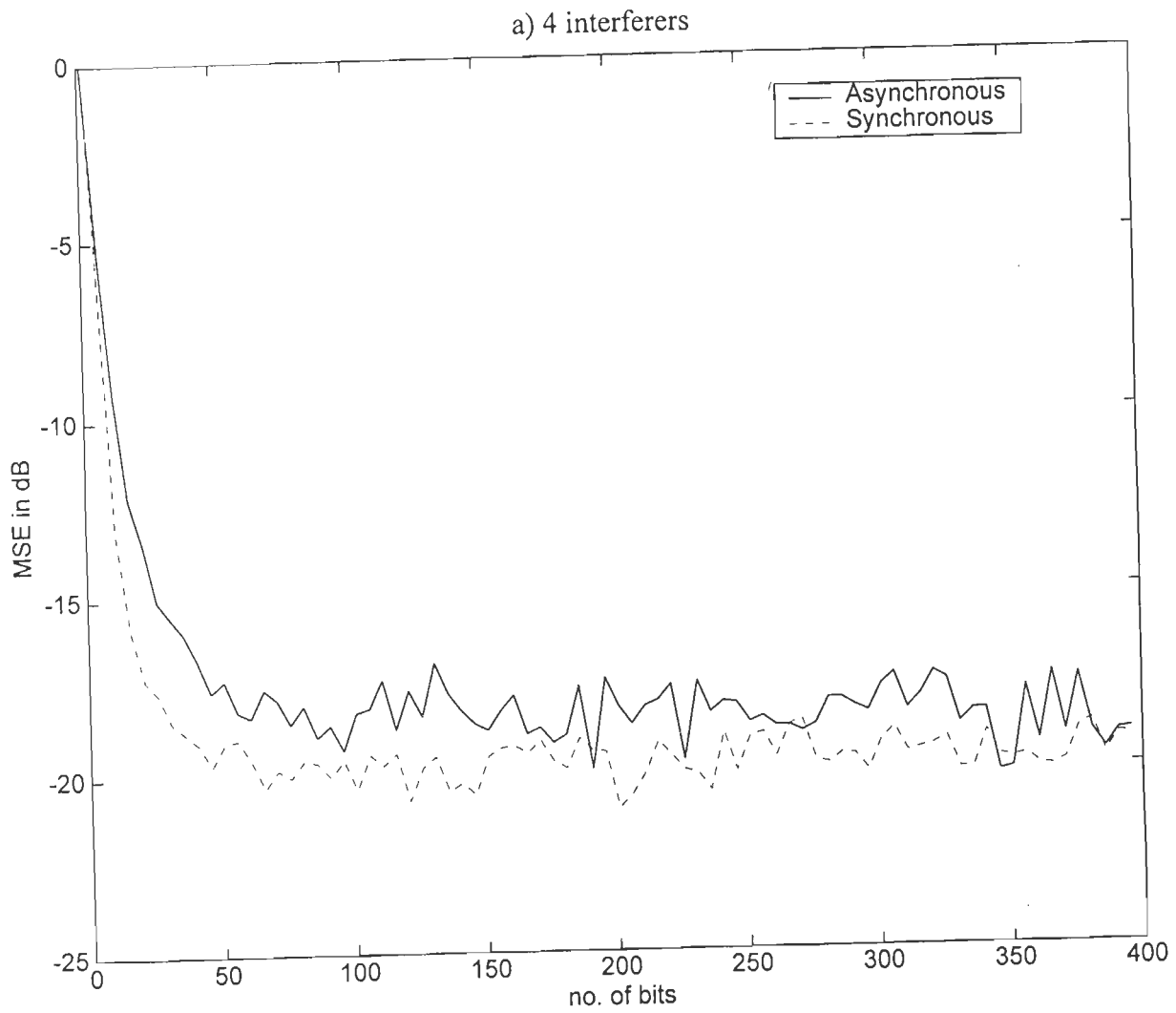


Fig.2.10 Convergence characteristics for the adaptive DS-CDMA receiver using the RLS algorithm for synchronous and asynchronous systems with a)4-interferers b)8 interferers (each interferer has 10dB power advantage over the desired user).

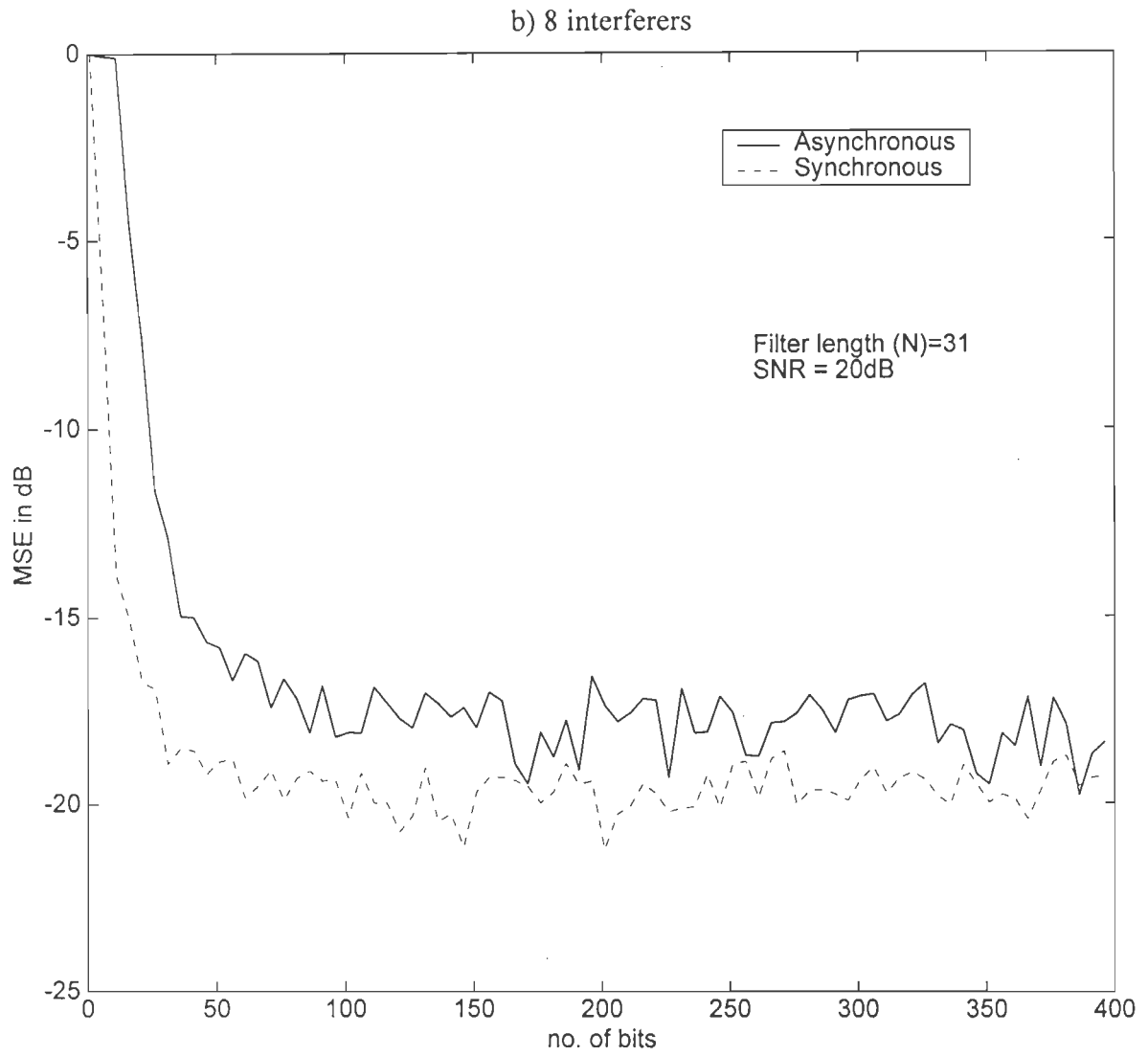


Fig.2.10.b

synchronous system. Fig.2.11 shows the probability of error performance for the adaptive DS-CDMA receiver for both the synchronous and asynchronous cases. It is clear that there is performance degradation for the asynchronous system as compared to the synchronous system. At an error rate of 10^{-3} , with 4 interferers, the performance degradation for the asynchronous receiver in terms of the input SNR is 0.65dB as compared to the synchronous system, while for the 8 interferers case the degradation is nearly 1.45dB.

A reason for this degradation in performance is that the crosscorrelation between different spreading codes is higher in the asynchronous system as compared to the synchronous system, and hence larger values of the MAI will be produced. This of course will result in an increase in the residual MSE value and hence the probability of error will be larger for the asynchronous system as compared to the synchronous system. Therefore, the asynchronous system represents the worst case of operation as compared to the synchronous case.

Example 2.8

In this example, the capacity, i.e. number of users that can be supported by the adaptive DS-CDMA receiver is investigated. The capacity is determined by evaluating the output SNR as a function of number of users. The near-far situation is assumed by setting all the interferers' power to have a 10 dB power advantage above the desired user. For both NLMS and the modified block algorithms, the step-size is tuned such that the single-user residual MSE is the same for the three algorithms. Fig.2.12 shows the output SNR versus number of users at input SNR=10, 30 and 50 dB. It is clear that the RLS algorithm performs much better than the NLMS algorithm, while the block algorithm performance is between NLMS and RLS algorithms. It is worth-noting that, while varying the number of users, the implemented step-size for both NLMS and block algorithms is fixed at the value in which the single-user

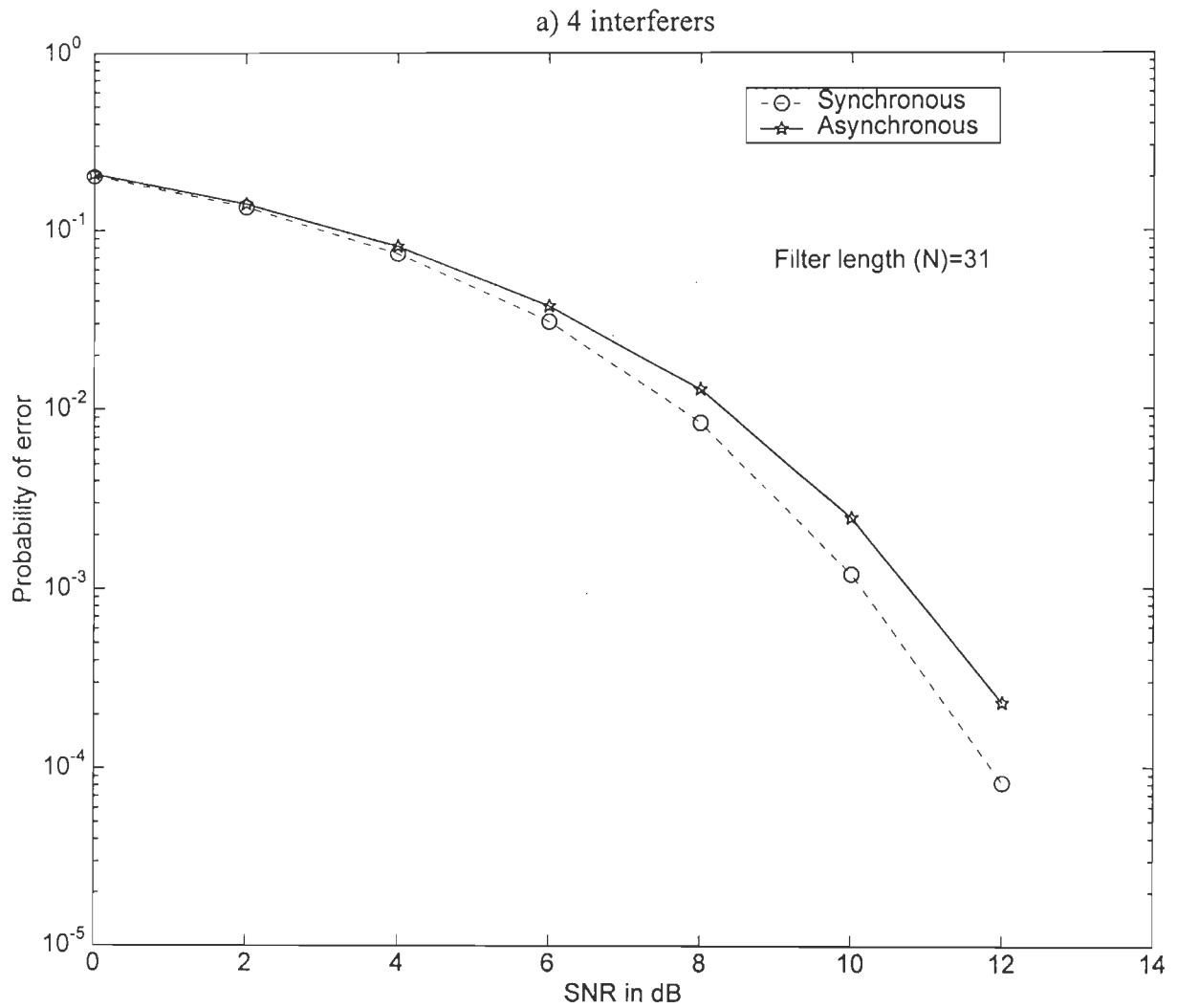


Fig.2.11 Probability of error performance for the adaptive DS-CDMA receiver using the RLS algorithm for synchronous and asynchronous systems with a)4 interferers b)8 interferers (each interferer has 10dB power advantage over the desired user).

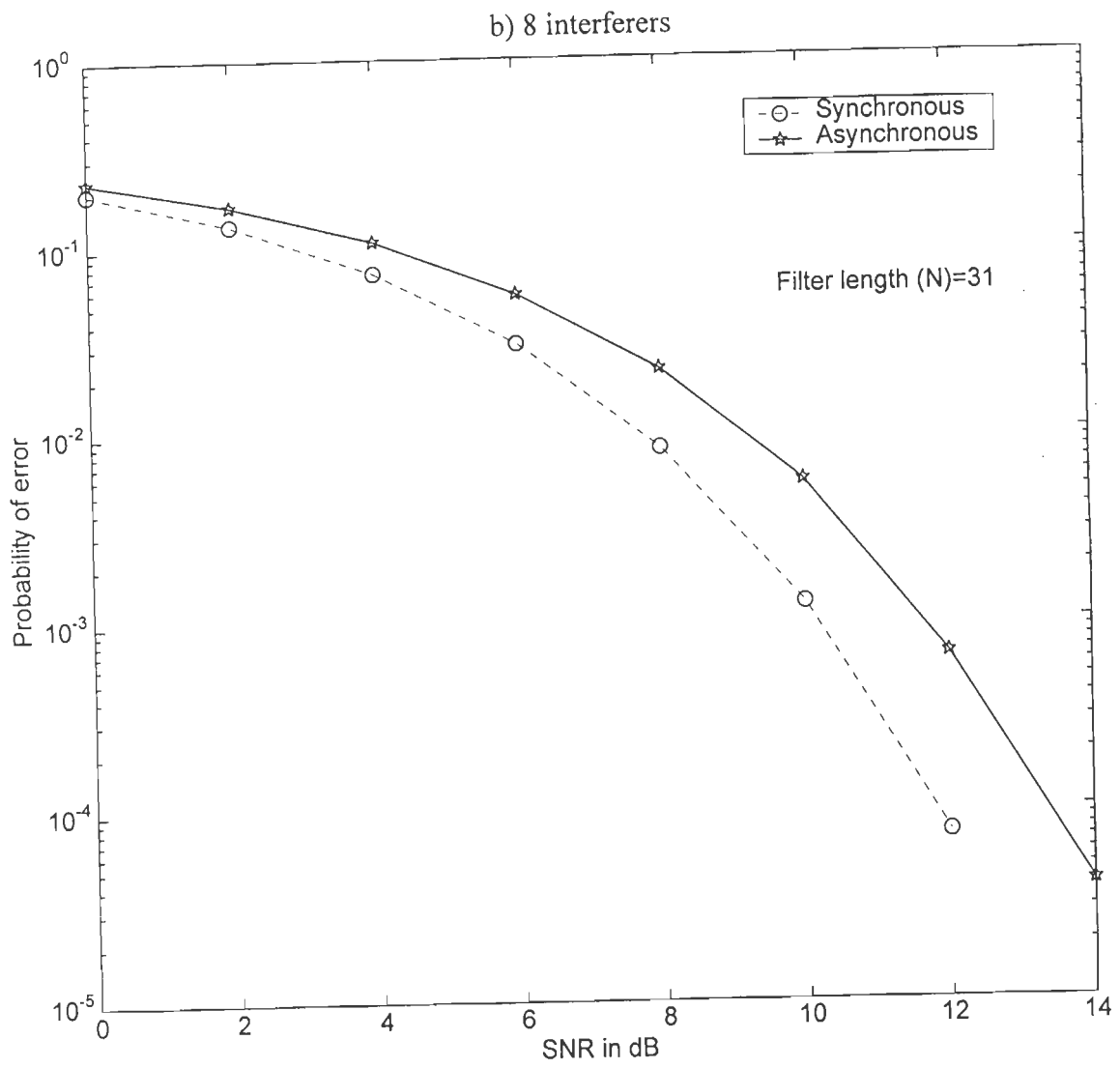


Fig.2.11b

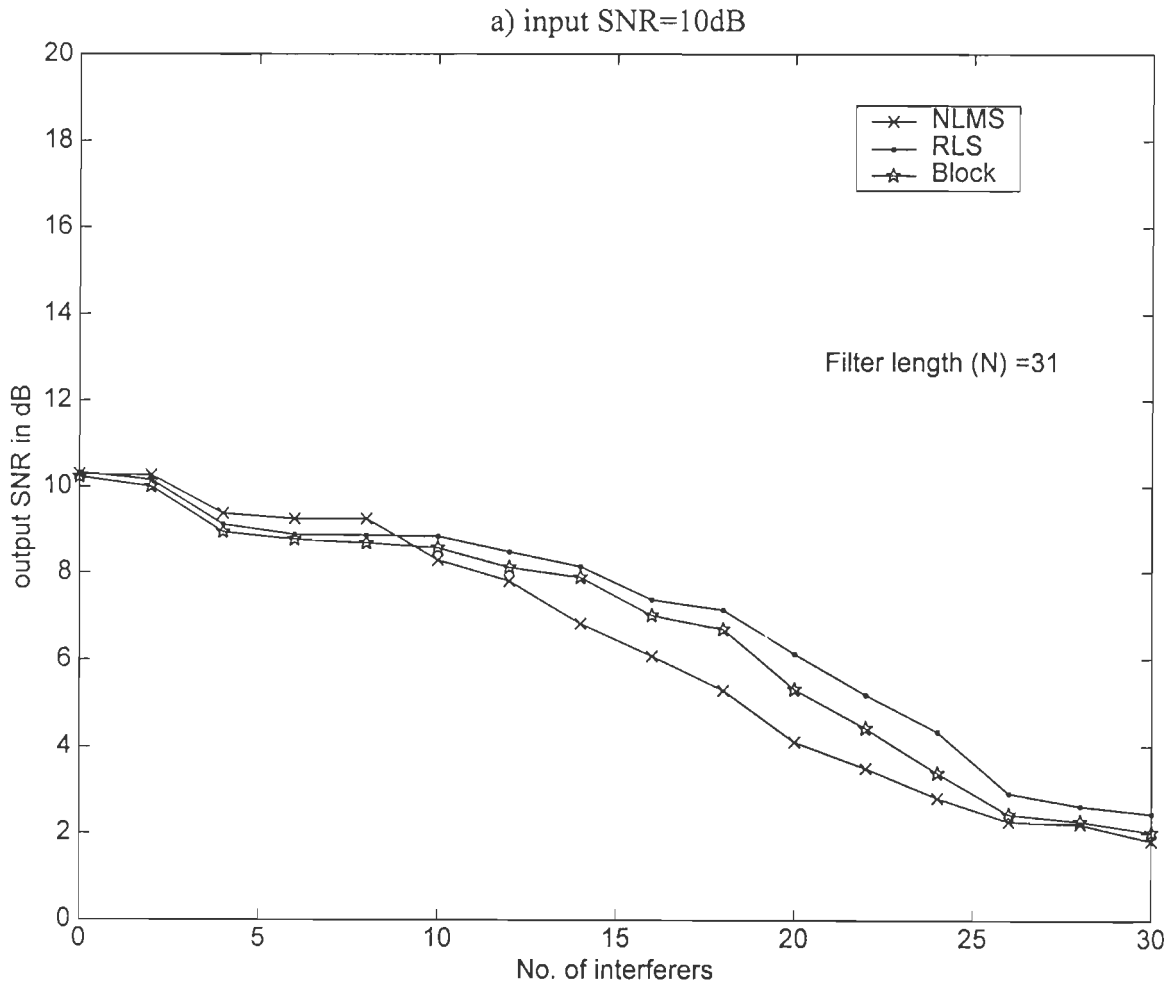


Fig.2.12 Comparison of the output SNR of adaptive DS-CDMA receiver using NLMS, RLS and block algorithms as a function of the number of interferers (each interferer has 10dB power advantage over the desired user) a)input SNR=10dB, b)input SNR=30dB c) input SNR=50dB.

b) input SNR=30dB.

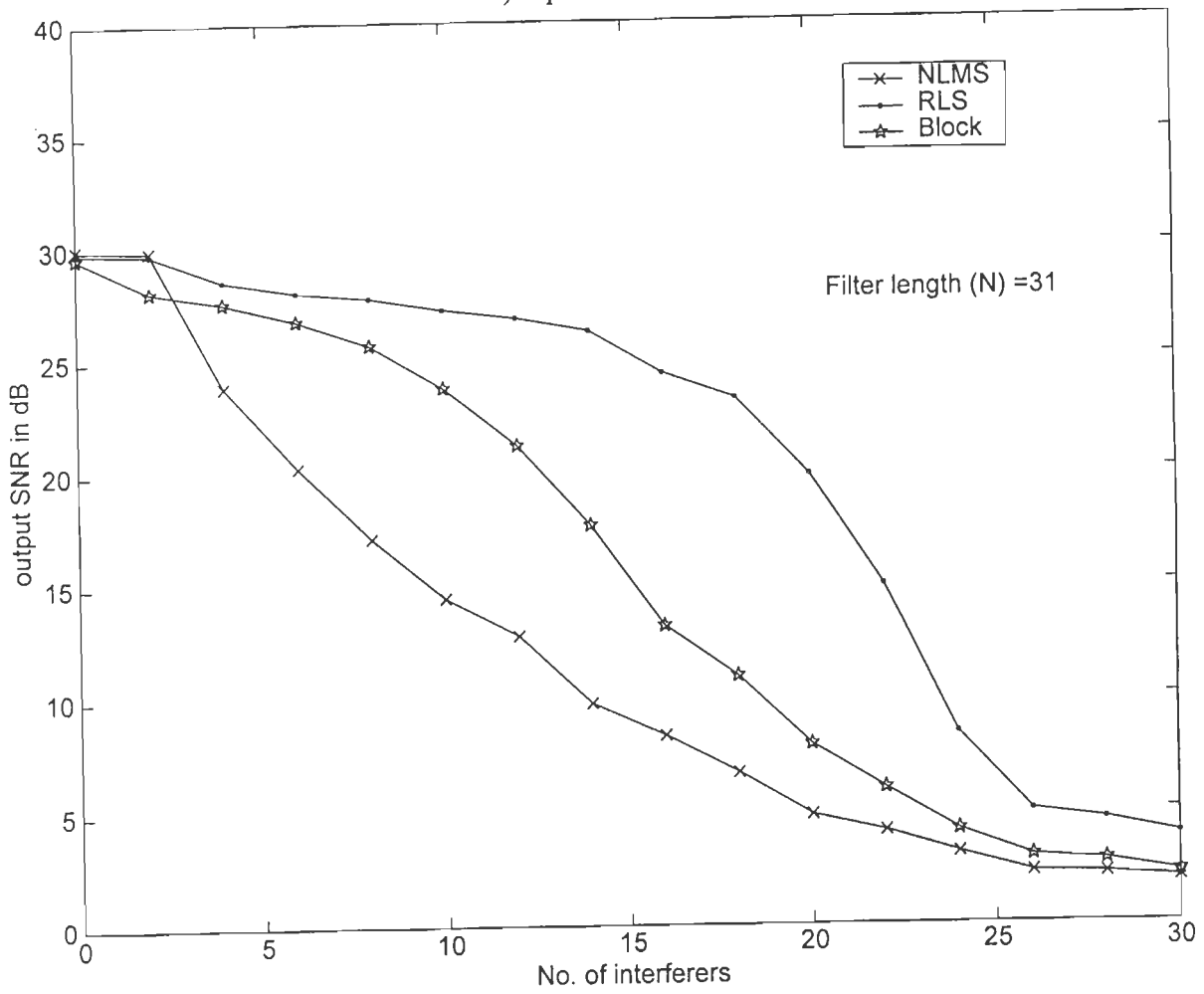


Fig.2.12b

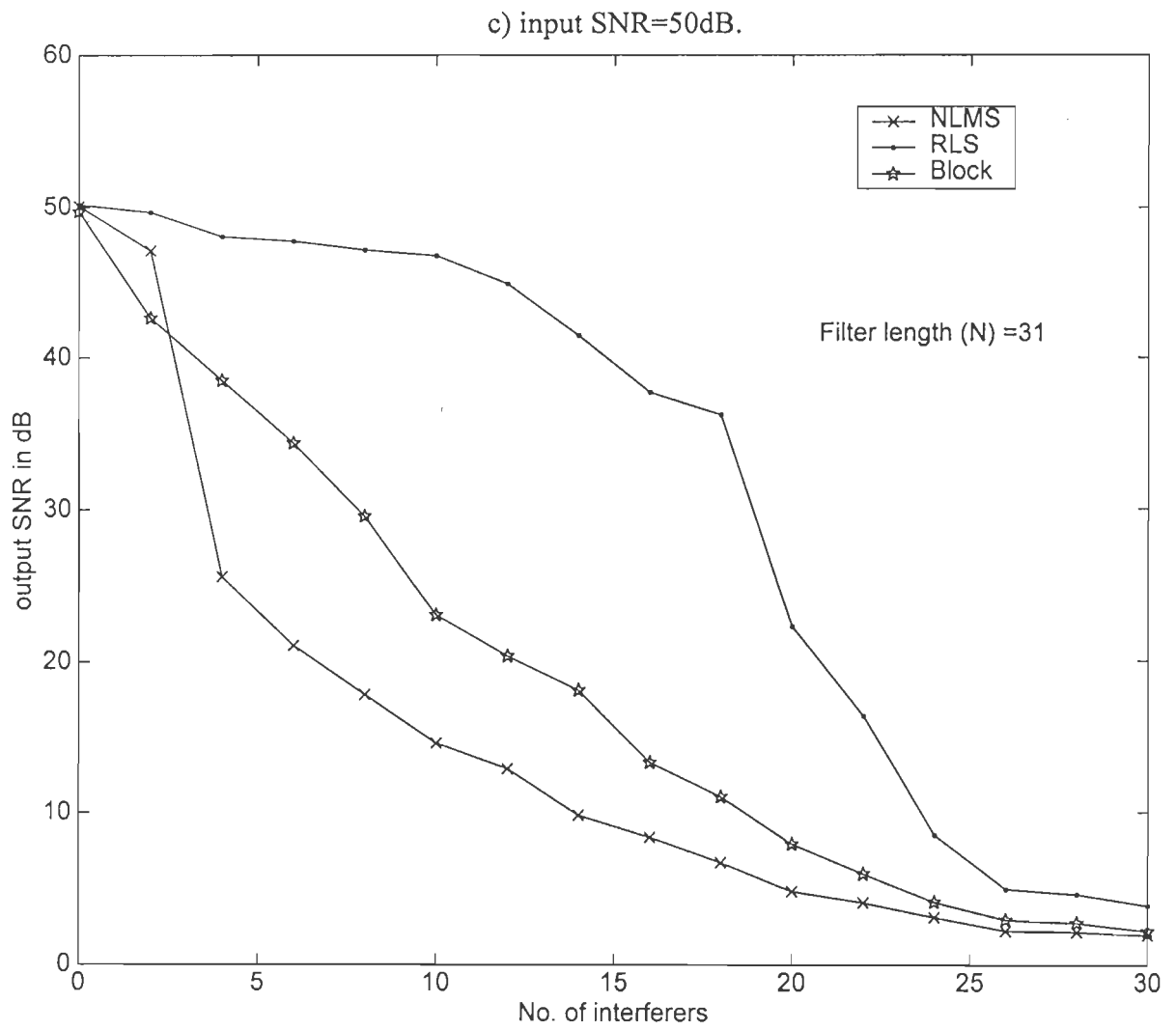


Fig.2.12c

residual MSE is the same for all algorithms. Of course, this is the cause of the performance degradation in both NLMS and block algorithms as compared to RLS algorithm. For example, at input SNR=30dB, suppose that the acceptable output SNR is equal to 20dB, then the RLS algorithm can support about 20 users, while about 14 users can be supported using the modified block algorithm and only 5 users can be supported using the NLMS algorithm. For an input SNR=50dB, if the acceptable output SNR=20dB, then the RLS algorithm can support 21 users and using the block algorithm only 14 users can be supported, while for the NLMS algorithm 6 users are supported only.

Example 2.9

In this example, an adaptive MMSE DS-CDMA receiver is simulated using RLS, NLMS and the block algorithms. The interferers' power is varied from -2dB to 12dB relative to the desired user at 10dB and 12dB values of input SNR. The step-size of the NLMS and the block algorithms is adjusted such that the single-user residual MSE for the three algorithms is the same. It is clear from Fig.2.13 that the probability of error remains constant even if the power of the interferers increases to 12dB relative to the desired user. At input SNR=10dB the probability of error remains constant at about 2×10^{-3} , while for input SNR=12 dB it remains constant at about 8×10^{-5} . Therefore, it is concluded that the adaptive MMSE DS-CDMA receiver based on the NLMS, RLS, and block algorithms is near-far resistant since its probability of error performance is not affected (remains constant) when the interferers power varies.

Example 2.10

In this example, the probability of error for the adaptive DS-CDMA receiver using NLMS, RLS and the block algorithm is calculated as a function of number of users. All interferers have a 10dB power advantage above the desired user. The simulation is performed

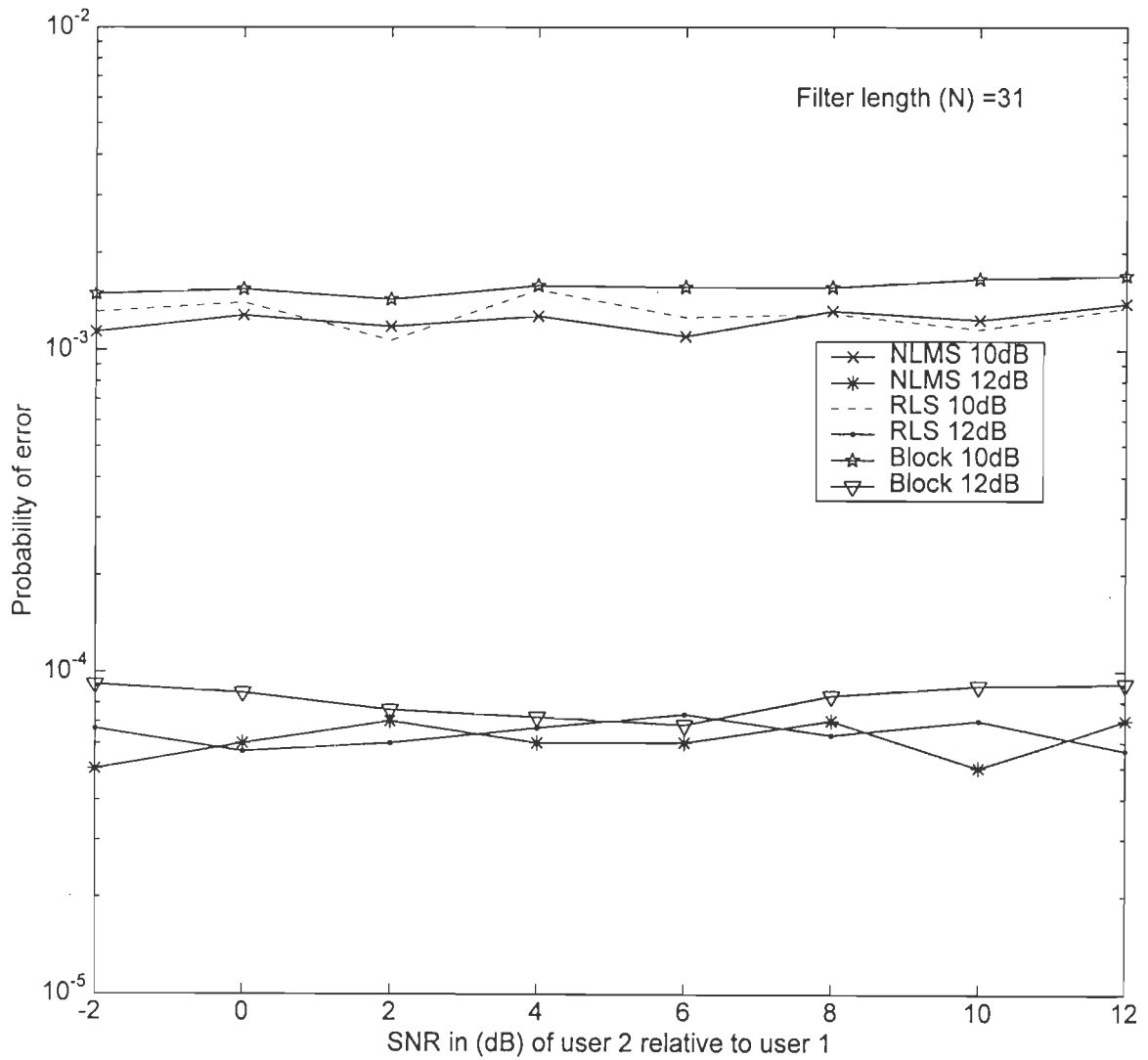


Fig.2.13 Probability of error performance for the desired user as a function of the second user power relative to the desired user, at input SNR of 10dB and 12dB using the NLMS, RLS and the block algorithm.

at input SNR of 10dB and 12dB respectively. It is clear from Fig.2.14 that the probability of error increases with the increase in the number of interferers, and there is a slight difference in the performance of the three adaptive algorithms.

In this chapter, we have implemented different adaptive algorithms for interference suppression in DS-CDMA systems. It has been shown that the RLS algorithm converges faster than the NLMS algorithm but at the expense of an increase in the computational complexity. To improve the convergence rate of the NLMS algorithm, an MVSS-LMS algorithm has been implemented, and simulation results demonstrate its improved convergence characteristics as compared to LMS algorithm. On the other hand, to deal with both the slow convergence rate of the NLMS and the high computational complexity of the RLS algorithm, we have proposed and implemented a novel block adaptive algorithm for the interference suppression in DS-CDMA systems. Results show that the proposed block algorithm possesses convergence characteristics, which is comparable to RLS algorithm while requiring much lower computational complexity.

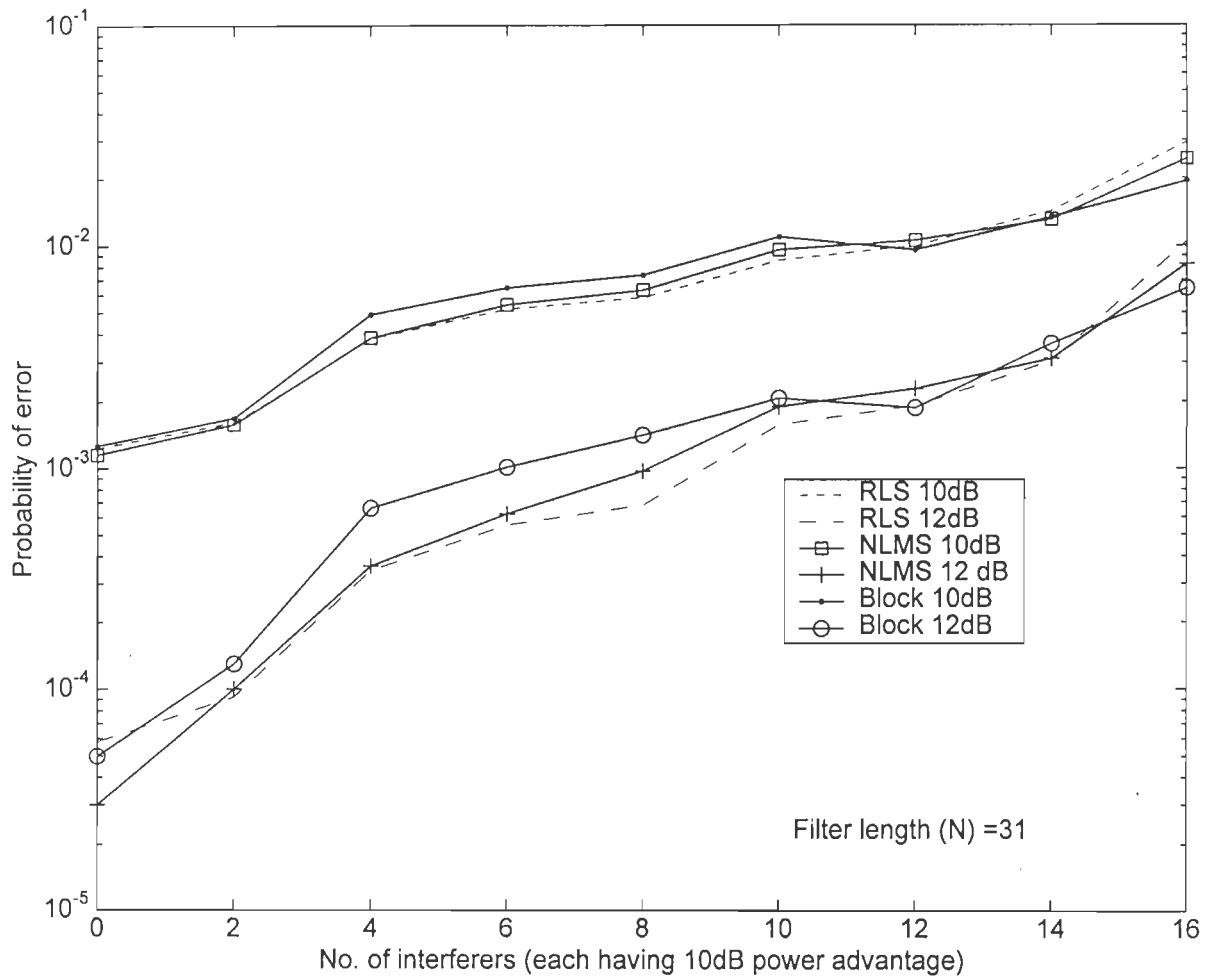


Fig.2.14 Probabilty of error performance for the adaptive DS-CDMA receiver as a function of the number of interferers at input SNR of 10dB and 12 dB using the NLMS, RLS and block algorithms.

ADAPTIVE DS-CDMA RECEIVER USING KALMAN FILTERING

In this chapter, we consider the application of the Kalman filter (KF) for the adaptation and demodulation of DS-CDMA signals. A motivation for using the KF is that it is optimal in the MMSE sense, and is considered as the best linear unbiased estimator. Moreover, the KF is usually formulated using the state-space approach, which contains all the necessary information about the system, and its solution may be computed recursively. Also it provides a general framework for the derivation of a family of RLS algorithms [101].

In section 3.1, we review the KF and its use in adaptive filtering problems. The KF-development and the state-space representation of multiuser CDMA signals are presented in section 3.2. The SQ-KF algorithm, which is numerically stable is introduced in section 3.3. Finally, section 3.4, presents simulation results and discussion.

3.1 Introduction

Lawrence and Kaufman [54] have considered the use of the KF for the equalization of digital channels in the presence of noise and ISI. The MMSE estimate of the transmitted symbols is obtained and the only constraints are stability and linearity. Benedetto and Biglieri [8] have investigated the steady state behavior of such receiver structures. Under steady-state situation, this linear receiver turns out to be a time-invariant, stable recursive filter. In the KF equalizer, the estimates of the symbols are fed back before a decision is made on them, and thus the receiver is linear and the effect of decision error propagation is thereby eliminated. The performance attainable with the KF equalizer is superior to that of the conventional linear equalizer (LE), for a given complexity of the receiver structure. However, for

implementation, the KF needs an exact knowledge of the channel tap-gains and a mismatch in tap setting may lead to performance degradation.

Godard [28] applied the Kalman filter algorithm to the estimation of the equalizer coefficient vector under some assumptions on the equalizer output error and input statistics. It is an ideal self-orthogonalizing algorithm in that the received equalizer input signals are used to build up the inverse of the input covariance matrix, which is applied to the coefficient adjustment process.

The Kalman filtering is prone to numerical instability due to the use of finite word-length arithmetic for calculating the Riccati difference equation. To solve this problem, a unitary transformation may be used at each iteration of the Kalman filtering algorithm [82].

In [60] an EKF-based detector for the joint estimation of symbols and delays of all users in asynchronous DS-CDMA is presented. The detector operates in the tracking mode and relies on the availability of accurate initial delay estimates. Due to the non-linear relationship between the estimator output and the delay estimates, linearization has been performed, which if introduces negligible errors, then the EKF reduces to the standard Kalman filter which produces MAP (maximum a posteriori) state estimate at each time, provided the first-order Gauss-Markov model of parameter time variation is exact and the noise covariance matrices are known exactly. In [61] a similar KF-based detector for the joint delay estimation/symbol detection algorithm in asynchronous multiuser CDMA systems is proposed. However, for simplicity it is assumed that the delay is known to the receiver. An improved performance of this algorithm over the conventional MMSE detector is demonstrated. An attractive property of this detector is that it provides very good performance without suffering long delays (long codes). The detector is near far resistant, both in bit error rate and channel estimation performance. In [62] it is shown that a first order

linear state-space model applies to the asynchronous CDMA channel, and thus the KF produces symbol estimates with the lowest possible MSE among all linear filters, in long- or short-code systems for a given detection delay. Moreover, the KF complexity is fixed for a given detection delay, unlike in the case of the windowed LMMSE detector, which for the same performance will require a window whose length increases with time.

In this chapter, we propose the use of the KF as an adaptive estimator of TDL filter weights for DS-CDMA signals.

3.2 The Kalman filter

The state-space equation of a linear system with random inputs can be described by:

$$\mathbf{x}(n+1) = \Phi_n \mathbf{x}(n) + \mathbf{v}_1(n) \quad (3.1)$$

$$\mathbf{y}(n) = \mathbf{H}_n \mathbf{x}(n) + \mathbf{v}_2(n) \quad (3.2)$$

where $\mathbf{x}(n)$ is an N-dimensional state-vector containing system variables which may not be directly measurable and $\mathbf{y}(n)$ is an M-dimensional measurement (observation) vector. Φ_n is an N-by-N state transition matrix relating the state of the vector at times $n+1$ and n . \mathbf{H}_n is a known M-by-N measurement (observation) matrix. The vector $\mathbf{v}_1(n)$ is modeled as a zero-mean white-noise process whose correlation matrix is defined by:

$$E[\mathbf{v}_1(n) \mathbf{v}_1^T(k)] = \begin{cases} \mathbf{Q}_1(n) & n = k \\ 0 & n \neq k \end{cases} \quad (3.3)$$

The vector $\mathbf{v}_2(n)$ is called the measurement noise modeled as a zero-mean, white-noise process whose correlation matrix is defined by:

$$E[\mathbf{v}_2(n) \mathbf{v}_2^T(k)] = \begin{cases} \mathbf{Q}_2(n) & n = k \\ 0 & n \neq k \end{cases} \quad (3.4)$$

Also it is assumed that the noise vectors $\mathbf{v}_1(n)$ and $\mathbf{v}_2(n)$ are statistically independent, so that

$$E[\mathbf{v}_1(n) \mathbf{v}_2^T(k)] = 0 \quad \text{for all } n \text{ and } k. \quad (3.5)$$

The recursive form of the KF involves the following steps in each symbol interval n [25,61]:

$$\mathbf{P}_n^- = \Phi_n \mathbf{P}_{n-1}^+ \Phi_n^T + \mathbf{Q}_1 \quad (3.6)$$

$$\mathbf{T}_n = \mathbf{P}_n^- \mathbf{H}_n^T (\mathbf{H}_n \mathbf{P}_n^- \mathbf{H}_n^T + \mathbf{Q}_2)^{-1} \quad (3.7)$$

$$\hat{\mathbf{x}}(n) = \Phi_n \hat{\mathbf{x}}(n-1) + \mathbf{T}_n [y(n) - \mathbf{H}_n \Phi_n \hat{\mathbf{x}}(n-1)] \quad (3.8)$$

$$\mathbf{P}_n^+ = (\mathbf{I} - \mathbf{T}_n \mathbf{H}_n) \mathbf{P}_n^- \quad (3.9)$$

The kalman filter delivers the MMSE estimate of $\mathbf{x}(n)$, defined as

$$\hat{\mathbf{x}}_{\text{MS}}(n | n) = \arg \min_{\hat{\mathbf{x}}(n)} E\{\|\mathbf{x}(n) - \hat{\mathbf{x}}(n)\|^2 | n\} \quad (3.10)$$

The Kalman filter operates on the sampled baseband signals $\mathbf{r}(n)$ to estimate the channel state $\mathbf{x}(n)$. It is a well established fact that the Kalman filter provides the mean-square optimum linear estimate of $\mathbf{x}(n)$. It minimizes not only the trace of the error covariance matrix, but also any linear combinations of main diagonal elements.

We assume asynchronous DS-CDMA system with K users simultaneously transmitting over the same channel with AWGN. Recalling the signal model of chapter 2, the received signal $y(t)$ is converted to the baseband signal $\mathbf{r}(t)$. After baseband conversion, the received signal is chip matched filtered and sampled at the chip rate, then it is fed to the TDL filter as $\mathbf{r}(n)=[r_0(n), r_1(n), \dots, r_{N-1}(n)]^T$.

In a stationary environment, the tap-weights vector $\mathbf{w}(n)$ of the TDL filter has a constant value such that,

$$\mathbf{w}(n)=\mathbf{w}(n-1) \quad (3.11)$$

where $\mathbf{w}(n)=[w_0(n), w_1(n), \dots, w_{N-1}(n)]^T$

The TDL filter output is equal to the inner product $\mathbf{r}^T(n)\mathbf{w}(n-1)$, and the desired response is:

$$d_1(n) = \mathbf{r}^T(n) \mathbf{w}(n-1) + \alpha(n) \quad (3.12)$$

where $\alpha(n)$ is the estimation error measured with respect to the desired response $d_1(n)$.

Equations (3.11 and 3.12) may be viewed as the state-space equations of a linear system defined in Eqs. (3.1) and (3.2). Comparing these equations, the following substitutions may be achieved.

- $\mathbf{x}(n)$, the state vector equals the tap-weights vector $\mathbf{w}(n)$, measured at time n .
- $y(n)$ is the measurement (observation) signal identified as the desired signal $d_1(n)$, measured at time n .
- Φ_n , the state transition matrix, equals the identity matrix \mathbf{I} .
- $\mathbf{v}_1(n)$, the process noise, equals to zero and hence $\mathbf{Q}_1(n)=0$, in this case.
- \mathbf{H}_n the measurement vector equal to the transposed tap-input vector $\mathbf{r}(n)$.
- $\mathbf{v}_2(n)$, the measurement noise, is identified as the estimation error $\alpha(n)$. Therefore $\mathbf{Q}_2(n)=E[\alpha^2(n)]$ which is denoted as ξ_{\min} , the minimum MSE.

Since in this case $\phi_n=\mathbf{I}$ and $\mathbf{Q}_1=0$, then Eq. (3.6) reduces to

$$\mathbf{P}_n^- = \mathbf{P}_{n-1}^+ \quad (3.13)$$

The Kalman filter uses the error between the desired and estimated data bits, $\alpha(n)$, to adapt the TDL filter weights in the sense of minimizing the MSE. The adopted Kalman filter for updating the estimated TDL filter weights $\mathbf{w}(n)$ for a stationary environment is as follows. Denoting \mathbf{T}_n by $\mathbf{g}(n)$, \mathbf{P}_{n-1}^+ by $\mathbf{k}(n-1)$ and \mathbf{P}_n^+ by $\mathbf{k}(n)$ in Eqs. (3.6-3.9), and based on the previous substitutions then Eq. (3.7) reduces to

$$\mathbf{g}(n) = \mathbf{k}(n-1) \mathbf{r}(n) [\mathbf{r}^T(n) \mathbf{k}(n-1) \mathbf{r}(n) + \xi_{\min}]^{-1} \quad (3.14)$$

Eq. (3.8) reduces to

$$\mathbf{w}(n) = \mathbf{w}(n-1) + \mathbf{g}(n) [d_1(n) - \mathbf{r}^T(n)\mathbf{w}(n-1)] \quad (3.15)$$

and Eq.(3.9) reduces to

$$\mathbf{k}(n) = \mathbf{k}(n-1) - \mathbf{g}(n) \mathbf{r}^T(n) \mathbf{k}(n-1) \quad (3.16)$$

with initial conditions, $\mathbf{w}(0)=\mathbf{0}$ and $\mathbf{k}(0)=c\mathbf{I}$ where $c>0$. $\xi_{\min}=E[\alpha^2(n)]$, the minimum MSE, is assumed to be known to the receiver clearly, however it could be measured during silent periods. Of course this is not the practical situation, therefore assuming a certain value for the channel noise power will result in a little difference in the performance between the assumed SNR and the correct one. The Kalman filter algorithm is summarized in Table 3.1.

Table 3.1 Summary of the Kalman filter algorithm.

<i>Input</i> $d_1(n)$, $\mathbf{r}(n)$, and J_{\min} .	
<i>Initializations</i> $\mathbf{w}(0)=\mathbf{0}$, $\mathbf{k}(0)=c\mathbf{I}$ ($c>0$.)	
<i>Algorithm</i>	<i>Complexity</i>
For $n=1, 2, \dots$ do	
$\mathbf{g}(n) = \mathbf{k}(n-1) \mathbf{r}(n) [\mathbf{r}^T(n) \mathbf{k}(n-1) \mathbf{r}(n) + \xi_{\min}]^{-1}$	$2N^2+N$ Mult. + N Div.
$\alpha(n) = d_1(n) - \mathbf{r}^T(n) \mathbf{w}(n-1)$	N Mult.
$\mathbf{w}(n) = \mathbf{w}(n-1) + \mathbf{g}(n) \alpha(n)$	N Mult.
$\mathbf{k}(n) = \mathbf{k}(n-1) - \mathbf{g}(n) \mathbf{r}^T(n) \mathbf{k}(n-1)$	N^2 Mult.
<i>TOTAL</i>	$3N^2 + 3N$ Mult. + N Div.

3.3 Square-Root Kalman Filter (SQRT-KF)

The previously mentioned implementation of the KF is the optimal solution to the linear filtering problem. However, the algorithm suffers from the numerical instability due to the way in which the Riccati difference equation is calculated. In particular $\mathbf{k}(n)$ in Eq. (3.16) is defined as the difference between two non-negative matrices, therefore, unless sufficient numerical accuracy is provided, the resulting matrix $\mathbf{k}(n)$ may be negative definite. This situation will make the KF unstable, which occurs due to the use of finite word-length arithmetic.

This problem may be overcome by using a numerically stable unitary transformations on the state error correlation matrix, $\mathbf{k}(n)$, at each iteration of the KF algorithm. The unitary transformation may be adopted using the Givens rotations or Householder transformations, as will be discussed later on in this section.

3.3.1 SQRT-KF Algorithm

The Cholesky factorization of the matrix $\mathbf{k}(n)$ is given by:

$$\mathbf{k}(n) = \mathbf{k}^{1/2}(n) \mathbf{k}^{T/2}(n) \quad (3.17)$$

where $\mathbf{k}^{1/2}(n)$ is a lower triangular matrix usually referred to as the square-root of $\mathbf{k}(n)$. The non-negative definite nature of $\mathbf{k}(n)$ is preserved by virtue of the fact that the product of any square matrix and its transpose is always non-negative definite matrix. The recursion in the square-root Kalman filter propagates the lower triangular matrix $\mathbf{k}^{1/2}(n)$. The Riccati difference equation for the Kalman filter, Eq. (3.16), may be rewritten as follows:

$$\mathbf{k}(n) = \mathbf{k}(n-1) - \mathbf{k}(n-1) \mathbf{r}(n) [\mathbf{r}^T(n) \mathbf{k}(n-1) \mathbf{r}(n) + 1]^{-1} \mathbf{r}^T(n) \mathbf{k}(n-1) \quad (3.18)$$

In light of the Riccati equation (3.18), the following two-by-two block matrix may be introduced [36]:

$$\mathbf{M}(n) = \begin{bmatrix} \mathbf{r}^T(n)\mathbf{k}(n-1)\mathbf{r}(n) + 1 & \mathbf{r}^T(n)\mathbf{k}(n-1) \\ \mathbf{k}(n-1)\mathbf{r}(n) & \mathbf{k}(n-1) \end{bmatrix} \quad (3.19)$$

Expressing the correlation matrix $\mathbf{k}(n-1)$ in its factored form (Eq. 3.17), and since the matrix $\mathbf{M}(n)$ is non-negative definite matrix we may use the Cholesky factorization

$$\mathbf{M}(n) = \begin{bmatrix} 1 & \mathbf{r}^T(n)\mathbf{k}^{1/2}(n-1) \\ \mathbf{0} & \mathbf{k}^{1/2}(n-1) \end{bmatrix} \begin{bmatrix} 1 & \mathbf{0}^T \\ \mathbf{k}^{T/2}(n-1)\mathbf{r}(n) & \mathbf{k}^{T/2}(n-1) \end{bmatrix} \quad (3.20)$$

where $\mathbf{0}$ is the null vector.

The matrix product on the right hand side of Eq. (3.20) may be interpreted as the product of a correlation matrix and its transpose. Invoking the matrix factorization lemma, according to which we may write [36],

$$\begin{bmatrix} 1 & \mathbf{r}^T(n)\mathbf{k}^{1/2}(n-1) \\ \mathbf{0} & \mathbf{k}^{1/2}(n-1) \end{bmatrix} \boldsymbol{\theta}(n) = \begin{bmatrix} b_{11}(n) & \mathbf{0}^T \\ \mathbf{b}_{21}(n) & \mathbf{B}_{22}(n) \end{bmatrix} \quad (3.21)$$

where $\boldsymbol{\theta}(n)$ is a unitary rotation and the scalar $b_{11}(n)$, the vector $\mathbf{b}_{21}(n)$ and the matrix $\mathbf{B}_{22}(n)$ denote the non-zero block elements of matrix \mathbf{B} .

To evaluate the unknown block elements, $b_{11}(n)$, $\mathbf{b}_{21}(n)$, and $\mathbf{B}_{22}(n)$ of the postarray, we proceed by squaring both sides of Eq. (3.21). Then, recognizing that $\boldsymbol{\theta}(n)$ is a unitary matrix, and therefore $\boldsymbol{\theta}(n)\boldsymbol{\theta}^T(n)$ equals the identity matrix \mathbf{I} for all n , we may write

$$\begin{bmatrix} 1 & \mathbf{r}^T(n)\mathbf{k}^{1/2}(n-1) \\ \mathbf{0} & \mathbf{k}^{1/2}(n-1) \end{bmatrix} \begin{bmatrix} 1 & \mathbf{0}^T \\ \mathbf{k}^{T/2}(n-1)\mathbf{r}(n) & \mathbf{k}^{T/2}(n-1) \end{bmatrix} = \begin{bmatrix} b_{11}(n) & \mathbf{0}^T \\ \mathbf{b}_{21}(n) & \mathbf{B}_{22}(n) \end{bmatrix} \begin{bmatrix} b_{11}(n) & \mathbf{b}_{21}^T(n) \\ \mathbf{0} & \mathbf{B}_{22}^T(n) \end{bmatrix} \quad (3.22)$$

Thus, comparing the respective terms on both sides of the equality (3.22), we get the following identities [36]:

$$|b_{11}(n)|^2 = \mathbf{r}^T(n) \mathbf{k}(n-1) \mathbf{r}(n) + 1 = \gamma(n) \quad (3.23)$$

$$\mathbf{b}_{21}(n) b_{11}(n) = \mathbf{k}(n-1) \mathbf{r}(n) \quad (3.24)$$

$$\mathbf{b}_{21}(n) \mathbf{b}_{21}^T(n) + \mathbf{B}_{22}(n) \mathbf{B}_{22}^T(n) = \mathbf{k}(n-1) \quad (3.25)$$

Eqs. (3.23) and (3.24) may be satisfied by choosing:

$$b_{11}(n) = \gamma^{1/2}(n) \quad (3.26)$$

$$\mathbf{b}_{21}(n) = \mathbf{k}(n-1) \mathbf{r}(n) \gamma^{-1/2}(n) = \mathbf{g}(n) \gamma^{1/2}(n) \quad (3.27)$$

$$\mathbf{B}_{22}(n) = \mathbf{k}^{1/2}(n) \quad (3.28)$$

where $\mathbf{g}(n)$ in Eq. (3.27) denotes the Kalman gain.

Then Eq. (3.21) can be rewritten as:

$$\begin{bmatrix} 1 & \mathbf{r}^T(n) \mathbf{k}^{1/2}(n-1) \\ \mathbf{0} & \mathbf{k}^{1/2}(n-1) \end{bmatrix} \boldsymbol{\theta}(n) = \begin{bmatrix} \gamma^{1/2}(n) & \mathbf{0}^T \\ \mathbf{g}(n) \gamma^{1/2}(n) & \mathbf{k}^{1/2}(n) \end{bmatrix} \quad (3.29)$$

Equation (3.29) shows that the element $\mathbf{k}(n)$ of the postarray is used to update the elements in the prearray, and therefore, initiate the next iteration of the algorithm. Moreover, the inclusion of the block elements $[1, \mathbf{0}]$ in the prearray induces the generation of block elements in the postarray which are used in the calculation of the Kalman gain $\mathbf{g}(n)$ and the variance of the estimation error $\gamma(n)$. Building on the latter result, we may readily update the state estimate, or the weight vector, as follows:

$$\mathbf{w}(n) = \mathbf{w}(n-1) + \mathbf{g}(n) \alpha(n) \quad (3.30)$$

where $\alpha(n)$ is the innovation defined by:

$$\alpha(n) = d(n) - \mathbf{r}^T(n) \mathbf{w}(n-1) \quad (3.31)$$

3.3.2 Givens rotations

The unitary transformation process may be carried out using the Givens rotations procedure. Through successive application of Givens rotations, we may develop a very efficient algorithm for solving the linear least squares problem, whereby the partial orthogonal triangularization of the data matrix is recursively updated as each new set of data enters the computation. To illustrate the procedure, assume that the partially triangularized data matrix of dimension $(N+1)$ -by- $(N+1)$ can, for simplicity, be written as:

$$\begin{bmatrix} 1 & A_{1,2} & A_{1,3} & \cdot & \cdot & A_{1,N+1} \\ 0 & A_{2,2} & 0 & 0 & \cdot & 0 \\ \cdot & \cdot & A_{3,3} & 0 & & 0 \\ \cdot & \cdot & & & & \cdot \\ \cdot & \cdot & & & \cdot & 0 \\ 0 & A_{N+1,2} & A_{N+1,3} & & & A_{N+1,N+1} \end{bmatrix}$$

To annihilate a block of zero entry in the top row of a partially triangularized matrix, a unitary matrix $\theta(n)$ may be adopted which is defined as follows:

$$\theta(n) = \prod_{k=1}^N \theta_k(n) \quad (3.32)$$

where $\theta_k(n)$ is a rotation matrix written as an identity matrix except for four elements on $(1,1)$, $(1,k+1)$, $(k+1,1)$ and $(k+1,k+1)$ positions defined by:

$$\theta_k(n) = \begin{bmatrix} c_k & & s_k^* & & & \\ & \mathbf{I}_{i-1} & & & & \\ -s_k & & c_k & & & \\ & & & \mathbf{I}_{N-k} & & \end{bmatrix} \quad (3.33)$$

where:

$$c_k = \cos \phi_k(n) \quad (3.34)$$

$$s_k = \sin \phi_k(n) e^{j\beta} \quad (3.35)$$

The proper selection of the rotation angles $\{\phi_k(n)\}$ will annihilate the non-zero element in the block row of the partially triangularized matrix. Then applying the first rotation $\theta_1(n)$ defined as

$$\theta_1(n) = \begin{bmatrix} c_1 & s_1^* & & & & \\ -s_1 & c_1 & & & & \\ & & \mathbf{I}_{N-1} & & & \end{bmatrix}$$

The resulting matrix will be:

$$\begin{bmatrix} c_1 - A_{1,2} s_1 & s_1^* + A_{1,2} c_1 & A_{1,3} & \cdot & \cdot & A_{1,N+1} \\ -A_{2,2} s_1 & A_{2,2} c_1 & 0 & 0 & \cdot & 0 \\ -A_{3,2} s_1 & \cdot & A_{3,3} & 0 & & \cdot \\ \cdot & \cdot & & & & \cdot \\ \cdot & \cdot & & & & 0 \\ -A_{N+1,2} s_1 & A_{N+1,2} c_1 & A_{N+1,3} & & & A_{N+1,N+1} \end{bmatrix}$$

The second element of the first row is set to zero, such that

$$s_1^* + A_{1,2} c_1 = 0. \quad (3.36)$$

and recognizing that

$$|s_1|^2 + |c_1|^2 = 1. \quad (3.37)$$

we get,

$$c_1 = \frac{1}{\sqrt{1 + |A_{1,2}|^2}}$$

and

$$s_1 = \frac{-A_{1,2}^*}{\sqrt{1 + |A_{1,2}|^2}} \quad (3.38)$$

The Givens rotation as described above operates on the first and second columns of the constructed matrix to annihilate the second element of the first row. In this process, all the elements of the first and second columns of the constructed matrix are modified. We then

choose $\theta_2(n)$ to annihilate the third element of the first row, and so on, until all the elements of the block array in the first row are annihilated. It is worth noting that the transformations $\theta_k(n)$ affect only the first and $(k+1)$ th column of the matrix, and the partially triangularized matrix form is preserved in each rotation.

The Givens rotation algorithm for annihilating the elements of the block entry in the first row is summarized in Table 3.2.

Table 3.2 Summary of the Givens rotation algorithm.

<i>Algorithm</i>	<i>Complexity</i>
For $n=1, 2, 3, \dots$ do For $k=1, N$ $a_{k,k} = \sqrt{ A_{1,1}(n-1) ^2 + A_{1,k+1}(n-1) ^2}$ If $ a_{k,k} > 0$., then $c_k = A_{1,1}(n-1)/a_{k,k}$ $s_k = A_{1,k+1}(n-1)/a_{k,k}$ Else $c_k = 1$. and $s_k = 0$. Endif $A_{1,1}(n) = A_{1,1}(n-1) c_k - A_{1,k+1}(n-1) s_k$ For $i = k+1, N+1$ $A_{i,1}(n) = A_{i,1}(n-1) c_k - A_{i,k+1}(n-1) s_k$ $A_{i,k+1}(n) = A_{i,1}(n-1) s_k^* + A_{i,k+1}(n-1) c_k$ End i End k	2N Mult. + N Square-root 2N Divisions 2N Mult N(N+1) Mult. N(N+1) Mult.
TOTAL	2N ² +6N Mult + 2N Divisions + N Square-roots

3.3.3 Householder transformation

The householder transformation may be used to annihilate the elements of the first row of the prearray, except for the first element. It is denoted by an $(N+1)$ -by- $(N+1)$ matrix [36]

$$\boldsymbol{\theta}(n) = \mathbf{I}(n) - \frac{2 \mathbf{u}(n) \mathbf{u}^T(n)}{\|\mathbf{u}(n)\|^2} \quad (3.39)$$

where $\mathbf{I}(n)$ is an $(N+1)$ -by- $(N+1)$ identity matrix, an $\mathbf{u}(n)$ is an $(M+1)$ -by-1 vector. To annihilate the elements of the vector $\mathbf{p}(n)$ except for the first, we may use one of the Householder transformations properties. It states that given a vector $\mathbf{p}(n)$, which may be defined as:

$$\mathbf{p}(n) = [1 \ \mathbf{r}^T(n) \mathbf{k}^{1/2}(n)]^T \quad (3.40)$$

then there exists a Householder transformation $\boldsymbol{\theta}(n)$ defined by the vector

$$\mathbf{z}(n) = \mathbf{p}(n) - \|\mathbf{p}(n)\| \mathbf{1} \quad (3.41)$$

where $\mathbf{1} = [1 \ 0 \ \dots \ 0]^T$ and $\|\mathbf{x}\|$ is the norm of the vector \mathbf{x} . The unitary transformation that annihilates the elements of the top row except the first element in the prearray is

$$\boldsymbol{\theta}(n) = \mathbf{I}(n) - \frac{2 \mathbf{z}(n) \mathbf{z}^T(n)}{\|\mathbf{z}(n)\|^2} \quad (3.42)$$

According to an error analysis under finite-precision computations [36], the Householder transformation is superior to the Givens rotation. However, the systolic array implementations are usually based on Givens rotation. On the other hand, the systolic array implementation based on Householder transformations is of block-oriented kind, with the block size providing a new variable. In particular increased stability is attained by increasing the block size, but at the expense of increased latency.

The SQRT-KF algorithm based on Givens rotations is summarized in Table 3.3. The computational complexity of the SQRT-KF algorithm is too high since it requires the

calculation of N arithmetic square-roots which is computationally expensive. Systolic array structures are used for parallel implementation of the algorithm which will reduce the complexity of the algorithm to $O[N]$. To avoid the use of the square roots, Omidi et al. [86] have proposed the use of a unit-lower-triangular-diagonal correction (LDC) method for the update of the Kalman filter. They used their algorithm for the joint estimation of channel and data detection over fading channels, in a mobile communication receiver. Systolic array structures are also proposed for its implementation. However, their algorithm is computationally expensive requiring $O[N^3]$ operations.

Table 3.3 Summary of the SQRT-KF algorithm.

<i>Input</i> $\mathbf{r}(n)$	
<i>Initialization</i> $\mathbf{w}(0)=\mathbf{0}$, $\mathbf{k}^{1/2}(0)=\delta^{1/2}\mathbf{I}$ where δ is a small number.	
<i>Algorithm</i>	<i>Complexity</i>
$\begin{bmatrix} 1 & \mathbf{r}^H(n) \mathbf{k}^{1/2}(n-1) \\ \mathbf{0} & \mathbf{k}^{1/2}(n-1) \end{bmatrix} \boldsymbol{\theta}(n) = \begin{bmatrix} \gamma^{1/2}(n) & \mathbf{0}^T \\ \mathbf{g}(n)\gamma^{1/2}(n) & \mathbf{k}^{1/2}(n) \end{bmatrix}$ $\mathbf{g}(n) = [\mathbf{g}(n)\gamma^{1/2}(n)] [\gamma^{1/2}(n)]^{-1}$ $\alpha(n) = d(n) - \mathbf{r}^H(n) \mathbf{w}(n-1)$ $\mathbf{w}(n) = \mathbf{w}(n-1) + \mathbf{g}(n) \alpha(n)$	$3N^2+6N$ Mult. $2N$ Divisions N Square-roots N Divisions N Mult. N Mult
TOTAL	$3N^2+8N$ Mult. $+ 3N$ Divisions $+ N$ Square-roots

3.4 Simulation results and discussion

In this section, a number of examples have been simulated to demonstrate the performance of the KF and SQRT-KF algorithms compared to other adaptive algorithms. Unless stated otherwise an asynchronous system is assumed, in which the delays are randomly generated from a uniform distribution. However, without loss of generality it is assumed that the receiver is synchronized with the desired user signal. The spreading codes are PN-sequences of length $N=31$. The receiver does not require the knowledge of the desired user spreading sequence. The SNR of the desired user is chosen to be equal to 20dB. Ensemble averaging over 100 independent trials is performed when the convergence characteristics curves are evaluated

Example 3.1

In this example, an asynchronous DS-CDMA receiver based on the KF algorithm has been simulated having a desired user with variable number of interferers. Each interferer has 10dB power advantage over the desired user at 20dB input SNR. Figure 3.1 shows the convergence characteristics using the KF algorithm. An assessment of this figure clearly shows that as the number of interferers increases the convergence rate becomes slower and the residual MSE increases. For example, for a single-user (no MAI) case, the receiver converges within 40 bits to a residual MSE of nearly -20dB, while for the four interferers case, the receiver converges within 60 bits to nearly -18dB residual MSE.

Example 3.2

In this example, KF, NLMS and the RLS adaptive algorithms are used to adapt the weights vector of the DS-CDMA receiver. For comparison purposes results for block algorithms are provided. Four and eight interferers have been considered, each interferer has 10 dB power advantage over the desired user. The block length, for the block algorithm, is

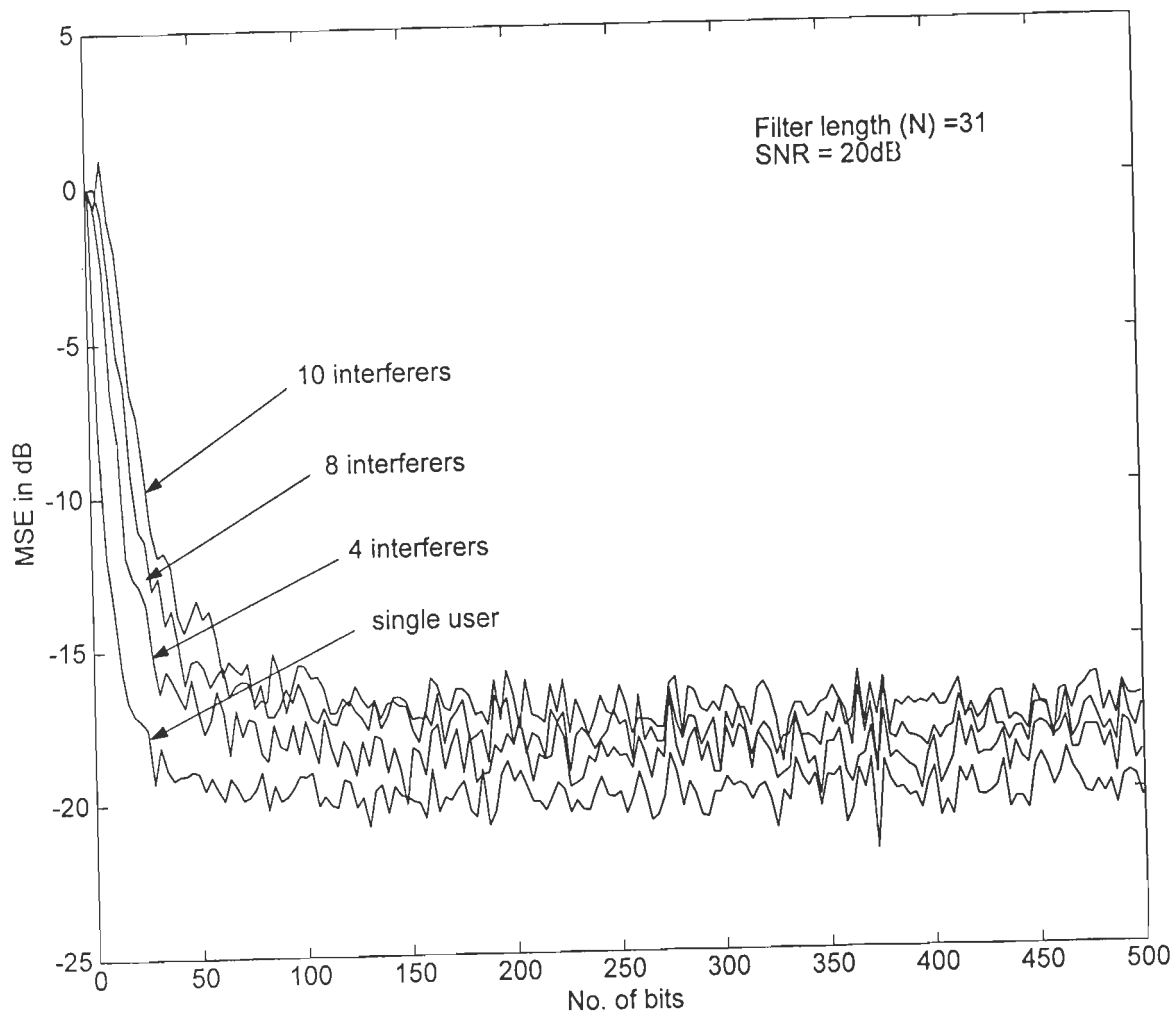


Fig 3.1 Convergence characteristics for the adaptive DS-CDMA receiver using the KF algorithm with different number of interferers (each interferer has 10dB power advantage over the desired user)

chosen to be $L=4$. The step-size of both the NLMS and the block algorithm has been tuned such that, in all the cases, the residual MSE is approximately the same, and, hence a fair comparison can be achieved.

It is clear from Fig.3.2 that the KF and RLS algorithms possess comparable convergence characteristics, which is better than the block algorithm and much faster than that of the NLMS algorithm. For example, for the 4-interferers case, the NLMS algorithm converges in about 500 bits compared to about 50 bits for the KF and RLS algorithms and about 80 bits for the block algorithm. For 8-interferers case, the NLMS algorithm converges in about 600 bits compared to about 80 bits for both KF and RLS algorithms and about 180 bits for the block algorithm. It is concluded that the KF algorithm provides a comparable performance to the RLS algorithm, but much better than the NLMS algorithm. However, the computational complexity of the KF algorithm is $O[N^2]$, which is comparable to that of the RLS algorithm, but it is an order of magnitude higher than that of the NLMS and block algorithms.

Example 3.3

In this example, the probability of error performance for the adaptive DS-CDMA receiver is examined using SQRT-KF and NLMS algorithms. Two cases are simulated, one with 8-interferers, while the other with 10-interferers, each having 10 dB power advantage above the desired user. The step-size of the NLMS algorithm is adjusted such that the two adaptive algorithms will possess approximately the same residual MSE in the single-user case. It is quite clear from Fig.3.3 that the probability of error performance for the two algorithms is almost comparable and is close to the theoretical values. Also provided with the figure are the lower (single-user) and upper (matched filter) bounds, for comparison purposes. It is quite clear that the proposed detector based on the SQRT-KF algorithm

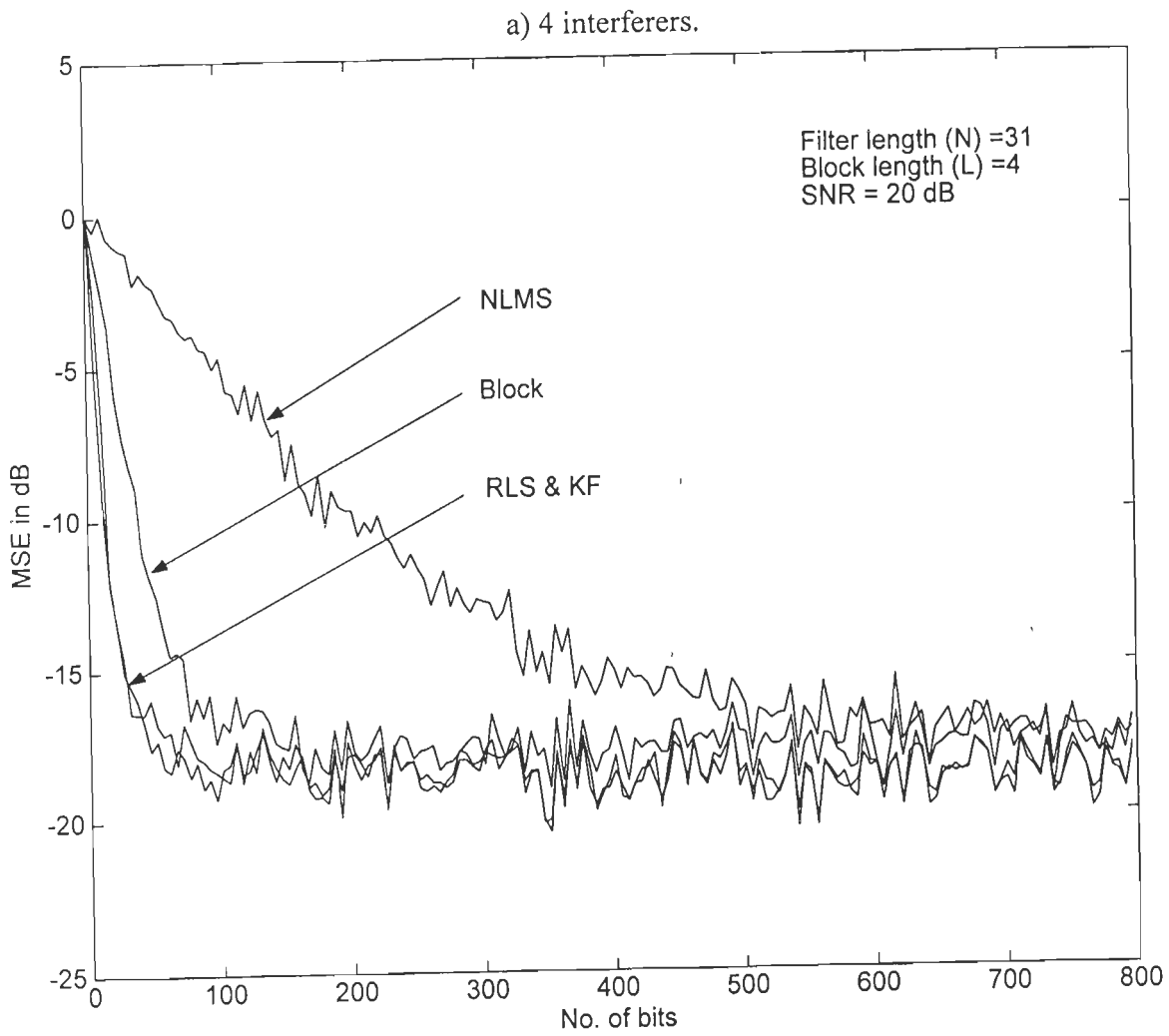


Fig.3.2 Comparison of the convergence characteristics for the adaptive DS-CDMA receiver using the NLMS, RLS, KF and block algorithm with a) 4 interferers
b) 8 interferers (each interferer has 10dB power advantage over the desired user)

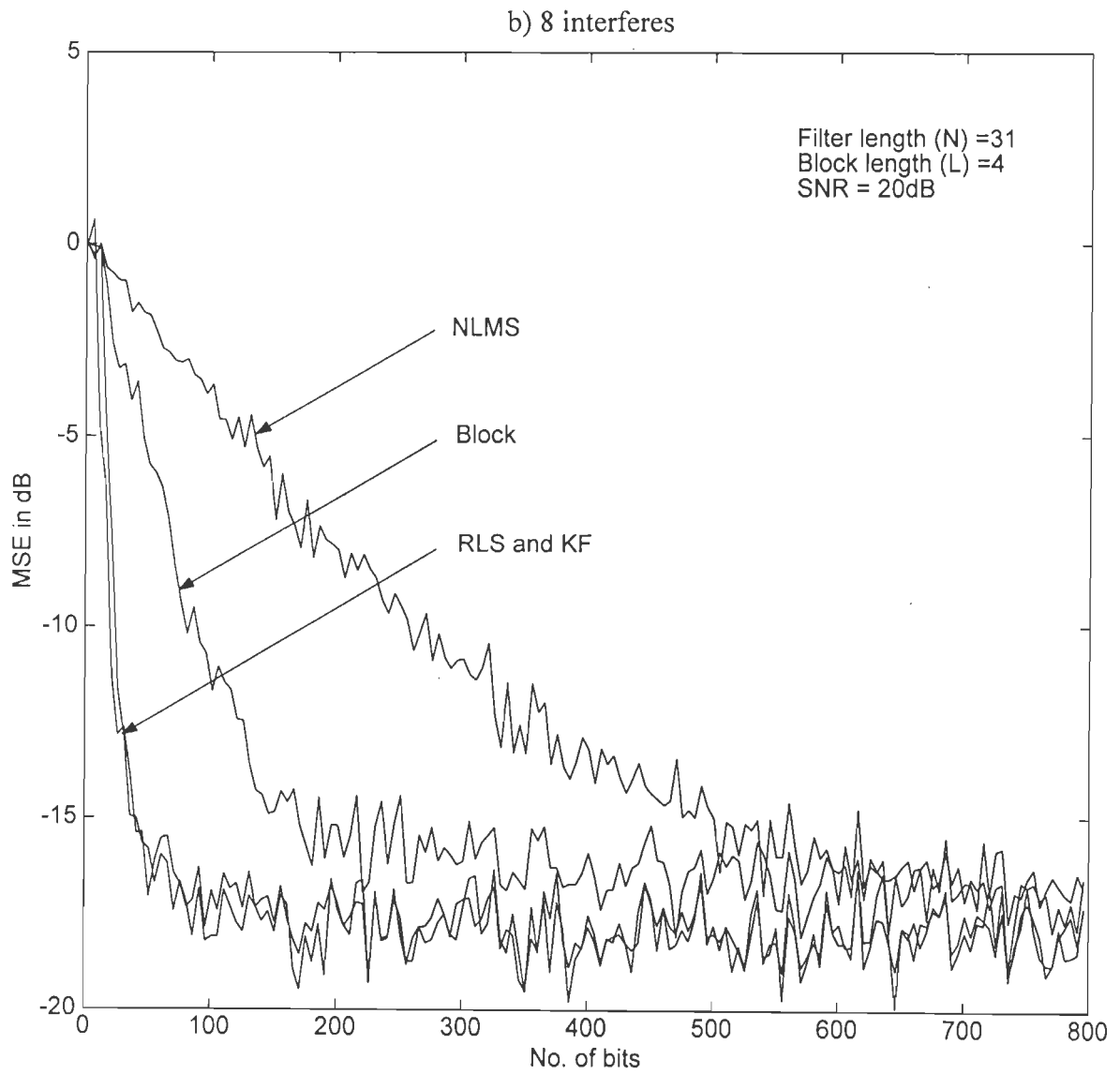


Fig.3.2b

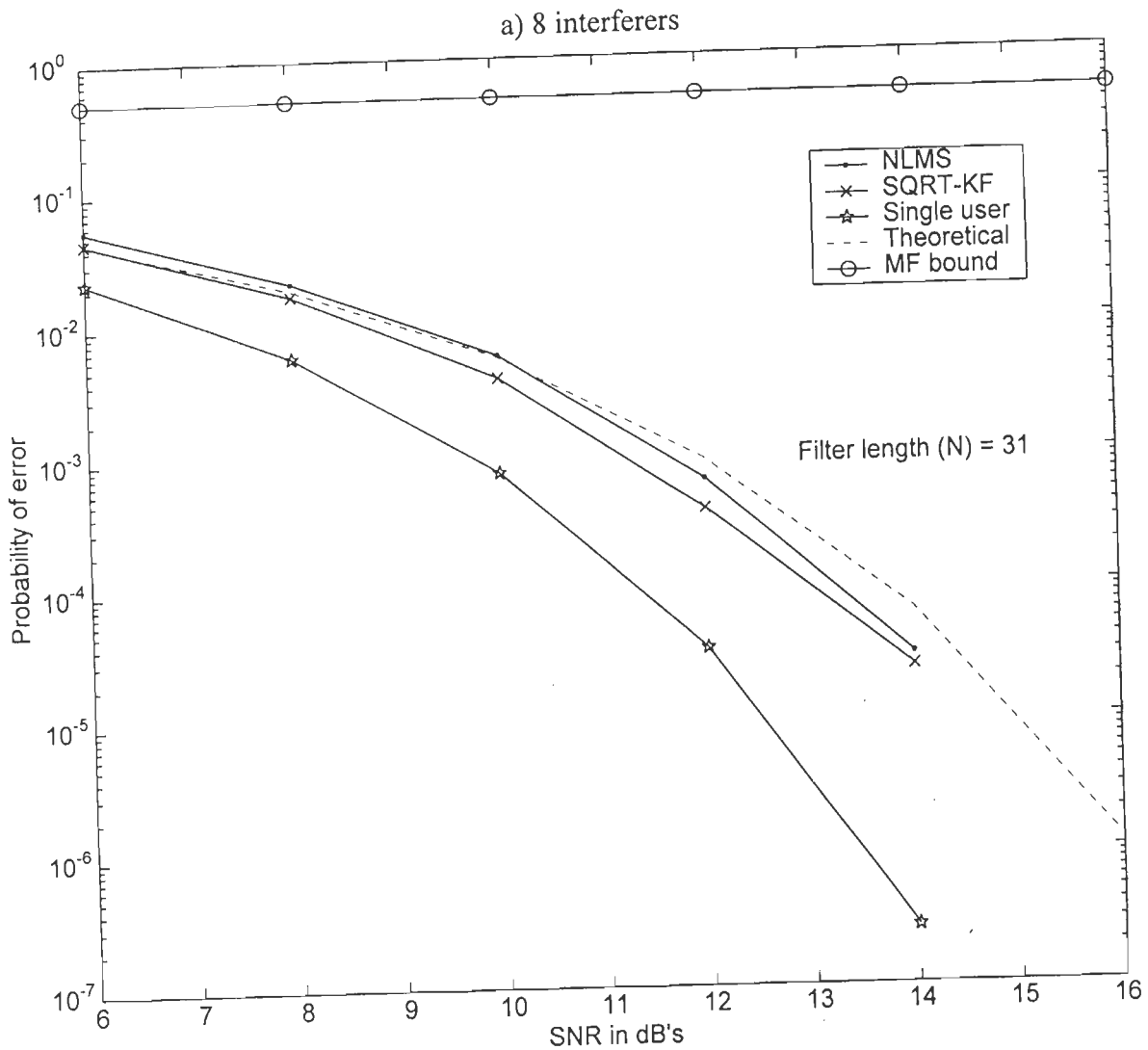


Fig.3.3 Probability of error performance for the adaptive DS-CDMA receiver using the NLMS and SQRT-KF algorithms with a) 8 interferers b) 10 interferers (each interferer has 10dB power advantage over the desired user).

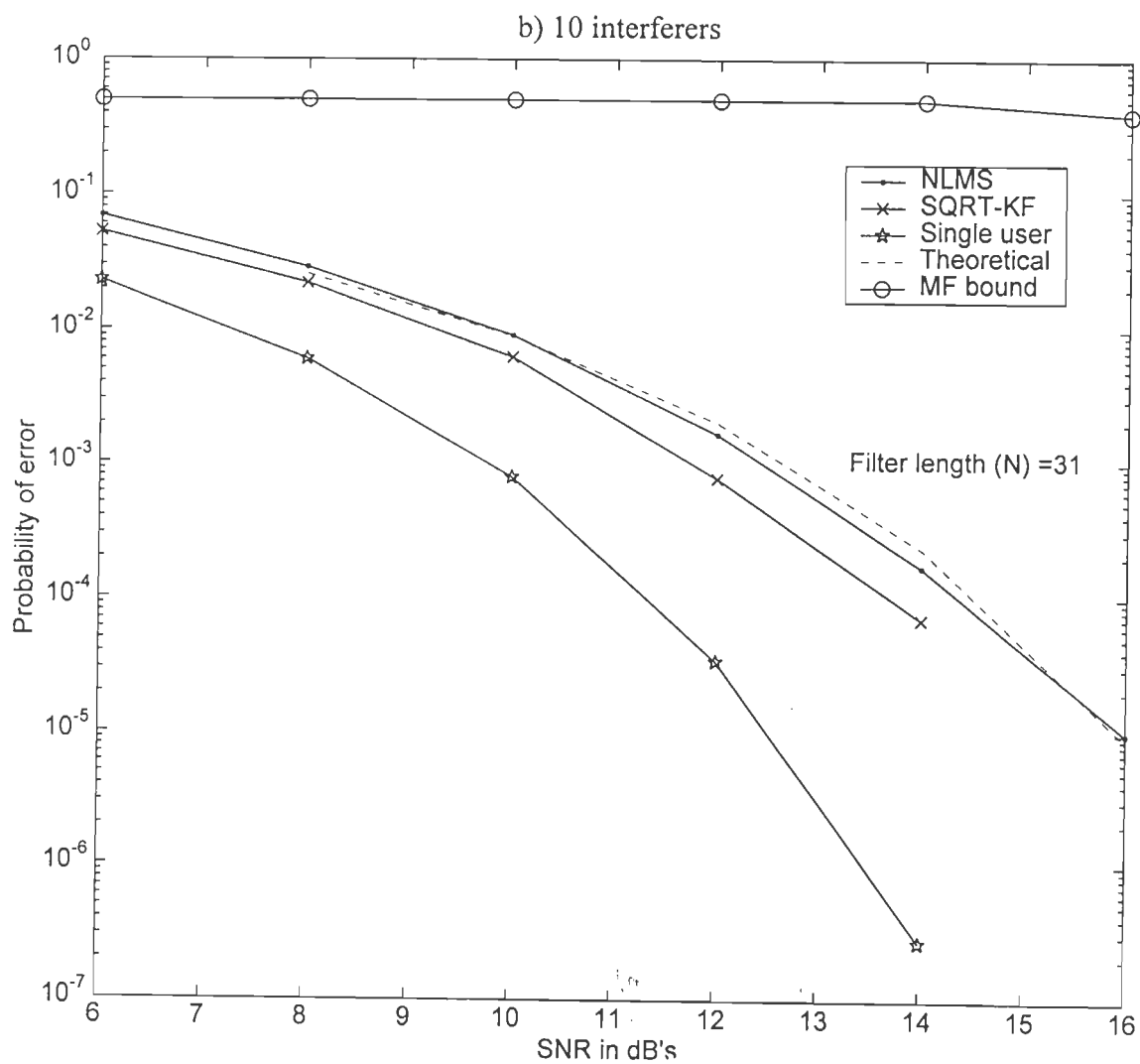


Fig.3.3b

outperforms the conventional detector. On the other hand for the 8-interferers case, the performance degradation in terms of the input SNR, using the SQRT-KF, is about 2dB as compared to the single user, while it is about 3dB for the 10-interferers case.

Example 3.4

In this example, an adaptive DS-CDMA receiver is simulated using the SQRT-KF and NLMS algorithms. The interferers' power is varied from -2dB to 10dB relative to the desired user at 10dB and 12dB input SNR respectively. The value of the step-size of the NLMS is adjusted such that the single-user residual MSE for the two algorithms is the same. It is shown in Fig.3.4a that the probability of error remains constant even if the power of the interferers increases by 10dB relative to the desired user. This clearly demonstrates the near-far resistance of the receiver based on the two algorithms. Also it is noticed that the SQRT-KF algorithm performs slightly better than the NLMS algorithm. In Fig.3.4b the effect of changing the number of interferers on the performance of the DS-CDMA based on the SQRT-KF algorithm is presented for 2- and 5-users cases. It is clear again that the SQRT-KF algorithm is near-far resistant for larger number of users. Also slight performance degradation is noticed when increasing the number of users.

Example 3.5

In this example, the probability of error for the adaptive DS-CDMA receiver using SQRT-KF and NLMS algorithms is evaluated as a function of number of users. All interferers have 10dB power advantage above the desired user. The simulation is performed at input SNR 10dB and 12dB . It is clear from Fig.3.5 that the probability of error increases with the increase in the number of interferers (since the overall interference power will increase), and also it is noticed that the SQRT-KF performs slightly better than the NLMS algorithm for both values of input SNR.

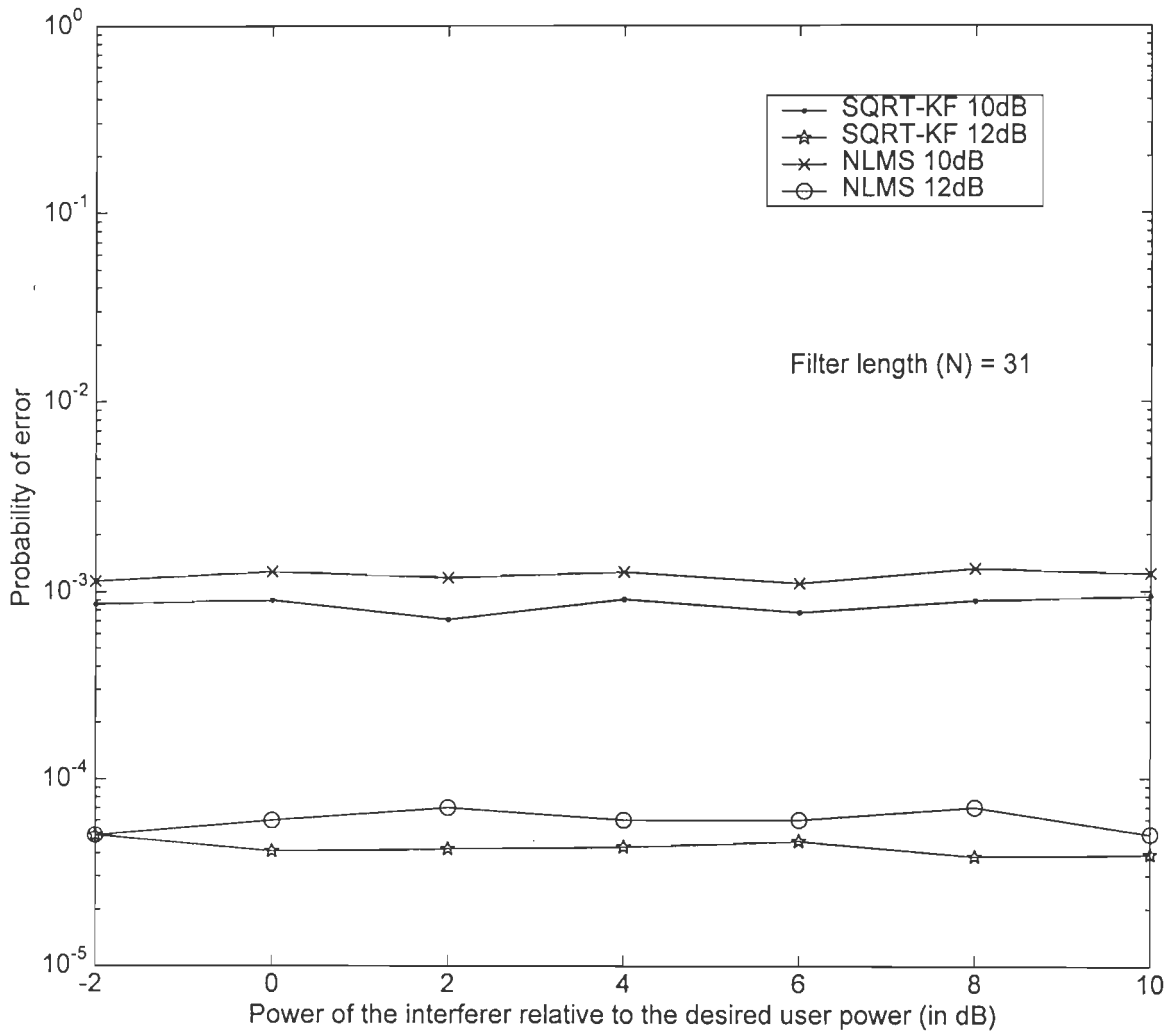


Fig.3.4a Probability of error performance for the desired user's as a function of the second user's power relative to the desired user power at input SNR 10dB and 12dB using the NLMS and SQRT- KF algorithms.

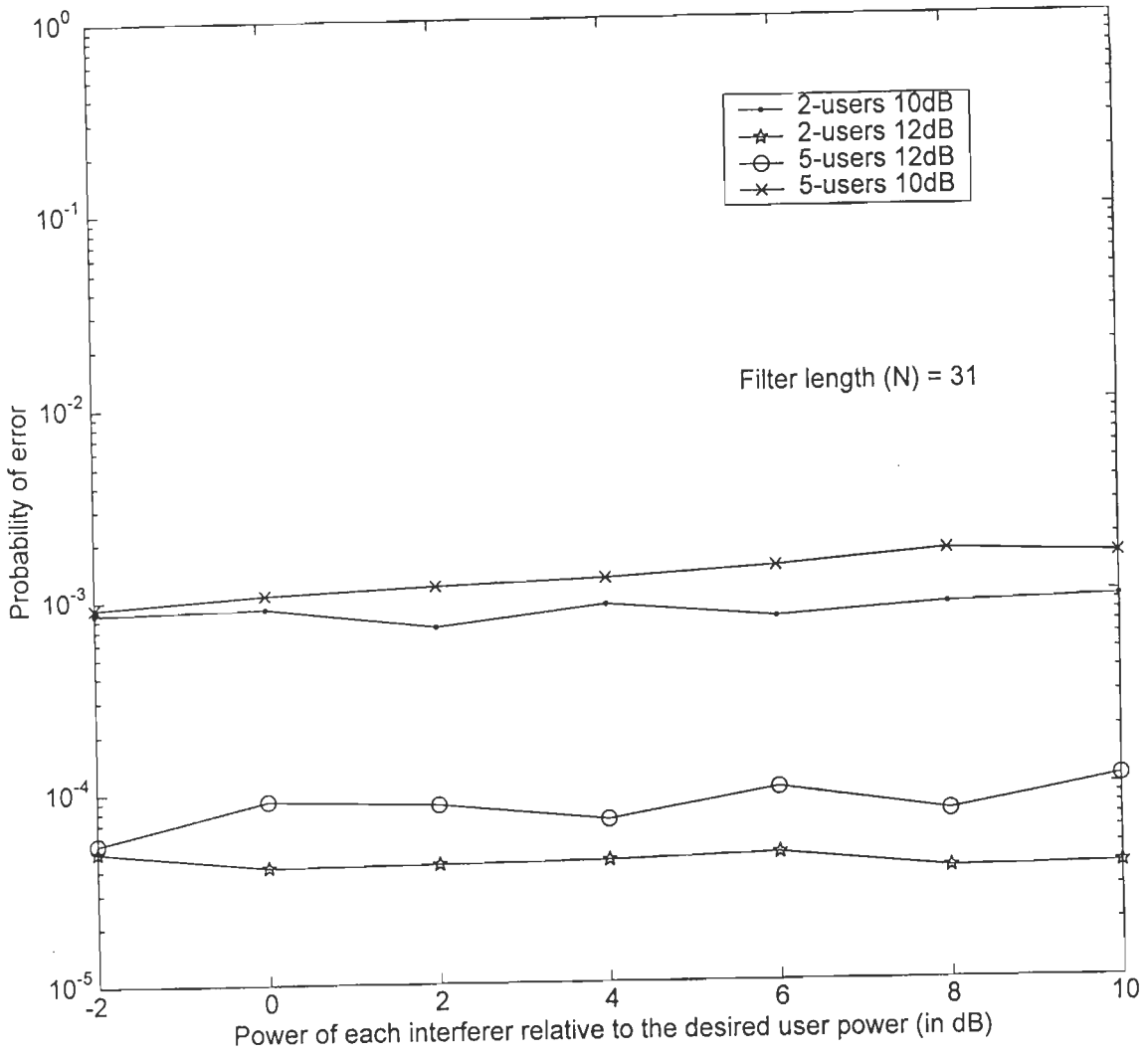


Fig.3.4b Probability of error performance for the desired user as a function of the interferer's power relative to the desired user power at input SNR of 10dB and 12dB using the SQRT-KF algorithm.

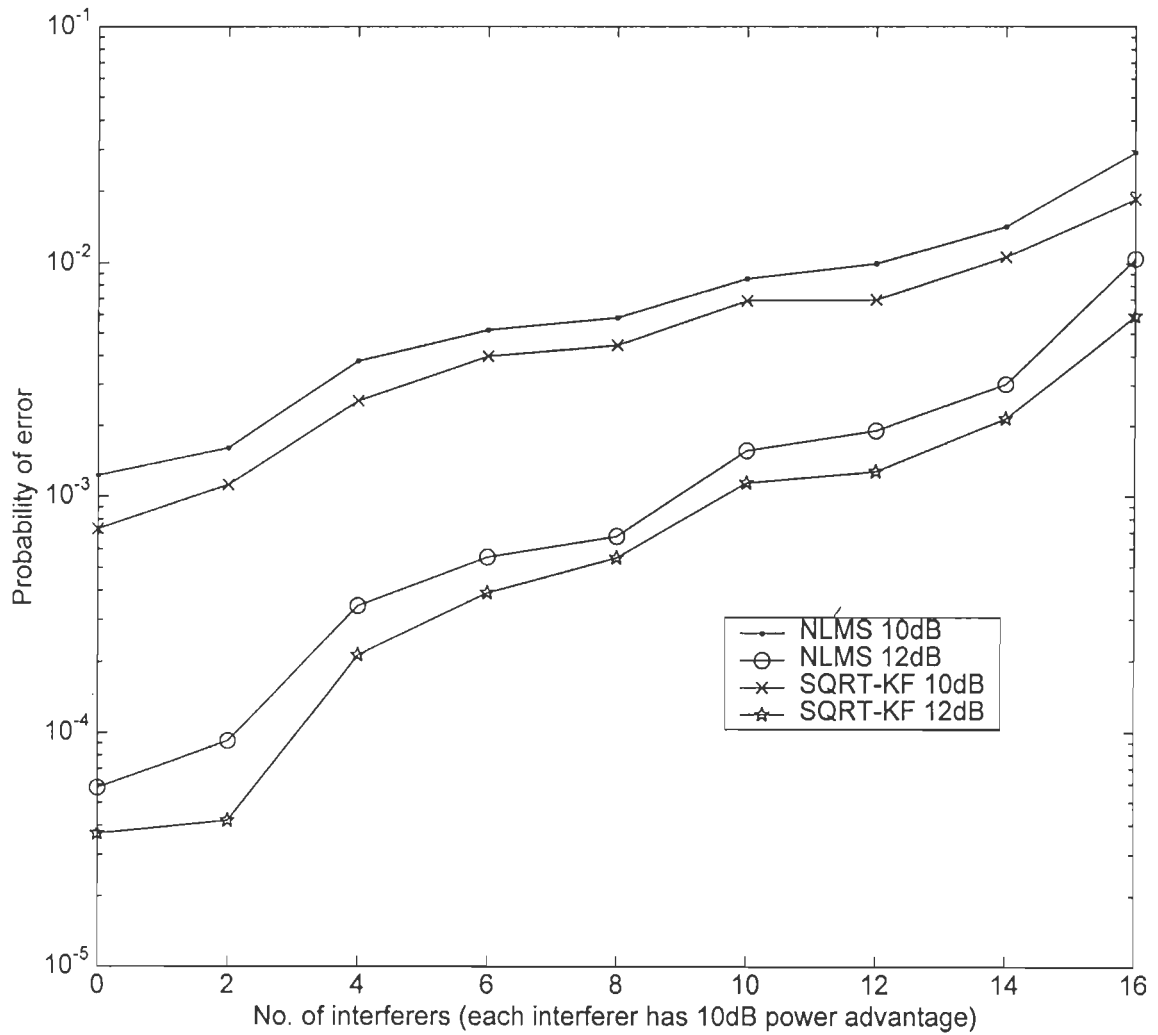


Fig.3.5 Probability of error performance for the adaptive DS-CDMA receiver as a function of the number of interferers using the NLMS and SQRT-KF algorithms at input SNR of 10dB and 12dB.

Due to its optimality in the MMSE sense, the KF algorithm has been used for the weights adaptation in DS-CDMA receivers. Improved performance of the KF algorithm as compared to the NLMS algorithm has been shown. To deal with the instability problem of the KF, the numerically stable SQRT-KF based on either Givens rotations or Householder transformations have been used. The near-far resistance of the DS-CDMA receiver based on the SQRT-KF algorithm has also been demonstrated.

RMGS-BASED ADAPTIVE INTERFERENCE SUPPRESSION IN DS-CDMA SYSTEMS

Computational complexity, rate of convergence, parallelism and numerical robustness are important issues for characterizing the performance of adaptive algorithms. Direct matrix inversion approach for finding the LS weights vector is computationally too expensive and can be avoided using the LMS algorithm. However, as mentioned in chapter two, the LMS algorithm suffers from slow convergence rate due to the dependence of the convergence time constant on the eigenvalue spread of the input autocorrelation matrix. This has motivated the development of adaptive LS algorithms, which are numerically robust, possess fast convergence rate and are insensitive to the input signal statistics. The most popular time-recursive LS estimation scheme is the classical RLS algorithm, but it is sensitive to the round off errors when finite precession arithmetic is used for its implementation. The Kalman filter, which is optimal in the MMSE sense, also suffers from the numerical instability problem and moreover, it requires the knowledge of the noise variance. On the other hand, the SQRT-KF is more stable, but requires high computational complexity. To remedy these problems, algorithms based on matrix factorizations and orthogonal transformations, of the input correlation matrix, have been used [55], which are less sensitive to roundoff errors, and, moreover can be efficiently mapped into systolic array structure for parallel implementation.

In this chapter, we propose the implementation of the recursive modified Gram-Schmidt (RMGS) algorithm for the adaptation and demodulation of DS-CDMA signals. The RMGS algorithm is more stable as compared to both RLS and KF algorithms, and moreover, it

require lower computations as compared to other QR-RLS algorithms. The organization of this chapter is as follows. In section 4.1, we review the matrix factorization and orthogonalization algorithms. The QR-RLS and the inverse QR-RLS algorithms, which are used to solve the LS problem in the data domain, via Givens rotations, are discussed in sections 4.2 and 4.3, respectively. Then the RMGS algorithm and its error feedback version for the adaptation and demodulation of DS-CDMA signals are presented in section 4.4. Parallel implementation of the RMGS algorithm on systolic array is also introduced along with its computational complexity. Finally, computer simulation results along with a comparison of the performance of the proposed algorithm with other algorithms are given in section 4.5.

4.1 Introduction

One of the problems encountered in applying the RLS algorithm, introduced in chapter two, is that of numerical instability due to the way in which the Riccati difference equation has been formulated. The same problem also occurs in the classical Kalman filter, introduced in chapter three, for exactly the same reason. It has been shown that the instability problem can be avoided by using square-root variant of the filter. Moreover, the computation of the least-squares weight vector of the adaptive filtering algorithm may be accomplished by working directly with the incoming data matrix, via matrix factorization and decomposition, rather than working with the (time-averaged) correlation matrix of the input data as in the conventional RLS algorithm [36]. Accordingly, factorization and orthogonalization of the data matrix will be numerically more stable than the conventional RLS algorithm. This has led to the development of a class of adaptive algorithms based on numerically robust QR factorization of the input data matrix via Givens rotation [30]. A Givens rotation-based QR decomposition has been developed in [24, 73] which updates the Cholesky factor of the input

data matrix and can be efficiently implemented on systolic arrays for parallel implementation. McWhirter [73] showed that the error could be extracted directly without computing the estimate of the transversal parameters of the unknown FIR system. Two rotation-based QR-RLS algorithms are proposed in [93] for blind adaptation of DS-CDMA systems. These algorithms exhibit high degrees of parallelism, and can be mapped to VLSI systolic arrays to exploit massively parallel signal processing computation. Using a single triangular array, demodulation of multiple synchronous streams of information bits can be carried out simultaneously. However, it is shown in the following that they are computationally expensive, and moreover they also involve computation of square roots.

Ling et al. have presented a time-recursive Gram-Schmidt algorithm (RMGS) for solving a general LS minimization problem, which is computationally more efficient than the QR-RLS algorithms mentioned above. This algorithm is reported to be robust to roundoff errors and can be implemented using systolic structure. Also, the authors have presented an improved error feedback version of the RMGS algorithm (RMGSEF), which is more robust as compared to RMGS algorithm. E.K.B. Lee has presented an adaptive orthogonalization technique, in which the coefficients are derived from the Cholesky factorization of the correlation matrix [123]. The result is the set of backward prediction errors that are well known to form an orthogonal set. It was demonstrated that with such prefiltering, convergence of an LMS MMSE filter for CDMA was rendered insensitive to eigenvalue spread. An alternative scheme based on the update of the inverse Cholesky factor of the data correlation matrix has also been developed in [4]. In this algorithm the error signal is obtained without using the computationally expensive back-substitution method.

In order to implement the adaptive algorithms based on matrix factorization and orthogonal transformations, for the adaptation and demodulation of the CDMA signals, the

problem is formulated as follows. After the baseband conversion, the complex baseband signal is chip-matched filtered and sampled at the chip rate. The sampled signal, $\tilde{\mathbf{r}}(n)$, is then fed into a tapped delay line (TDL) filter of length N (Fig. 2.3). The output of the TDL filter is sampled at the bit interval, and hard-limited to form an estimate of the desired user data bit $d_1(n)$. The output of the TDL filter may be written as,

$$y(n) = \tilde{\mathbf{w}}^H(n) \tilde{\mathbf{r}}(n) \quad (4.1)$$

where H stands for the Hermitian (complex transpose), $\tilde{\mathbf{r}}(n) = [\tilde{r}_0(n), \tilde{r}_1(n), \dots, \tilde{r}_{N-1}(n)]^T$ is the TDL contents, and $\tilde{\mathbf{w}}(n) = [w_0(n), w_1(n), \dots, w_{N-1}(n)]^T$ and are the TDL filter weights during interval $(n-1)T < t < nT$, which minimizes $\varepsilon(n)$, the exponentially weighted sum of squared errors defined as:

$$\varepsilon(n) = \sum_{i=1}^n \lambda^{n-i} e^2(i) = \sum_{i=1}^n \lambda^{n-i} |d_1(i) - \tilde{\mathbf{w}}^H(n) \tilde{\mathbf{r}}(n)|^2 \quad (4.2)$$

where λ , the forgetting factor, is less than but close to unity. This is the well-known least-squares problem. The minimization of Eq.(4.2) is equivalent to the LS problem for solving the linear system of equations:

$$\mathbf{A}(n) \tilde{\mathbf{w}}(n) = \mathbf{D}(n) \quad (4.3)$$

where

$$\mathbf{D}(n) = [\sqrt{\lambda^n} d_1(1), \sqrt{\lambda^{n-1}} d_1(2), \dots, d_1(n)]^T$$

and

$$\mathbf{A}(n) = [\tilde{\mathbf{r}}(1), \tilde{\mathbf{r}}(2), \dots, \tilde{\mathbf{r}}(n)]$$

4.2 The QR-RLS algorithm

Square-root adaptive filtering algorithms for RLS estimation are known as QR-RLS algorithm, extended QRLS and inverse QR-RLS algorithm [36]. The derivation of the QR-

RLS algorithm has traditionally relied on the use of orthogonal triangularization process known as QR-decomposition [36]. The motivation for using the QR-decomposition technique is to exploit its good numerical properties. The QR-RLS algorithm works directly with the data matrix rather than with the correlation matrix, and since the condition number ($\lambda_{\max}/\lambda_{\min}$) of the data matrix is much smaller than the condition number of the correlation matrix, the QR-RLS algorithm is numerically more stable than the RLS algorithm.

Assuming that the input-data matrix can be constructed as $\mathbf{A}(n) = [\tilde{\mathbf{r}}(1), \tilde{\mathbf{r}}(2), \dots, \tilde{\mathbf{r}}(N)]$ of dimension N-by-N, where N is the TDL filter length, then the correlation matrix of the input data is defined by:

$$\mathbf{R}(n) = \sum_{i=1}^n \lambda^{n-i} \tilde{\mathbf{r}}(i) \tilde{\mathbf{r}}^H(i) = \mathbf{A}(n) \Lambda(n) \mathbf{A}^H(n) \quad (4.4)$$

The matrix $\Lambda(n)$ is called the exponential weighting matrix defined by:

$$\Lambda(n) = \text{diag} [\lambda^{n-1}, \lambda^{n-2}, \dots, 1] \quad (4.5)$$

The tap-weight vector $\mathbf{w}(n)$ is defined by:

$$\mathbf{R}(n) \tilde{\mathbf{w}}(n) = \mathbf{P}(n) \quad (4.6)$$

where $\mathbf{P}(n) = E[d_1(n) \tilde{\mathbf{r}}(n)]$ is cross-correlation vector between the desired response $d_1(n)$ and the input vector $\tilde{\mathbf{r}}(n)$. Let $\mathbf{R}(n)$ be expressed in its factored form:

$$\mathbf{R}(n) = \mathbf{R}^{1/2}(n) \mathbf{R}^{H/2}(n) \quad (4.7)$$

Then, premultiplying Eq.(4.6) By the square root $\mathbf{R}^{-1/2}(n)$, we may introduce a new vector variable $\mathbf{u}(n)$ defined by:

$$\mathbf{u}(n) = \mathbf{R}^{H/2}(n) \mathbf{w}(n) = \mathbf{R}^{-1/2}(n) \mathbf{P}(n) \quad (4.8)$$

To formulate the QR-RLS algorithm for linear predictive filtering, the following matrices are constructed in [36, 101]:

$$\begin{bmatrix} \lambda^{1/2} \mathbf{R}^{1/2}(n-1) & \tilde{\mathbf{r}}(n) \\ \lambda^{1/2} \mathbf{u}^H(n-1) & d(n) \\ \mathbf{0}^T & 1 \end{bmatrix} \boldsymbol{\theta}(n) = \begin{bmatrix} \mathbf{R}^{1/2}(n) & \mathbf{0} \\ \mathbf{u}^H(n) & \kappa \gamma^{1/2}(n) \\ \tilde{\mathbf{r}}^H(n) \mathbf{R}^{-H/2}(n) & \gamma^{1/2}(n) \end{bmatrix} \quad (4.9)$$

where $\boldsymbol{\theta}(n)$ is a unitary rotation that operates on the elements of the input vector $\tilde{\mathbf{r}}(n)$ in the prearray, annihilating them one by one so as to produce a block zero entry in the block row of the postarray. The unitary rotations may be performed via Givens rotations or Householder transformations discussed in chapter three. Naturally, the lower triangular structure of the square root of the correlation matrix, namely $\mathbf{R}^{1/2}(n)$, is preserved in its exact form after the transformation.

The computed updated block values $\mathbf{R}^{1/2}(n)$ and $\mathbf{u}^H(n)$ are used to solve the LS weight vector:

$$\tilde{\mathbf{w}}^H(n) \mathbf{R}^{1/2}(n) = \mathbf{u}^H(n) \quad (4.10)$$

where the back-substitution method is used in the last computation exploiting the lower triangular structure of $\mathbf{R}^{1/2}(n)$. For the initialization of the QR-RLS algorithm, we may set $\mathbf{R}^{1/2}(0)=\mathbf{0}$ and $\mathbf{u}(0)=\mathbf{0}$. A summary of the QR-RLS algorithm is presented in Table 4.1.

The unitary matrix can be expressed as:

$$\boldsymbol{\theta}(n) = \prod_{k=1}^N \boldsymbol{\theta}_k \quad (4.11)$$

where $\boldsymbol{\theta}_k$ consists of a unitary matrix except for four strategic elements located at the points where the pair of rows, k and $N+1$ intersects the pair of columns, k and $N+1$. These four elements denoted by $\theta_{k,k}$, $\theta_{N+1,k}$, $\theta_{k,N+1}$ and $\theta_{N+1,N+1}$, are defined as follows:

$$\begin{aligned} \theta_{k,k} &= \theta_{N+1,N+1} = c_k \\ \theta_{N+1,k} &= s_k^* & (k=1, 2, \dots, N) \\ \theta_{k,N+1} &= -s_k \end{aligned} \quad (4.12)$$

The cosine parameters c_k are real, whereas the sine parameters s_k are complex.

Table 4.1 Summary of the QR-RLS algorithm.

<i>Input</i> $\tilde{\mathbf{r}}(n), d_1(n), \lambda$	
<i>Initial condition</i> $\mathbf{R}^{1/2}(0)=\mathbf{0}, \mathbf{u}(0)=\mathbf{0}$.	
<i>Algorithm</i>	<i>Complexity</i>
For $n=1, 2, \dots$ compute	
$\begin{bmatrix} \lambda^{-1/2} \mathbf{R}^{1/2}(n-1) & \tilde{\mathbf{r}}(n) \\ \lambda^{1/2} \mathbf{u}^H(n-1) & d_1(n) \\ \mathbf{0}^T & 1 \end{bmatrix} \boldsymbol{\theta}(n) = \begin{bmatrix} \mathbf{R}^{1/2}(n) & \mathbf{0} \\ \mathbf{u}^H(n) & \kappa \gamma^{1/2}(n) \\ \tilde{\mathbf{r}}^H(n) \mathbf{R}^{-H/2}(n) & \gamma^{1/2}(n) \end{bmatrix}$	$3N^2+7.5N$ Mult. $+ 2N$ Div. $+ N$ Square-roots.
$\tilde{\mathbf{w}}^H(n) \mathbf{R}^{1/2}(n) = \mathbf{u}^H(n)$	$N(N-1)/2$ Mult. $+ N$ Div.
TOTAL	$3.5N^2+7$ Mult. $+ 3N$ Div. $+ N$ Square-roots

4.3 Inverse QR-RLS algorithm

In this algorithm, instead of operating on the correlation matrix $\mathbf{R}(n)$, as in the conventional QR-RLS algorithm, the operation is performed on the inverse of $\mathbf{R}(n)$ [4]. Referring to Eq. (3.29), the inverse QR-RLS algorithm may be written as follows (after canceling common terms) [36, 101]:

$$\begin{bmatrix} 1 & \lambda^{-1/2} \tilde{\mathbf{r}}^H(n) \mathbf{R}^{-1/2}(n-1) \\ \mathbf{0} & \lambda^{-1/2} \mathbf{R}^{-1/2}(n-1) \end{bmatrix} \boldsymbol{\theta}(n) = \begin{bmatrix} \gamma^{-1/2}(n) & \mathbf{0}^T \\ \mathbf{g}(n) \gamma^{-1/2} & \mathbf{R}^{-1/2}(n) \end{bmatrix} \quad (4.13)$$

where $\boldsymbol{\theta}(n)$ is a unitary rotation, based on Givens rotations, that operates on the block entry $\lambda^{-1/2} \tilde{\mathbf{r}}^H(n) \mathbf{R}^{-1/2}(n-1)$ in the prearray by annihilating its elements, one by one, so as to produce a block zero entry in the first row of the postarray. The gain factor $\mathbf{g}(n)$ is computed by:

$$\mathbf{g}(n) = [\mathbf{g}(n) \gamma^{-1/2}] [\gamma^{-1/2}]^{-1} \quad (4.14)$$

The LS weight vector may be updated by:

$$\tilde{\mathbf{w}}(n) = \tilde{\mathbf{w}}(n-1) + \mathbf{g}(n) \alpha^*(n) \quad (4.15)$$

where $\alpha(n)$ is the a priori estimation error defined as:

$$\alpha(n) = d(n) - \tilde{\mathbf{w}}^H(n-1) \tilde{\mathbf{r}}(n) \quad (4.16)$$

A summary of the inverse QR-RLS algorithm is presented in Table 4.2 [36, 101].

Table 4.2 Summary of the inverse QR-RLS algorithm.

Input $\tilde{\mathbf{r}}(n), d_1(n), \lambda$	
Initialization $\mathbf{R}^{1/2}(0) = \delta^{-1/2} \mathbf{I}$, δ is a small positive number, $\tilde{\mathbf{w}}(0) = \mathbf{0}$.	
Algorithm	Complexity
For $n=1, 2, \dots$, compute	
$\begin{bmatrix} 1 & \lambda^{-1/2} \tilde{\mathbf{r}}^H(n) \mathbf{R}^{-1/2}(n-1) \\ \mathbf{0} & \lambda^{-1/2} \mathbf{R}^{-1/2}(n-1) \end{bmatrix} \boldsymbol{\theta}(n) = \begin{bmatrix} \gamma^{-1/2}(n) & \mathbf{0}^T \\ \mathbf{g}(n) \gamma^{-1/2}(n) & \mathbf{R}^{-1/2}(n) \end{bmatrix}$	$4N^2 + 7N$ Mult. $+ 2N$ Div. $+ N$ Square roots
$\mathbf{g}(n) = [\mathbf{g}(n) \gamma^{-1/2}] [\gamma^{-1/2}]^{-1}$	N Div.
$\tilde{\mathbf{w}}(n) = \tilde{\mathbf{w}}(n-1) + \mathbf{g}(n) \alpha^*(n)$	N Mult.
$\alpha(n) = d(n) - \tilde{\mathbf{w}}^H(n-1) \tilde{\mathbf{r}}(n)$	N Mult.
TOTAL	$4N^2 + 9N$ Mult. $+ 3N$ Div. $+ N$ Square-roots

where $\boldsymbol{\theta}(n)$ is a unitary rotation that produces a zero in the first row of the postarray. Since the square root $\mathbf{R}^{1/2}(n)$ is lower triangular, then its inverse matrix $\mathbf{R}^{-1/2}(n)$ is upper triangular.

The inverse QR-RLS [36] algorithm differs from the conventional QR-RLS algorithm in a fundamental way. Specifically, the input data vector $\tilde{\mathbf{r}}(n)$ does not appear by itself as a block entry in the prearray of the algorithm; rather it is multiplied by $\lambda^{-1/2} \mathbf{R}^{-1/2}(n)$. Hence, the

input data vector has to be preprocessed prior to performing the rotations. This adds computational complexity to the parallel implementation of the inverse QR-RLS algorithm. The computation of the weights vector in the inverse QR-RLS algorithm does not involve the back substitution method as in the conventional QR-RLS algorithms, where it requires additional computations.

4.4 The RMGS algorithm

The Gram-Schmidt procedure for solving the LS estimation problem has very poor numerical characteristics. A rearrangement of the steps of the Gram-Schmidt procedure, known as Modified GS (MGS) procedure yields a method, which is computationally sound with good numerical properties [55]. However, the MGS is a block-processing algorithm and is not efficient when it is implemented in time recursive form. Ling et al. [63] have derived a time recursive form of the MGS procedure, viz., the recursive MGS and its error feedback form for the least squares estimation. Jagdeesha et al. [45] have derived the complex form of the RMGS algorithm.

The LS problem can be solved using the modified Gram-Schmidt method as follows [55]. First, we combine $\mathbf{A}(n)$ and $\mathbf{D}(n)$, defined in section 4.1, as:

$$\mathbf{A}_t(n) = [\mathbf{A}(n), \mathbf{D}(n)] \quad (4.17)$$

and define a set of $N+1$, $(n+1)$ -dimensional orthogonal vectors $\mathbf{q}_i(n)$, ($i=1, \dots, N$) and $\mathbf{e}(n)$, that satisfy

$$\mathbf{A}_t(n) = [\mathbf{q}_1(n), \mathbf{q}_2(n), \dots, \mathbf{q}_N(n), \mathbf{e}(n)] \mathbf{K}_t(n) \quad (4.18)$$

where $\mathbf{K}_t(n)$ is an $(N+1)$ -by- $(N+1)$ upper-triangular matrix with unit diagonal elements, given as:

$$\mathbf{K}_t(n) = \begin{bmatrix} 1 & k_{12}(n) & k_{13}(n) & \dots & k_{1N}(n) & k_1^d(n) \\ & 1 & k_{23}(n) & \dots & k_{2N}(n) & k_2^d(n) \\ & & \dots & \dots & \dots & \dots \\ & & & 1 & k_{N-1,N} & k_{N-1}^d(n) \\ 0 & & & & 1 & k_N^d(n) \\ & & & & & 1 \end{bmatrix} = \begin{bmatrix} \mathbf{K}(n) & \mathbf{K}^d(n) \\ 0 & \mathbf{I} \end{bmatrix} \quad (4.19)$$

The elements $\mathbf{q}_i(n)$, $\mathbf{e}(n)$ and the elements of the upper triangular matrix $k_{ij}(n)$ and $k_i^d(n)$ are determined using the modified Gram-Schmidt (MGS) algorithm given in Table 4.3[63].

Table 4.3 Modified Gram-Schmidt (MGS) algorithm.

Input	$\tilde{\mathbf{r}}_i(n)$ ($i=1, \dots, N$), $d_1(n)$, λ
Initialization	$\mathbf{q}_i^{(1)}(n) = \tilde{\mathbf{r}}_i(n)$ ($i=1, \dots, N$) $\mathbf{e}^{(1)}(n) = \mathbf{D}(n)$
For $i=1$ to N do	
	$\mathbf{q}_i(n) = \mathbf{q}_i^{(1)}(n)$
	$a_{ii}(n) = \mathbf{q}_i^H(n) \mathbf{q}_i(n)$
	For $j = i + 1$ to N do
	$a_{ij}(n) = [\mathbf{q}_j^{(i)}(n)]^H \mathbf{q}_i(n)$
	$k_{ij}(n) = a_{ij}(n)/a_{ii}(n)$
	$\mathbf{q}_j^{(i+1)}(n) = \mathbf{q}_j^{(i)}(n) - k_{ij}(n) \mathbf{q}_i(n)$
	$a_i^d(n) = [\mathbf{e}^{(i)}(n)]^H \mathbf{q}_i(n)$
	$k_i^d(n) = a_i^d(n) / a_{ii}(n)$
	$\mathbf{e}^{(i+1)}(n) = \mathbf{e}^{(i)}(n) - k_i^d(n) \mathbf{q}_i(n)$
	$\mathbf{e}(n) = \mathbf{e}^{N+1}(n)$

It can be shown that $\tilde{\mathbf{w}}(n)$ satisfies the equation $\mathbf{K}(n)\tilde{\mathbf{w}}(n) = \mathbf{K}^d(n)$ which can be solved by back substitution.

Since the MGS algorithm is a block processing scheme, the vectors $\tilde{\mathbf{r}}_i(n)$ and $\mathbf{D}(n)$, $n=1$ through N , are involved in the computation of error $\mathbf{e}(n)$ or the weight vector $\tilde{\mathbf{w}}(n)$.

Therefore, the computational complexity will increase as 'n' increases. Hence, the use of MGS algorithm in real time application is inefficient.

It can be easily seen from Table 4.3 that the nth component of the vectors $\mathbf{q}_j^{(i)}(n)$, $\mathbf{q}_i(n)$ and $\mathbf{e}^{(i)}(n)$ namely, $q_j^{(i)}(n)$, $q_i(n)$ and $e^{(i)}(n)$, satisfy the same order recursive equations as their corresponding vectors. Therefore,

$$q_i(n) = q_i^{(1)}(n) \quad (4.20)$$

$$q_j^{(i+1)} = q_j^{(i)}(n) - k_{ij}(n) q_i(n) \quad (4.21)$$

$$e^{(i+1)}(n) = e^{(i)}(n) - k_i^d(n) q_i(n) \quad (4.22)$$

$$e(n) = e^{(N+1)}(n) \quad (4.23)$$

In order to obtain a time-recursive algorithm, we only have to derive time-update formulas for the coefficients $a_{ij}(n)$ and $a_i^d(n)$. These are given by [63]:

$$a_{ij}(n) = \lambda a_{ij}(n-1) + q_j^{(i)}(n) q_j^*(n) / \alpha_i(n) \quad (4.24)$$

$$a_i^d(n) = \lambda a_i^d(n-1) + e^{(i)}(n) q_i^*(n) / \alpha_i(n) \quad (4.25)$$

where $i=1$ to N and $j=i+1$ to N , $\alpha_i(n)$ is a scalar quantity, which has a magnitude close to but less than unity. The order recursive equation for $\alpha_i(n)$ is given by:

$$\alpha_{i+1}(n) = \alpha_i(n) - |q_j(n)|^2 / a_{ij}(n) \quad (4.26)$$

Replacing the vector operations in Table 4.3 by their corresponding time recursive form, we obtain the RMGS algorithm, which is summarized in Table 4.4.

The RMGS algorithm has good numerical properties, however, in [63] a modified form has also been obtained which is more efficient and has even better numerical properties by using an a priori error form and incorporating the error feedback formula. The complete error feedback RMGS (RMGSEF) algorithm is given in Table 4.5. A distinct feature of this algorithm is that the error $e^{(i+1)}(n)$ and $\alpha_i(n)$ are feedback to time update the elements $k_{ij}(n)$ of the upper triangular matrix and the elements of the vector $\mathbf{K}^d(n)$. Therefore, the algorithm

exhibits better numerical accuracy and is more robust to round off errors as compared to RMGS algorithm without error feedback [63, 45].

Table 4.4 Recursive Modified Gram-Schmidt (RMGS) algorithm

Input $\tilde{\mathbf{r}}(n)$ ($i=1, \dots, N$), $d_1(n)$, λ	
Initialization $\alpha_1(n)=1$	(T4.4.1)
$q_i^{(i)}(n)=\tilde{\mathbf{r}}(n)$ ($i=1, \dots, N$), $e^{(1)}(n)=d_1(n)$	(T4.4.2)
<i>Algorithm</i>	<i>Complexity</i>
For $i=1$ to N do	
$q_i(n) = q_i^{(i)}(n)$	(T4.4.3)
$a_{ii}(n) = \lambda a_{ii}(n-1) + q_i(n) ^2 / \alpha_i(n)$	(T4.4.4)
$\alpha_{i+1}(n) = \alpha_i(n) - q_i(n) ^2 / a_{ii}(n)$	(T4.4.5)
For $j = i + 1$ to N do	
$a_{ij}(n) = \lambda a_{ij}(n-1) + q_j^{(i)}(n) q_j^*(n) / \alpha_i(n)$	(T4.4.6)
$k_{ij}(n) = a_{ij}(n) / a_{ii}(n)$	(T4.4.7)
$q_j^{(i+1)}(n) = q_j^{(i)}(n) - k_{ij}(n) q_i(n)$	(T4.4.8)
$a_i^d(n) = \lambda a_i^d(n-1) + e^{(i)}(n) q_i^*(n) / \alpha_i(n)$	(T4.4.9)
$k_i^d(n) = a_i^d(n) / a_{ii}(n)$	(T4.4.10)
$e^{(i+1)}(n) = e^{(i)}(n) - k_i^d(n) q_i(n)$	(T4.4.11)
$e(n) = e^{N+1}(n)$	(T4.4.12)
TOTAL	1.5N ² +4.5N Mult. + 3N Div.

4.4.1 Parallel implementation on systolic arrays

The RMGS algorithm can be implemented using a highly modular structure (systolic array) shown in Fig.4.1. The systolic array operates directly on the input data represented by $\tilde{\mathbf{r}}^H(n)$. The output of the systolic array is the estimated weight vector $\tilde{\mathbf{w}}^H(n)$. The structure consists of two sections: the triangular systolic array and the linear systolic array. A single clock controls the entire systolic array. Each section of the triangular systolic array consists

Table 4.5 RMGS algorithm using the error feedback formula.

Input	$\tilde{r}_i(n)$ ($i=1, \dots, N$), $d_i(n)$, λ	
Initialization	$\alpha_1(n)=1$	(T4.5.1)
	$a_{ii}(-1)=\delta$ ($i=1, \dots, N$)	(T4.5.2)
	$q_i^{(1)}(n)=r_n(i)$ ($i=1, \dots, N$),	(T4.5.3)
	$e^{(1)}(n)=d_1(n)$	(T4.5.4)
Algorithm		Complexity
For $i=1$ to N do		
	$q_i(n) = q_i^{(i)}(n)$	(T4.5.5)
	$a_{ii}(n) = \lambda a_{ii}(n-1) + \alpha_i(n) q_i(n) ^2$	(T4.5.6)
	$\alpha_{i+1}(n) = \alpha_i(n) - \alpha_i^2(n) q_i(n) ^2 / a_{ii}(n)$	(T4.5.7)
	For $j = i + 1$ to N do	
	$q_j^{(i+1)}(n) = q_j^{(i)}(n) - k_{ij}(n-1) q_i^*(n)$	(T4.5.8)
	$k_{ij}(n) = k_{ij}(n-1) + \alpha_i(n) q_j^{(i+1)}(n) q_i^*(n) / a_{ii}(n)$	(T4.5.9)
	$e^{(i+1)}(n) = e^{(i)}(n) - k_i^d(n-1) q_i(n)$	(T4.5.10)
	$k_i^d(n) = k_i^d(n-1) + \alpha_i(n) e^{(i+1)}(n) q_i^*(n) / a_{ii}(n)$	(T4.5.11)
	$e(n) = e^{N+1}(n)$	(T4.5.12)
TOTAL		N^2+5N Mult. + N Div.

of two types of processing cells: internal cells (represented by squares) and boundary cells (represented by circles). The internal cells compute Eqs. (T4.4.4) and (T4.4.5), while, the boundary cells, on the other hand, compute Eqs. (T4.4.6), (T4.4.7) and (T4.4.8) or (T4.4.9), (T4.4.10) and (T4.4.11). When the entire orthogonal triangularization is completed, each particular row of the upper triangular matrix $\mathbf{K}^H(n)$ or the associated 1-by- N vector $[\mathbf{K}_n^d]^H$ is clocked out for subsequent processing by the linear systolic array section. This section computes the estimated weight vector $\tilde{\mathbf{w}}^H(n)$ by the method of backward substitutions using the following equations:

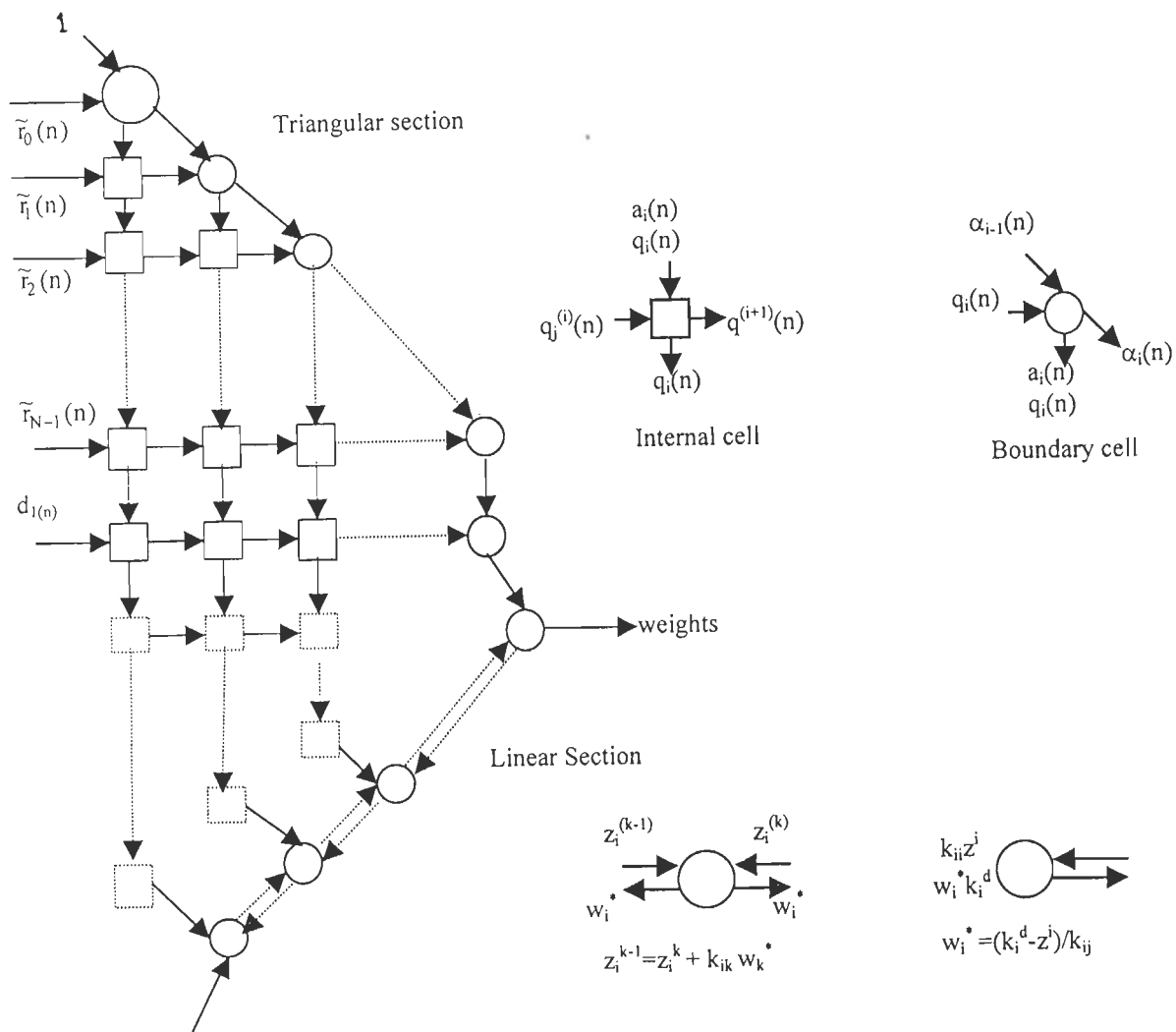


Fig. 4.1 Systolic array implementation of the RMGS algorithm.

$$z_i^{(N)} = 0.$$

$$z_i^{(k-1)} = z_i^{(k)} + k_{ik}(n) w_k^*(n)$$

$$w_k^*(n) = \frac{k_i^d(n) - z_i^{(i)}}{k_{ii}(n)} \quad (4.27)$$

where $i, k = N-1, \dots, 1$, and Z_i^k are intermediate variables, $k_{ik}(n)$ are elements of upper triangular matrix $\mathbf{K}^H(n)$, $k_i^d(n)$ are elements of the vector $\mathbf{K}^d(n)$, and $w_k^*(n)$ are elements of the weights vector $\tilde{\mathbf{w}}^H(n)$. The linear systolic array section consists of one boundary cell and $(N-1)$ internal cells that perform the arithmetic functions defined in Fig.4.1 according to Eq. (4.27). The elements of the weight vector appear at the output of the boundary cell at different clock cycles, with $w_N^*(n)$ leaving this cell first, followed by $w_{N-1}^*(n)$ and so on right up to $w_1^*(n)$

4.4.2 Computational complexity

Direct computation of the RMGS algorithm needs $1.5N^2 + 4.5N$ operations per output point. Here each operation is defined as one multiplication plus one addition. In addition it requires $2N$ divisions. Using the error feedback form of the RMGS algorithm (RMGSEF), the number of operations required is $N^2 + 5N$ operation in addition to N divisions per output bit. If it is required to calculate the weights, then using backward substitution method, then an additional $N(N-1)/2$ operations and N divisions are required.

The QR-RLS method of solving the LS problem requires $3N^2 + 7.5N$ operations, as well as $2N$ divisions and N square roots. Additional $N(N-1)/2$ operations and N divisions are required to calculate the filter weights. The inverse QR-D method proposed in [4, 36], which solves directly the time-recursive LS filter vector without using the backward substitution method, requires $4N^2 + 9N$ multiplications, $3N$ divisions and N square-roots. The computational complexity of the above methods, as well as the complexity of the

conventional RLS algorithm, is given in Table 4.6. It is clear that the highest complexity is required when using the square root algorithms (i.e. QR-RLS, inverse QR-RLS and the SQRT-KF algorithms) since they involve the calculation of further N square roots, which is computationally expensive. On the other hand, it may be noted from Table 4.6 that the RMGSEF algorithm requires the lowest computational complexity.

Table 4.6 Computational complexity of various adaptive algorithms.

<i>Algorithm</i>	<i>Multiplications</i>	<i>Divisions</i>	<i>Square-roots</i>
RLS	$3N^2+3N$	N	–
QR-RLS	$3.5N^2+7N$	$3N$	N
Inverse QR-RLS	$4N^2+9N$	$3N$	N
SQRT-KF	$3N^2+8N$	$3N$	N
RMGS	$2N^2+4N$	$3N$	–
RMGSEF	$1.5N^2+4.5N$	$2N$	–

4.5 Simulation Results and Discussion

In order to assess the performance of the proposed RMGS algorithm for the adaptation and demodulation of DS-CDMA signals in comparison to NLMS and RLS algorithms, several examples have been simulated. An asynchronous DS-CDMA system is assumed, in which the interferer's delays are chosen from a uniform distribution. However, it is assumed that the receiver is synchronized with the desired user data bits. Moreover, the receiver

requires a training sequence in the training mode, but it does not require the knowledge of the spreading sequence of the desired user. AWGN channel is assumed, in which different levels of noise power are used. The TDL filter length N is assumed to be 31, and the number of users is varied. Ensemble averaging over 100 independent trials is performed for evaluating the convergence characteristics.

Example 4.1

In this example, an asynchronous DS-CDMA system has been simulated with different number of interferers, each having 10dB power advantage over the desired user. The input SNR is fixed at 20dB.

Fig.4.2a shows the convergence characteristics for the DS-CDMA receiver based on the RMGS algorithm using 4, 8 and 10 interferers, as well as the single user case. It may be seen that by increasing the number of users the convergence becomes slower and the residual MSE is slightly increased. Figure4.2b shows the convergence characteristics for the adaptive DS-CDMA receiver based on NLMS, RLS and RMGS algorithms for 4 and 8 interferers cases. The step-size of the NLMS algorithm has been tuned, such that while using the different algorithms, the residual MSE is the same, and hence a fair comparison is achieved. It is observed that the RMGS algorithm has a much faster convergence rate as compared to the NLMS algorithm, while it has indistinguishable convergence characteristics in comparison with the RLS algorithm. For 4-interferers case, the RLS and RMGS algorithms converge in about 70 bits while the NLMS converges in about 500 bits, while for the 8-interferers case, both the RLS and RMGS algorithm converges in nearly 100 bits while the NLMS converges in about 650 bits.

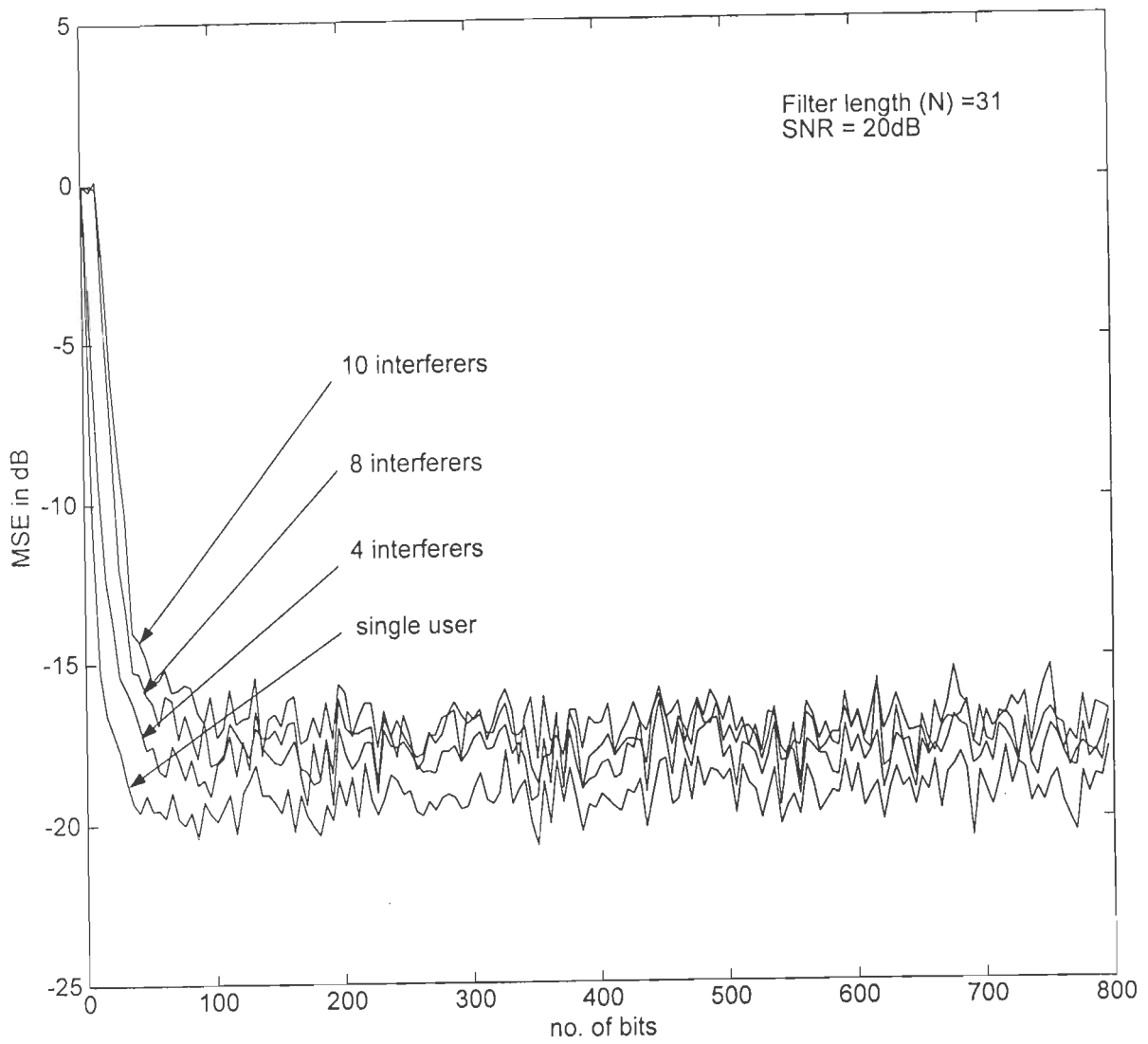


Fig.4.2a Convergence characteristics of the adaptive DS-CDMA receiver using the RMGS algorithm with different number of interferers (each interferer has 10dB power advantage over the desired user).

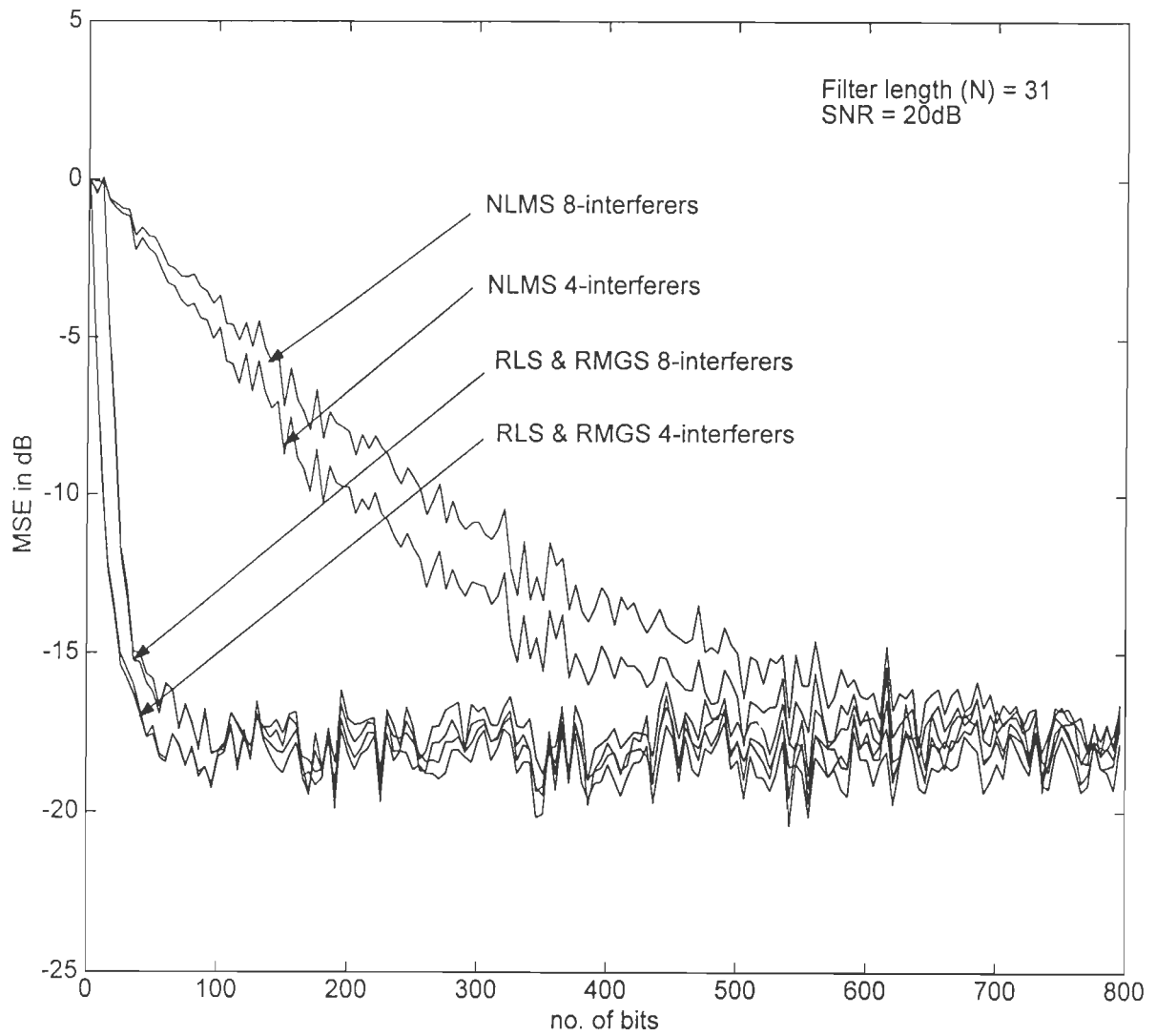


Fig.4.2b Comparison of the convergence characteristics for the adaptive DS-CDMA receiver using NLMS, RLS and RMGS algorithms with 4 and 8 interferers (each interferer has 10dB power advantage).

Example 4.2

In this example an asynchronous DS-CDMA system with 4 interferers, each having 10dB power advantage, has been simulated using both RLS and RMGS algorithms in the training and decision directed modes. The input SNR is fixed at 20dB. 800 bits are used for the training mode before switching to the decision-directed mode, and the forgetting factor is set equal to $\lambda=0.992$. From Fig.4.3, it is clear that the convergence characteristics for both the RLS and RMGS algorithms are indistinguishable in the training mode. However, in the decision directed mode, this example shows that, the RLS algorithm becomes unstable after 1750 bit intervals, while the RMGS algorithm remains stable. As has been stated earlier, this is because the condition number of the RMGS algorithm is lower than the condition number of the RLS algorithm, and also due to the use of the finite word-length arithmetic in the calculation of the Riccati difference equation. Solution to the instability problem of the RLS algorithm is either to use periodic re-initialization, or to use rescue initialization procedure whenever the RLS algorithm tends to diverge. Of course, this is another reason that has motivated us to propose the use of the RMGS algorithm as an alternative to the RLS algorithm.

Example 4.3

In this example, an asynchronous MMSE DS-CDMA receiver based on the RMGS algorithm has been simulated. The system includes four interferers each having 10dB power advantage over the desired user and the input SNR is set at 20dB. The initial weights vector is set to $\mathbf{w}(0)=\mathbf{0}$. The aim of this example is to show that the weight vector, which is obtained by simulation, will converge to the optimal weight vector at the end of the training phase.

Fig.4.4a shows a plot of the theoretical weights (calculated using Eqs. 2.11-2.16, 2.25, 2.26 and 2.27) and the weights obtained by simulation using the RMGS algorithm. It is

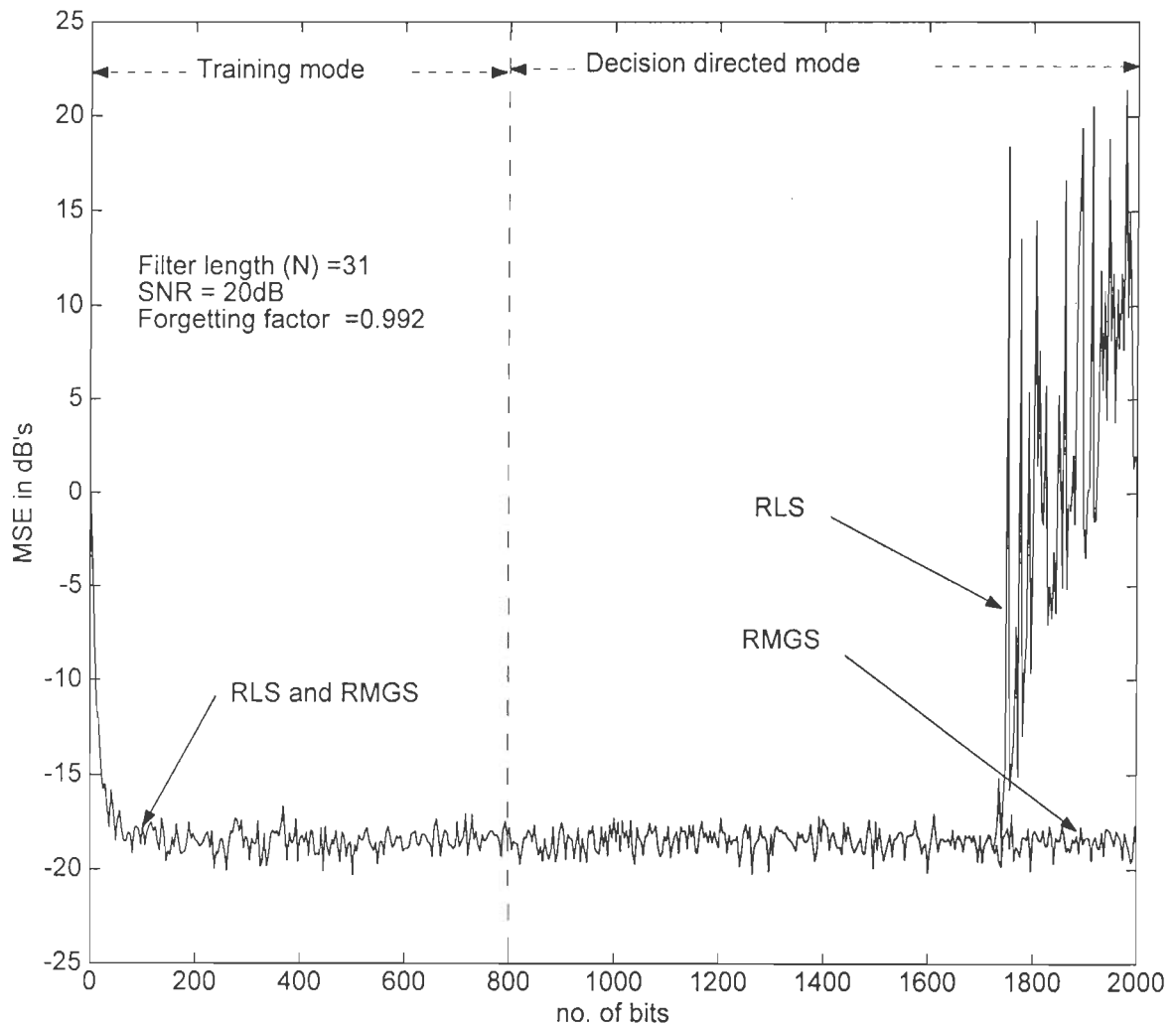


Fig.4.3 Convergence characteristics for the adaptive DS-CDMA receiver using RLS and RMGS algorithms in both training mode (up to 800 bits) and decision directed modes. The system includes 4 interferers (each interferer has 10dB power advantage).

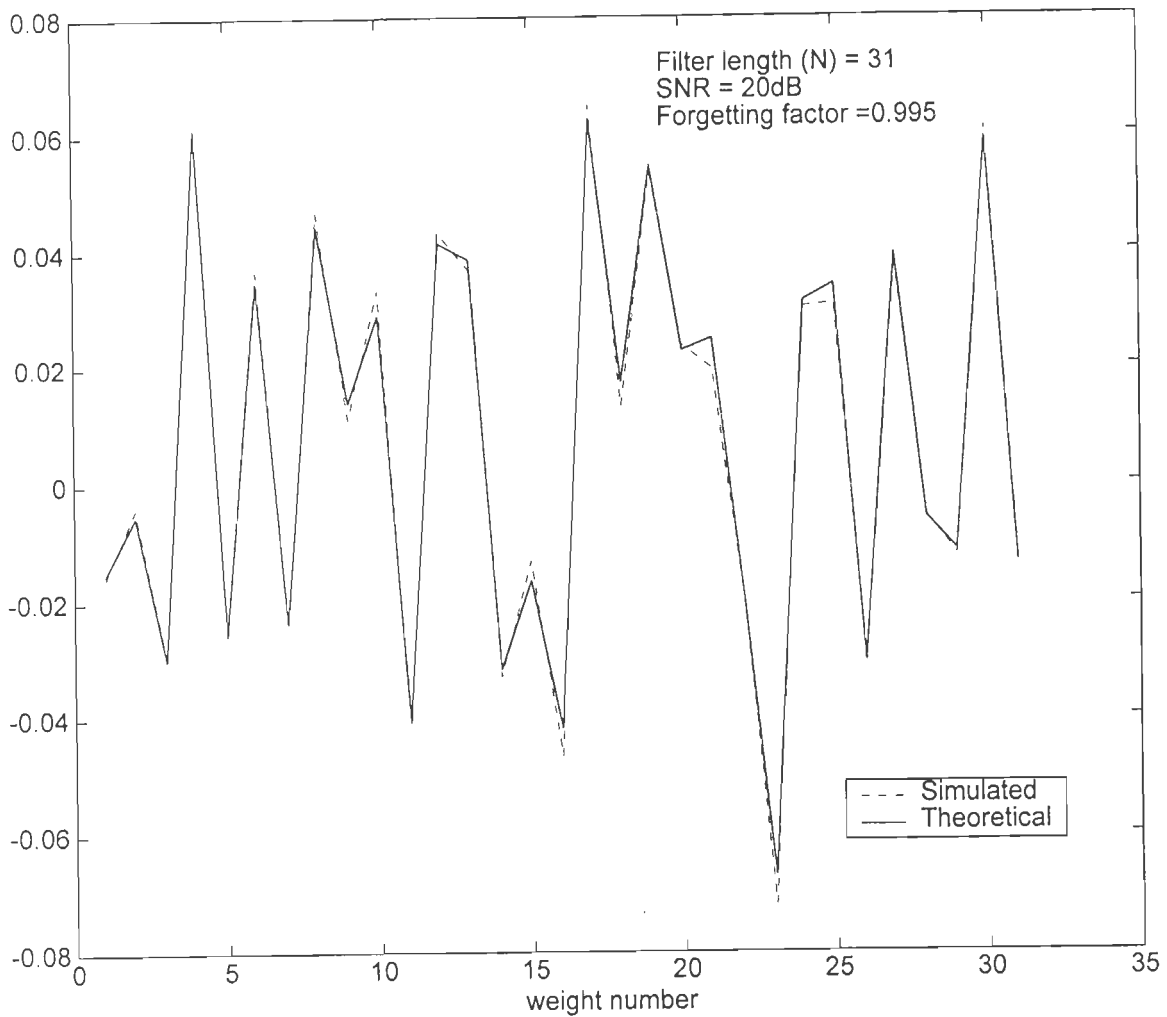


Fig.4.4a Theoretical and simulated weight vector at the end of the training mode for the adaptive DS-CDMA receiver using the RMGS algorithm with 4-interferers (each interferer has 10dB power advantage over the desired user)

observed that the weights that are obtained by simulation are very close to the theoretical weight value. Fig.4.4b shows the trajectory of a single weight (w_{17} in this case), which shows that the weight w_{17} converges in about 150 bits to its optimum value, and after that it fluctuates around that value. It may therefore be concluded that the RMGS algorithm converges to the optimal solution at the end of the training phase.

Example 4.4

In this example, the error rate performance of the MMSE DS-CDMA receiver is examined. Eight and ten interferers' cases have been simulated in which each interferer has 10dB power advantage over the desired user. In the evaluation of the probability of error, sufficiently large number of samples has been considered and a training period of 800 bits is allowed for the RMGS algorithm to converge to the steady state MSE value. For comparison we have also provided, the single user lower bound (in which only one user is using the channel) and the matched filter upper bound (in which the interference from other users is treated as thermal Gaussian noise) calculated using Eqs. (2.63 and 2.64), respectively. Also provided is a plot of the theoretical value of the probability of error for the adaptive MMSE receiver based on the RMGS algorithm which is calculated using Eq.(2.60).

Fig.4.5 shows that the probability of error for the adaptive DS-CDMA receiver based on the RMGS algorithm, which is obtained by simulation, is very close to the theoretical value. A comparison of the probability of error for the adaptive DS-CDMA receiver with the single user lower bound shows performance degradation due to the existence of MAI. At probability of error of 10^{-3} the performance degradation in terms of input SNR is nearly 1.75dB for the 8-interferers case and about 2.5dB for the 10-interferers case.

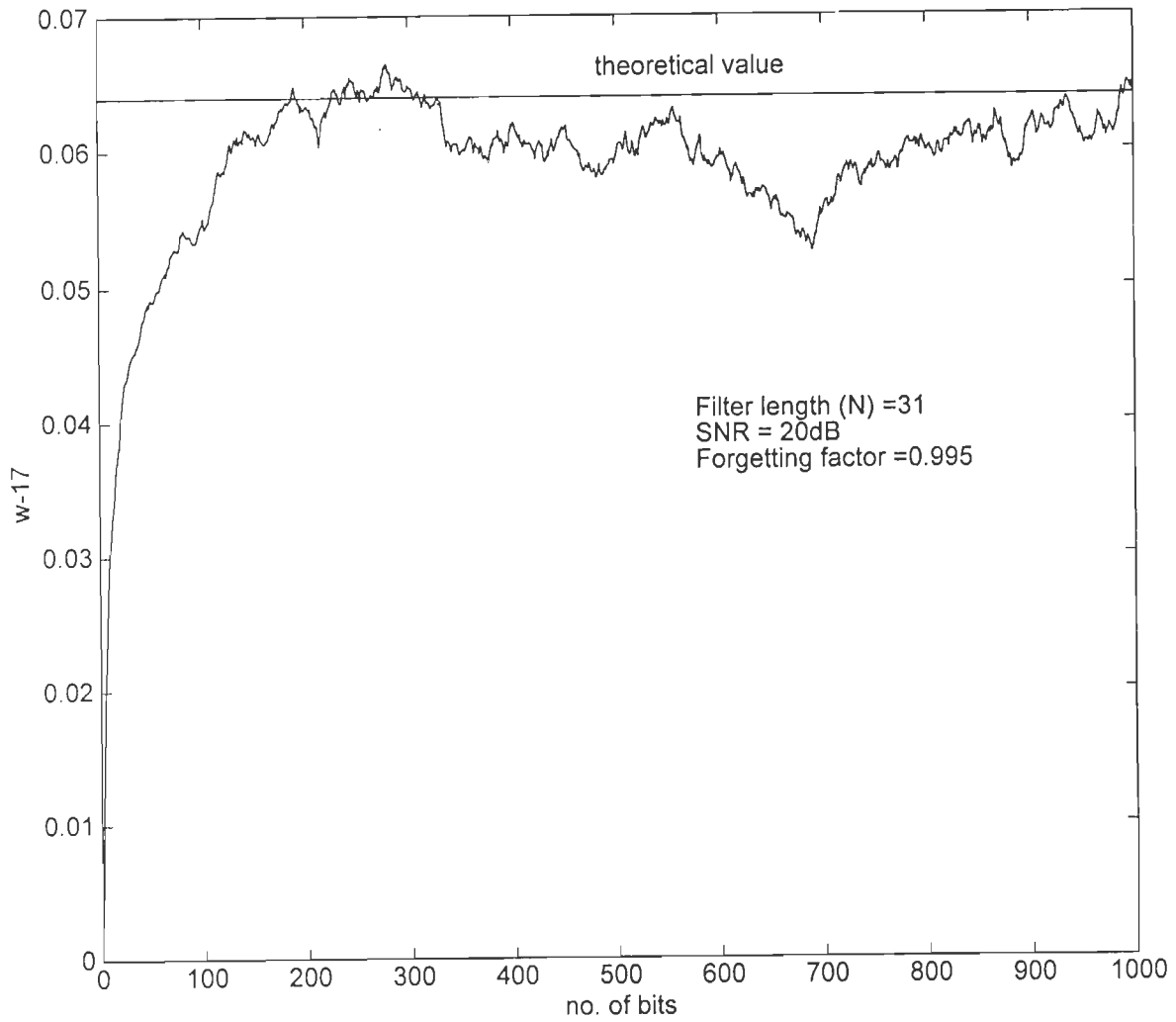


Fig.4.4b The trajectory of a single weight (w_{17}) of the TDL filter for the adaptive DS-CDMA receiver with using the RMGS algorithm with 4 interferers (each interferer has 10dB power advantage over the desired user).

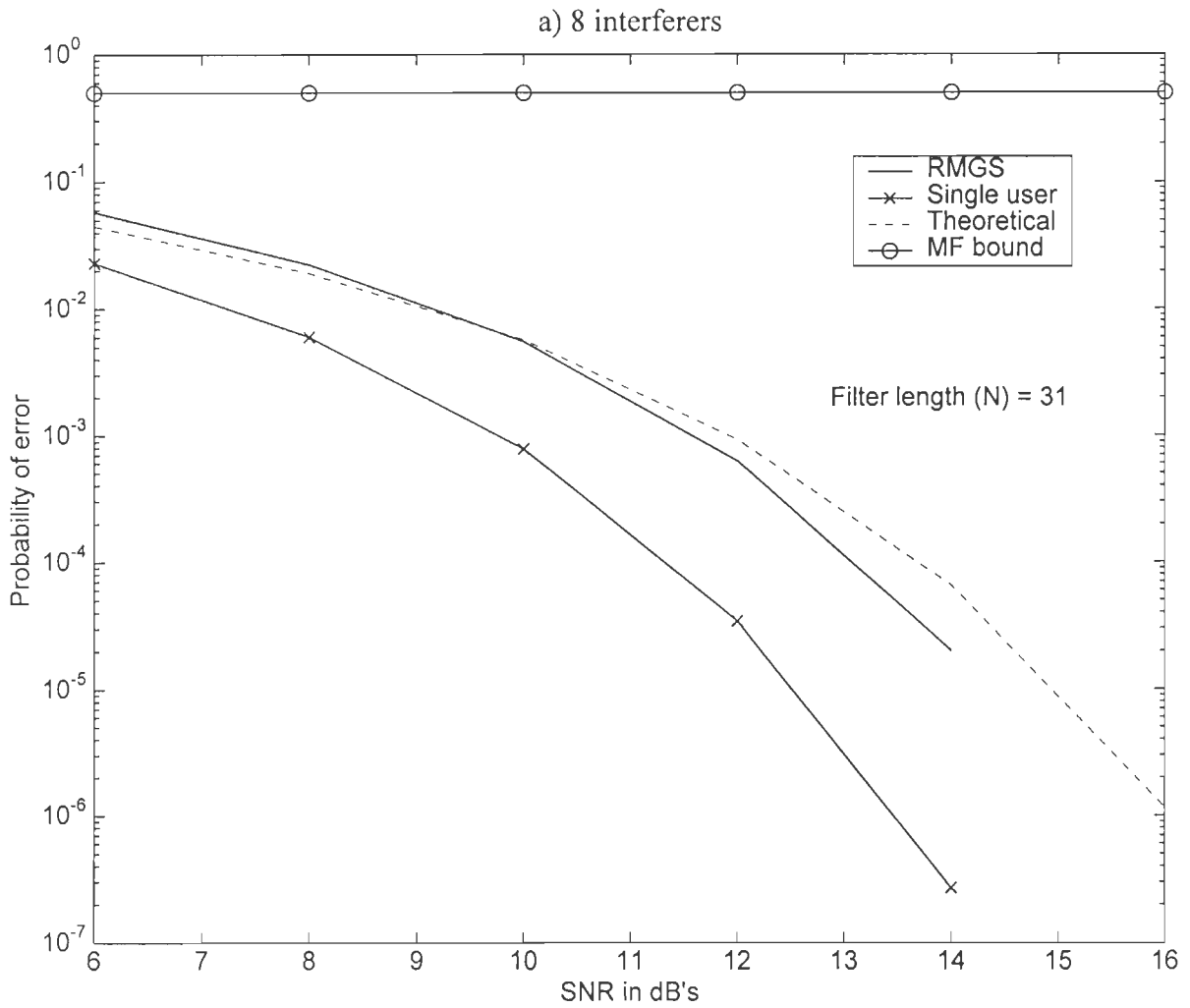


Fig.4.5 Probability of error performance for the adaptive DS-CDMA receiver using the RMGS algorithm with a) 8 interferers b) 10 interferers (each interferer has 10dB power advantage over the desired user).

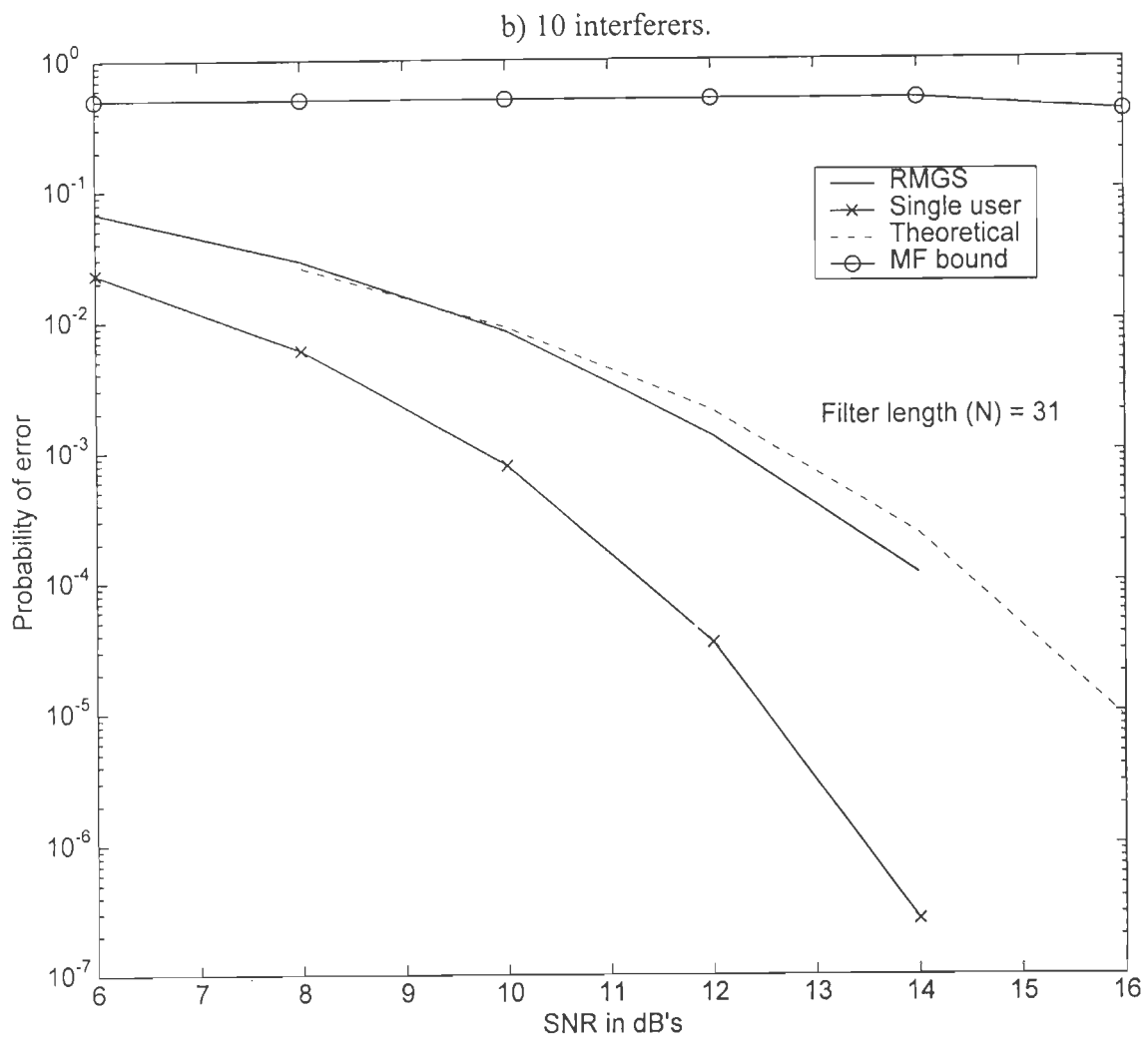


Fig.4.5b

Example 4.5

In this example, the capacity, i.e., number of users, of the adaptive MMSE DS-CDMA receiver is evaluated by calculating the output SNR as a function of number of users at certain value of the input SNR. The output SNR is calculated using Eq.(2.66). The near far situation is assumed in which each interferer has 10dB power advantage over the desired user. The step size of the NLMS algorithm is tuned such that the steady state residual MSE for both the NLMS and RMGS algorithms has the same value.

Fig.4.6 shows the output SNR plot of the adaptive DS-CDMA receiver using both NLMS and RMGS algorithms as a function of number of users at different values of the input SNRs. It is clear that the RMGS algorithm outperforms the NLMS algorithm in terms of the number of users that can be supported at both 30dB and 50dB input SNRs. For example, at input SNR=30dB, if the acceptable output SNR=20dB, then the RMGS algorithm can support about 21 users while the NLMS can support only 6 users. At input SNR=50dB, if the acceptable output SNR=20dB, then the RMGS algorithm can support about 22 users while the NLMS can support only 7 users.

Example 4.6

In this example, the near far resistance of the adaptive MMSE DS-CDMA receiver based on the RMGS algorithm is demonstrated, by plotting the probability of error as a function of the SNR of the second user (interferer) relative to the SNR of the desired user. The step size of the NLMS algorithm is tuned such that the single user steady state residual MSE for the adaptive DS-CDMA receiver has the same value using both NLMS and RMGS algorithms. The input SNR is set to 10dB and 12dB, respectively.

Fig.4.7 shows that the probability of error remains constant even when the interferer's MAI changes from -2dB to 12dB relative to the desired user. This indicates that the residual

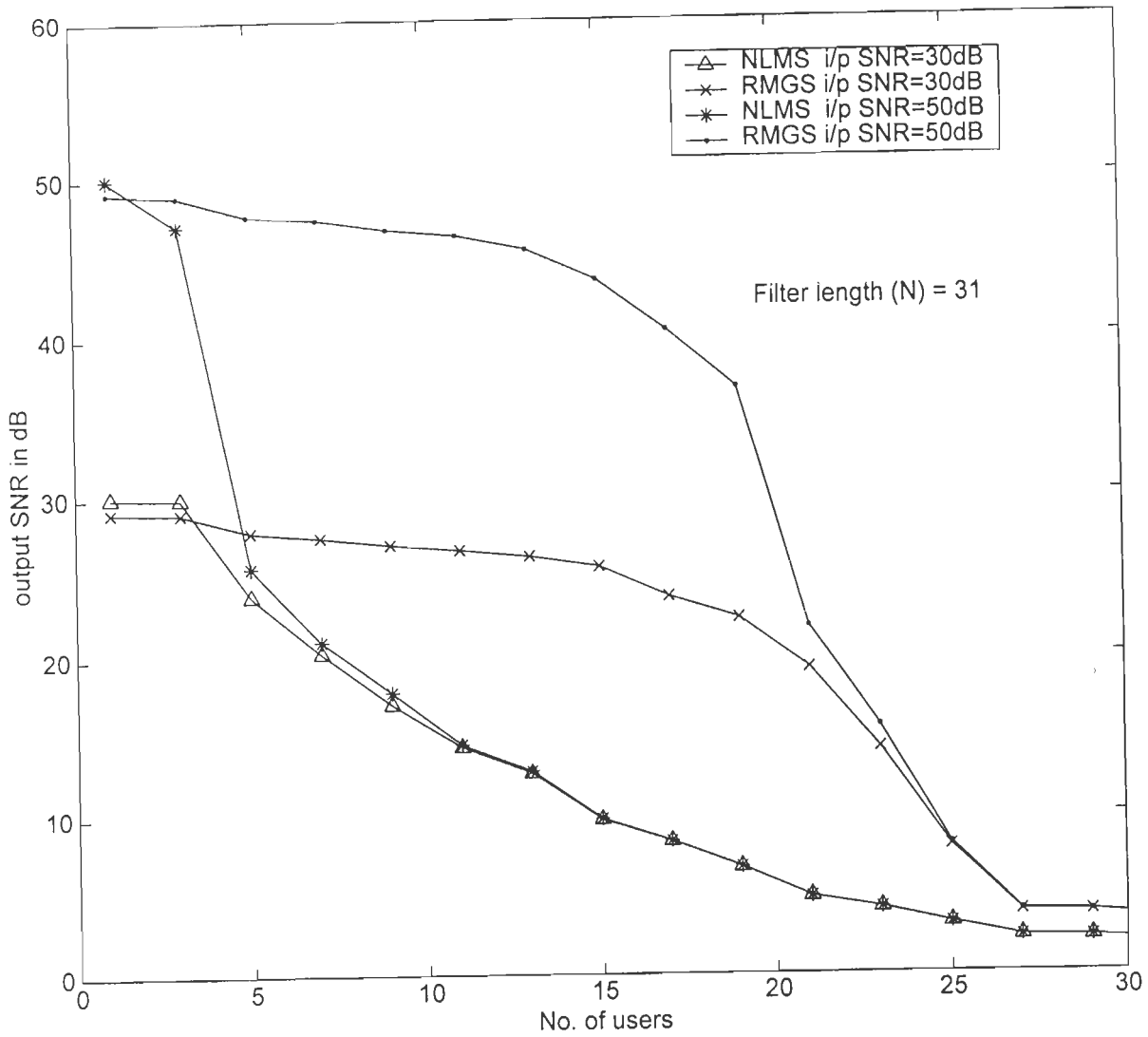


Fig.4.6 Comparison of the output SNR for the adaptive DS-CDMA receiver using NLMS and RMGS algorithms with different number of users (each interferer has 10dB power advantage over the desired user).

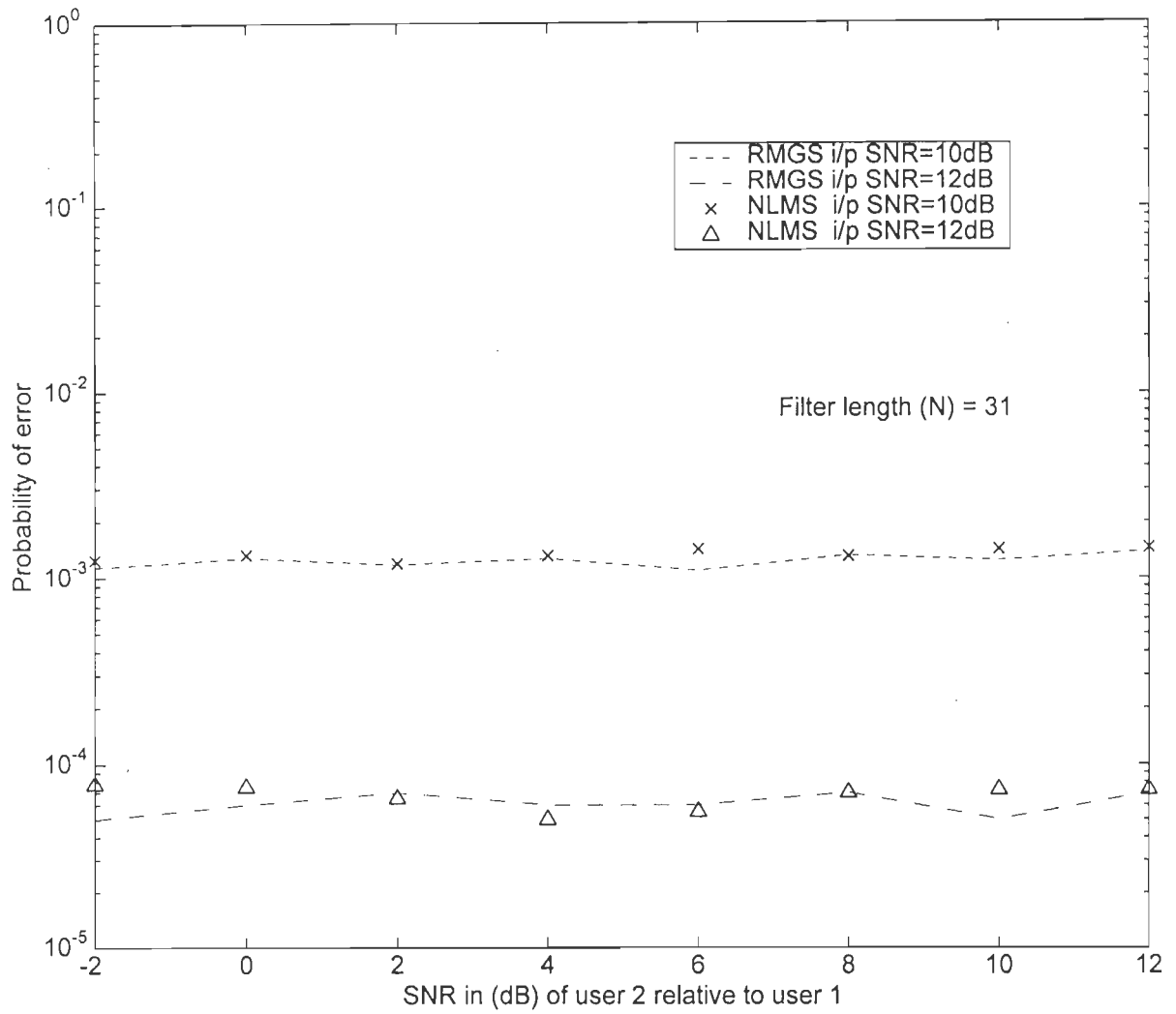


Fig.4.7 Probability of error performance for the desired user as a function of the second user's power relative to the desired user, at input SNR 10dB and 12 dB, for NLMS and RMGS algorithms.

MSE remains constant in the presence of changing MAI, and the receiver's performance is not affected with the increase of the interferer's power. It is, therefore, concluded that the MMSE receiver based on the RMGS algorithm is near far resistant.

Example 4.7

In this example, the probability of error performance as a function of the number of active users for the adaptive MMSE DS-CDMA receiver based on both NLMS and RMGS algorithms is studied at input SNR of 10dB and 12dB, respectively. Each interferer has 10dB power advantage over the desired user. The step size for the NLMS algorithm is tuned such that the single user steady state MSE for both NLMS and RMGS algorithms has the same value.

Fig.4.8 shows that the probability of error increases as the number of interferers increases due the increase in MAI. It may be observed that the RMGS algorithm performs better than the NLMS algorithm.

Example 4.8

In this example, the performance of the adaptive DS-CDMA receiver under fading dispersive environment is studied. We consider the transmission of DS-CDMA signals over a multipath fading dispersive channel having a fading rate lower than the bit rate so that the channel parameters are fixed during several bit intervals. The fading dispersive channel is represented by an equivalent discrete-time (EDT) channel, which can be realized by an FIR filter with time-variant tap gains $g_m(n)$ [37] as shown in Fig.4.9. The fading dispersive channel model is introduced in appendix A, and the procedure for generating the complex tap-gains that model the channel is also provided.

It can be easily shown that the output of the fading dispersive channel for the k th chip of the n th symbol, for DS-CDMA signal, can be computed as (Appendix A):

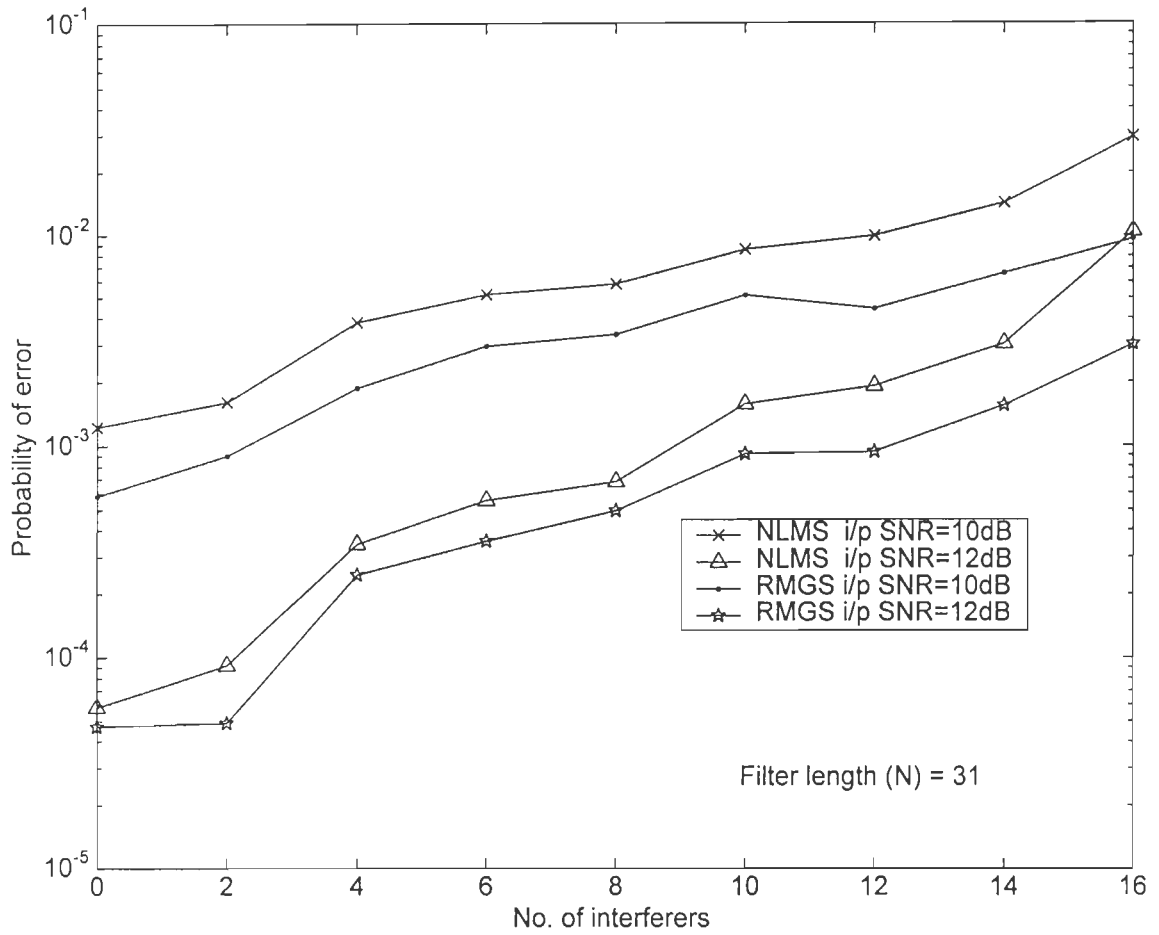


Fig.4.8 Probability of error performance for the desired user as a function of the number of interferers (each interferer has 10dB power advantage)using the NLMS and RMGS algorithms at input SNR 10dB and 12 dB.

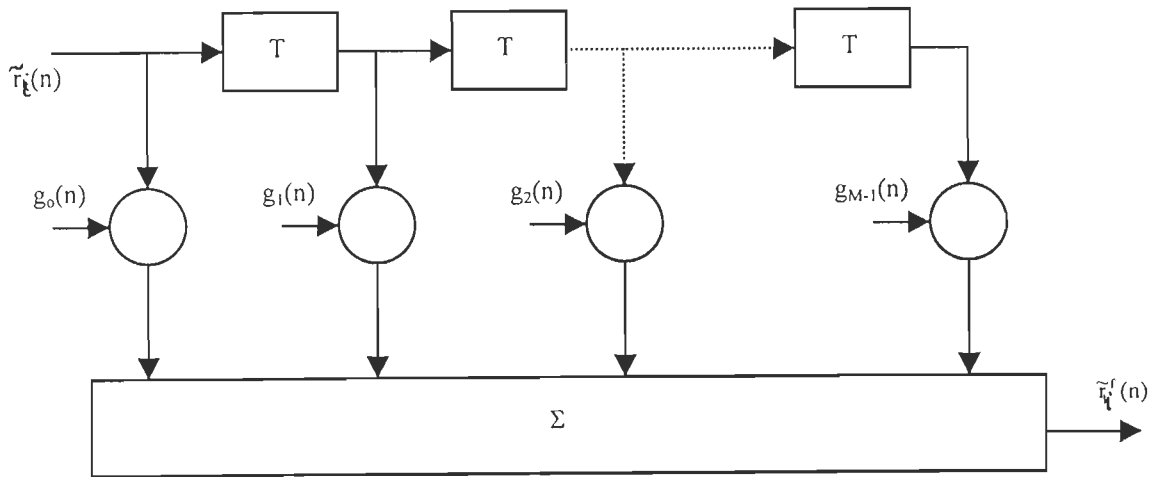


Fig.4.9 The equivalent discrete-time channel model for fading dispersive channel.

$$\tilde{r}_i^f(n) = \sum_{m=0}^{M-1} \begin{cases} \tilde{r}_{i+m}(n)g_m(n) & \text{if } (i+m) \leq N-1 \\ \tilde{r}_{i+m-N+1}(n-1)g_m(n) & \text{if } (i+m) > N-1 \end{cases} \quad \text{for } i=0, 1, \dots, N-1 \quad (4.28)$$

and the faded received vector will be $\tilde{\mathbf{r}}^f(n) = [\tilde{r}_0^f(n) \tilde{r}_1^f(n) \dots \tilde{r}_{N-1}^f(n)]^T$ where M is the total number of paths. A good approximation for M is $M = \lfloor \tau' / T_c \rfloor + 1$ where τ' is the maximum delay spread and $\lfloor x \rfloor$ is the largest integer that is less than or equal to x [58].

In our simulation, we have assumed that the maximum delay spread is $15\mu\text{sec}$ and the data rate is 9600 bit/sec , which yields a total number of paths $M=5$. The maximum Doppler frequency is kept at any of the three values (1Hz , 10 Hz and 100 Hz). Assuming that the carrier frequency is 900MHz , then a receiver moving at the walking speed of 3km/hr will produce a maximum Doppler shift of 2.5 Hz , while for a receiver moving at the highway speed of 120km/hr then a maximum Doppler frequency of 100Hz will be produced. The number of interferers has been changed between eight or ten interferers each having 10dB power advantage above the desired user.

Fig.4.10 shows the error rate performance of the adaptive MMSE DS-CDMA receiver based on both NLMS and RMGS algorithms at different values of the Doppler frequency. It

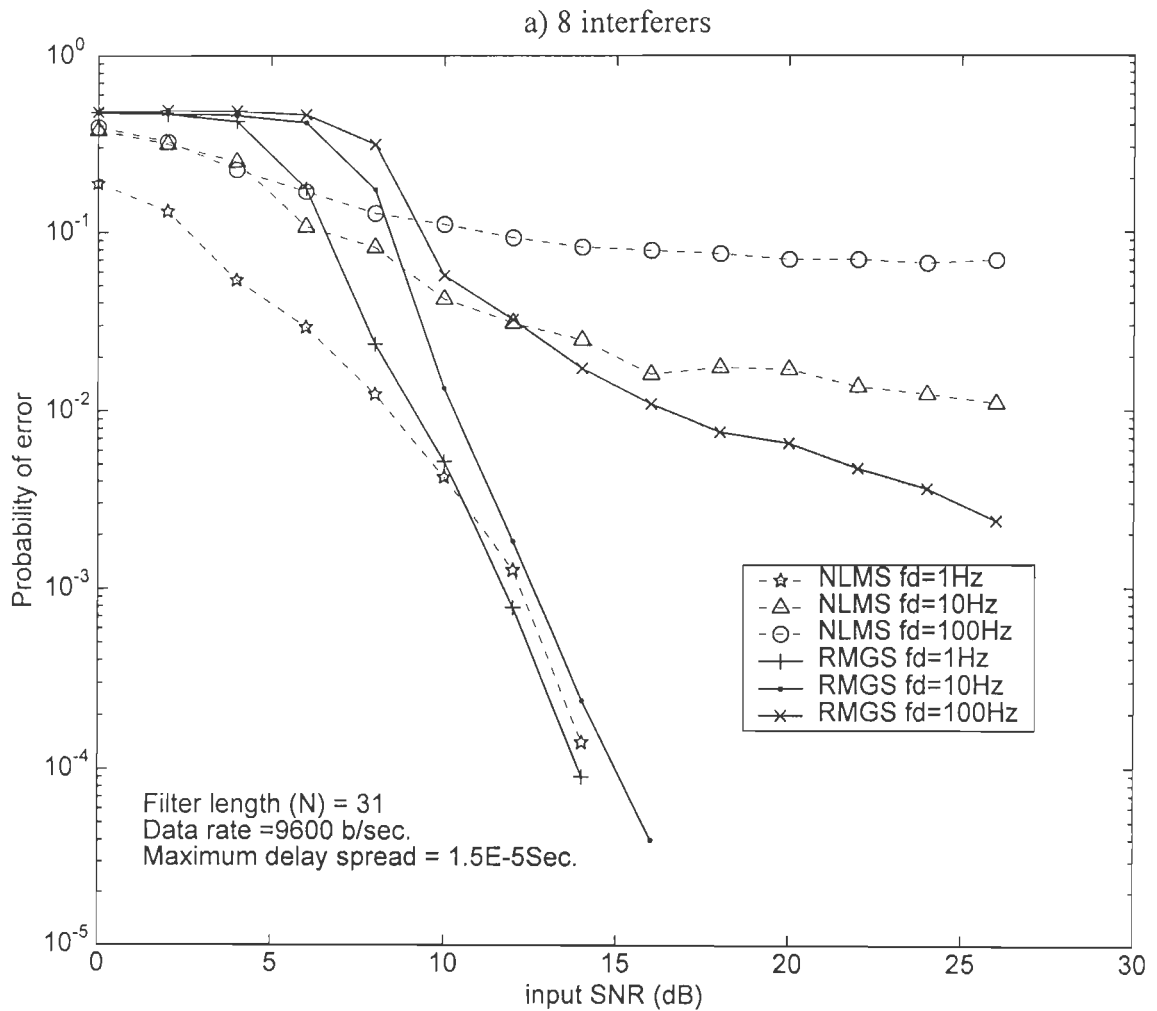


Fig.4.10 Probability of error for the adaptive DS-CDMA receiver using the NLMS and RMGS algorithms in a fading multipath environment for a) 8 interferers b) 10 interferers (each having 10dB power advantage over the desired user).

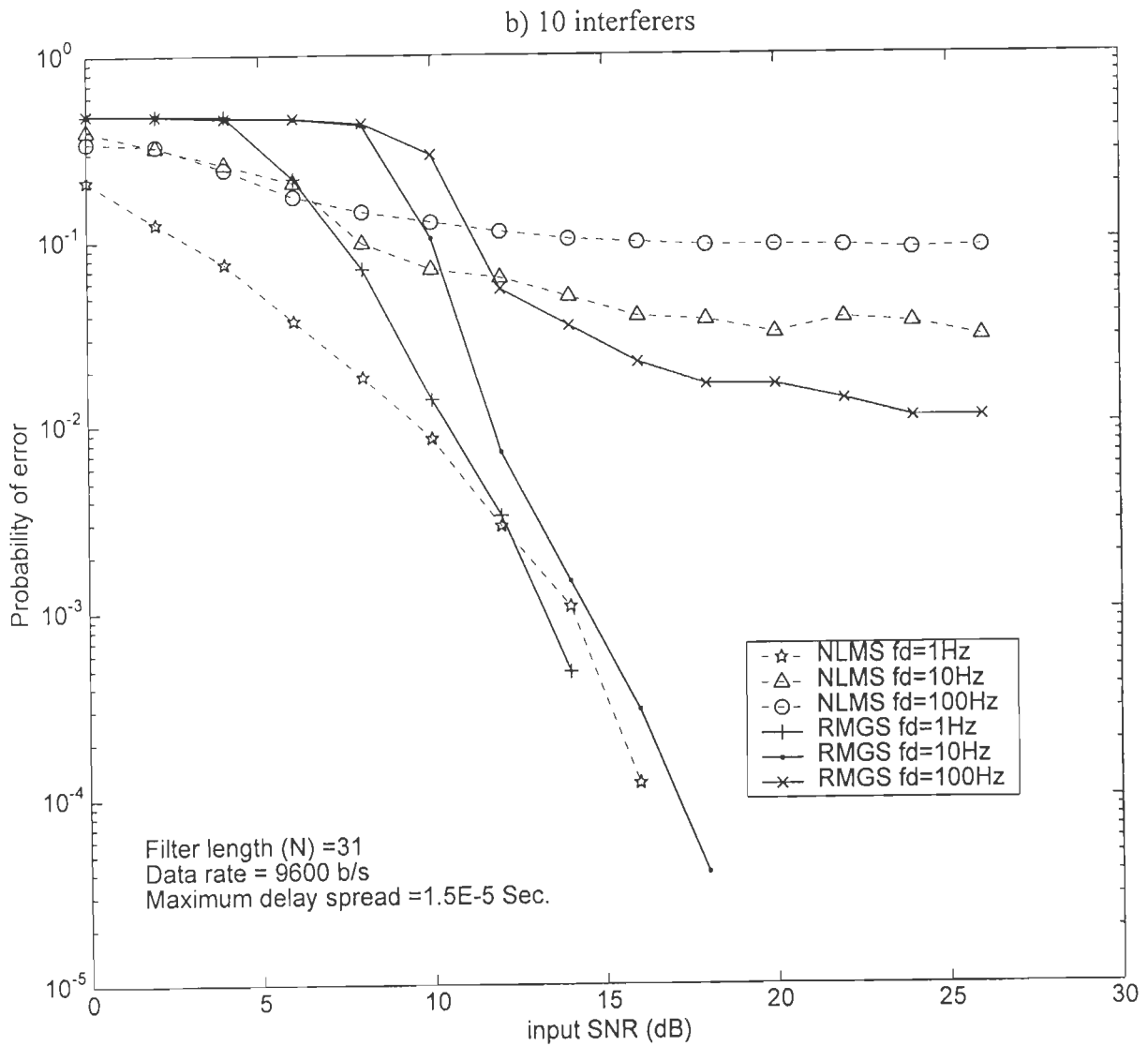


Fig.4.9b

is observed that the error rate performance of the RMGS algorithm is always better than the NLMS algorithm. Also the RMGS algorithm provides a lower error floor at all values of Doppler frequencies, input SNRs and number of users. It is also shown that there is considerable improvement in the error rate performance with the increase in the SNR, but at higher Doppler frequencies, there is degradation in the performance of both algorithms. It is also noticed that there will be irreducible value of the probability of error (error floor), which becomes independent of the SNR. At error rate of 10^{-2} and using 8-interferers, there is a degradation in terms of input SNR of nearly 1.3dB for Doppler frequency $f_d=10\text{Hz}$, and 7.5 dB for $f_d=100\text{ Hz}$, as compared to the case of $f_d=1\text{Hz}$. For the 10-interferers case, and at error rate of 10^{-2} , the degradation is nearly 1.3dB for $f_d=10\text{Hz}$ as compared to $f_d=1\text{Hz}$, while for the case of $f_d=100\text{Hz}$ the error floor is higher than 10^{-2} for all input SNR values. At error rate of 10^{-3} and using the RMGS algorithm, it is observed that the degradation in terms of the input SNR is about 0.9 dB for the $f_d=10\text{Hz}$ case as compared to the $f_d=1\text{Hz}$ when using 8 near-far interferers, while the degradation is nearly 1.2 dB when using 10 near-far interferers. It is also observed that the error floor of the NLMS algorithm is higher than 10^{-2} for $f_d=10\text{Hz}$ and $f_d=100\text{Hz}$. For the RMGS algorithm with $f_d=100\text{Hz}$, the error floor is at higher also higher than 10^{-2} .

We have also studied the effect of changing the maximum delay spread on the performance of the adaptive MMSE DS-CDMA receiver based on the RMGS algorithm. Assuming that the carrier frequency is fixed at 900MHz, the data rate is 9600 bit/sec and the maximum delay spread is chosen to be either 15 μsec or 30 μsec , which corresponds to a total of 5 or 9 paths, respectively. Fig.4.11 shows the error rate performance of the adaptive DS-CDMA receiver in fading multipath dispersive environment for 10Hz and 100Hz Doppler frequencies and for 8 and 10 interferers. For these cases, it is observed that the performance

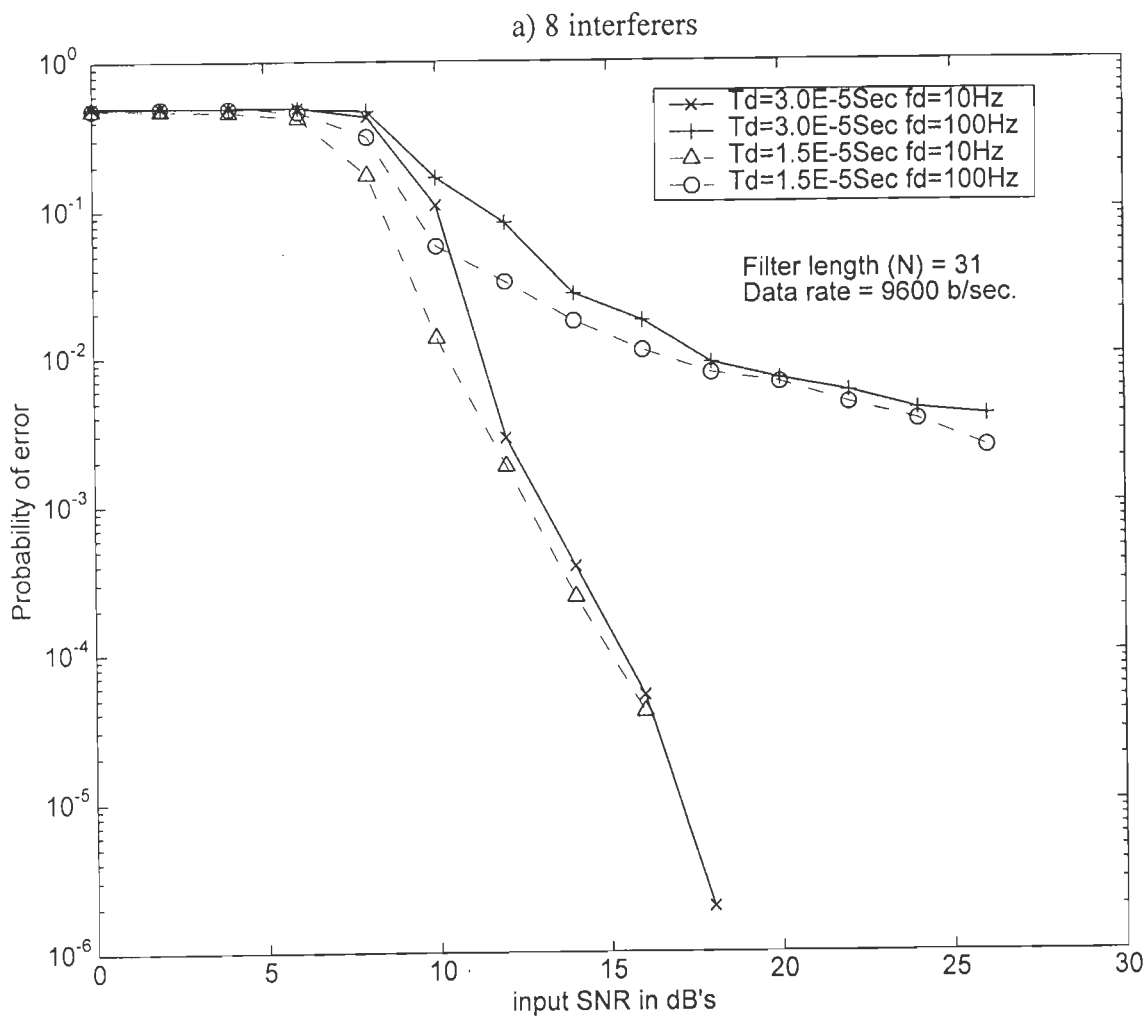


Fig.4.11 Probability of error for the adaptive DS-CDMA receiver using the NLMS and RMGS algorithms in a fading multipath environment for different values of maximum delay spread (T_d) with a)8 interferers b)10 interferers (each interferer has 10dB power advantage).

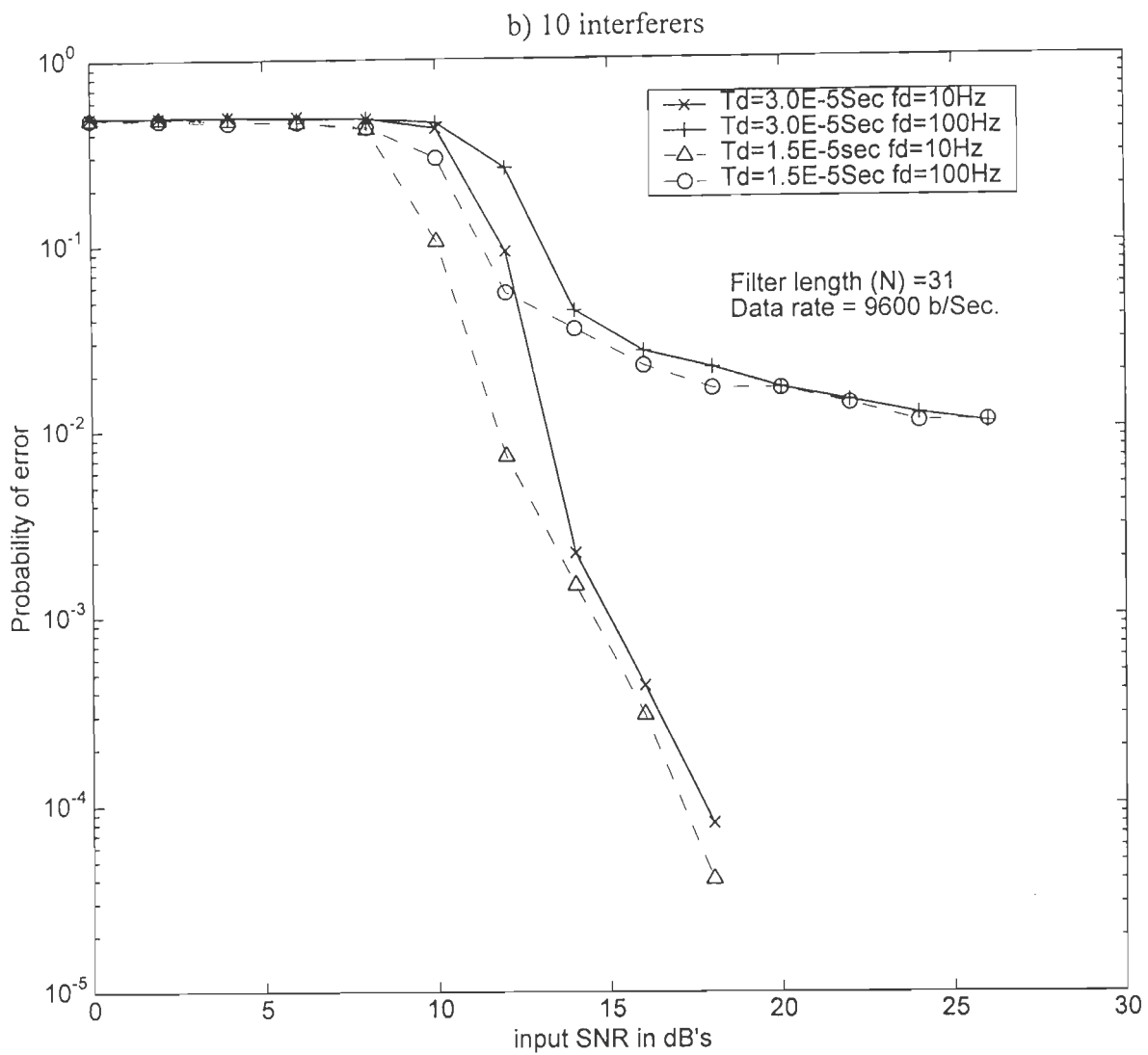


Fig.4.11b

of the receiver degrades slightly as the maximum delay spread increases, which is due to the increase of the ISI.

In this chapter, we have considered the RMGS algorithm for updating the TDL weight vector for the MMSE DS-CDMA receiver in the presence of both MAI and ISI. Simulation results show that the convergence rate of the RMGS algorithm is same as compared to the RLS algorithm. However it has been shown that the RMGS algorithm is more stable than the RLS algorithm. Moreover, it may be noted that the RMGS algorithm requires the lowest computational complexity as compared to other adaptive LS algorithms (Table 4.6). The parallel implementation of the RMGS algorithm via systolic array will further reduce the computational complexity to $O[N]$ per processor.

BLIND ADAPTIVE INTERFERENCE SUPPRESSION ALGORITHMS FOR DS-CDMA SYSTEMS

The operation of the adaptive algorithms discussed so far require the use of training sequence for the desired user during initial adaptation, and then switching to the decision directed mode during actual data transmission. A fresh training may be required when the receiver loses synchronization due to deep fading or due to the interference from a strong interferer entering the network. However, in some applications the use of training sequence may be impractical. Therefore, there is a need for adaptive receivers which do not require a training sequence (blind) or the knowledge about the parameters of the interfering users.

In this chapter, blind adaptive algorithms for interference suppression in DS-CDMA systems are presented. Section 5.1 reviews blind algorithms in DS-CDMA systems. Blind equalization algorithms based on Bussgang techniques are introduced in section 5.2. Then, in section 5.3, we present blind minimum output energy (MOE) algorithms based on LMS, RLS and QR-RLS techniques. Moreover, since as stated earlier the RMGS algorithm can be implemented using systolic arrays which reduces the computational complexity proportional to $O[N]$ per processor, we have proposed a new RMGS-based blind adaptive algorithm. Finally, simulation results are presented in section 5.4.

5.1 Introduction

In a non-stationary environment, it is impractical to use training sequence-based algorithms. Therefore, in such a case the adaptive filter has to suppress the interference in a self-organized (blind) manner. Interference suppression in DS-CDMA systems is analogous to adaptive equalization of dispersive channels, by the virtue of the analogy between MAI

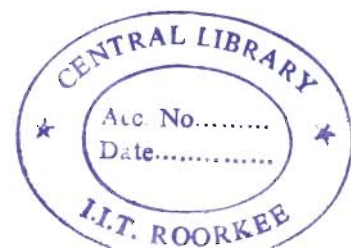
and ISI, and a considerable amount of work has been done in the area of blind equalization. Blind adaptive interference suppression algorithms in DS-CDMA systems have been developed based on the above analogy.

The Bussgang technique was first proposed by Godfrey and Rocca [29] for the equalization of seismic traces. Special cases of the Bussgang methods are the Sato algorithm and the Godard algorithm, as reviewed below. Sato in [100] proposed a blind equalization scheme for multilevel digital transmission systems, which was successful in situations in which zero-forcing and MMSE algorithms failed. The Sato algorithm differs from the MMSE equalization only in the use of error signal it makes use of, as it minimizes a different cost function. Benveniste [11] extended the Sato work to QAM systems, in which a heuristic combination of the Sato and MMSE techniques was used providing some forms of automatic switching between them. Godard [28] suggested another approach to blind equalization in QAM systems guaranteeing the equalizer convergence independently of the carrier phase recovery. The Godard algorithm is based on higher order statistics and is considered as one of the simplest blind algorithm. This algorithm was also developed independently as constant modulus algorithm (CMA) for pulse amplitude (PAM) and FM signals in [109, 110].

The stochastic gradient-descent blind minimum output energy (MOE) technique, for the interference suppression in DS-CDMA systems, was proposed by Honig et al. [38]. The receiver requires the knowledge of the spreading sequence and the timing of the user of interest. The MOE based on the stochastic method suffers from slow convergence rate and has difficulty in adapting the step-size to ensure the stability of the algorithm in a dynamic environment. Also the MOE method suffers from the switching back and forth during new user entering the network. The idea of MOE has been proposed for the joint acquisition and demodulation of DS-CDMA signals in [67], and for NBI suppression in [22]. The

generalized structure of the blind adaptive interference mitigation detector based on the MOE technique has been introduced by De Gaundenzi et al. [18], and a few modifications to the algorithm of [38] have been performed which makes it suitable for practical implementations. In [111] linear blind CDMA receivers are derived using inverse filtering criteria. The receiver parameters are directly obtained without explicit estimation of the system/channel. The method is based on minimizing the receiver's output energy subject to appropriate constraints. Batch and adaptive blind algorithms are derived that are near-far resistant and do not require knowledge of the interferers' codes. An accelerated convergence stochastic-gradient algorithm, which uses second round averaging of the stochastic-gradient has been derived and analyzed in [52]. The algorithm yields convergence rate identical to RLS algorithm but has a computational cost similar to LMS algorithm. However, the algorithm performs worse than RLS with the existence of strong NBI, also the step size has to be obtained accurately and the algorithm suffers from ill-convergence condition when the filter length becomes large. Poor and Wang [93] proposed an RLS-based blind adaptive algorithm for MAI and NBI suppression in DS-SS systems. The algorithm possesses a high convergence rate but it suffers from numerical instability and requires the recursive update of the inverse autocorrelation matrix, which severely limits the parallelism and pipelining in implementation. The major limitation of the MOE approach to blind MUD is that there is a saturation effect in the steady-state, which causes a significant performance gap between the MOE detection and the true MMSE detector.

Blind algorithms using classical approach of subspace estimation through either eigenvalue decomposition or singular-value decomposition of the data matrix is computationally too expensive for adaptive applications. The projection approximation subspace tracking algorithm (PASTd), proposed in [121], ensures almost sure global convergence and lower



residual MSE as compared to MOE criterion, but suffers from relatively slow convergence rate. Wang and Poor [120] extended the blind subspace technique to combat both MAI and ISI in a high-rate dispersive CDMA system. Improved detector characteristics, using the subspace method compared to MOE criterion, are also presented in [99]. However some decreased sensitivity to perturbation is anticipated. On the other hand, although the subspace-based detectors outperform the MOE detectors in the steady state, they either require more computational complexity or possess slower convergence rate.

As it will be discussed in the next sections, the CMA algorithm suffers from poor convergence rate and it does not ensure global convergence. The gradient stochastic based MOE algorithm suffers from slow convergence rate and has difficulty in adapting the step-size to ensure stability in a dynamic environment. The blind RLS-based algorithm converges much faster but suffers from the well-known numerical instability. The blind QR-RLS algorithm is more stable than the blind RLS algorithm while possessing a comparable convergence rate. However, the QR-RLS algorithm is computationally expensive, since it also requires the calculation of N -square roots. Moreover, as discussed in chapter four, since the RMGS algorithm can be implemented in a highly modular structure via parallel systolic array implementations, its computational complexity can be reduced to $O[N]$ per processor. For the above reasons, we propose in the next section the blind RMGS-based adaptive algorithm, which possesses all the attractive features of the previous algorithms while avoiding their drawbacks.

In CDMA systems, the channel is shared by K users, where each user is assigned a spreading waveform $c_k(t)$, which is zero outside the interval $[0, T]$, defined by:

$$c_k(t) = \sum_{j=0}^{N-1} c_{k,j} \psi(t - jT_c) \quad (5.1)$$

where T is the signal bit interval, $N=T/T_c$ is the processing gain, $\psi(t)$ is the chip waveform of rectangular shape and duration T_c , and $c_{kj} \in \{-1,1\}$ is the j th element of the spreading code of the k th user. The k th user transmit a signal, in the interval $0 \leq t \leq T$ corresponding to first bit, of the form

$$s_k(t) = d_k(t)c_k(t)\cos(\omega_c t + \theta_k) \quad 0 \leq t \leq T \quad (5.2)$$

where $d_k(t)$ is the k th user data bit, ω_c is the carrier frequency and θ_k is the phase. The received signal is of the form:

$$y(t) = \sum_{k=1}^K \sqrt{P_k} s_k(t - \tau_k) + n(t) \quad (5.3)$$

where P_k is the received power of the k th user and τ_k is its delay which is assumed to be uniformly distributed over $[0, T]$, and $n(t)$ is additive white Gaussian noise. The receiver converts the received signal $y(t)$ to the baseband signal $r(t)$. After the baseband conversion, the received signal $r(t)$ is chip-matched filtered and sampled at the chip rate and fed to the TDL filter as $\mathbf{r}(n) = [r_0(n), r_1(n), \dots, r_{N-1}(n)]^T$.

5.2 Blind equalization based on Bussgang technique

Blind equalization, consists of retrieving the input signal, and possibly the channel impulse response, given the channel output and some statistical information on the channel input but not the channel itself [6]. A nice feature of this algorithm is that it differs from the MMSE equalizer only in the non-linear function $g[\cdot]$ it makes use of.

The system under consideration is considered in Fig.5.1 [36]. The output signal of the transversal filter $\bar{d}(n)$ is computed by

$$\bar{d}(n) = \mathbf{w}^T(n) \mathbf{r}(n) \quad (5.4)$$

where the output of the transversal filter is defined as

$$\bar{d}(n) = d(n) + v(n) \quad (5.5)$$

where the term $v(n)$ is the convolutional noise, and $d(n)$ is the transmitted data bits. The filter output $\bar{d}(n)$ is then processed by the zero-memory nonlinear estimator, producing the estimate $\hat{d}(n)$ for the data symbol $d(n)$, i.e.

$$\hat{d}(n) = g[\bar{d}(n)] \quad (5.6)$$

where $g[\cdot]$ is the nonlinear function. The estimation error, $e(n)$ may be calculated by:

$$e(n) = \hat{d}(n) - \bar{d}(n) \quad (5.7)$$

The tap-weights vector $\mathbf{w}(n)$ of the adaptive filter may be adjusted using the formula

$$\mathbf{w}(n+1) = \mathbf{w}(n) + \mu \mathbf{r}(n) e(n) \quad (5.8)$$

where μ is the step size, and $\mathbf{r}(n)$ is the input vector.

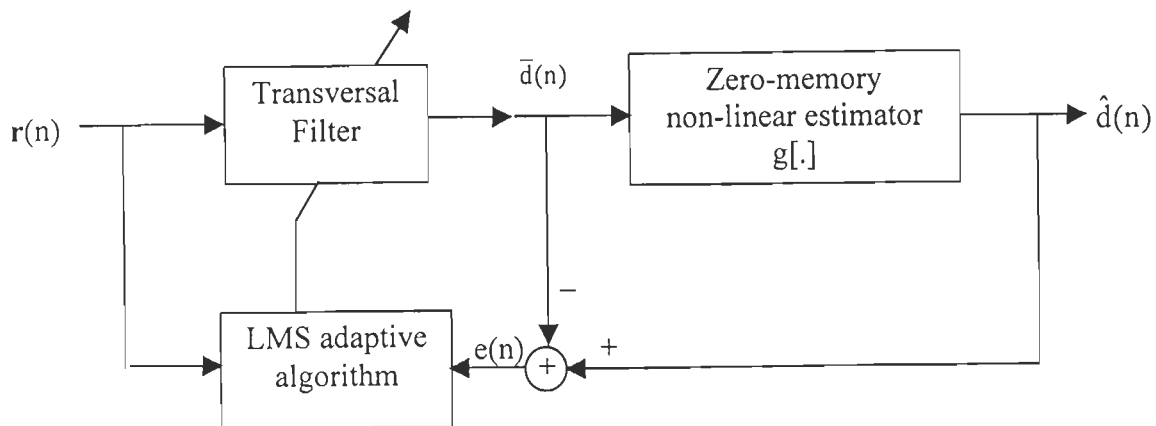


Fig.5.1. Block Diagram of blind equalizer using non-linear estimator.

To update the TDL filter weights, minimization of the following cost function is performed,

$$\begin{aligned}
J(n) &= E[e^2(n)] = E[\{\hat{d}(n) - \bar{d}(n)\}^2] \\
&= E[\{g[\bar{d}(n)] - \bar{d}(n)\}^2] \tag{5.9}
\end{aligned}$$

In the LMS algorithm, the cost function is a quadratic function of the tap weights, and therefore, has a well-known minimum point. In contrast, the cost function defined by (5.9) may possess local minima in addition to the global minima. This might happen due to the effect of zero-memory nonlinearity applied to the filter output $\bar{d}(n)$. Local minima may result in an ill convergence of the algorithm. It is worth mentioning here, that to date, no zero-memory nonlinear function $g[\cdot]$ is known which would result in global convergence of the blind equalizer, to the unknown inverse of the unknown channel [36].

When the Bussgang algorithm converges, the equalizer should be switched smoothly to the decision directed mode of operation based on the MMSE weights update criterion. The only difference between the two modes of operation lies in the type of the non-linearity employed in the blind equalization mode. More specifically, in the decision directed mode, the nonlinear estimator of the blind equalizer is replaced by a threshold device (hard-limiter).

A special case of the Bussgang algorithm is the Godard algorithm [28] in which the author had proposed a family of constant modulus blind equalization algorithms for use in two-dimensional digital communication systems. The Godard algorithm minimizes a non-convex cost function of the form

$$J(n) = E[(|\bar{d}(n)|^p - R_p)^2] \tag{5.10}$$

where p is a positive integer, and R_p is a positive real constant defined by

$$R_p = \frac{E[|d(n)|^{2p}]}{E[|d(n)|^p]} \tag{5.11}$$

The Godard algorithm is designed to penalize the deviations of the blind equalizer output $\bar{d}(n)$ from a constant modulus. The constant R_p is chosen in such a way that the gradient of the cost function $J(n)$ is zero when perfect equalization is attained.

The tap-weights vector is adapted in accordance with the stochastic gradient algorithm [28]:

$$\mathbf{w}(n+1) = \mathbf{w}(n) + \mu \mathbf{r}(n) e(n) \quad (5.12)$$

$$e(n) = \bar{d}(n) |\bar{d}(n)|^{p-2} [R_p - |\bar{d}(n)|^p] \quad (5.13)$$

As a special case, assuming that $p=2$, the cost function reduces to:

$$J(n) = E[\{|\bar{d}(n)|^2 - R_2\}^2] \quad (5.14)$$

where $R_2 = \frac{E[|d(n)|^4]}{E[|d(n)|^2]}$ (5.15)

This case of the Godard algorithm ($p=2$) is referred to as the constant modulus algorithm (CMA). Its cost function for binary valued signals (± 1) will have a constant squared modulus equal to 1. The stochastic descent based CMA algorithm will update the weights vector as follows:

$$\mathbf{w}(n+1) = \mathbf{w}(n) + \mu \mathbf{r}(n) \bar{d}(n) [1 - |\bar{d}(n)|^2] \quad (5.16)$$

The CMA is considered as the most successful and the simplest higher-order statistics (HOS) based algorithm among the Bussgang family of blind equalization algorithms. It chooses a linear receiver that minimizes the deviation of the receiver output from a constant modulus. The CMA cost function does not distinguish between desired and interfering symbols because each symbol of all users are local minima of the cost function. The CMA based adaptive DS-CDMA receiver is summarized in Table 5.1.

Table 5.1 CMA-based algorithm for DS-CDMA systems.

<i>Input</i> $\mathbf{r}(n)$, μ	
<i>Initialization</i> $\mathbf{w}(0)=\mathbf{c}_1/\text{SQRT}(N)$.	
<i>Algorithm</i>	<i>Complexity</i>
$\bar{d}(n) = \mathbf{w}^T(n) \mathbf{r}(n)$	N Mult.
$R_2 = \frac{E[d(n) ^4]}{E[d(n) ^2]^2} = 1$ (for binary signals $=\pm 1$)	
$e(n) = \bar{d}(n) [R_2 - \bar{d}(n) ^2]$	2 Mult.
$\mathbf{w}(n+1) = \mathbf{w}(n) + \mu \mathbf{r}(n) e(n)$	N+1 Mult.
<i>TOTAL</i>	2N+3 Mult.

5.3 Blind MOE multiuser detector

In this section, we present the constrained blind MOE detector for the interference suppression in DS-CDMA systems. It is easy to show that the MSE and MOE differ by a constant factor [38], which is equal to the desired user power. In contrast to the MMSE detector, the MOE detector does not require the knowledge of the data in order to implement a gradient descent algorithm for the minimization of the MSE. This will remove the requirement for a training sequence, and leads to the blind adaptation rule. On the other hand, it could also be shown that the MOE has no local minima, since the MOE cost function is strictly a convex function over a set of signals orthogonal to the desired user spreading sequence.

5.3.1 LMS-based blind MOE detector

A linear multiuser detector for DS-CDMA signals, which uses the blind MOE criterion, performs the following hard decision at the output of the TDL filter to estimate the desired user data bit:

$$\hat{d}_1(n) = \text{sgn}(\langle \mathbf{r}(n), \mathbf{z}_1 \rangle) \quad (5.17)$$

where, the inner product is given by

$$\langle \mathbf{x}, \mathbf{y} \rangle = \sum_{n=0}^{N-1} x(n)y(n) \quad (5.18)$$

and \mathbf{z}_1 is the desired user linear detector defined by[38]:

$$\mathbf{z}_1 = \mathbf{c}_1 + \mathbf{x}_1 \quad (5.19)$$

where \mathbf{c}_1 is the normalized spreading sequence of user 1 (which is considered as the fixed part), and \mathbf{x}_1 is the adaptive part of the linear detector. The fixed and adaptive parts, \mathbf{c}_1 and \mathbf{x}_1 , are assumed to be orthogonal to each other, such that $\langle \mathbf{c}_1, \mathbf{x}_1 \rangle = 0$. It is also assumed that

$$\langle \mathbf{c}_1, \mathbf{z}_1 \rangle = \|\mathbf{c}_1\|^2 = 1. \quad (5.20)$$

This normalization, of course, will not affect the decision in (5.17).

The linear MMSE detector minimizes the MSE, sum of the noise plus interference,

$$E[(\sqrt{P_1} d_1(n) - \langle \mathbf{r}(n), \mathbf{z}_1 \rangle)^2] \quad (5.21)$$

while the MOE detector minimizes the output energy defined by

$$E[(\langle \mathbf{r}(n), \mathbf{c}_1 + \mathbf{x}_1 \rangle)^2] \quad (5.22)$$

It is important to restrict the detector to be in canonical form, otherwise the output energy is trivially minimized with $\mathbf{z}_1=0$ [38].

Assuming that the n th output of the conventional single user matched filter given by:

$$y_{MF}(n) = \langle \mathbf{r}(n), \mathbf{c}_1 \rangle \quad (5.23)$$

The output of the linear detector is

$$y(n) = \langle \mathbf{r}(n), \mathbf{c}_1 + \mathbf{x}(n-1) \rangle \quad (5.24)$$

$$\text{and } \hat{d}_1(n) = \text{sgn}(y(n)) \quad (5.25)$$

Minimization of the MOE cost function will provide the following adaptation rule:

$$\mathbf{x}_1(n) = \mathbf{x}_1(n-1) - \mu y(n) [\mathbf{r}(n) - y_{MF}(n) \mathbf{c}_1] \quad (5.26)$$

This algorithm converges regardless of the initial condition to the MMSE detector, if the step-size decreases as $\mu(n) = 1/n$ [38]. However, in practice, a lower bounded step size $\mu(n)$ is often needed to track channel variations. The blind LMS-based MOE algorithm is summarized in Table 5.2.

Table 5.2 Blind LMS-based MOE algorithm.

Input $\mathbf{r}(n), \mathbf{c}_1, \mu$	
Initialization $\mathbf{x}_1(n)=\mathbf{0}$.	
<i>Algorithm</i>	<i>Complexity</i>
$y_{MF}(n) = \mathbf{r}^T(n) \mathbf{c}_1$	N Mult.
$y(n) = \mathbf{r}^T(n) [\mathbf{c}_1 + \mathbf{x}(n-1)]$	N Mult.
$\mathbf{x}_1(n) = \mathbf{x}_1(n-1) - \mu y(n) [\mathbf{r}(n) - y_{MF}(n) \mathbf{c}_1]$	2N+1 Mult.
TOTAL	4N+1 Mult.

5.3.2 RLS-based blind MOE detector

The exponentially windowed RLS algorithm selects the weight vector $\mathbf{z}_1(n)$, to minimize the sum of exponentially weighted energy [93]:

$$\text{minimize } \sum_{i=1}^n \lambda^{n-i} [\mathbf{z}_1^T(n) \mathbf{r}(i)]^2 \quad (5.27)$$

$$\text{subject to } \mathbf{z}_1^T(n) \mathbf{c}_1 = 1 \quad (5.28)$$

where $0 < \lambda < 1$ is the forgetting factor ($1 - \lambda \ll 1$). The solution to this constrained optimization problem is given by (see appendix B):

$$\mathbf{z}_1(n) = \frac{1}{\mathbf{c}_1^T \mathbf{R}^{-1}(n) \mathbf{c}_1} \mathbf{R}^{-1}(n) \mathbf{c}_1 \quad (5.29)$$

$$\text{where } \mathbf{R}(n) = \sum_{i=1}^n \lambda^{n-i} \mathbf{r}(i) \mathbf{r}^T(i) \quad (5.30)$$

A recursive procedure for updating $\mathbf{z}_1(n)$ can be obtained as follows [93]:

$$\mathbf{k}(n) = \frac{\mathbf{R}^{-1}(n-1)\mathbf{r}(n)}{\lambda + \mathbf{r}^T(n)\mathbf{R}^{-1}(n-1)\mathbf{r}(n)} \quad (5.31)$$

$$\mathbf{h}(n) = \mathbf{R}^{-1}(n-1) \mathbf{c}_1 = \frac{1}{\lambda} [\mathbf{h}(n-1) - \mathbf{k}(n) \mathbf{r}^T(n) \mathbf{h}(n-1)] \quad (5.32)$$

$$\mathbf{z}_1(n) = \frac{1}{\mathbf{c}_1^T \mathbf{h}(n)} \mathbf{h}(n) \quad (5.33)$$

$$\mathbf{R}^{-1}(n) = \frac{1}{\lambda} [\mathbf{R}^{-1}(n-1) - \mathbf{k}(n) \mathbf{r}^T(n) \mathbf{R}^{-1}(n-1)] \quad (5.34)$$

The blind RLS-based algorithm is summarized in Table 5.3, together with its computational complexity.

Table 5.3 The blind RLS algorithm.

<i>Input</i> $\mathbf{r}(n), \mathbf{c}_1, \lambda$	
<i>Algorithm</i>	<i>Complexity</i>
$\mathbf{k}(n) = \frac{\mathbf{R}^{-1}(n-1)\mathbf{r}(n)}{\lambda + \mathbf{r}^T(n)\mathbf{R}^{-1}(n-1)\mathbf{r}(n)}$	N^2+N Mult. + N Div.
$\mathbf{h}(n) = \mathbf{R}^{-1}(n-1) \mathbf{c}_1 = \frac{1}{\lambda} [\mathbf{h}(n-1) - \mathbf{k}(n) \mathbf{r}^T(n) \mathbf{h}(n-1)]$	N^2 Mult.
$\mathbf{z}_1(n) = \frac{1}{\mathbf{c}_1^T \mathbf{h}(n)} \mathbf{h}(n)$	N Mult. + N Div.
$\mathbf{R}^{-1}(n) = \frac{1}{\lambda} [\mathbf{R}^{-1}(n-1) - \mathbf{k}(n) \mathbf{r}^T(n) \mathbf{R}^{-1}(n-1)]$	N^2+N Mult + N Div.
<i>TOTAL</i>	$3N^2+3N$ Mult. + N^2+2N Div.

5.3.3 QR-RLS based blind adaptive multiuser detector [93]

Assuming that the autocorrelation matrix $\mathbf{R}(n)$ is positive definite and can be factorized by the Cholesky decomposition as

$$\mathbf{R}(n) = \mathfrak{R}^T(n)\mathfrak{R}(n) \quad (5.35)$$

where $\mathfrak{R}(n)$ an upper triangular matrix. Then define the following quantities:

$$\mathbf{u}(n) = \mathfrak{R}^{-1}(n) \mathbf{c}_1 \quad (5.36)$$

$$\mathbf{v}(n) = \mathfrak{R}^{-1}(n) \mathbf{r}(n) \quad (5.37)$$

$$\alpha(n) = \frac{1}{\mathbf{c}_1^T \mathbf{R}^{-1}(n) \mathbf{c}_1} = \frac{1}{\mathbf{u}^T(n) \mathbf{u}(n)} \quad (5.38)$$

Since $\mathbf{R}(n-1)$ and $\mathbf{u}(n-1)$ are available from the previous recursion, and at time n , a new data vector $\mathbf{r}(n)$ becomes available. Then the following matrix will be constructed, which will be processed by a series of orthogonal transformations as follows:

$$\boldsymbol{\theta}(n) \begin{bmatrix} \sqrt{\lambda} \mathfrak{R}(n-1) & \mathbf{u}(n-1)/\sqrt{\lambda} & \mathbf{0} \\ \mathbf{r}^T(n) & 0 & 1 \end{bmatrix} = \begin{bmatrix} \mathfrak{R}(n) & \mathbf{u}(n) & \mathbf{v}(n) \\ \mathbf{0} & \eta(n) & \gamma(n) \end{bmatrix} \quad (5.39)$$

where: $\boldsymbol{\theta}(n)$ is a unitary transformation (of N successive Givens rotations or Householder transformation discussed in chapter three) that zeros the first N elements on the last row of the constructed matrix at the left hand side of (5.39).

The demodulation of the data bits can be obtained by:

$$\hat{d}_1(n) = \text{sgn}[\eta(n)\gamma(n)] \quad (5.40)$$

And the algorithm is initialized by setting $\mathfrak{R}(n) = \sqrt{\delta} \mathbf{I}$ and $\mathbf{u}(0) = \mathbf{c}_1 / \sqrt{\delta}$, where δ is a small positive number, i.e. the adaptation starts with the matched filter case. At each iteration orthogonal transformation is performed on the prearray to form a block of zero at the bottom row of the postarray and updating $\mathfrak{R}(n)$ and $\mathbf{u}(n)$. The QR-RLS algorithm is summarized in Table 5.4.

Table 5.4 The blind QR-RLS algorithm.

<p>Input $\mathbf{r}(n), \lambda$</p> <p>Initialization $\mathfrak{R}(n) = \sqrt{\delta}\mathbf{I}$ where δ is a small positive number. \mathbf{I} is the identity matrix.</p> <p>$\mathbf{u}(0) = \mathbf{c}_1 / \sqrt{\delta}$</p>	
<i>Algorithm</i>	<i>Complexity</i>
$\theta(n) \begin{bmatrix} \sqrt{\lambda}\mathfrak{R}(n-1) & \mathbf{u}(n-1)/\sqrt{\lambda} & \mathbf{0} \\ \mathbf{r}^T(n) & 0 & 1 \end{bmatrix} = \begin{bmatrix} \mathfrak{R}(n) & \mathbf{u}(n) & \mathbf{v}(n) \\ \mathbf{0} & \eta(n) & \gamma(n) \end{bmatrix}$ <p>$\hat{d}_1(n) = \text{sgn}[\eta(n)\gamma(n)]$</p>	<p>$3N^2 + 7.5N$ Mult. $2N$ Div. N SQRT</p> <p>1 Mult.</p>
TOTAL	<p>$3N^2 + 7.5N + 1$ Mult. $2N$ Div. N SQRT</p>

5.3.4 RMGS-based blind adaptive algorithm

In this section, we propose the blind MOE based on the RMGS algorithm for the adaptation and interference suppression in DS-CDMA systems, due to its attractive features in terms of stability, fast convergence rate and its ability to be implemented in a highly modular systolic structure.

The exponentially weighted LS criterion selects the weight vector $\mathbf{z}_1(n)$ to minimize the sum of exponentially weighted output energy according to Eqs. (5.31-5.34). Assuming that

$$\mathbf{h}(n) = \mathbf{R}^{-1}(n) \mathbf{c}_1 \quad (5.41)$$

then
$$\mathbf{z}_1(n) = \frac{1}{\mathbf{c}_1^T \mathbf{h}(n)} \mathbf{h}(n) \quad (5.42)$$

The weight vector can be updated by updating $\mathbf{R}^{-1}(n)$ recursively. Based on the RMGS algorithm, $\mathbf{R}^{-1}(n)$ can be updated using $\mathbf{k}(n)$, the upper triangular matrix, as follows:

$$\mathbf{R}(n) = \mathbf{k}^T(n) \mathbf{A}(n) \mathbf{k}(n) \quad (5.43)$$

where $\mathbf{A}(n)$ is a diagonal matrix with elements $a_{ij} = 0$, for all $i \neq j$, or

$$\mathbf{R}^{-1}(n) = \mathbf{k}^{-1}(n) \mathbf{A}^{-1}(n) \mathbf{k}^{-T}(n) \quad (5.44)$$

Substituting in Eq. (5.41) we get

$$\mathbf{h}(n) = \mathbf{R}^{-1} \mathbf{c}_1 = \mathbf{k}^{-1}(n) \mathbf{A}^{-1}(n) \mathbf{k}^{-T}(n) \mathbf{c}_1 \quad (5.45)$$

Let $\mathbf{p}(n) = \mathbf{k}^{-T}(n) \mathbf{c}_1$ which can be calculated by back substitution method. Then

$$\mathbf{h}(n) = \mathbf{k}^{-1}(n) \mathbf{A}^{-1}(n) \mathbf{p}(n) = \mathbf{k}^{-1}(n) \mathbf{b}(n) \quad (5.47)$$

where: $\mathbf{b}(n) = \mathbf{A}^{-1}(n) \mathbf{p}(n)$. Again, using the back substitution method, we calculate $\mathbf{h}(n) = \mathbf{k}^{-1}(n) \mathbf{b}(n)$. The vector $\mathbf{h}(n)$ is then used in (5.42) to update the weights vector $\mathbf{z}_1(n)$.

Therefore in order to update the weights vector $\mathbf{z}_1(n)$, the RMGS algorithm updates the upper triangular matrix $\mathbf{k}(n)$, while $\mathbf{R}^{-1}(n)$ is updated using (5.44) and $\mathbf{h}(n)$ is updated in (5.45) by applying the back substitution method twice. The complete RMGS-based blind adaptive algorithm along with its computational complexity is summarized in Table 5.5.

Table 5.5 Summary of the Blind RMGS algorithm.

Input	$r_i(n)$ ($i=1, \dots, N$), λ	
Initialization	$\alpha_1(n)=1$ $a_{ii}(-1)=\delta$, $q_i^{(i)}(n)=r_n(i)$ ($i=1, \dots, N$),	
Algorithm		
1) For $i=1$ to N do $q_i(n) = q_i^{(i)}(n)$ $a_{ii}(n) = \lambda a_{ii}(n-1) + \alpha_i(n) q_i^2(n)$ $\alpha_{i+1}(n) = \alpha_i(n) - \alpha_i^2(n) q_i^2(n) / a_{ii}(n)$ For $j = i + 1$ to N do $q_j^{(i+1)}(n) = q_j^{(i)}(n) - k_{ij}(n-1) q_i(n)$ $k_{ij}(n) = k_{ij}(n-1) + \alpha_i(n) q_j^{(i+1)}(n) q_i(n) / a_{ii}(n)$	3N Mult. N Mult. + N Div.	
2) $\mathbf{h}(n) = \mathbf{R}^{-1} \mathbf{c}_1 = \mathbf{k}^{-1}(n) \mathbf{D}^{-1}(n) \mathbf{k}^{-T}(n) \mathbf{c}_1$	N^2 Mult	
3) $\mathbf{z}_1 = \frac{1}{\mathbf{c}_1^T \mathbf{h}(n)} \mathbf{h}(n)$	N Mult. + N Div.	
TOTAL		$2N^2 + 4N$ Mult. + 2N Div.

The computational complexity of the previously mentioned blind algorithms is summarized in Table 5.6.

Table 5.6 Computational complexity for the blind adaptive algorithms

<i>Algorithm</i>	<i>Multiplications</i>	<i>Divisions</i>	<i>Square-roots</i>
CMA	$2N + 3$	—	—
LMS	$4N + 1$	—	—
RLS	$3N^2 + 2N$	—	—
QR-RLS	$3N^2 + 7.5N + 1$	$2N$	N
RMGS	$2N^2 + 4N$	$2N$	—

5.4 Simulation Results and Discussion

In this section, we consider the blind adaptation and demodulation of DS-SS signals. Unless stated otherwise, an asynchronous system is assumed in which the delays of different users are uniformly distributed random numbers over the interval $[0, T]$ and are kept fixed during the simulation. PN spreading sequences of length $N=31$ are used. Without loss of generality it is assumed that the receiver is synchronized with the desired user (user number 1). The desired user SNR is set equal to 20dB. The near-far situation is assumed in which all the interferers have a 10dB power advantage over the desired user. The performance characteristic is averaged over 100 independent runs in both the blind and decision-directed modes. The optimum signal-to-interference ratio is defined as:

$$SIR^* = \frac{[E\{z_1^T(n)r(n)\}]^2}{\text{var}\{z_1^T(n)r(n)\}} \quad (5.47)$$

The steady state SIR can be shown to be [93]:

$$\text{SIR}^\infty = \frac{\text{SIR}^*}{(1 + \alpha) + \alpha \text{SIR}^*} \quad (5.48)$$

where $\alpha = \frac{1 - \lambda}{2\lambda} (N - 1)$.

Example 5.1

In this example the performance of the blind adaptive DS-CDMA receiver is investigated using the CMA, blind-LMS, Blind-RLS and blind-RMGS algorithms. The near-far situation is assumed, in which nine synchronous interferers are included in the system each having a 10dB power advantage over the desired user. The spreading sequences of length $N=10$ are randomly generated. Fig.5.2 shows the convergence characteristics of the adaptive DS-CDMA receiver in the blind mode. It is clear that the CMA algorithm converges poorly as compared to other blind adaptive schemes, though it is noted from simulation that the convergence characteristics of CMA depends essentially on the initial values setting of the tap-weights. It is also observed that the blind LMS algorithm converges slowly as compared to both RLS and RMGS algorithms, which possess identical convergence characteristics. The CMA algorithm converges in nearly 300 bits and the blind-LMS converges in about 130 bits while the blind-RLS and blind-RMGS algorithms converge in about 40 bits.

Example 5.2

This example shows the tracking capability of the blind adaptive DS-CDMA receiver based on the RMGS algorithm in a dynamic environment. The performance of the receiver is plotted in terms of SIR as a function of the number of bits when the number of interferers is varied with time. The receiver starts with a desired user and four interferers each having 10dB power advantage above the desired user. At time $n=400$, one strong interferer of 10dB

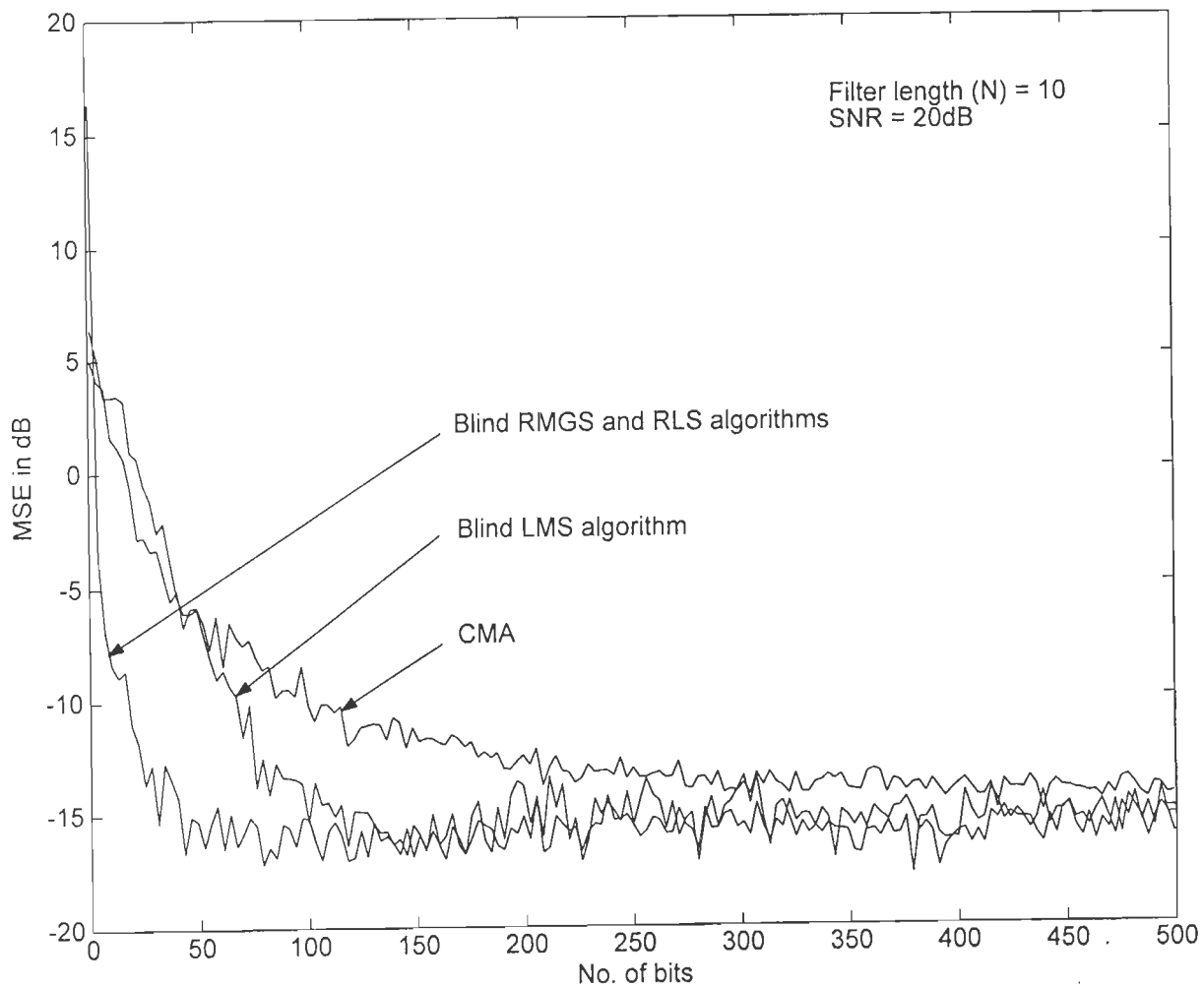


Fig.5.2 Convergence characteristics for the adaptive DS-CDMA receiver using the CMA, LMS RLS and RMGS blind algorithms with nine synchronous interferers (each interferer has 10dB power advantage over the desired user).

power advantage is added to the system. At time $n=800$, another two interferers of 10dB power advantage enter the system and at time $n=1200$, four interferers leave the system. It is clear from Fig. 5.3 that when the interferers access the system the SIR will spike to about 0dB and then in a blind mode adapt to the steady-state SIR value. It is concluded that the RMGS algorithm can adapt quickly in a dynamic environment, which makes it attractive for a mobile communication environment.

Example 5.3

In this example, the effect of changing the forgetting factor (λ) on the steady-state SIR of the adaptive DS-CDMA receiver, in the blind mode adaptation, is presented. The system consists of a desired user and four interferers each having 10dB power advantage over the desired user. The forgetting factor is assumed to be one of these values ($\lambda= 0.98, 0.99, 0.995$ and 0.999). Fig.5.4 shows the SIR plot versus number of bits in the blind mode for different values of the forgetting factor. It is observed that the SIR converges to its steady state value in the same way as the MSE converges to its optimum value. Also it is obvious that the steady state SIR increases as λ increases which is governed by Eq.(5.48).

Example 5.4

In this example, we show the difference between the SIR in the blind and decision-directed modes. The system includes a desired user and four interferers each having 10dB power advantage over the desired user, which incorporates the near-far situation. The decision directed mode operates in the following manner: at time n , the input vector $\mathbf{r}(n)$ is available and the previously calculated weights vector $\mathbf{w}(n-1)$ is used to find the estimate of the desired user data bit $\hat{d}_1(n) = \text{sgn}[\mathbf{r}^T(n)\mathbf{w}(n-1)]$. Assuming that the demodulated data bit

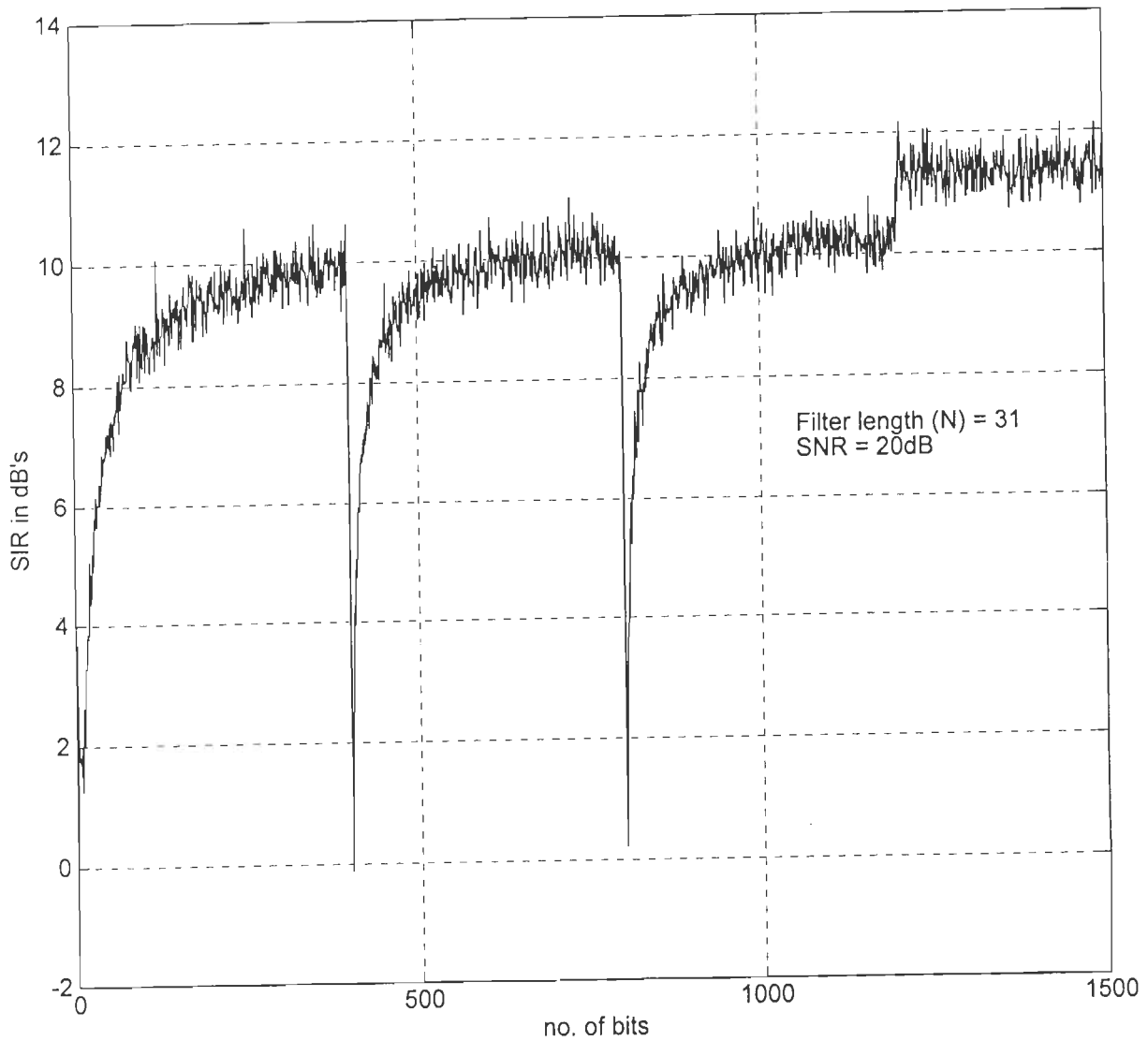


Fig.5.3 The behavior of the adaptive DS-CDMA receiver based on the blind RMGS algorithm in a dynamic environment as given by example 5.2.

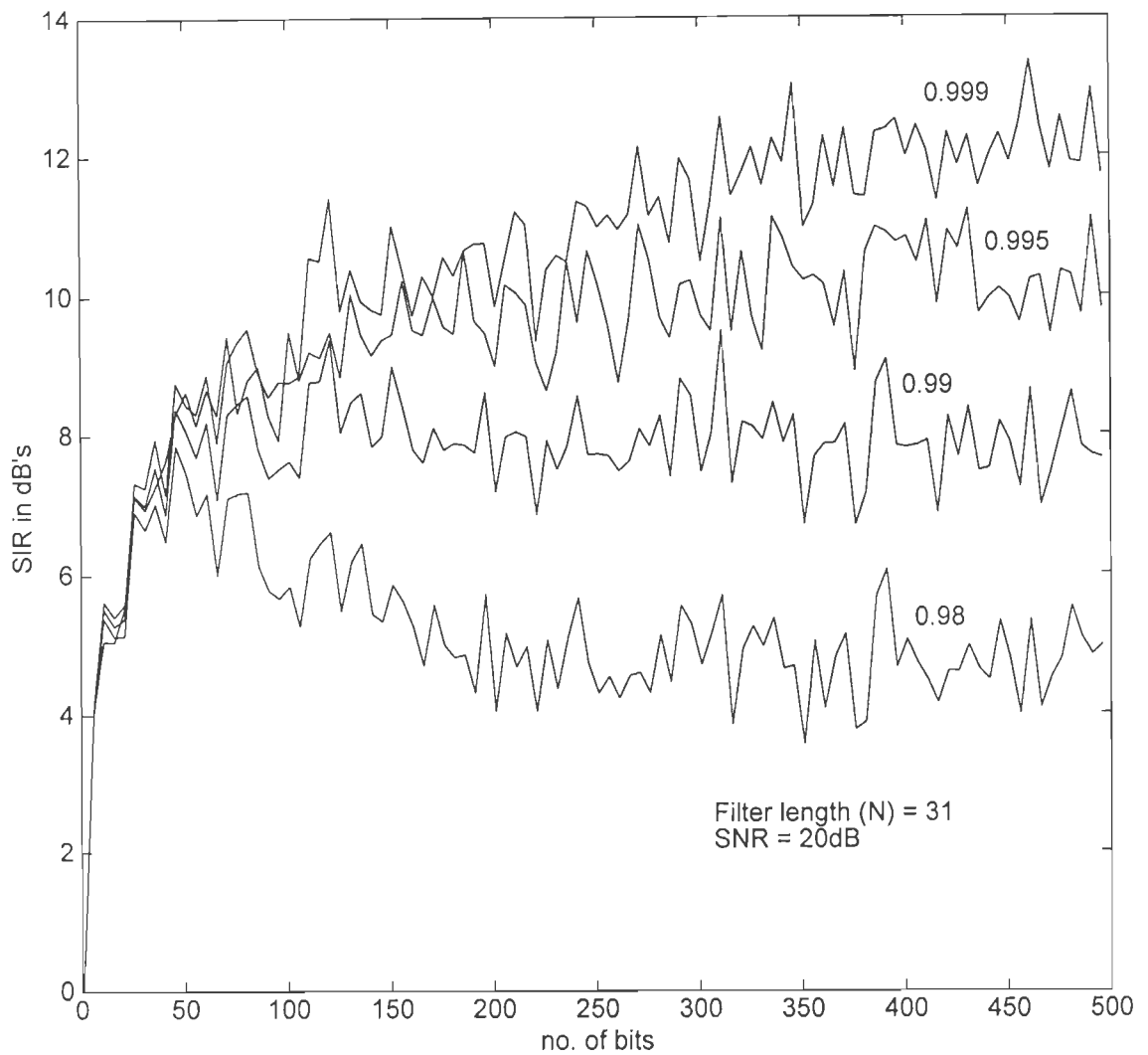


Fig.5.4 Effect of changing the forgetting factor (λ) on the time-averaged SIR versus number of bits in the blind adaptation mode for the adaptive DS-CDMA receiver using the RMGS algorithm with 4 interferers (each interferer has 10dB power advantage over the desired user).

is the true data bit i.e., $d_1(n) = \hat{d}_1(n)$, then we use it to update the weight vector in the conventional (non-blind) adaptive algorithm.

The system starts in the blind adaptation mode and then at $n=500$ bit it changes to the decision directed mode. Fig.5.5 shows the SIR plot versus number of bits for the adaptive DS-CDMA receiver based on the RLS and RMGS algorithms. It is observed that the system converges to SIR value of 10dB in about 120 bits in the blind mode, and after it switches to the decision directed mode it converges to the steady state SIR value of about 18dB in nearly 100 bits. It is clear that there is an 8dB gap in the SIR between the blind and decision-directed modes, which is considered an important drawback of the MOE criterion. It is also clear that the SIR in the decision directed mode is very close to the optimum value.

Example 5.5

In this example, we aim to demonstrate the near-far resistance of the blind adaptive DS-CDMA receiver based on the blind-RMGS algorithm. The probability of error performance of the RMGS-based blind adaptive algorithm is measured by varying the power of each interferer from -2 dB to 10dB relative to the desired user. Two cases have been simulated; in the first case one asynchronous interferer and in the second case with four asynchronous interferers have been assumed. The input SNR is chosen to be 10dB, 12dB or 15dB. Fig.5.6 shows that the probability of error remains nearly constant even though the interference power varies, or the number of interferers changes. This clearly demonstrates the near-far resistance of the blind RMGS-algorithm in the blind adaptation mode.

Example 5.6

In this example, the probability of error performance of the adaptive DS-CDMA receiver based on either training sequence based adaptation or blind adaptation modes are examined. Two cases are simulated. In the first case, the system is adapted using training

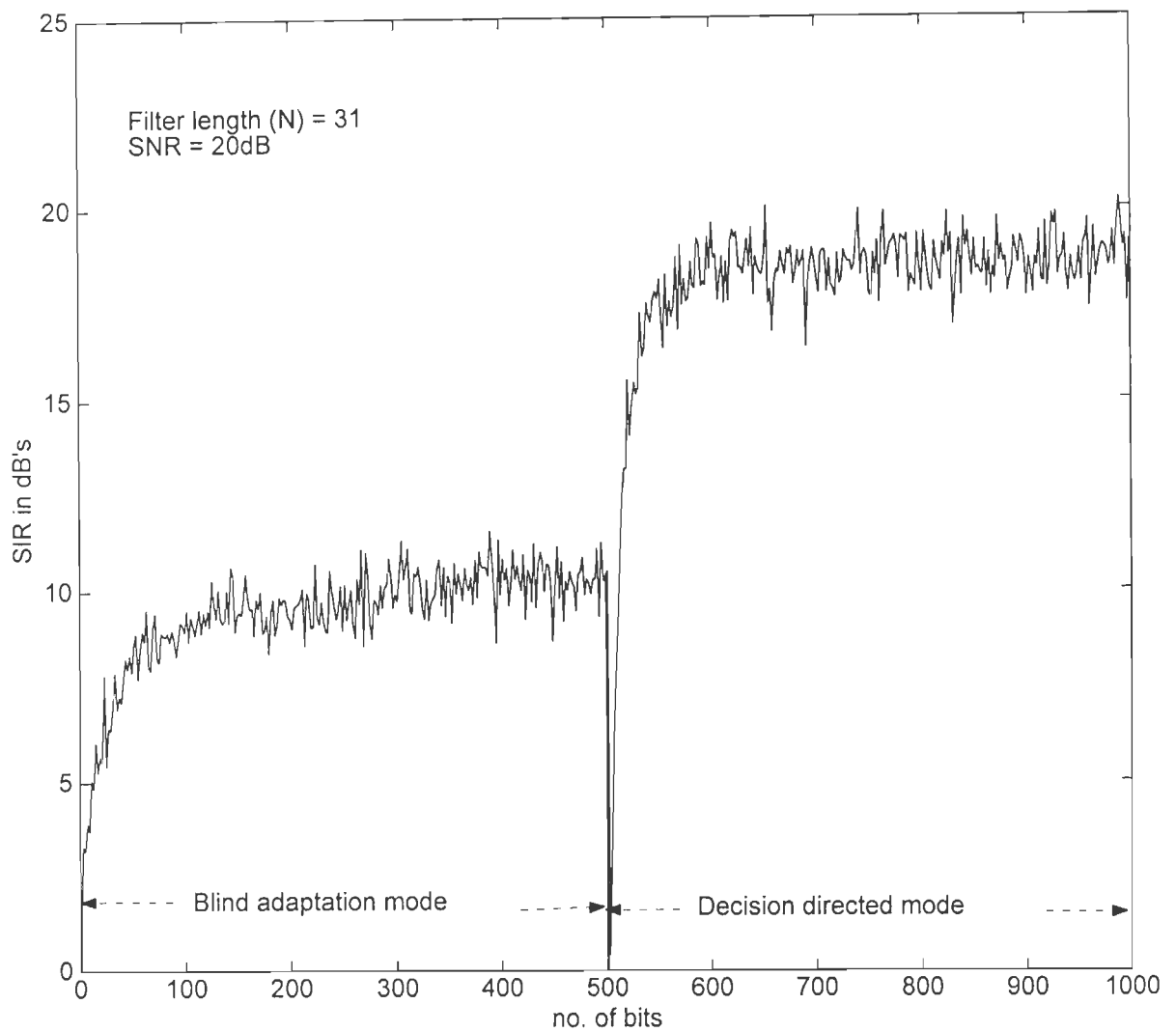


Fig.5.5 Time averaged SIR versus number of bits for the RMGS algorithm using the blind adaptation rule and the decision directed mode, with 4 interferers (each interferer has 10dB power advantage over the desired user).

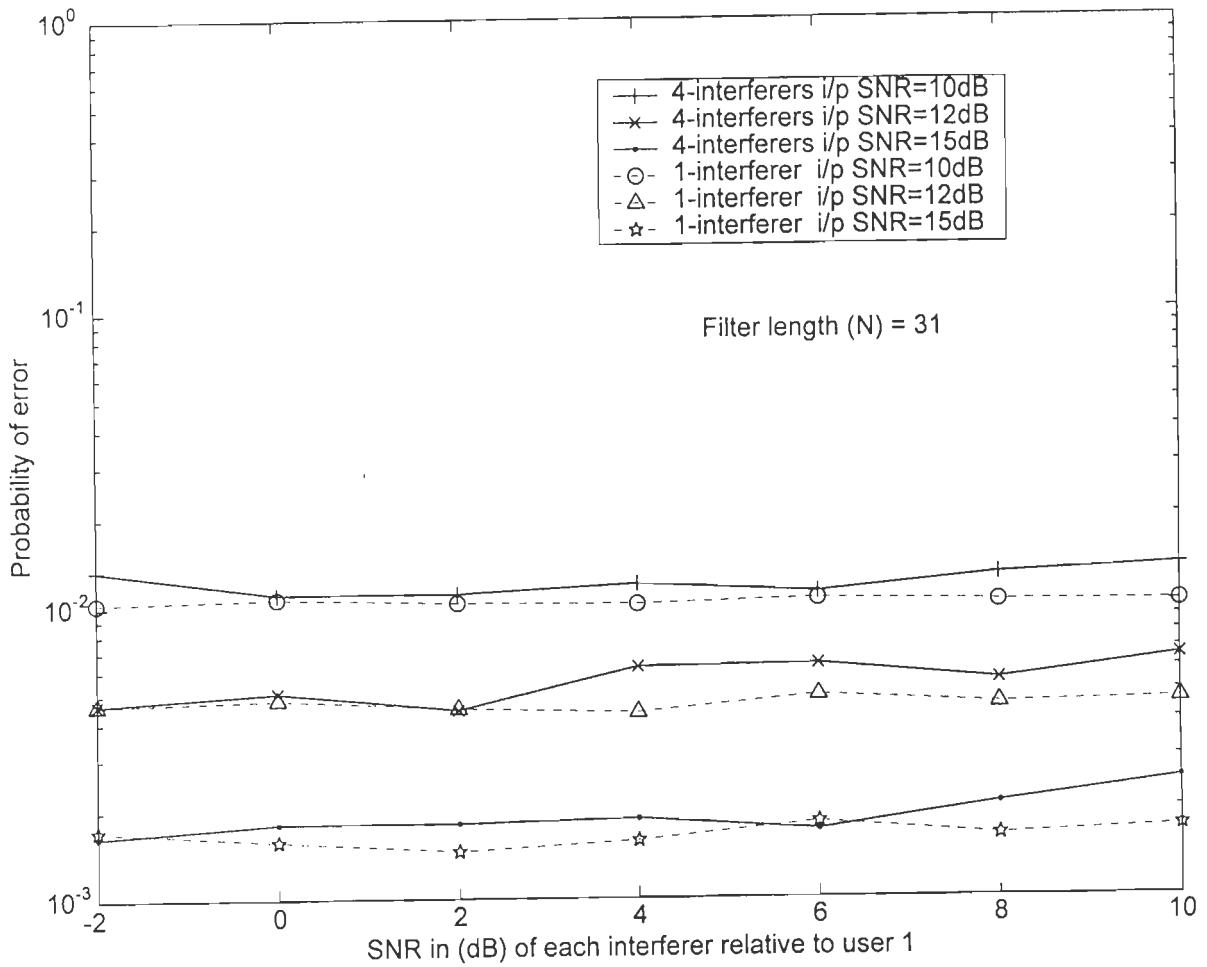


Fig.5.6 Probability of error performance versus interferer's power for the RMGS-based blind adaptive DS-CDMA receiver at different input SNRs for one and four interferers cases.

sequence before switching to the decision directed mode, while in the second case the system is adapted blindly. For comparison, we have also provided in the plot, the single user lower bound and the matched filter upper bound, which are calculated using Eqs.(2.63 and 2.64), respectively. Also provided is a plot of the theoretical values of the probability of error for the adaptive MMSE receiver which is calculated using Eq.(2.60). Eight and ten interferers cases have been simulated each having 10dB power advantage over the desired user.

It is clear from Fig.5.7 that the probability of error performance based on the blind adaptation matches with that of the training sequence based adaptation. This is due to the reason that, while switching from the blind mode to the decision directed mode, the receiver adapts quickly to the same steady-state MSE as that of the training sequence based adaptation, and hence the same probability of error is achieved. Also performance degradation is observed in terms of input SNR as compared to the single user case.

In this chapter, we have considered blind adaptive algorithms based on the Bussgang technique and the MOE criterion for the adaptation and demodulation of DS-CDMA signals. These algorithms include the CMA, blind LMS, blind RLS, and blind QR-RLS algorithms as well as a new blind RMGS algorithm. The proposed RMGS algorithm is shown to be near far resistant and possesses fast convergence rate same as that of the blind-RLS algorithm, and is more stable as compared to the RLS algorithm. Also the proposed blind RMGS algorithm requires lower computational complexity as compared to the blind QR-RLS algorithm. Parallel implementation of the proposed blind RMGS algorithm will reduce the computational complexity to $O[N]$ per processor.

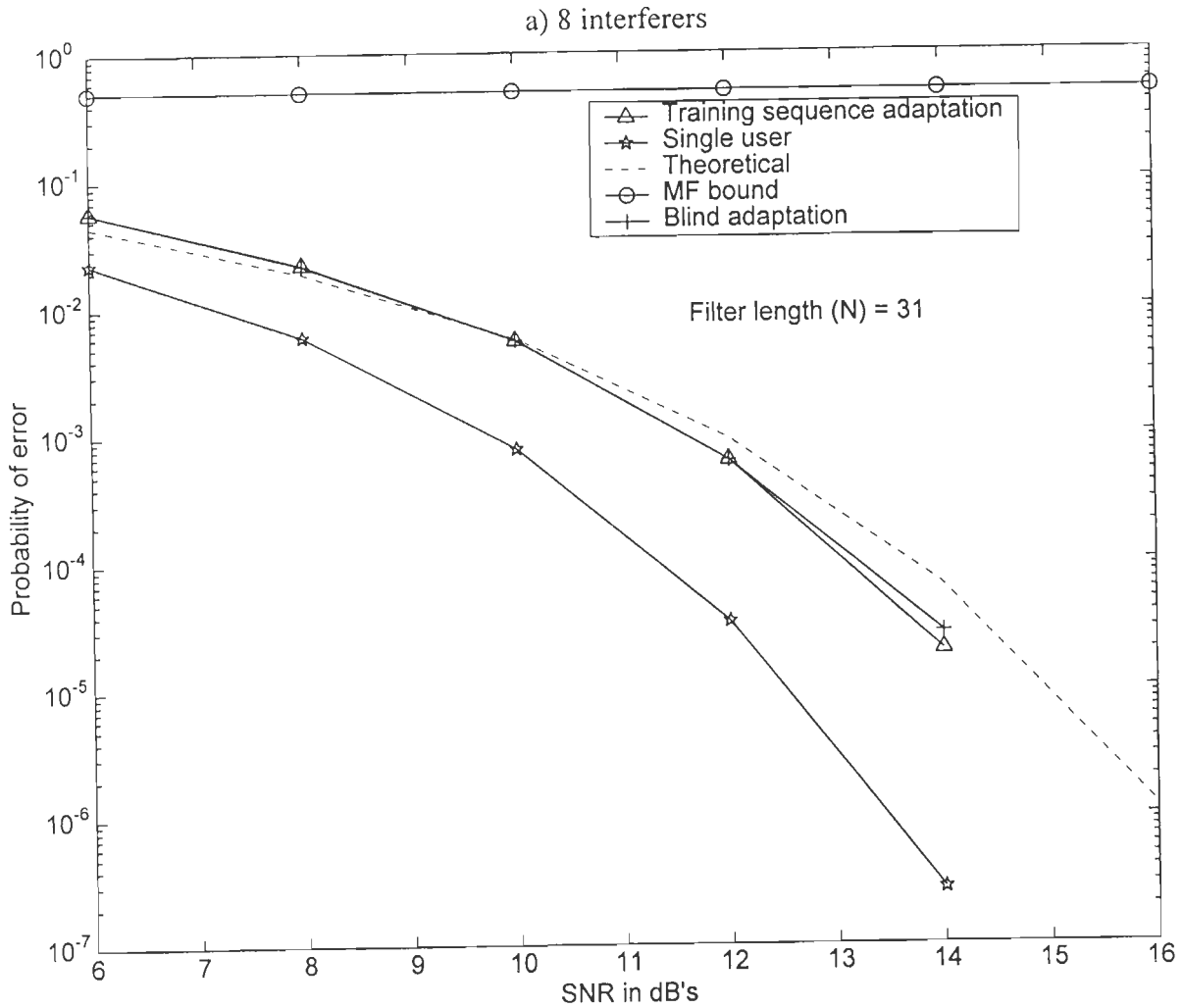


Fig.5.7 Probability of error performance for the adaptive DS-CDMA receiver with blind-adaptation and training sequence adaptation using the RMGS algorithm for a) 8-interferers b) 10 interferers (each interferer has 10dB power advantage over the desired user)

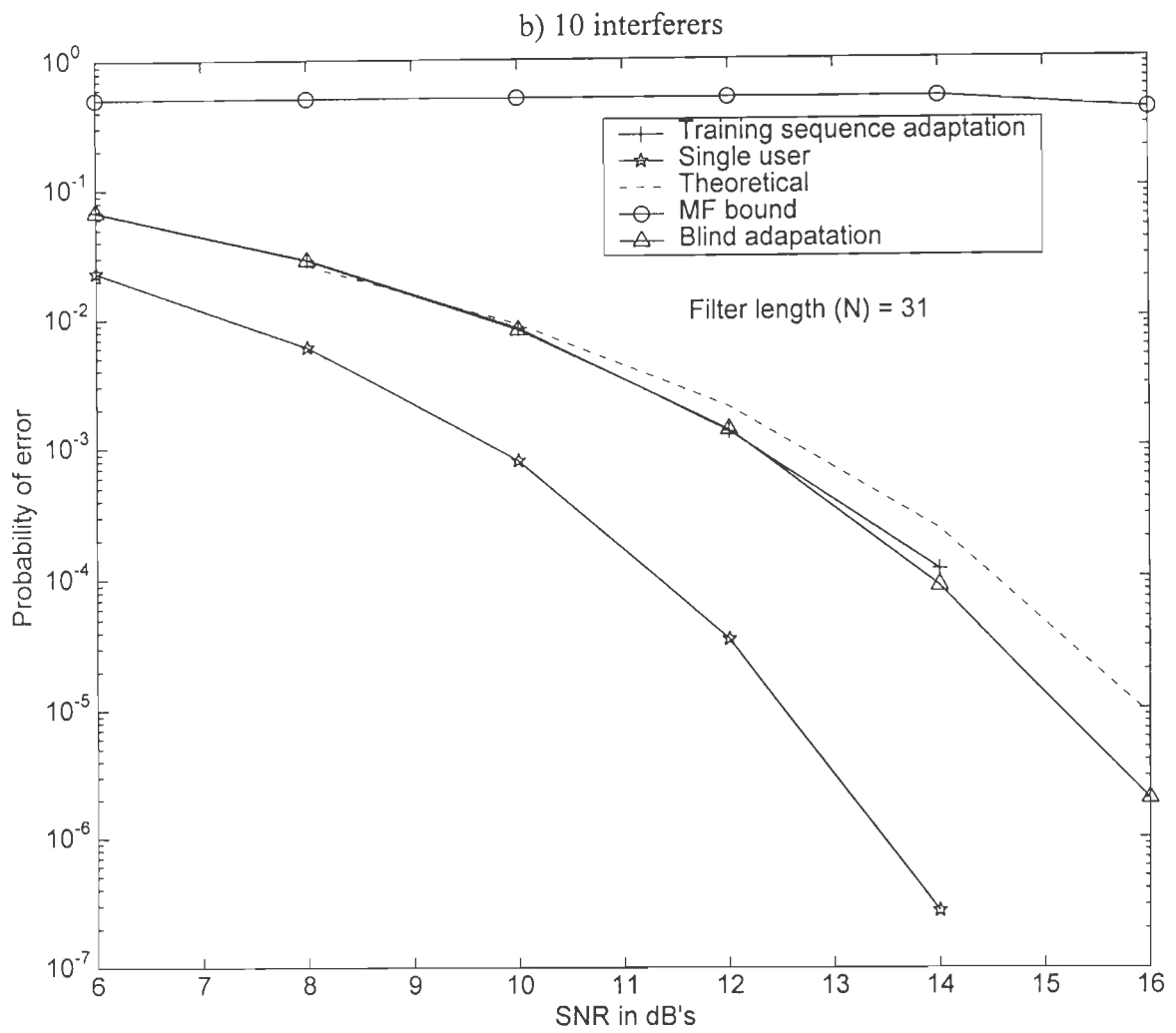


Fig.5.7b

ADAPTIVE TIME-DELAY ESTIMATION USING RMGS

ALGORITHM

The adaptive implementation of the MMSE receiver for interference suppression in DS-CDMA systems requires the knowledge of the training sequence for the desired user before switching to the decision directed mode. This of course assumes the knowledge of the code timing for the desired user, which we have assumed to be known in the previous chapters. In this chapter, we remove this restriction by presenting adaptive algorithms for time-delay estimation, of the desired user, in both the initialization and the tracking modes. Section 6.1 introduces some theoretical background and reviews the time-delay estimation algorithms. In section 6.2, a time-delay estimator based on processing the MMSE weights vector using the RMGS algorithm is presented. Another TDE for both the initialization and tracking modes is presented in section 6.3, which is based on running N-parallel MMSE algorithms at different hypothetical values of the desired user delay. Section 6.4 presents a blind version of the TDE method. The computational complexity of the blind adaptive algorithms is provided in section 6.5. Finally, simulation results and discussion are given in section 6.6.

6.1 Introduction

Because of the nonlinear dependence of the received signal on the user's time delay in DS-CDMA systems, time delay appears to be the hardest to estimate and there has been a considerable effort devoted towards solving this problem.

Assuming asynchronous DS-CDMA system with K users simultaneously transmitting over the same channel with AWGN, the baseband transmitted signal due to the k th user is given by:

$$s_k(t) = \sum_{n=-\infty}^{\infty} d_k(n) c_k(t - nT) \quad (6.1)$$

where $d_k(n)$ is the data bits of the k th user, and T is the signaling bit interval. The spreading sequence of the k th user may be defined as:

$$c_k(t) = \sum_{j=0}^{N-1} c_{k,j} \psi(t - jT_c) \quad (6.2)$$

where $N=T/T_c$ is the processing gain, $\psi(t)$ is the chip waveform of rectangular shape and duration T_c , and $c_{k,j} \in \{-1,1\}$ is the j th element of the spreading code of the k th user. The total received signal is given by:

$$y(t) = \sum_{k=1}^K \sqrt{P_k} s_k(t - \tau_k) \cos(\omega_c t + \theta_k) + n(t) \quad (6.3)$$

where P_k is the k th user power and τ_k is its delay which is assumed to be uniformly distributed over $[0,T]$, θ_k is its phase, ω_c is the carrier frequency and $n(t)$ is AWGN. Further it is assumed that θ_1 , the phase of the desired user =0.

The receiver is asynchronous with all users including the desired user, the user 1. It is, therefore, required to estimate its delay τ_1 , which is assumed to be within a single bit interval (i.e. $0 \leq \tau_1 \leq T$).

The time-delay estimate, in the cross-correlation technique of [48, 91], is given by the peak location of the crosscorrelation between the true signal and its filtered delayed version. This is a single user method and works reasonably well in a multiuser environment if the received powers are similar, but it fails in a near-far environment.

The time-delay can also be modeled as an FIR filter, whose coefficients represents the estimate of the time-delay and may be updated using the LMS algorithm [15]. A class of gradient-based algorithms has been introduced in [59] for joint estimation of time delay and

IIR filtering. However, the algorithm exhibits local minima and in order to ensure global convergence of the algorithm, extra conditions are needed. Boudrea and Kabal [13] proposed a least square (LS) estimation criterion to perform the joint estimation of the delay and filter coefficients. The filter is updated using the FTF-RLS algorithm, while the delay is updated using a form of derivative. It is shown that both stationary and time-varying delays are effectively tracked. Drawbacks of this method is that the algorithm restrict adaptive delay values to integer numbers of samples and also the time averaging for the LS error is required for each new lag, which will introduce additional delay for the convergence to occur and large data have to be gathered.

Algorithms based on the maximum likelihood (ML) rule, for estimating the users delays, amplitudes and phases have been developed in [10]. It has been shown that this ML estimator is capable of eliminating the near-far effect as well as processing the signals propagated through multiple paths. However, it requires the knowledge of the transmitted symbols, which can be accomplished by using feedback decisions from the detector. Zheng et al. [127] have presented a large sample ML (LSML) algorithm for estimating the code timing of a known training sequence in an asynchronous DS-CDMA system. This algorithm is a single-user TDE and is shown to be near far resistant. One limitation of the LSML estimator is that it is applicable to stationary systems where the channel remains reasonably static over the duration of time in which the code acquisition is performed. G. Ye et al. [125] have extended the ML algorithm of [127]. It is shown by simulation that the proposed estimator is near-far resistant with reduced computational complexity.

Bensely et al. [9] have considered the estimation of the channel parameters for DS-CDMA communication systems operating over channels with either single or multiple propagation paths and the time-delay of each propagation path is to be estimated. The

channel estimate is formed by projecting a given user's spreading waveform into the estimated noise subspace and then by either maximizing the likelihood or minimizing the Euclidean norm of this projection. The algorithm is near-far resistant but requires $O[N^3]$ computational complexity. Strom et al. [106] have proposed algorithms to deal with the propagation delay, phase and amplitude estimation of all users in DS-CDMA systems. These are the ML, MUSIC and the sliding correlator algorithms. The computational complexity of the sliding correlator is simple, however, it is only optimal in a single-user system (i.e. in the presence of WGN only), but is highly suboptimal in the presence of MAI, especially in a near-far situation. On the other hand, both the ML and MUSIC algorithms are shown to be near-far resistant, but with increased computational complexity, $O[N^3]$. Parkvall et al. [89] proposed a CDMA receiver using the modified MUSIC estimator in conjunction with the MMSE interference suppression to obtain a near-far resistant receiver without a priori synchronization. Parameters that are required by the MMSE suppression receiver are readily obtained from the MUSIC estimator and are not assumed to be known in advance.

Smith et al. [105] have presented a single user code timing estimation algorithm that is based on processing the weight vector of an adaptive DS-CDMA receiver. The performance of this detector is better than the traditional correlator-based approach, and it is found to be near-far resistant when the RLS adaptive filter is used. However, the technique requires an all-ones training sequence or it requires the filter's length to be doubled (i.e. $2N$) such that the bit transitions will be within the observation interval. Madhow [68] has suggested a near-far resistant method, which automatically accounts for the delays and amplitudes of the desired signal without explicitly estimating these parameters. The technique runs N -parallel adaptive MMSE receivers at N -hypothetical values of the delay; then finding the delay, which produces the lowest MSE. The only requirements are a training sequence for the

desired user and a finite uncertainty regarding the symbol timing. A drawback of this method is that it is not designed to recover chip timing, which causes some performance loss. In [67] a similar idea has been proposed, but it is based on the blind MOE algorithms as a building block. The delay is found by the location that possesses the best MOE. Some performance degradation is noticed as compared to training-based algorithms.

Work on joint data detection and parameter estimation was presented in [44]. The algorithm is made adaptive and the likelihood metric is updated using a set of EKF filters. Lim et al. [60] had introduced adaptive multiuser detector structures using the EKF and RLS formulation to jointly estimate the transmitted bits and individual amplitudes and time delay of each user. The proposed detector works in the tracking mode and it outperforms a bank of single user detectors in terms of near-far resistance. Caffery and Stüber [14] have presented a joint channel and time-delay tracking technique for CDMA systems using an iterative non-linear filtering algorithm. The complexity is reduced from that of the standard of EKF when the number of users is large. However, the above algorithms are computationally complex (exponential in the number of users).

Based on the MMSE criterion, in this chapter, we have considered two near-far resistant TDE estimation methods using the RMGS algorithm, namely: the MMSE weights processing method and the parallel MMSE algorithm.

6.2 TDE by processing the MMSE weights vector

In this section, we present a time-delay estimation algorithm that is based on processing the weight vector obtained using the MMSE criterion. It has been shown in [105] that the weights vector adapts in the mean to a scaled time-shifted version of the spreading code of the desired user.

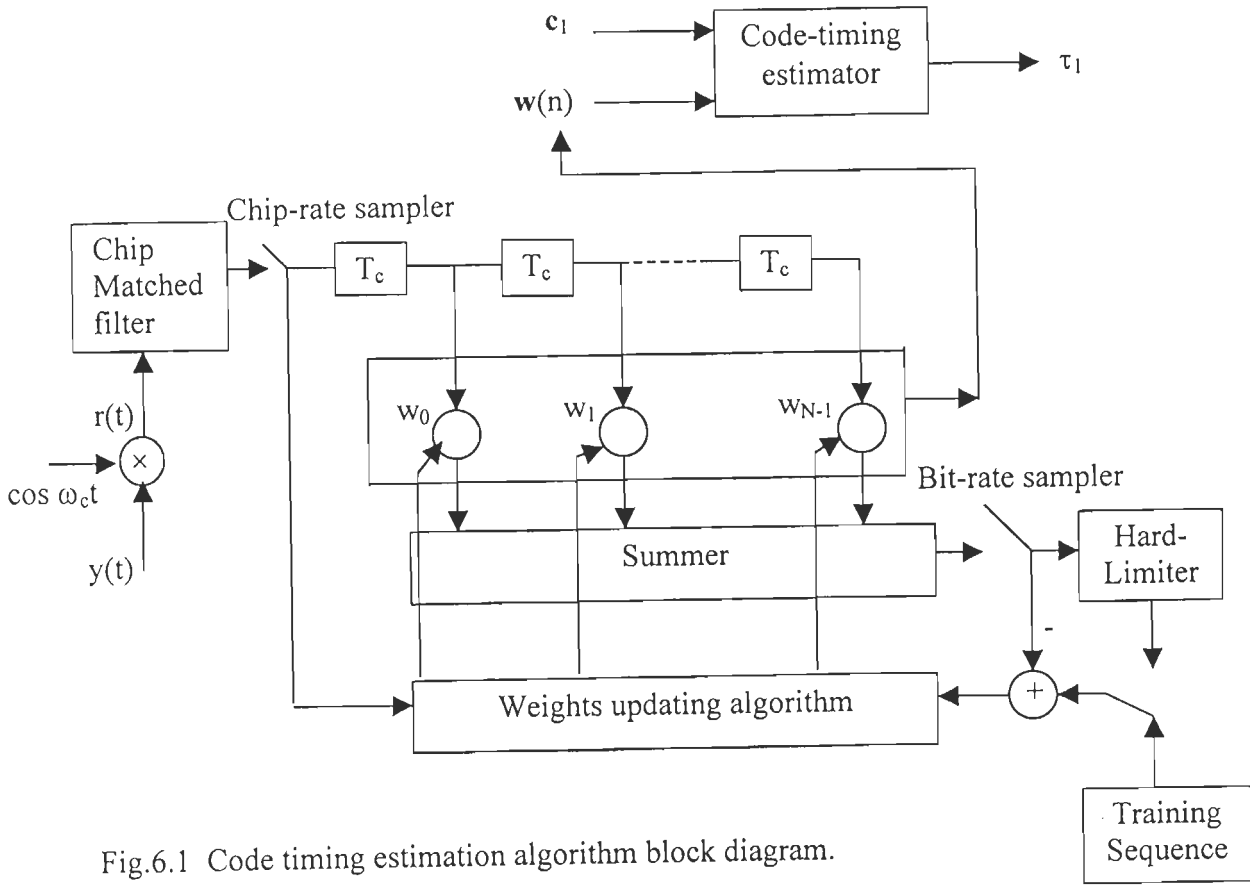


Fig.6.1 Code timing estimation algorithm block diagram.

The receiver converts the received signal $y(t)$ to the baseband signal $r(t)$. After the baseband conversion, the signal $r(t)$ is chip matched-filtered and sampled at the chip rate producing the vector $\mathbf{r}(n)=[r_0(n) \ r_1(n) \ \dots \ r_{N-1}(n)]^T$ which represents the contents of the TDL at the n th data sample time. Assuming that $\mathbf{c}_k=[c_{0,k} \ c_{1,k} \ \dots \ c_{N-1,k}]^T$ is the spreading sequence for the k th user, then the TDL filter contents can be written as [see chapter 2]:

$$\mathbf{r}(n)=d_1(n) \mathbf{c}_1 + \sum_{k=2}^K \sqrt{P_k} \ d_k(n) \mathbf{I}_k(n) \cos(\theta_k) + \boldsymbol{\eta}(n) \tag{6.4}$$

$$\mathbf{I}_k(n) = z_{2k-1}(n)\mathbf{a}_{2k-1}(\rho_k, \delta_k) + z_{2k}(n)\mathbf{a}_{2k}(\rho_k, \delta_k) \tag{6.5}$$

$$z_{2k-1}(n)=[d_k(n)+d_k(n-1)]/2 \tag{6.6}$$

$$z_{2k}(n)=[d_k(n)-d_k(n-1)]/2 \tag{6.7}$$

where:

$$\mathbf{a}_{2k-1}(\rho_k, \delta_k) = \left\{ \delta_k \mathbf{c}_k^{(\rho_k+1)} + (1-\delta_k) \mathbf{c}_k^{(\rho_k)} \right\} \quad (6.8)$$

$$\mathbf{a}_{2k}(\rho_k, \delta_k) = \left\{ \delta_k \hat{\mathbf{c}}_k^{(\rho_k+1)} + (1-\delta_k) \hat{\mathbf{c}}_k^{(\rho_k)} \right\} \quad (6.9)$$

$$\mathbf{c}_k^{(m)} = [c_{k,N-m} \ c_{k,N-m+1} \ \dots \ c_{k,N-1} \ c_{k,0} \ c_{k,1} \ \dots \ c_{k,N-m-1}]^T \quad (6.10)$$

$$\hat{\mathbf{c}}_k^{(m)} = [-c_{k,N-m} \ -c_{k,N-m+1} \ \dots \ -c_{k,N-1} \ c_{k,0} \ c_{k,1} \ \dots \ c_{k,N-m-1}]^T \quad (6.11)$$

$\mathbf{r}(n)$ is a vector of random Gaussian noise variables with zero mean and variance of σ^2 and $\tau_k = \rho_k T_c + \delta_k T_c$ with $\rho_k \in \{0, 1, \dots, N-1\}$ and $0 < \delta_k < 1$ is the delay of the k th user.

The optimal weight vector for the MMSE receiver is given by the Wiener-Hopf solution $\mathbf{w}_o(n) = \mathbf{R}^{-1}(n) \mathbf{P}(n)$, where $\mathbf{R}(n) = E[\mathbf{r}(n) \mathbf{r}^T(n)]$ is the autocorrelation matrix, and $\mathbf{P}(n) = E[d_1(n) \mathbf{r}(n)]$ is the crosscorrelation vector. In a stationary environment, the forms of $\mathbf{R}(n)$ and $\mathbf{P}(n)$ are independent of n and are given by [105]:

$$\begin{aligned} \mathbf{R} = & \mathbf{a}_1(\rho_k, \delta_k) \mathbf{a}_1^T(\rho_k, \delta_k) + \sigma^2 \mathbf{I} + \sum_{k=2}^K \frac{P_k}{P_1} \mathbf{a}_{2k-1}(\rho_k, \delta_k) \mathbf{a}_{2k-1}^T(\rho_k, \delta_k) \\ & + \sum_{k=2}^K \frac{P_k}{P_1} \mathbf{a}_{2k}(\rho_k, \delta_k) \mathbf{a}_{2k}^T(\rho_k, \delta_k) \end{aligned} \quad (6.12)$$

$$\mathbf{P} = \mathbf{a}_1(\rho_k, \delta_k) \quad (6.13)$$

Since it is assumed that the receiver is not synchronized with the desired user, then the observation interval of length (T) will obviously include portions of two adjacent bits. This of course, might turn out to have bit transitions within the observation interval. To avoid bit transitions, it is suggested that the desired user might use an all one training sequence. However, this poses a problem when new users are planning to access the network. Possible solutions to this problem are to use a side channel to control the addition of a new user, or to

increase the received vector length to $2N$. However, this means doubling the filter length, leading to increased computational complexity.

In order to justify the use of the crosscorrelation between the MMSE weights vector and the spreading sequence in the TDE algorithm, we will observe the weight vector for the following case. We assume that there is only one chip-synchronous user with phase shift $\theta_1=0$, which implies that

$$\mathbf{r}(n) = \mathbf{c}_1^{(m)} + \boldsymbol{\eta}_n \quad (6.14)$$

Using the Wiener-Hopf equation, it can be shown that:

$$\mathbf{w}(n) = \frac{\mathbf{c}_1^{(m)}}{\|\mathbf{c}_1\|^2 + \sigma^2} \quad (6.15)$$

It is clear that the optimal weight vector is a scaled delayed version of the desired user spreading sequence, therefore, the delay of the desired user could be found by the location of the peak of the crosscorrelation magnitude between \mathbf{c}_1 and $\mathbf{w}(n)$. It has been shown in [105] that adding near-far interferers to the system will introduce small perturbation of the filter weight vector around the solution given by (6.15). However, we are still able to find delay-estimates with reasonable accuracy.

The weights of the adaptive MMSE filter could be obtained using the LMS or RLS algorithms. However, we propose the use of the RMGS algorithm due its attractive features as discussed earlier in chapter four. The code timing estimation is performed using the following procedure. The MMSE weight vector, obtained by adopting the RMGS algorithm, is crosscorrelated with the desired user spreading sequence. This is followed by a search for the chip that provides the largest crosscorrelation peak, which will give the delay estimate. The MMSE timing estimate is thus given by:

$$\hat{\tau}_1 = \arg \max_{(\rho, \delta)} \left\{ \frac{|\mathbf{a}_1^T(\rho, \delta) \mathbf{w}(n)|^2}{\|\mathbf{a}_1(\rho, \delta)\|^2} \right\} \quad \delta=1 \quad (6.16)$$

This of course, will produce an estimate equal to integer multiples of the chip interval, which leads to an estimation error up to T_c . Therefore, to estimate the timing within a fraction of a chip, a quadratic interpolation between this chip and its two neighboring chips is performed. Denoting the chip with the maximum cross-correlation by τ_a and its two neighboring chips by τ_b , and τ_c , and their corresponding crosscorrelation values to be designated by $f(\tau_a)$, $f(\tau_b)$ and $f(\tau_c)$, respectively, then the estimated code-timing delay may be calculated by [94]:

$$\tau_1 = \tau_b - \frac{1}{2} \frac{(\tau_b - \tau_a)^2 [f(\tau_b) - f(\tau_a)] - (\tau_b - \tau_c)^2 [f(\tau_b) - f(\tau_c)]}{(\tau_b - \tau_a)[f(\tau_b) - f(\tau_c)] - (\tau_b - \tau_c)[f(\tau_b) - f(\tau_a)]} \quad (6.17)$$

The justification for using quadratic interpolation is that there exists a maximum value of the crosscorrelation residing somewhere nearby or within this chip. However, though the use of quadratic interpolation is not completely precise in this case, simulation results show that it provides reasonable accuracy in the time-delay estimate. In conclusion, the above method may be summarized as:

- Find the MMSE weight vector $\mathbf{w}(n)$ using the RMGS algorithm.
- Crosscorrelate the weight vector $\mathbf{w}(n)$ with desired user spreading sequence \mathbf{c}_1 , delayed at integer chip intervals.
- Find the chip τ_a , which corresponds to the largest (peak) crosscorrelation value.
- Estimate the time delay τ_1 by interpolating τ_a and its neighbors τ_b and τ_c .

6.3 Parallel adaptive MMSE TDE scheme

The previous TDE method suffers form performance degradation as the number of interferers grows up due to the perturbation error introduced in the relation between the

weight vector and the desired user spreading sequence [105]. Therefore, in this section, we present a near-far resistant MMSE time-delay estimation algorithm for DS-CDMA systems which will avoid the weights processing TDE drawback. We assume a near-far situation in which strong interferers exist in the system, and that the delay of the desired user is within one bit interval T , (i.e. $0 \leq \tau_1 \leq T$). Also we assume that the desired user phase is $\theta_1=0$, such that real signal representation is used. The received signal is defined as in (6.4). The observation interval is chosen to be equal to $2T$ (i.e. $2N$ chips) such that it will guarantee the inclusion of the desired bit within it. This means that three consecutive bits might be included within this observation interval as indicated in Fig.(6.2). Therefore the observation vector will include $2N$ samples defined as $\mathbf{r}_E(n)=[r(nN), r(nN+1), \dots, r\{nN+(2N-1)\}]^T$.

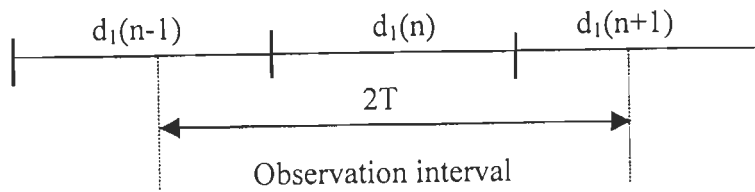


Fig.6.2 The observation interval includes three consecutive bits.

We run N -parallel adaptive MMSE algorithms at the following hypothetical delay values of the desired user; $\tau=0, T_c, \dots, iT_c, \dots, (N-1)T_c$. Therefore, the processed part of the observation vector $\mathbf{r}_E(n)$ will be, $\mathbf{r}(n) \in R^N$, $\mathbf{r}(n)=[r(nN+i), r(nN+1+i), \dots, r\{nN+N-1+i\}]^T$. Again the optimal weight vector for the MMSE receiver is given by the Wiener-Hopf solution $\mathbf{w}_o(n)=\mathbf{R}^{-1}(n)\mathbf{P}(n)$, where $\mathbf{R}(n)=E[\mathbf{r}(n)\mathbf{r}^T(n)]$ is the autocorrelation matrix and $\mathbf{P}(n)=E[d_1(n)\mathbf{r}(n)]$ is the crosscorrelation vector.

The MMSE receiver forms an estimate of the desired data bit given by:

$$\hat{d}_1(n) = \text{sgn}[\mathbf{w}^T(n) \mathbf{r}(n)] \quad (6.18)$$

where $\mathbf{w}(n) \in R^N$ is the weight vector which minimizes the MSE between the estimated and the actual data bits of the desired user, $d_1(n)$, defined by:

$$\text{MSE} = E[\{d_1(n) - \mathbf{w}^T(n) \mathbf{r}(n)\}^2] \quad (6.19)$$

The receiver requires a training sequence before switching to the decision directed mode. In the training phase, we find the delay at which the receiver will provide the largest crosscorrelation value between the weight vector and the desired user spreading sequence. This will be the estimated delay measured in multiples of the chip delay. To find the TDE within a fraction of a chip, we may sample the received signal at T_c/m intervals, which will provide improved TDE accuracy within $\{-T_c/(2m) \leq \tau_1 \leq +T_c/(2m)\}$, however, this will cause an m -fold increase in the received vector length and hence leading to higher computational complexity. A better solution is to sample the received signal at the chip rate and using quadratic interpolation between the chip with the largest crosscorrelation peak and its two neighboring chips find the value of the delay at which the crosscorrelation peak occurs. (which resides inside this chip or the two neighboring chips). The estimated delay of the desired user will be selected at the interpolated maximum. Denoting the chip with the largest crosscorrelation peak by τ_a , and its two neighboring chips by τ_b and τ_c , and their corresponding crosscorrelation values by $f(\tau_a)$, $f(\tau_b)$ and $f(\tau_c)$, respectively, the interpolated value of delay can be computed using Eq.(6.20). The Parallel MMSE TDE method may be summarized as follows:

- Find the weight vector $\mathbf{w}(n)$ for each hypothesis using the RMGS algorithm.
- For each hypothetical delay, find the crosscorrelation of $\mathbf{w}(n)$ with the desired user spreading sequence \mathbf{c}_1 .
- Find the hypothesis, which provides the largest crosscorrelation peak.

- The delay τ_1 is estimated, within a fraction of a chip, by using quadratic interpolation between the chip of best hypothesis and its two neighboring chips.

6.4 Blind TDE

In this section, we implement the TDE method presented in section 6.3 in the blind adaptation mode (by removing the requirement of a training sequence). We use the blind MOE detector based on the RMGS (introduced in section 5.4) as a building block for the joint demodulation and TDE of the desired user signal. The philosophy of implementing this method is the same as that of the TDE of section 6.3 except for the removal of the training sequence restriction. The only side information required is the knowledge of the spreading sequence of the desired user. The length of the observation interval is chosen to be $2T$, such that one complete bit of the desired user, $d_i(n)$, falls in this interval. This observation interval corresponds to $2N$ samples such that $\mathbf{r}_E(n)=[r(nN), r(nN+1), \dots, r(nN+(2N-1))]^T$. We run N -parallel RMGS-based blind adaptive algorithms at hypothetical values of the delay equal to integer multiples of the chip interval, i.e., $\tau=0, T_c, \dots, iT_c, \dots, (N-1)T_c$, such that the processed part of the observation vector $\mathbf{r}_E(n)$ will be, $\mathbf{r}(n) \in R^N$, $\mathbf{r}(n)=[r(nN+i), r(nN+i+1), \dots, r(nN+i+N-1)]^T$.

Based on the MOE criterion, the exponentially weighted LS criterion selects the weights vector $\mathbf{w}(n)$ to minimize the sum of exponentially weighted output energy:

$$\text{minimize } \sum_{i=1}^n \lambda^{n-i} [\mathbf{w}^T(n) \mathbf{r}(n)]^2 \quad (6.20)$$

$$\text{subject to } \mathbf{c}_1^T \mathbf{w}(n) = 1 \quad (6.21)$$

where $0 < \lambda < 1$ is the forgetting factor. The solution of this constrained optimization problem is given by (see appendix B):

$$\mathbf{w}(n) = \frac{1}{\mathbf{c}_1^T \mathbf{R}^{-1}(n) \mathbf{c}_1} \mathbf{R}^{-1}(n) \mathbf{c}_1 \quad (6.22)$$

$$\text{where } \mathbf{R}(n) = \sum_{i=1}^n \lambda^{n-i} \mathbf{r}(i) \mathbf{r}^T(i) \quad (6.23)$$

The mean output energy is:

$$=E[(\mathbf{w}^T(n) \mathbf{r}(n))] = \mathbf{w}^T(n) \mathbf{R}(n) \mathbf{w}(n) = \frac{1}{\mathbf{c}_1^T \mathbf{R}^{-1}(n) \mathbf{c}_1} \quad (6.24)$$

All signal vectors are normalized to unit energy to enable a fair comparison of the MOE's for different hypothesis. The normalized MOE is then defined as [67]:

$$=E\left[\left(\frac{\mathbf{w}^T(n) \mathbf{r}(n)}{\|\mathbf{w}(n)\|^2}\right)^2\right] = \frac{\mathbf{w}^T(n) \mathbf{R}(n) \mathbf{w}(n)}{\|\mathbf{w}(n)\|^2} \quad (6.25)$$

At each hypothesis, the normalized MOE solution is found by simulation. Then we choose the best hypothesis as the estimated delay of the desired user. Again, this delay is equal to integer multiple of the chip interval, and a quadratic interpolation between this bit and its two neighboring chips is performed to estimate the delay within a fraction of a chip using (6.17).

An attractive feature of this receiver is that no side information about the user is required except the knowledge of the desired user spreading sequence. Moreover, the method is shown to be near far resistant. It requires $O[N^3]$ computational complexity in the acquisition mode when the RMGS algorithm is used, then after switching to the decision directed mode for tracking, the method requires $O[3N^2]$ computations.

6.5 Computational complexity

The computational complexity of the above TDE methods, based on the using the LMS and the RMGS algorithms, is summarized in Table 6.1.

Table 6.1 Computational complexity of the implemented TDE methods in the acquisition mode (The observation interval equal $2N$).

<i>Method</i>		<i>Multiplications</i>	<i>Divisions</i>
TDE based on MMSE weights processing	LMS	$8N+8$	2
	RMGSEF	$6N^2+13N+7$	$4N+2$
TDE based on parallel adaptive MMSE weights processing	LMS	$2N^2+N+7$	1
	RMGSEF	$1.5N^3+4.5N^2+7$	$2N^2+1$
	Blind RMGSEF	$2N^3+4N^2+7$	$2N^2+1$

It is clear that the computational complexity of the RMGSEF-based TDE algorithms, in the acquisition mode, is an order of magnitude higher than that of the LMS-based TDE algorithms. However, the RMGSEF-based TDE algorithms converge much faster and possess better performance as compared to the LMS-based TDE algorithm. In the tracking mode, the computational complexity of weights processing TDE method will be the same as that of the acquisition mode, while for the parallel TDE method the computational complexity will be an order of magnitude lower than that of the acquisition mode (since in the tracking mode we run only 3-parallel adaptive algorithms compared to N -parallel adaptive algorithms in the acquisition mode). For example, for the LMS-based Parallel TDE method requires $6N+10$ multiplications and one-division in the tracking mode compared to $2N^2+N+7$ multiplications and one-division in the acquisition mode. On the other hand, the RMGS-based parallel TDE algorithm requires $1.5N^3+4.5N^2+7$ multiplications and one-division in the tracking mode compared to $2N^2+1$ multiplications and one-division in the acquisition mode. It is worth mentioning that the computational complexity of the TDE

methods implemented in this chapter, in the tracking mode, is lower than other TDE methods based on subspace or MUSIC algorithms which require $O[N^3]$ computational complexity.

6.6 Simulation results and discussion

In this section, we provide simulation results for several examples, in order to assess the performance of the TDE methods presented in this chapter. For both TDE methods, we compare their performance using the LMS and RMGS algorithms. In all simulation results presented in this section, an asynchronous system is assumed, in which the delays of all users (τ_k) are chosen from a uniform random distribution having values in the range $[0, T)$. The near-far situation is assumed in which the system includes strong interferers having 10dB power advantage over the desired user, unless stated otherwise, and the input signal to noise ratio SNR=20dB.

One performance measure, to assess the performance of the timing estimator is the average acquisition time of the estimator. It is defined as the number of training bits required by the estimator such that the probability that the timing estimate is within one half-chip of the propagation delay is greater than 90% [105], i.e.

$$\Pr [|\hat{\tau}_1 - \tau_1| \leq \frac{T_c}{2}] \geq 90\% \quad (6.26)$$

In the simulation, the calculation of the probability of correct acquisition is evaluated as follows. 500 independent trials are performed for estimating the delay, and then a correct acquisition of the TDE is achieved if the probability of having an estimation error within $\pm T_c/2$ is greater than 90%.

Another important performance measure is the root mean-square estimation error (RMSE) given the correct acquisition, i.e.

$$\text{RMSE} = \sqrt{E[(\hat{\tau}_1 - \tau_1)^2 \mid (|\hat{\tau}_1 - \tau_1| \leq T_c/2)]} \quad (6.31)$$

which is a measure of how well the receiver could be synchronized if the timing estimate was used to update the receiver timing relative to the desired user. The RMSE is evaluated by averaging the TDE error (conditioned on correct acquisition) over 500 independent trials.

Example 6.1

In this example, we study the performance of the two time-delay estimation methods in the acquisition (initialization) mode. An asynchronous CDMA system is assumed in which, the delays of all users are assumed to be unknown but fixed during the acquisition mode. The system includes 4-interferers, each having 10dB power advantage over the desired user, and the spreading code is PN-sequence of length 31.

Fig.6.3a shows the performance of the two TDE methods based on the RMGS algorithm. It is clear that both methods achieve correct acquisition (i.e. $|\hat{\tau}_1 - \tau_1| \leq T_c / 2$) within less than 8 bits in a near far situation. Fig.6.3b shows the performance of the two TDE methods for the same situation, using the LMS algorithm. It is therefore concluded that the two TDE methods based on both LMS and RMGS algorithms can achieve correct time delay acquisition within few bits in a near-far environment.

Example 6.2

In this example, the performance of the two TDE methods based on the LMS and RMGS algorithms is examined by measuring the average acquisition time (i.e. no. of training bits required to achieve correct acquisition) with different number of active users and with varying multiple access interference (MAI). The spreading codes are random sequences of length $N=24$. All the simulation results are averaged over 500 independent trials, in which different values of users' delays are chosen at each trial.

Fig.6.4a shows the acquisition performance (i.e. number of training bits as a function of number of interferers, each having 10dB power advantage over the desired user) for the two

a) RMGS algorithm.

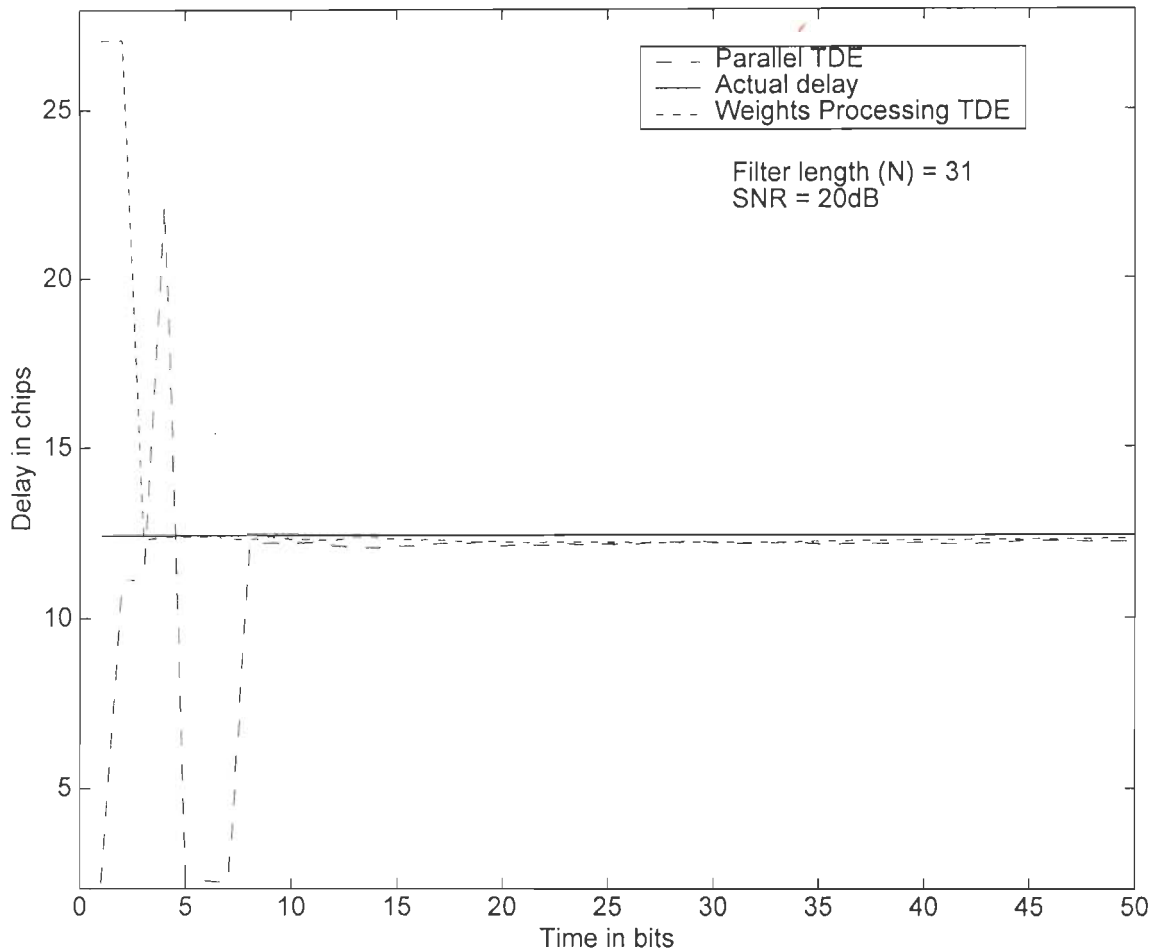


Fig.6.3 Performance of the two TDE methods based on a) RMGS b) LMS algorithms for the adaptive DS-CDMA receiver with 4 interferers (each interferer has 10dB power advantage over the desired user).

b) LMS algorithm.

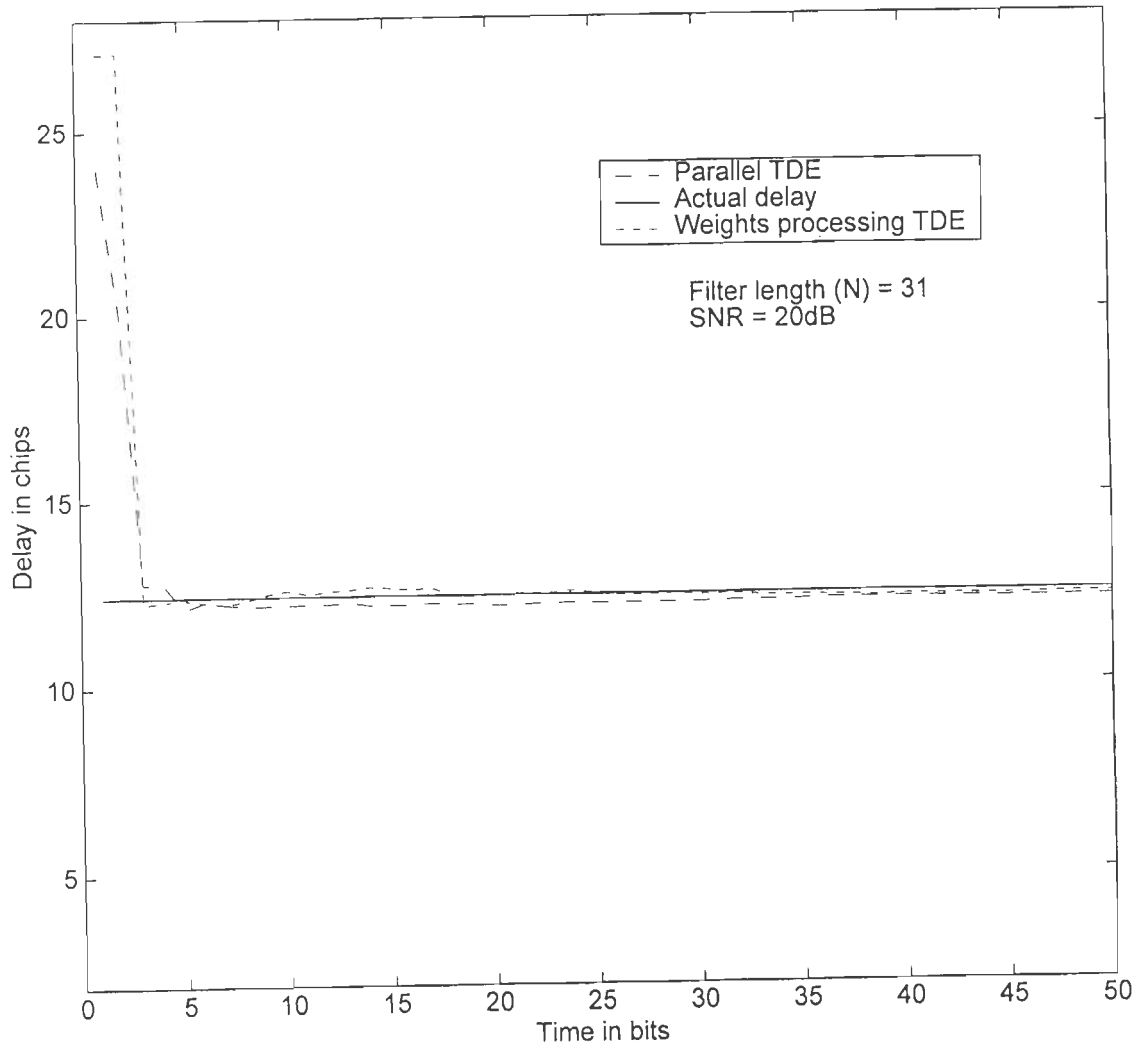


Fig.6.3b

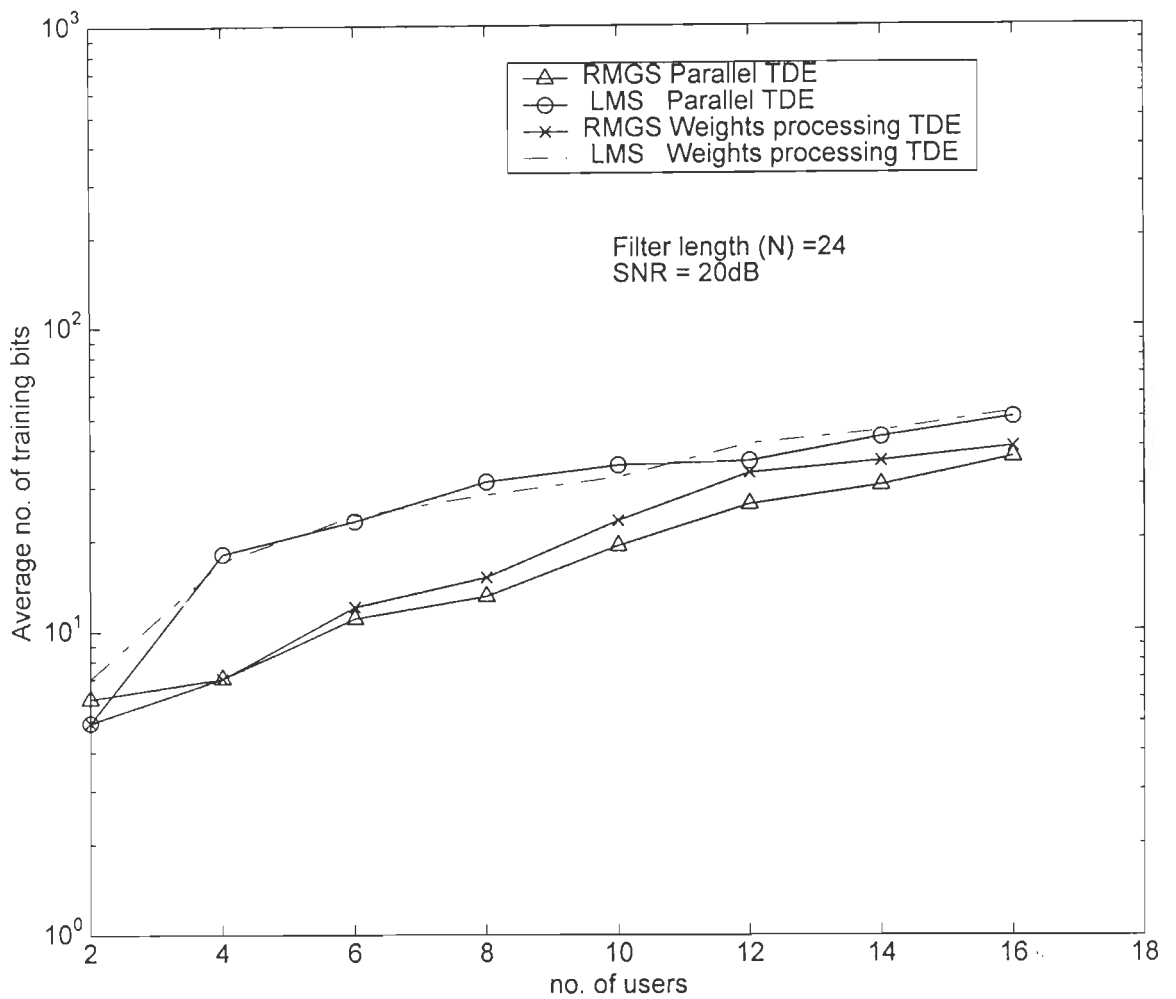


Fig.6.4a Average number of training bits required for correct acquisition as a function of number of users using the two TDE methods based on LMS and RMGS algorithms (each interferer has 10dB power advantage over the desired user)..

TDE methods based on the LMS and RMGS algorithms. It is clear that the average number of training bits required to achieve the correct acquisition increases as the number of users increase. Also it is clear that the two TDE methods possess similar performance using either the LMS or the RMGS algorithm. The results also indicate that the RMGS algorithm performs better than the LMS algorithm. For example, for four users system the number of training bits required for correct acquisition using the RMGS algorithm is 7 bits compared to 20 bits for the LMS algorithm. For 10-users system, the number of bits is 14 bits for the RMGS algorithm compared to 38 bits for the LMS algorithm. Therefore, for 4-users system the RMGS algorithm achieves acquisition three times faster than the LMS based timing estimator.

To examine the near-far resistance of the two TDE methods, we have plotted in Figs.6.4b,c&d their acquisition performance as a function of interferer's power, i.e. MAI from each interferer. In other words, it is required to show how the number of training bits required to achieve correct acquisition is affected by the MAI level. The simulated system includes 3-users and 11-users cases. From Fig.6.4b&c it is quite clear that the RMGS algorithm performs better than the LMS algorithm for the two cases. From Fig.6.4d, it is noticed that the parallel TDE method performs better than the weights processing method for the 3- and 11-users cases. It is also clear that the LMS-based TDE methods are not truly near-far resistance while based on the RMGS-algorithm, for the three users case, the TDE could be considered as near-far resistant. For example for the 3-users RMGS-based TDE the average number of acquisition bits required for correct acquisition is 4 for MAI level of 4dB and 7 bits for 12dB MAI, while for the 11-users case it is 11 bits for 4dB MAI and 22 for 12dB MAI.

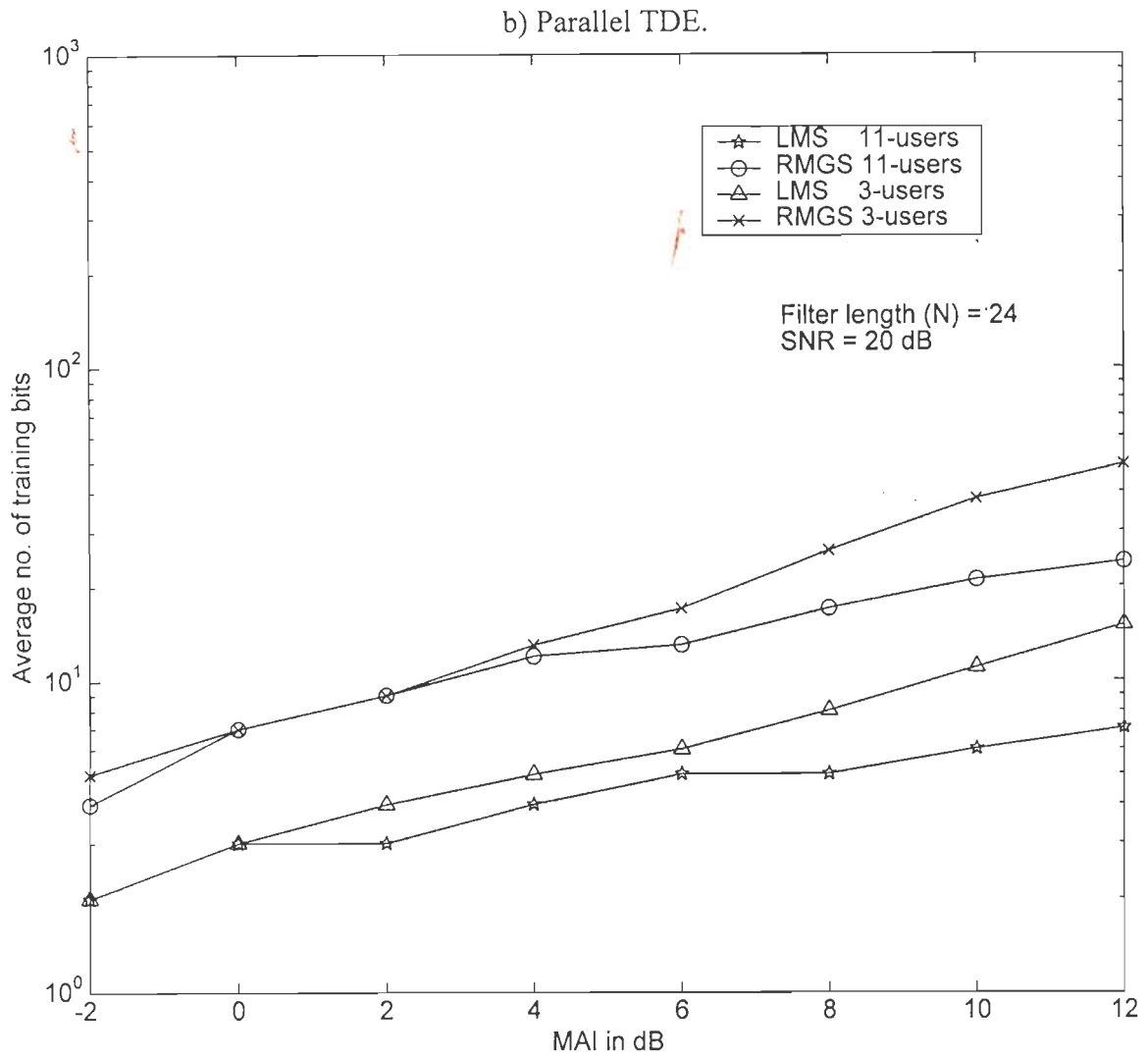


Fig.6.4b Average number of training bits required for correct acquisition as a function of MAI from each user based on the parallel TDE method for 3 and 11 users, using LMS & RMGS algorithms

c) Weights processing TDE.

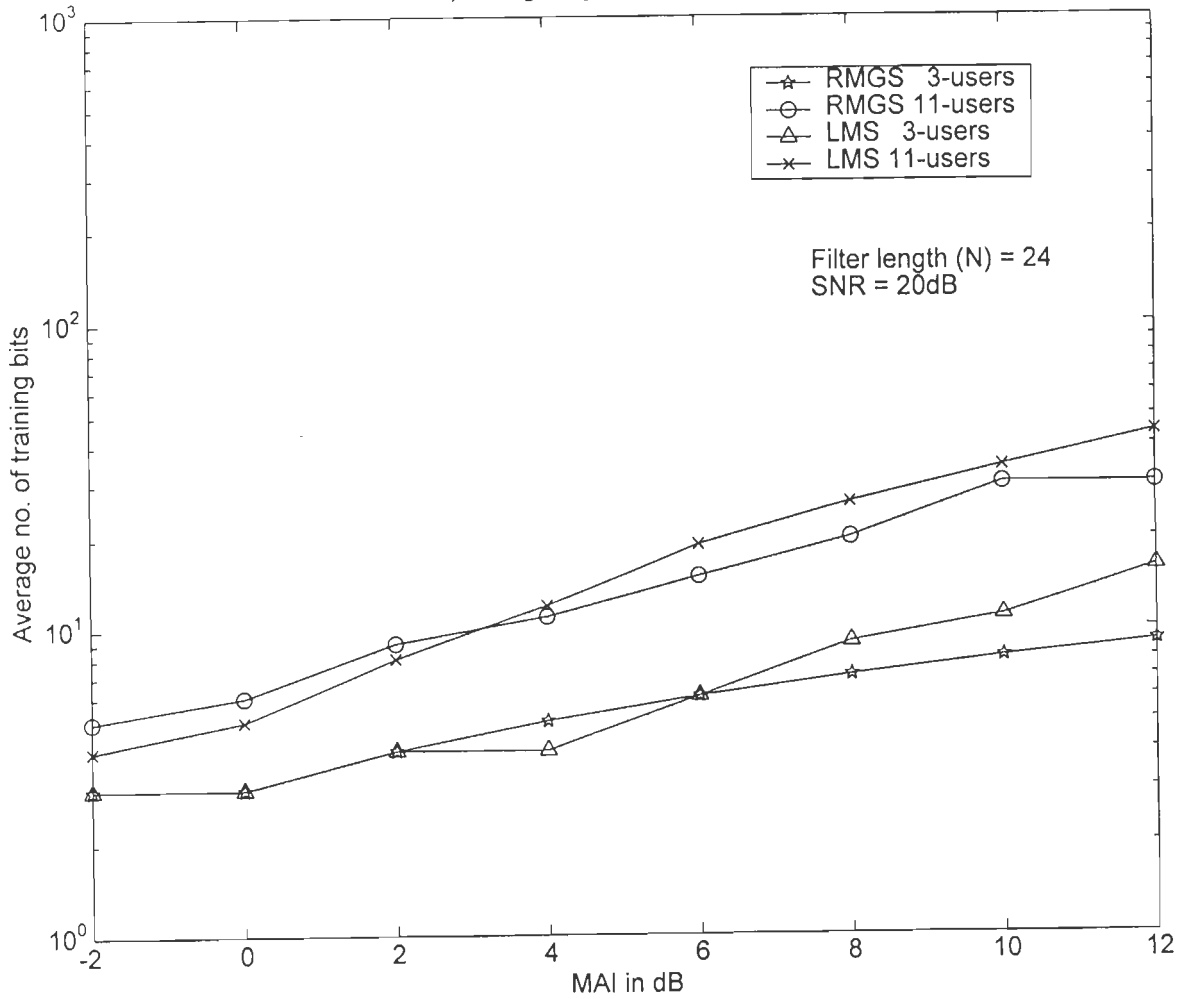


Fig.6.4c Average number of training bits required for correct acquisition as a function of MAI from each user based on the weights processing method for 3 and 11 users using LMS and RMGS algorithms.

d) RMGS algorithm.

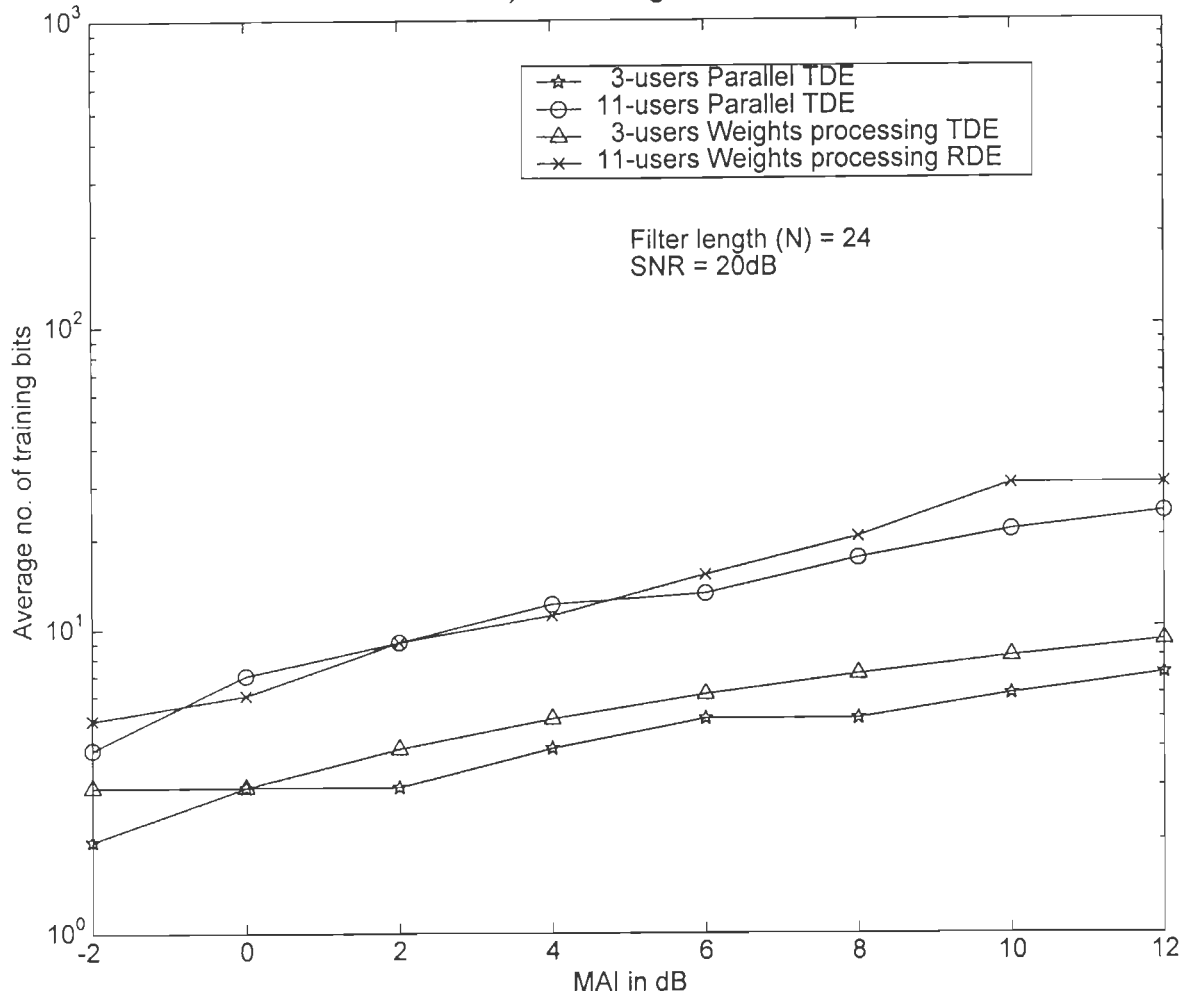


Fig.6.4d Average number of training bits required for correct acquisition as a function of the MAI for 3 and 11 users using the two TDE methods based on the RMGS algorithm.

Example 6.3

In this example, we study the probability of correct acquisition for the two estimators presented in this chapter. The near-far situation is assumed in which all interferers possess 10dB power advantage over the desired user. The spreading codes are randomly generated sequences of length $N=24$. The simulation results presented are averaged over 500 independent trials in which the delays and spreading sequences are changed in each trial.

Fig.6.5a shows the probability of correct acquisition as a function of the number of training bits using the two TDE methods with 4 interferers based on the LMS and RMGS methods. It is clear that the RMGS method achieves correct acquisition faster than the LMS-based TDE methods. Also it is noticed that the parallel TDE method performs better than that of the weights processing methods.

Fig.6.5b shows the probability of acquisition performance of the two TDE methods as a function of number of users. It is clear that for small number of users the weights processing TDE methods performs better than the parallel TDE method and possesses higher value of probability of acquisition. However, for large number of users the probability of correct acquisition for the weights processing TDE method degrades faster than the parallel TDE method and approaches a value of 0.7 for 22 users. The degradation in the performance of the weights processing method is due to the perturbation error induced in the relation between the desired user's weight vector and its spreading sequence, which will make the crosscorrelation criterion deviates from achieving the correct delay estimate as the number of users increases,

Fig.6.5c shows the probability of correct acquisition as a function of the power of each interferer for the two TDE methods in 11-users system. It is clear that initially both methods are near-far resistant and beyond certain value of MAI, the probability of correct acquisition

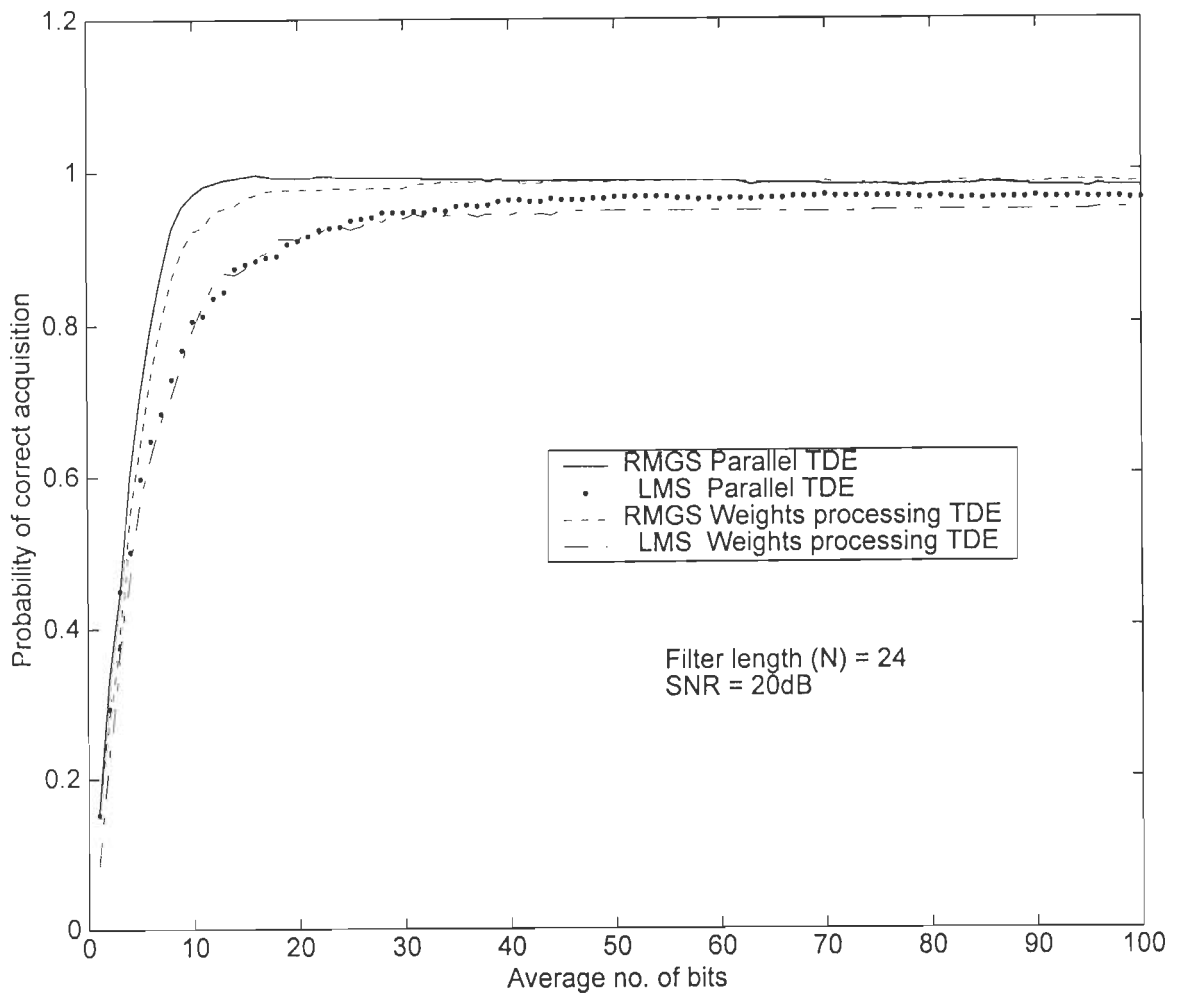


Fig.6.5a Probability of correct acquisition as a function of the average number of training bits for the two TDE methods based on the LMS and RMGS algorithms with 4-interferers (each interferer has 10dB power advantage over the desired user).

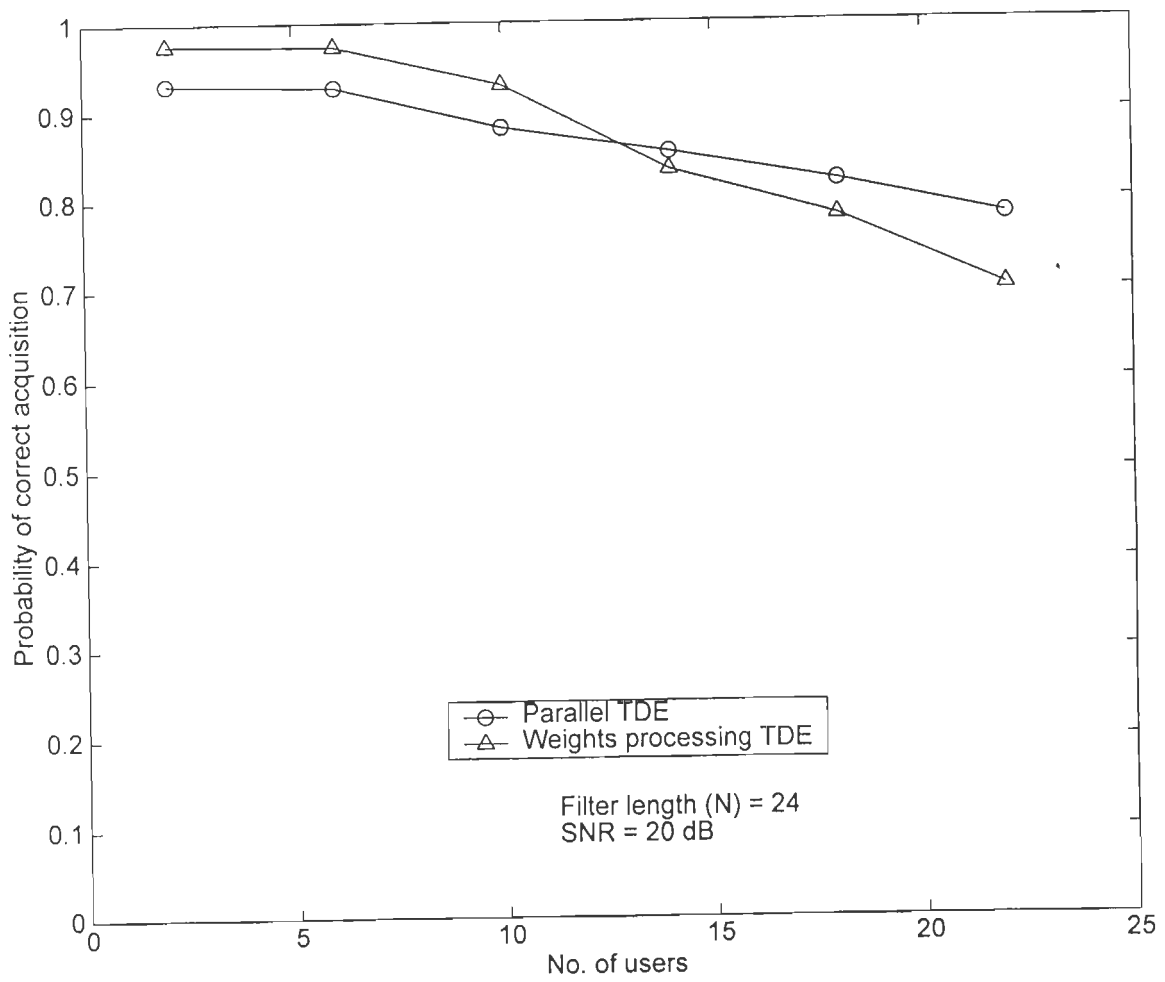


Fig.6.5b Probability of correct acquisition as a number of users using the two TDE methods based on the RMGS algorithm (each interferer has 10dB power advantage over the desired user)..

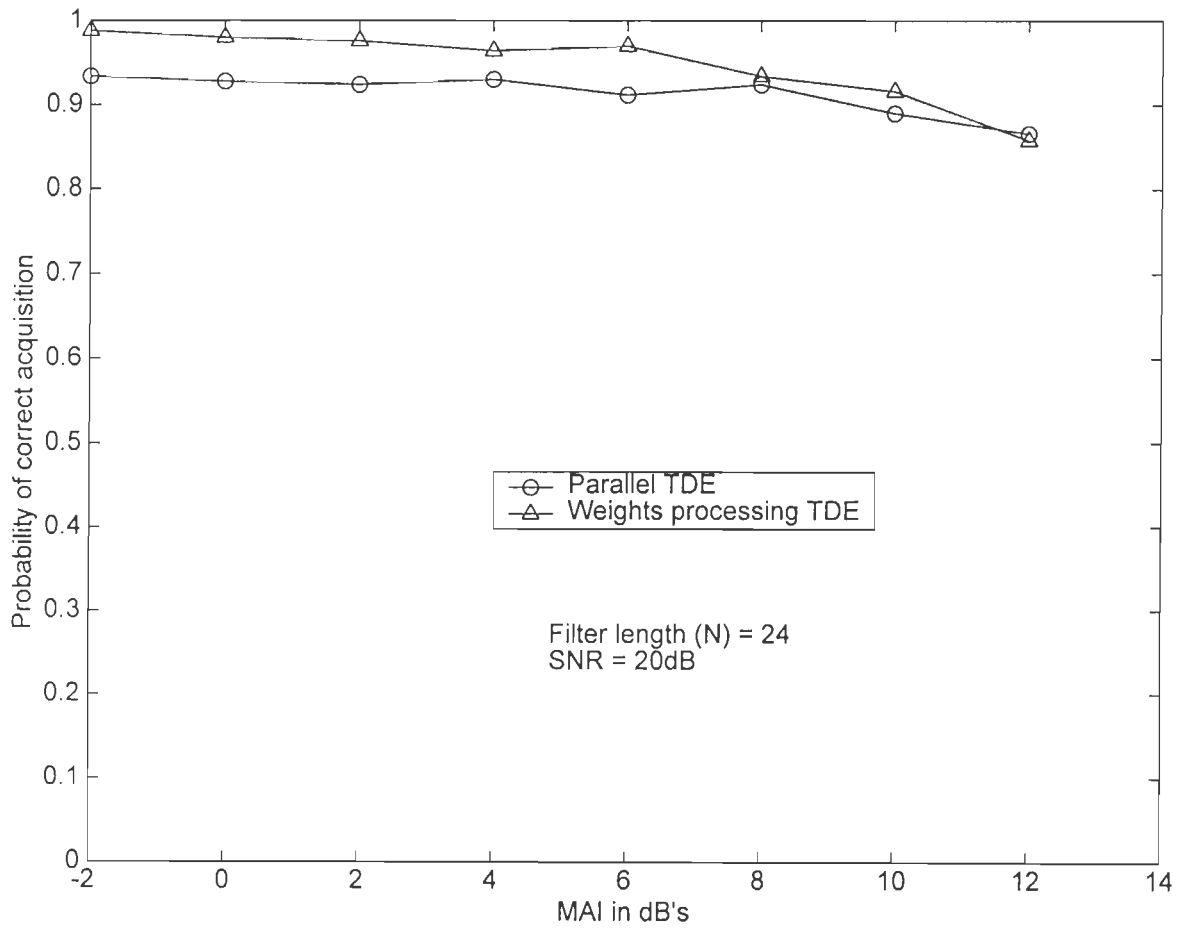


Fig.6.5c Probability of correct acquisition as a function of the MAI from each user for the two TDE methods using the RMGS algorithm with 10 interferers.

degrades as the MAI level increases. Also it is noticed that for low MAI level the probability of correct acquisition for the weights processing TDE method is higher than that of the parallel TDE method. But as the level of MAI increases, the probability of correct acquisition for the weights processing TDE method degrades faster as compared to that of the parallel TDE method.

Example 6.4

In this example, we study the performance of the two TDE methods in terms of the RMSE after the correct acquisition has been achieved. The spreading codes are randomly generated sequences of length $N=24$. The near-far situation is assumed, and the simulation results are averaged over 500-independent trials in which all the users delays and spreading codes are changed in each trial.

Fig.6.6a shows the RMSE plot for the two TDE methods as a function of the average number of training bits using both LMS and RMGS algorithms. The system includes 4-interferers each having 10dB power advantage over the desired user. It is shown that the RMGS based TDE converges, to the steady state RMSE, faster than the LMS based TDE. It is also clear that the parallel TDE method based on the RMGS algorithm possesses lower RMSE as compared to the weights processing TDE method.

Fig. 6.6b shows the near-far resistance for the two TDE methods by plotting the RMSE as a function of the power of each interferer. Three and eleven users cases are simulated. It is clear that for the 3-users case, the two methods are near far resistant, in which the RMSE remains constant at a value of $0.14T_c$ when the MAI values varies form -2dB to 12 dB . On the other hand, for 11-users case, the two methods are not considered as truly near-far resistant, since the RMSE for -2dB MAI is $0.15T_c$ while it is $0.2T_c$ for 12dB MAI.

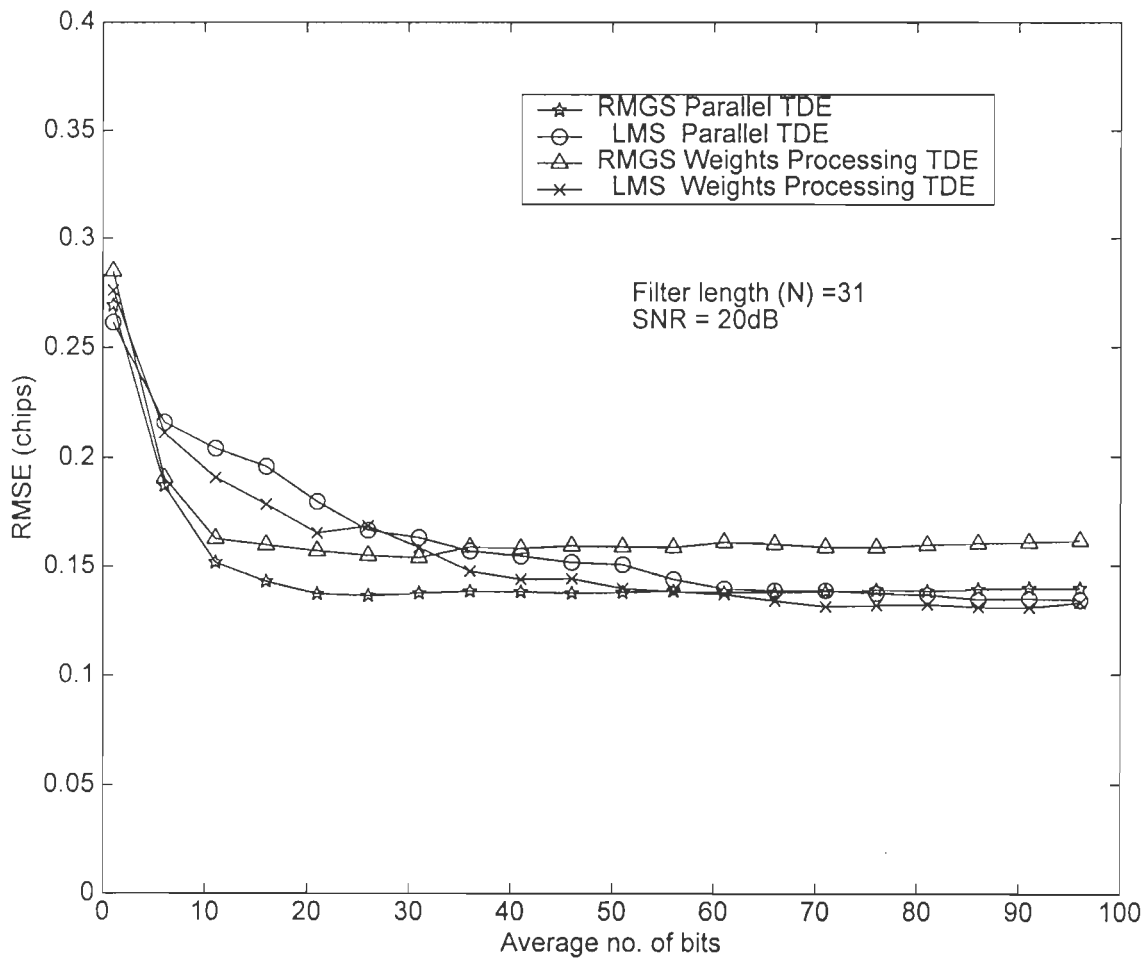


Fig.6.6a RMSE of timing estimate in chips as a function of the average number of training bits for the two TDE methods based on LMS and RMGS algorithms with 4-interferers (each interferer has 10dB power advantage over the desired user).

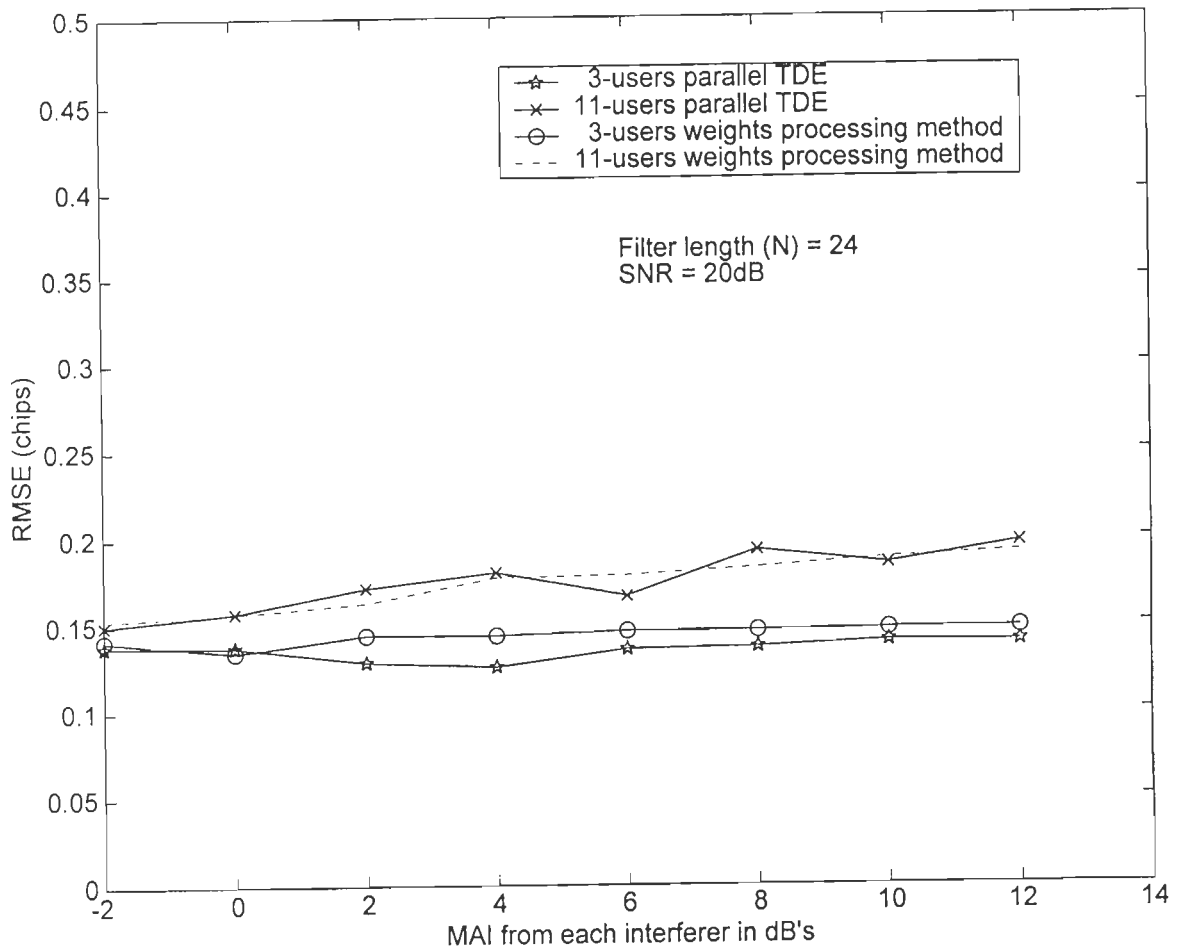


Fig.6.6b RMSE of the timing estimate in chips as a function of the MAI from each interferer for the two TDE methods based on the RMGS algorithm with 3 and 11 users.

Fig. 6.6c shows the RMSE plot as a function of number of users, in which each interferer has a 10dB power advantage over the desired user. Again the RMSE is calculated assuming that the correct acquisition is achieved. It is clear that the RMSE increases as the number of users increase.

Example 6.5

In this example, we study the performance of the two time-delay estimation methods in the tracking mode. An asynchronous system is assumed with 4-interferers, each having 10dB power advantage over the desired user. The spreading codes are PN-sequence of length 31. The delays of all interferers are assumed to be unknown but fixed, while, the desired user's time-delay is assumed to be correctly acquired in the initialization mode and its delay grows linearly with time in the tracking mode, as follows:

$$\tau_1(n+1) = \tau_1(n) + 0.0005 T \tag{6.32}$$

This variation in the time-delay ($5 \cdot 10^{-4} T$) corresponds to a vehicular velocity of $1.74 \cdot 10^5$ km/Hr for bit-rate of 9600 bit/sec, which much higher than the realistic speed.

Fig.6.7a shows the performance of the two TDE methods based on the RMGS algorithm. It is clear that the two methods perform similarly. Fig.6.7b shows the performance of the two TDE methods for the same situation, using the LMS algorithm. Some performance degradation is noticed as compared to the RMGS algorithm. It is also observed that, based on the LMS algorithm, the parallel TDE method performs better than the weights processing TDE method in the tracking mode.

Example 6.6

In this example, the performance of the TDE method based on the blind adaptation is examined and compared to the TDE method based on training sequence adaptation. Both TDE methods are using the RMGS algorithm. The simulated system uses random spreading

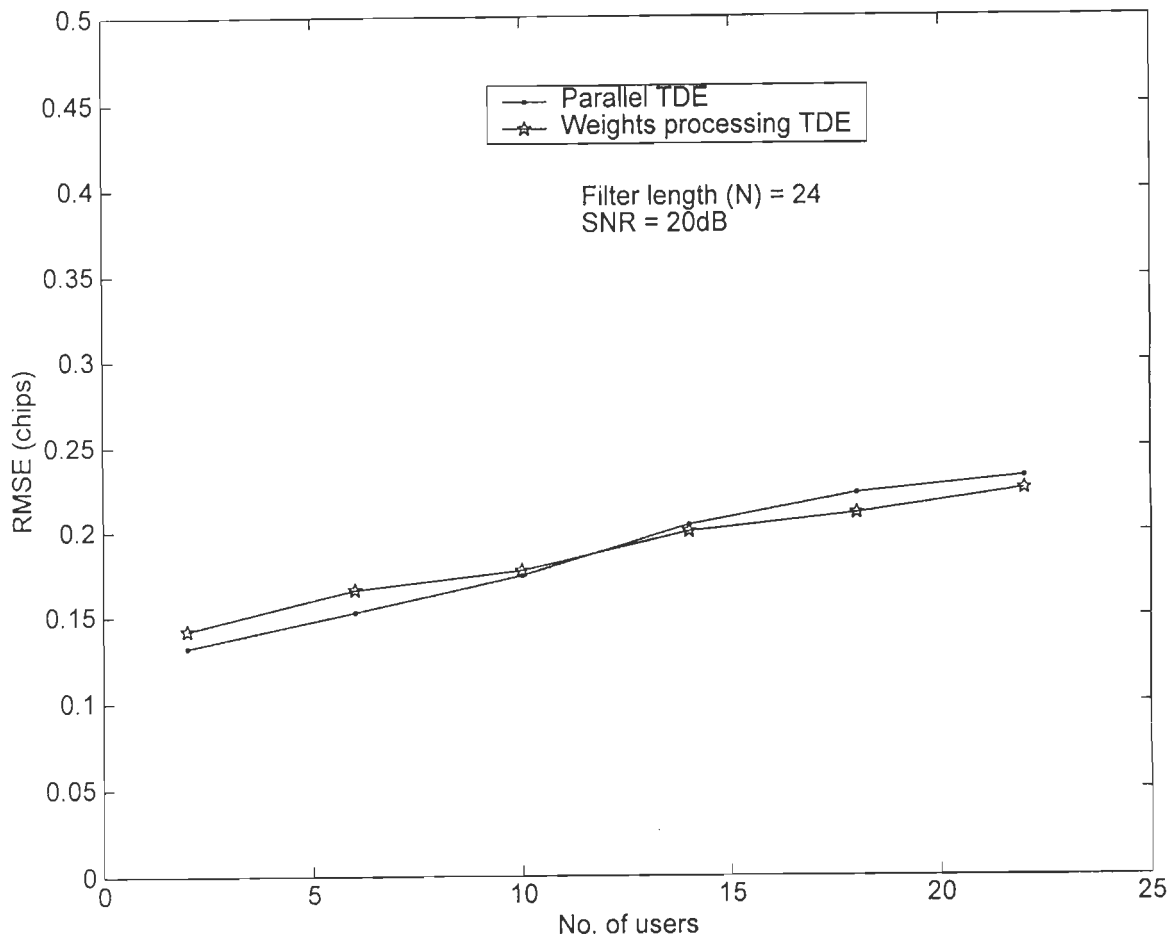


Fig.6.6c RMSE of the timing estimate in chips as a function of number of users for the two TDE methods based on the RMGS algorithm (each interferer has 10dB power advantage over the desired user).

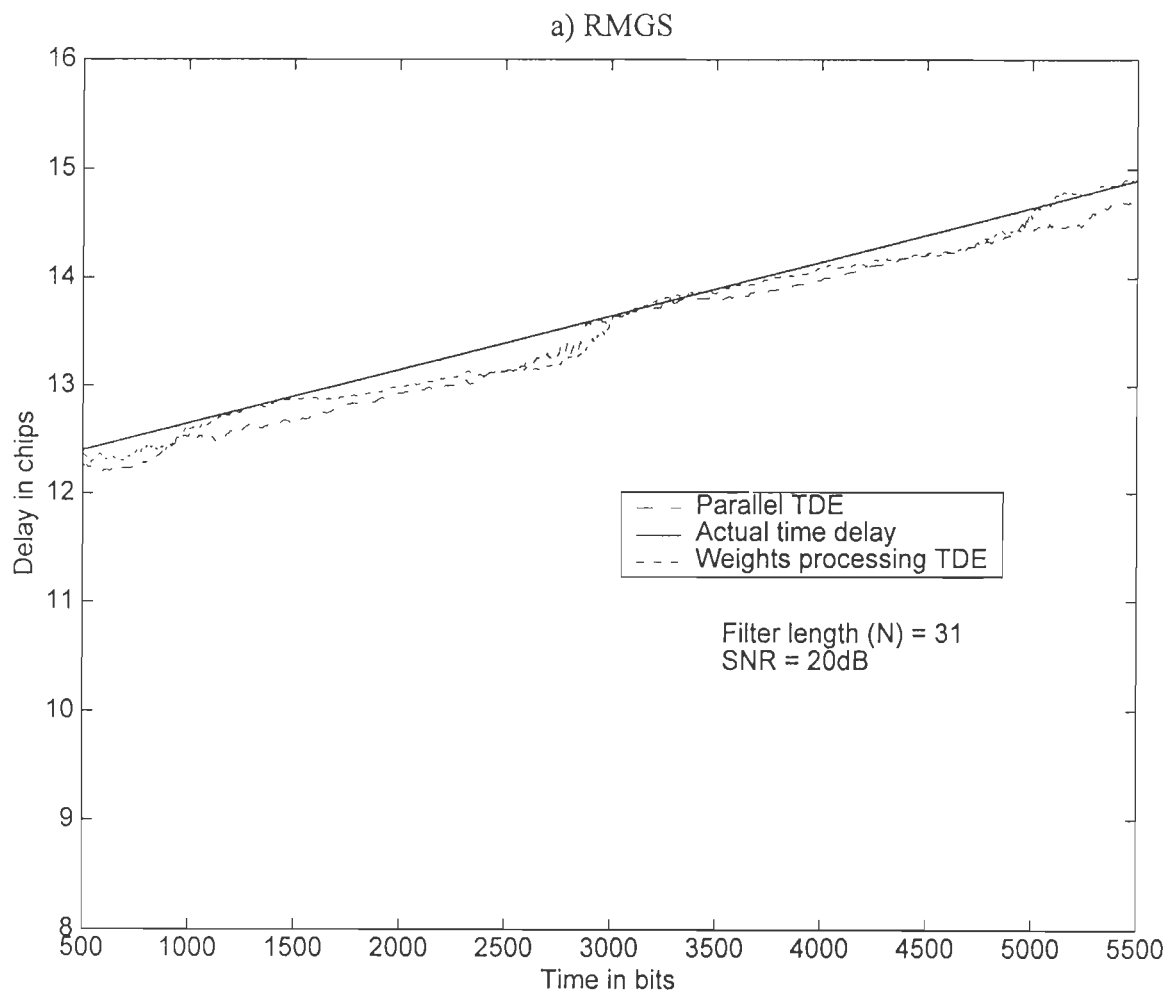


Fig.6.7 Performance of the two TDE methods in the tracking mode using a) RMGS b) LMS algorithms with 4-interferers (each interferer has 10dB power advantage over the desired user).

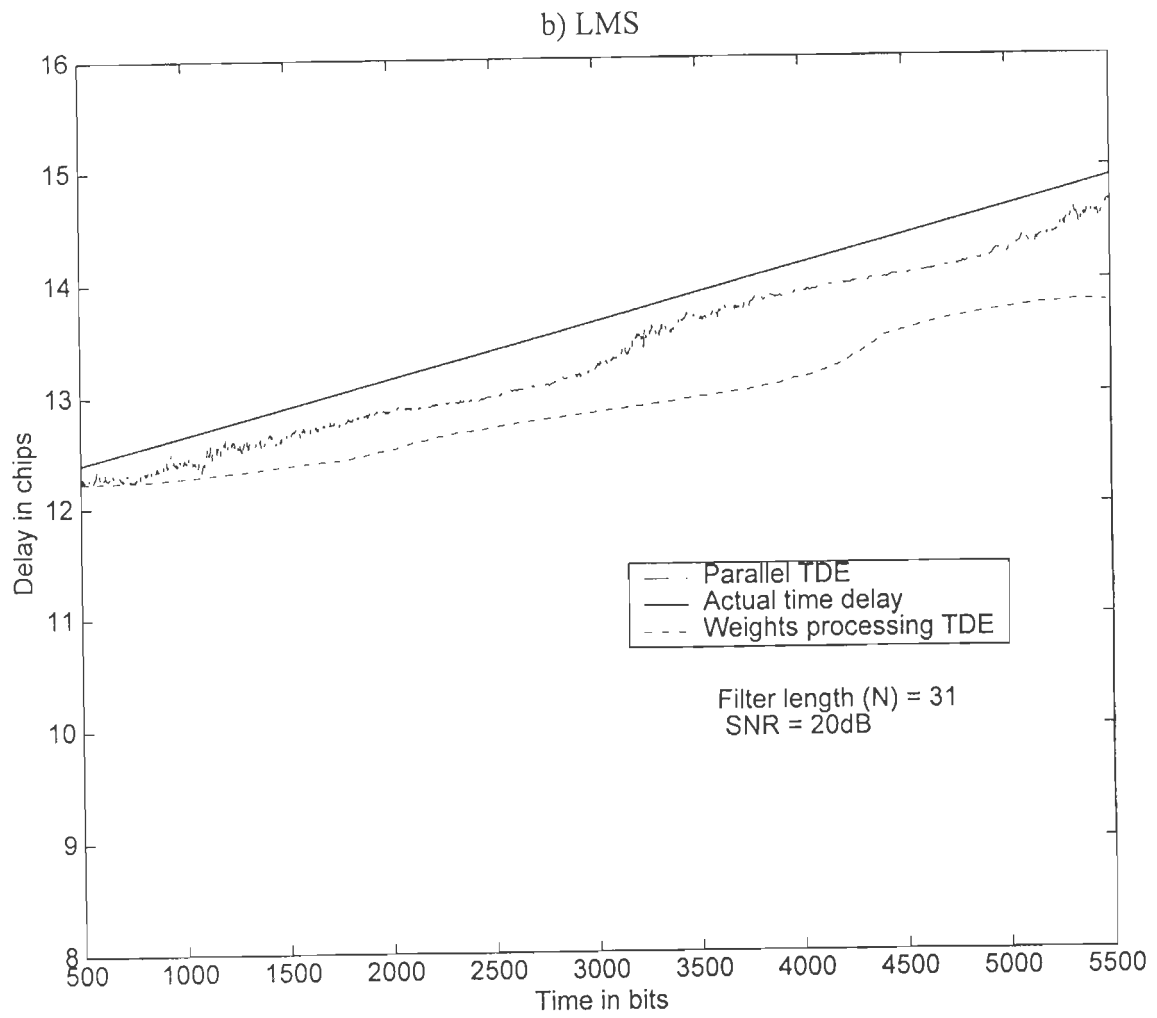


Fig.6.7b

sequences of length $N=24$, which is the only side information required to be known by the receiver. All the simulated results are averaged over 500 independent trials, in which the delays of all the interferers and their spreading sequences are varied in each trial.

Fig.6.8a shows the probability of correct acquisition plot as a function of the number of interferers (each interferer has 10dB power advantage over the desired user). It is shown that the performance of the TDE method based on blind adaptation degrades very fast as compared to the TDE method based on the training sequence adaptation. This degradation in performance is due to the large increase in the total MAI.

Fig.6.8b shows the probability of correct acquisition as a function of MAI of each interferer using 3-users system. It is shown that, for 3-users system, the performance of the TDE based on blind adaptation is worse than that of the TDE method based on training sequence adaptation, however, both methods may be considered as near-far resistant, since their performance remains constant as MAI levels varies from -2dB to 12dB. Fig.6.9a shows the RMSE as a function of the number of users for the two TDE methods. It is shown that the RMSE using the TDE method based on blind adaptation is higher than that of TDE method based on training sequence adaptation. Also it is noticed that the RMSE increases with the increase of the number of users. Fig.6.9b shows the RMSE as a function of MAI of each interferer for 3-users system. It may be seen that the RMSE for the TDE method based on blind adaptation is higher than that of the TDE method based on training sequence adaptation. However, for 3-users system it is noticed that the RMSE remains constant for MAI values of -2dB to 12 dB, and therefore the algorithm can be considered as near far resistant.

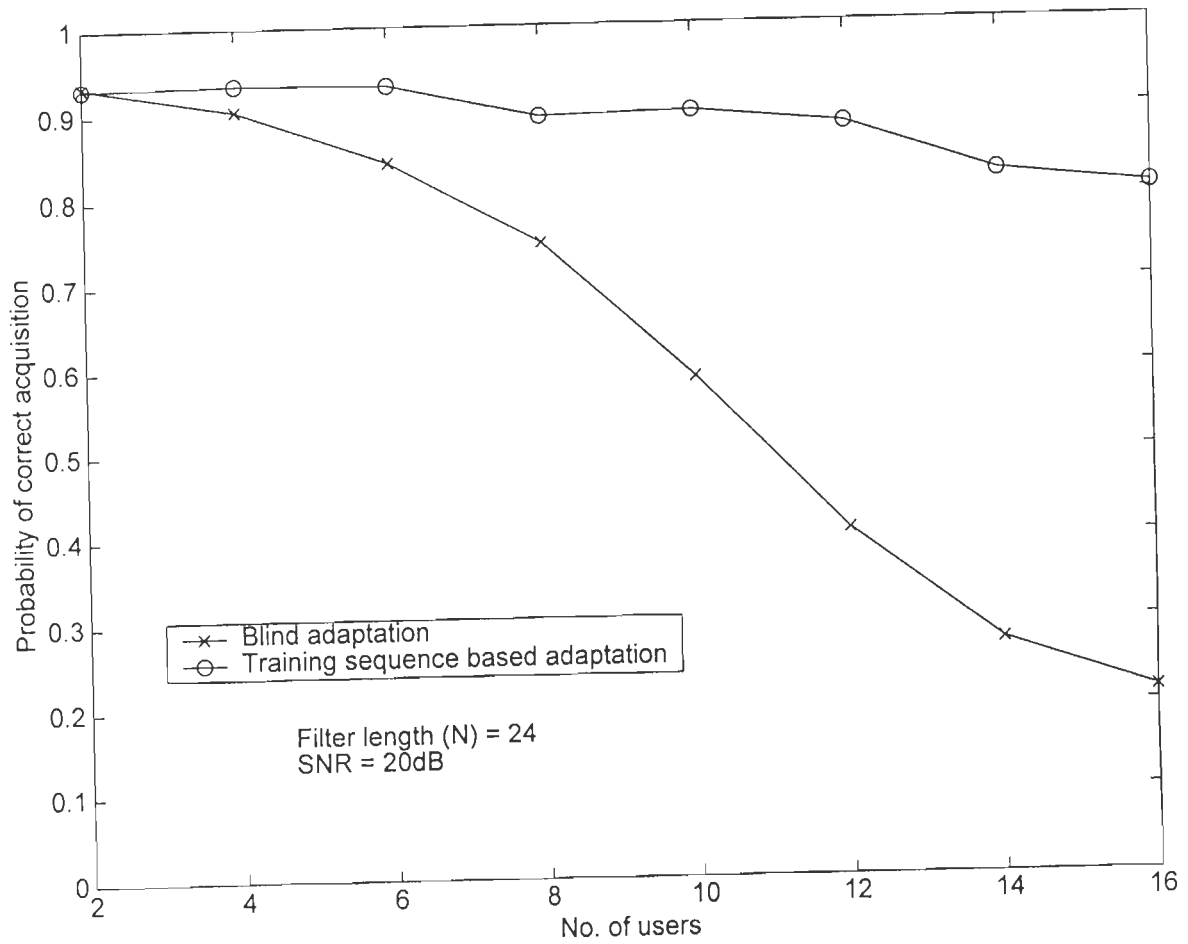


Fig.6.8a Probability of correct acquisition for the parallel TDE method based on the RMGS algorithm as a function of number of users using training sequence based adaptation and blind adaptation modes (each interferer has 10dB power advantage over the desired user).

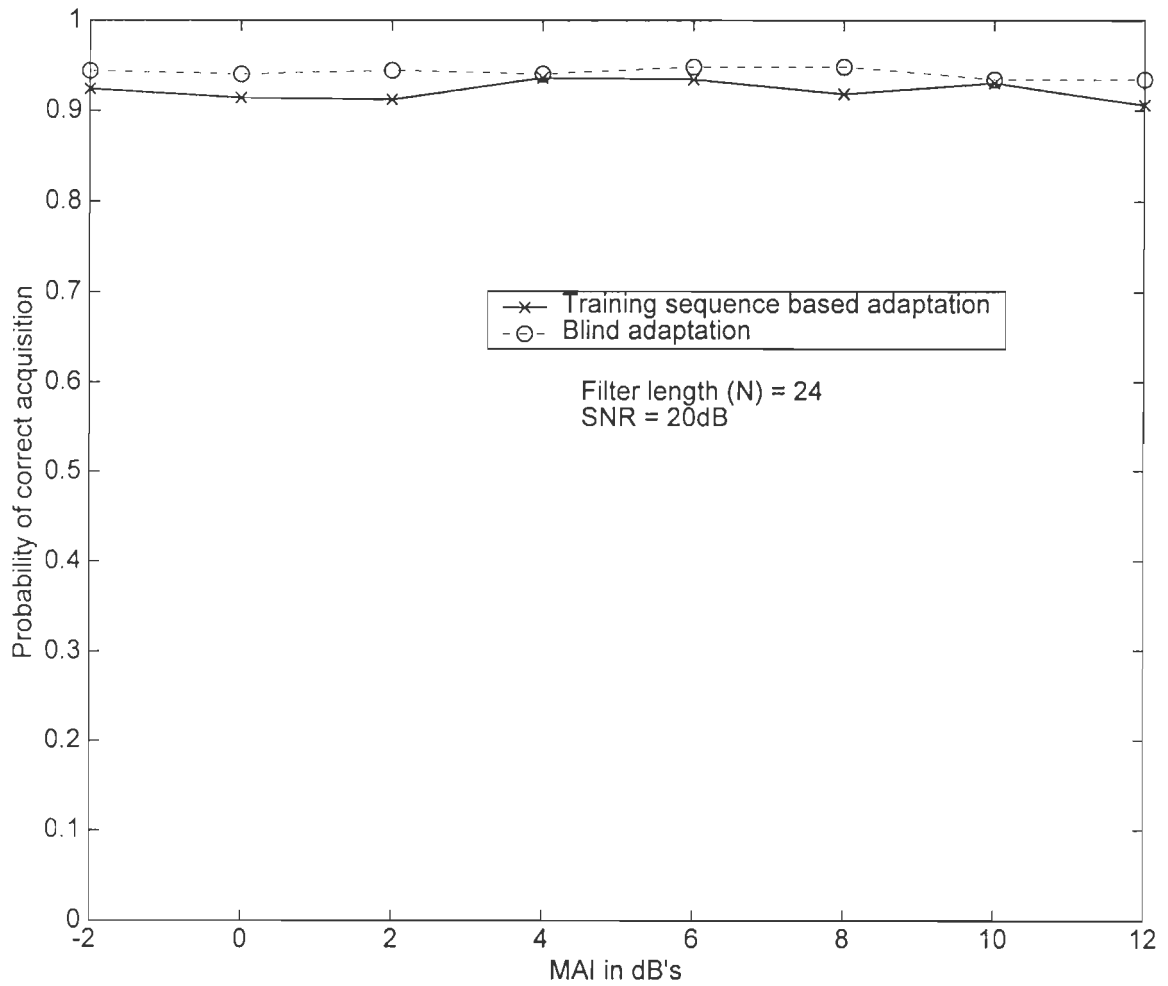


Fig.6.8b Probability of correct acquisition for the parallel TDE method based on the RMGS algorithm as a function of MAI from each user using training sequence based adaptation and blind adaptation modes, with 3-users.

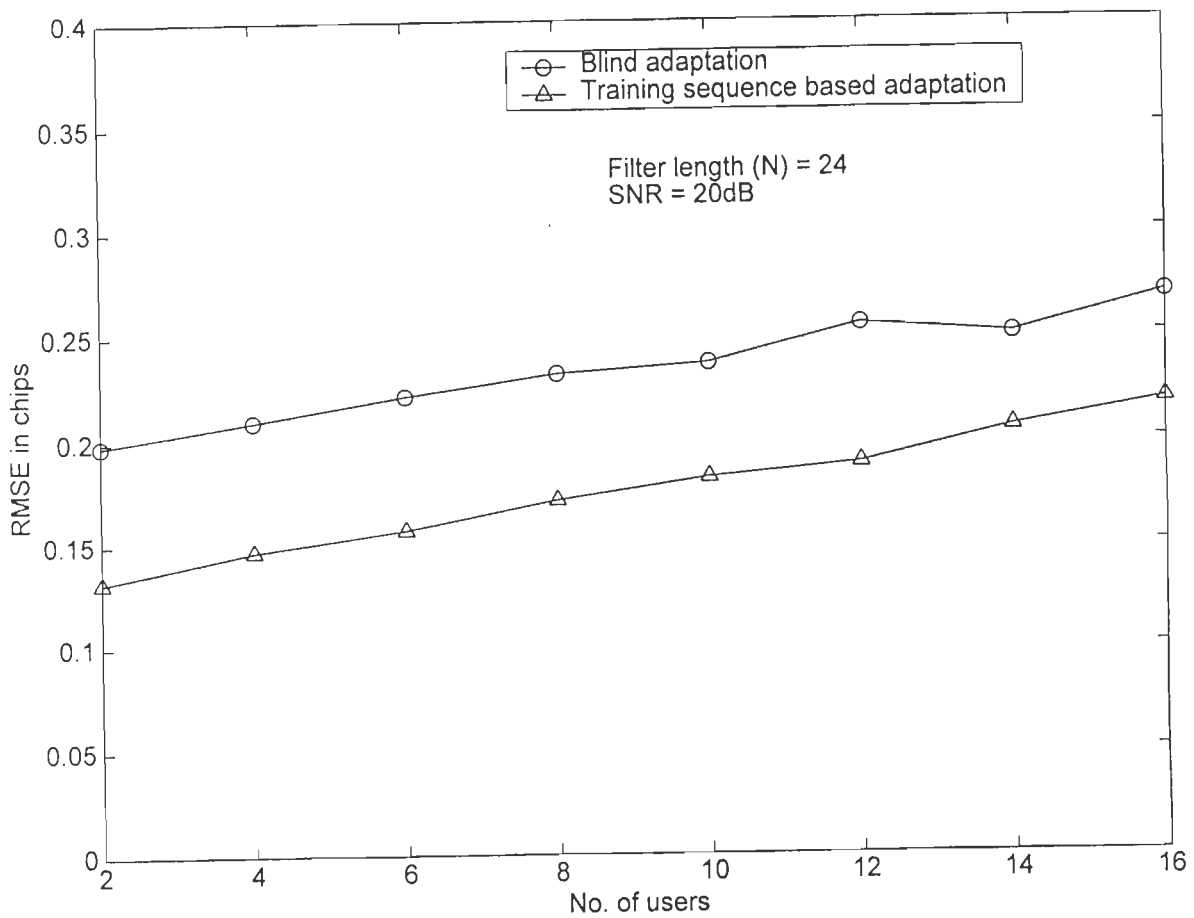


Fig.6.9a RMSE of the timing estimate in chips for the parallel TDE method as a function of number of users using training sequence based adaptation and blind adaptation modes based on theRMGS algorithm, (each interferer has 10dB power advantage over the desired user).

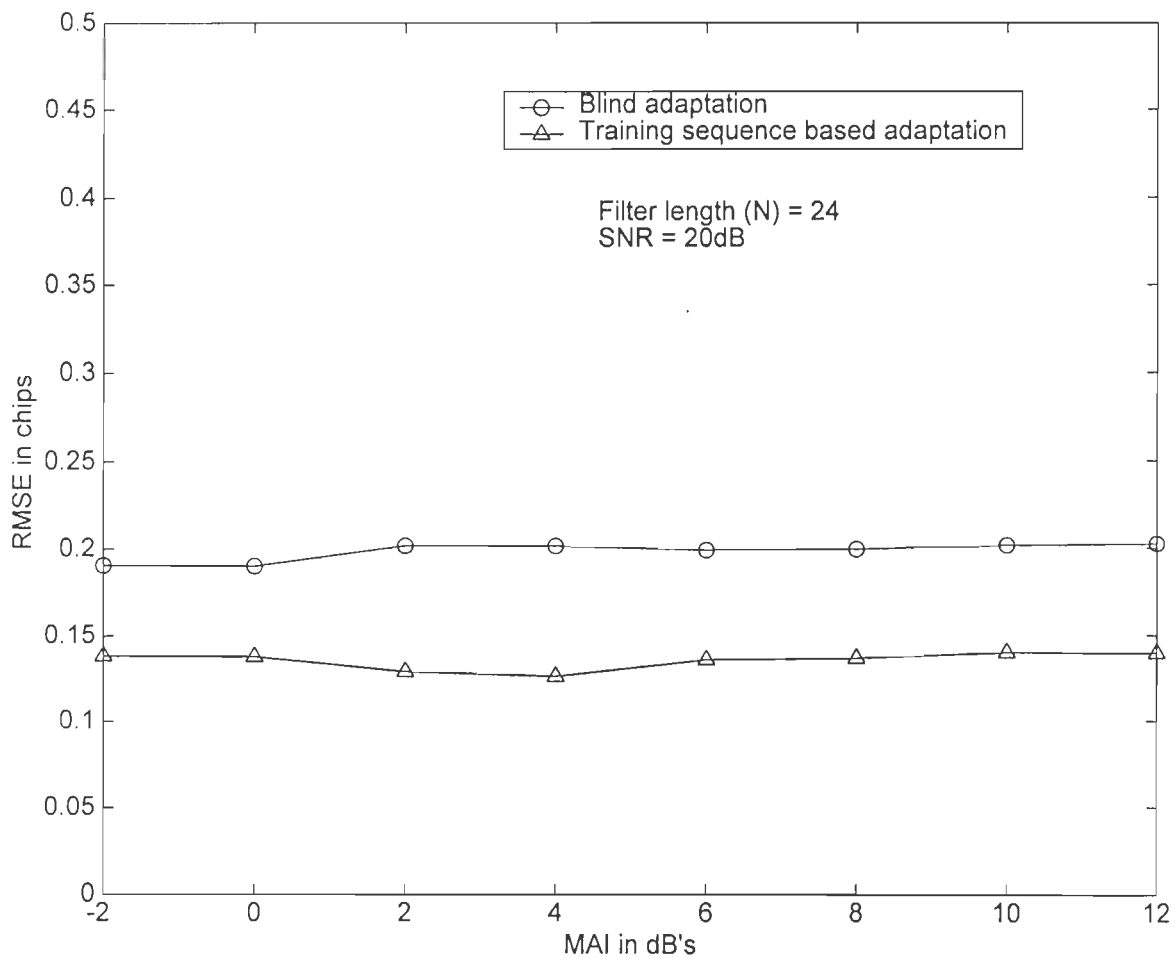


Fig.6.9b RMSE of the timing estimate in chips for the parallel TDE method as a function of the MAI of each interferer using the training sequence based adaptation and blind adaptation modes with two interferers.

Example 6.7

In this example, a comparison of the probability of error performance for the adaptive DS-CDMA receiver for synchronous system with known value of delay and for asynchronous system based on estimated time-delay is presented. The time-delay has been estimated based on parallel TDE method using both training sequence based adaptation and blind based adaptation modes presented in (sections 6.3 and 6.4). After achieving correct acquisition of the desired user's time-delay, the receiver switches to the decision directed mode. The estimated time-delay is then kept fixed during the whole simulation run. The system includes 4-interferers each having 10dB power advantage over the desired user. The results are averaged over 500 independent trials in which all the users' delays and spreading codes are changes in each trial.

It is clear that there is performance degradation in the probability of error performance for the adaptive DS-CDMA receiver using the TDE methods based on either blind based adaptation or training sequence based adaptation as compared to the synchronous system (Fig.6.10). The SNR degradation is within a maximum value of 3dB corresponding to estimation error of $T_c/2$

In this chapter, we have considered two adaptive methods for TDE in DS-CDMA systems, which can be used during both the acquisition and tracking modes. The first method is based on cross-correlating the MMSE weights vector with the desired user spreading sequence, while in the second method we run N-parallel TDE methods at N-hypothetical delay values. The two TDE methods are shown to be near far resistant, and require lower computational complexity as compared to other adaptive TDE methods. A novel blind adaptive DS-CDMA receiver for interference suppression, which does not require any side information except the desired user's spreading sequence, has also been implemented.

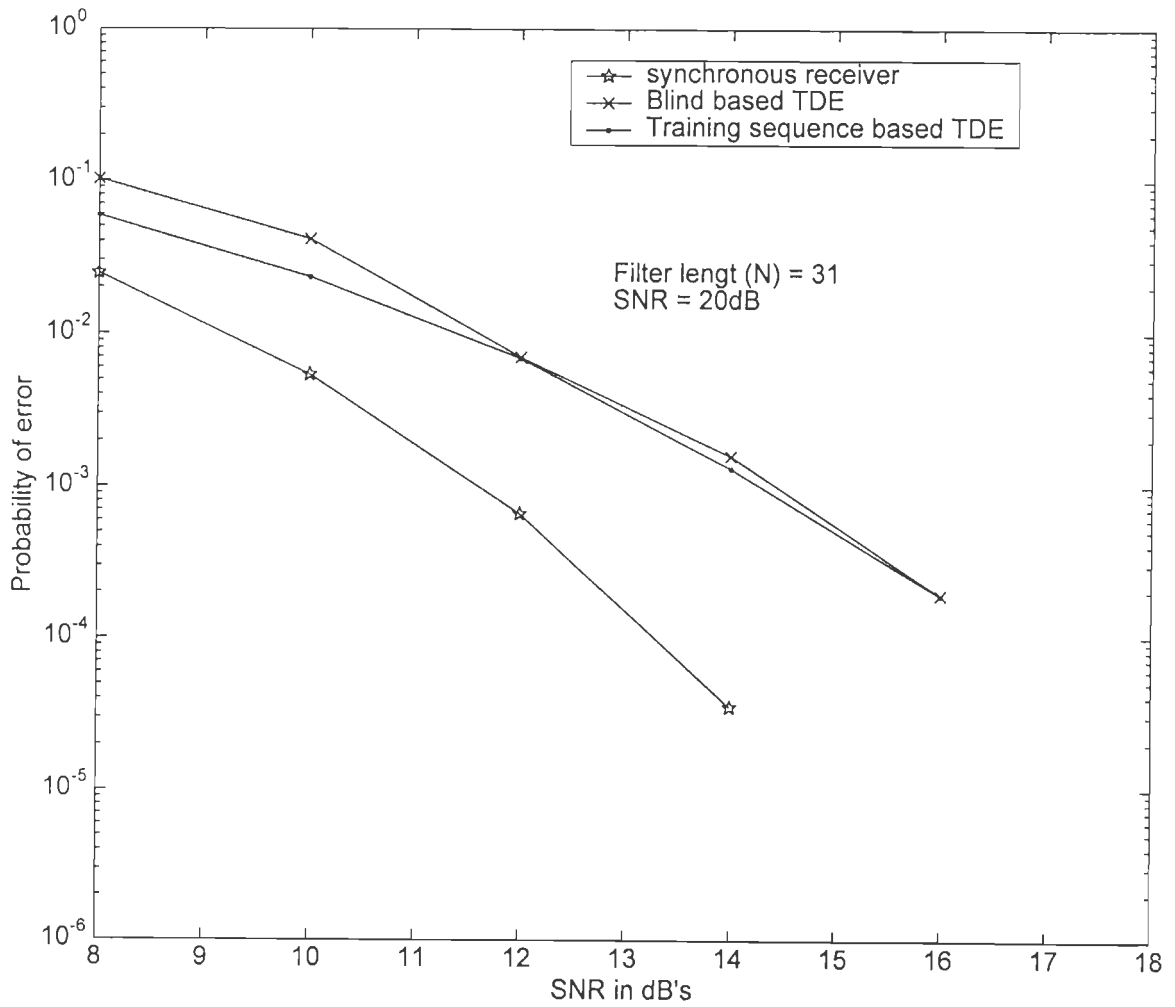


Fig.6.10 Probability of error performance for the adaptive DS-CDMA receiver for the synchronous, training sequence based TDE and blind based TDE cases with 4-interferers (each interferer has 10dB power advantage).

CONCLUSIONS

In this chapter, we conclude the thesis by summarizing some of the important results of the present work and also suggest some problems for further investigation.

This thesis addresses itself to the consideration of the interference suppression in multiuser DS-CDMA systems using adaptive signal processing algorithms. MUD techniques jointly detect all signals, in order to mitigate the non-orthogonal properties of the received signals. The optimum detector based on the MLSD [116] has a computational complexity that is exponential with the number of users, which has motivated the design of many suboptimal detectors with lower computational complexity. However, we have, in this thesis, restricted ourselves to the use of adaptive algorithms based on the MMSE criterion. We consider the transmission of DS-CDMA signals over AWGN channel with the existence of MAI. The main issues considered are the convergence rate, near far resistance, stability and the computational complexity of the adaptive algorithms.

We have first introduced the asynchronous DS-CDMA signal model. We then considered the performance comparison of MMSE adaptive algorithms (including the LMS, MVSS-LMS and RLS) for the interference suppression in DS-CDMA systems. It is well known that the LMS algorithm requires low computational complexity, $O[N]$, but it suffers from slow convergence. In order to speed up the convergence the RLS algorithm is used, which converges much faster but possesses higher computational complexity, $O[N^2]$. To reduce the computational complexity, while maintaining fast convergence rate, we have implemented a novel block algorithm for the adaptation and interference suppression of DS-CDMA signals. It has been shown that the block algorithm possesses fast convergence rate,

comparable to the RLS algorithm while requiring lower computational complexity. It has also been shown that the block algorithm performs well using moderate block sizes. To improve the convergence rate, we have implemented the MVSS algorithms for both conventional LMS and block LMS algorithms. Simulation results show that variable step-size algorithms perform better than fixed step-size algorithms in terms of convergence rate and residual MSE for both conventional LMS and block LMS algorithms. The MMSE receiver based on LMS, RLS and block algorithms has also been shown to be near far resistant. Further results show that the RLS algorithm can support larger number of users (i.e. capacity) than the LMS algorithm, while for the block algorithm capacity lies between the capacity realized by the two algorithms.

Next, we have proposed the implementation of the KF algorithm for the adaptation and interference suppression in DS-CDMA systems. A motivation for using the KF is that it is optimal in the MMSE sense and is considered as the best linear unbiased estimator. Moreover, the KF is usually formulated using the state-space approach, which contains all the necessary information about the system. However, the KF algorithm suffers from the well-known numerical instability problem due to the way in which the Riccati difference equation is calculated and also due to the use of finite word-length arithmetic. The instability problem of the KF algorithm has been overcome by using the SQRT-KF algorithm. In the SQRT-KF algorithm, we have used unitary transformations on the state error correlation matrix, which is adopted using the Givens rotations or Householder transformation.

It has been shown that the KF, SQRT-KF and RLS algorithms possess comparable convergence characteristics. However, the SQRT-KF algorithm is shown to be more stable as compared to the RLS and conventional KF algorithms. The near-far resistance of the DS-CDMA receiver based on the SQRT-KF algorithm has also been demonstrated.

As stated above, the SQRT-KF is stable, but requires high computational complexity. To remedy this problem, the RMGS algorithm [63] has been used for the adaptation and interference suppression of DS-CDMA signals due its good numerical properties. A modified form of the RMGS algorithm (RMGSEF) has also been used which is more efficient and has better numerical properties. Parallel implementation of the RMGS algorithm using systolic arrays has been presented, thus reducing the computational complexity to $O[N]$ per processor. It has been shown that the RMGSEF algorithm requires the lowest computational complexity as compared to other square root algorithms (namely the SQRT-KF, the QR-RLS and the inverse QR-RLS algorithms), since these algorithms involve the calculation of the computationally expensive square roots. It has also been shown that the RMGS algorithm outperforms the LMS algorithm in terms of convergence rate and capacity, while it possesses the same convergence rate as that of the RLS algorithm but is more stable. The performance of the adaptive MMSE DS-CDMA receiver based on the RMGS algorithm has also been studied in a fading dispersive environment. The fading dispersive channel is represented by an equivalent discrete-time (EDT) channel, which is realized by an FIR filter with time-variant tap gains. It is shown that the RMGS algorithm outperforms the NLMS algorithm and provides lower error floor for different values of the maximum Doppler frequency and for different number of interferers.

Then we have dealt with the adaptation techniques for interference suppression of DS-CDMA systems in a blind manner (i.e. without the use of a training sequence). We have first implemented the CMA algorithm, which minimizes the deviation of the receiver output from a constant modulus. It has been shown that the CMA algorithm suffers from slow convergence rate, and moreover, it does not ensure global convergence since its cost function possesses local minima.

Next, blind adaptation algorithms based on the MOE criterion, which minimizes the output energy subject to a certain constraint, have also been used for the adaptation and interference suppression of DS-CDMA systems. It has been shown that the blind-LMS algorithm suffers from slow convergence rate and it is difficult to adapt the step-size to ensure stability in a dynamic environment. However, it ensures convergence in contrast to CMA algorithm. The blind-RLS algorithm, on the other hand, is shown to converge much faster than the blind-LMS algorithm but it suffers from the well-known numerical instability. The blind QR-RLS algorithm possesses comparable convergence as that of the RLS algorithm but it is more stable, however, the blind QR-RLS algorithm requires the calculation of the computationally expensive N square roots. To deal with the above drawbacks, we have proposed and used a novel blind-RMGS algorithm based on the MOE-criterion. It has been shown that the blind RMGS algorithm possesses the same convergence rate as that of the RLS algorithm, but it is more stable. Moreover, the blind-RMGS algorithm requires lower computational complexity as compared to the blind QR-RLS algorithm since it does not involve the calculation of N -square roots, and it can be implemented in a highly modular systolic structure. The near-far resistance of the proposed blind-RMGS algorithm has also been demonstrated.

The implementation of the adaptive MMSE DS-CDMA receiver requires the knowledge of the time-delay of the desired user, which motivates its estimation. Conventional TDE method based on the crosscorrelation of the received signal with its scaled time-shifted version fails in a near far environment. Therefore, in this thesis, we have used two near-far resistant TDE methods: one is based on crosscorrelating the desired user spreading code with the MMSE weights, and the other is based on running N -parallel adaptive MMSE algorithms.

The second TDE method has also been developed to work in the blind mode, such that the only requirement is the knowledge of the desired user spreading code.

The TDE methods implemented in the present work are shown to be near far resistant. It has also been shown that the RMGS-based TDE algorithms converge much faster and possess better performance in terms of probability of correct acquisition and RMSE as compared to the LMS-based TDE algorithm, but at the expense of increase in the computational complexity. It is worth mentioning that, in the tracking mode, the computational complexity of the implemented TDE methods using the RMGS algorithm is lower than other TDE methods based on subspace or MUSIC algorithms which require $O[N^3]$ computational complexity. It has also been shown that for a small number of users the weights processing TDE methods performs better, in terms of probability of correct acquisition and RMSE, than the parallel TDE method, however, for large number of users the parallel TDE performs better than the weights processing TDE which is due to the perturbation error induced in the relation between the weights vector and the spreading sequence as the number of users increases. The performance of the blind adaptation based TDE is shown to degrade faster as compared to the training sequence based TDE. Also some performance degradation is noticed in the probability of error of the TDE methods using both training sequence based adaptation and blind adaptation as compared to the synchronous system. The SNR degradation is within a maximum value of 3dB, which corresponds to timing estimation error of $\leq T/2$.

7.1 Suggestions for further work

The third generation (3G) mobile systems are designed to support wideband services at data rates as high as 2Mb/sec, with the same quality as fixed networks. Wideband CDMA (WCDMA) [77] is emerging as the main wireless access technology for 3G systems, and it

offers services such as wideband wireless Internet access and video transmission. The physical limitations and impairments to radio channels (bandwidth constraints, multipath fading, noise and interference) present a fundamental technical challenge to the goal of reliable high data rate communications. Since in WCDMA more ISI is inherited in the received signal there is a need to use adaptive signal processing algorithms to remove such interference. It is therefore of interest to investigate the use of the single user MMSE receiver, presented in this thesis, for the interference suppression in WCDMA systems operating over a fading multipath environment.

The use of trellis codes for multiuser CDMA systems using the MMSE receiver offer an increase in system efficiency and improvement in BER for a given value of E_b/N_o [87]. It has been shown in this thesis that the RMGS based algorithm can support larger number of users as compared to LMS based algorithms. Therefore, it is of interest to use the trellis codes in WCDMA and to employ the RMGS based MMSE single user receiver, which is expected to provide improved system capacity.

In the presence of cochannel interference (CCI) with delay spread a space-time MMSE receiver is more attractive. This receiver combines the input space and time to generate an output that minimizes the squared error between itself and the desired signal. The space-time MMSE combines the strengths of time-only and space only processing, and trades CCI and ISI reduction against noise enhancement [90]. Array receivers are designed to extract information directly from all antenna elements [33] and then treat them as an adaptive optimization problem. By using spatial processing of the adaptive array, multipath signals and ISI can be suppressed. Moreover, the use of an equalizer can further enhance the capability of suppressing the ISI. The combination of the adaptive array and the equalizer may be developed to suppress the MAI and ISI in mobile communication [57]. It will be of

interest to implement low complexity adaptive signal processing techniques for the combined spatial smoothing and equalization of WCDMA signals in a fading multipath environment.

Turbo coding is a way to approach the Shannon limit on channel capacity, while space-time processing is a way to increase the possible capacity by exploiting the rich multipath nature of fading wireless environments. Combining the two concepts provide even a practical way to both increase and approach the possible channel capacity [5]. It is of interest to investigate the use of the combined turbo coding and space-time processing for the capacity enhancement of CDMA systems.

Space-time coding is a coding/signal-processing framework for wireless communication systems with multiple transmit and multiple receive antennas [84]. This framework may be used to enhance the data rate and/or capacity of DS-SS systems. A spatio-temporal vector coding (STVC) communication structure is suggested as a means for achieving MIMO channel capacity [98]. The complexity of STVC motivates a more practical reduced-complexity discrete matrix multitone (DMMT) space-frequency coding approach. Both of these structures are shown to be asymptotically optimum. The implementation of the STVC communication structure for the capacity enhancement using adaptive signal processing techniques deserves further investigation.

MULTIPATH FADING DISPERSIVE CHANNEL MODEL

We consider the transmission of a DS-CDMA signal over a multipath fading dispersive channel having a fading rate lower than the bit rate so that the channel parameters are fixed during several bit intervals. The fading dispersive channel is represented by an equivalent discrete-time (EDT) channel, which can be realized by an FIR filter with time-variant tap gains as given earlier in Fig.4.9 [37]. Based on theoretical and empirical considerations [7] the time-variant tap-gains $g_m(n)$ are taken to be complex valued random variables with zero mean and variance equal to $\frac{1}{2} E[|g_m(n)|^2]$.

The tap gains $g_m(n)$ can be generated by $\mathbf{G}(t)=\mathbf{Z}\mathbf{F}(t)$, where $\mathbf{G}(t)=[g_0(n) \ g_1(n) \ \dots \ g_{M-1}(n)]^T$, M is the total number of paths (or taps) and \mathbf{Z} is an M -by- M matrix which satisfies the relation $\mathbf{A}=\mathbf{Z}\mathbf{Z}^T$ (the Cholesky factorization), while \mathbf{A} denotes an M -by- M covariance matrix of the tap-gains $g_m(n)$ with coefficients $a_{m,n}$, $m, n \in \{0, 1, \dots, M-1\}$. The coefficients $a_{m,n}$ of the covariance matrix \mathbf{A} is related to the delay power spectrum $Q(\tau)$ by the following relation [37, 126]:

$$a_{m,n}=E[g_m(n) g_n^*(n)]= \int 2Q(\tau)W(mT_s - \tau)W(nT_s - \tau)d\tau \quad (\text{A-1})$$

$$\text{where } W(\tau)=(T)^{-1} \int_0^T \psi(t) \psi(t+\tau) dt \quad (\text{A-2})$$

and $\psi(t)$ is the symbol waveform defined earlier in chapter two, and $Q(\tau)$, the multipath intensity profile, is given by the exponential relation

$$Q(\tau)= (2\tau_{rms})^{-1} \exp(-\tau/\tau_{rms}) \quad \tau \geq 0 \quad (\text{A-3})$$

where τ_{rms} is the rms delay spread of the channel. The integration in eq.(A-1) is evaluated numerically using Simpson's rule. Assuming a channel composed of N_p echos, each has a phase γ_n , a delay τ_n and rotates with Doppler frequency f_d . Therefore, the elements of the vector $\mathbf{F}(t) = [f_N(t,0) \ f_N(t,1) \ \dots \ f_N(t,M-1)]^T$, can be computed as [126]:

$$f_N(t) = \frac{1}{\sqrt{N_p}} \sum_{n=0}^{N_p-1} e^{j(\gamma_n - 2\pi f_d t)} \quad (\text{A-4})$$

where N_p is the number of random phasors assumed to be equal to 10 in the simulation, γ_n 's are independent identically distributed (i.i.d) random variables uniformly distributed over $[0, 2\pi)$ generated as

$$\gamma_n = 2\pi u_n - \pi \quad (\text{A-5})$$

where u_n 's are the uniform random variables distributed between 0 to 1, and f_d are i.i.d. random variables which are generated as

$$f_d = f_{\text{max}} \cos(2\pi u_n) \quad (\text{A-6})$$

where f_{max} is the maximum Doppler frequency of the channel. The Doppler variation of the channel is assumed to follow the Jakes spectrum model (which models the Doppler power spectrum as an isotropic scattering) [37, 126]:

$$S(f) = \left[2\pi f_{\text{max}} \sqrt{1 - \left(\frac{f_d}{f_{\text{max}}} \right)^2} \right]^{-1} \quad \text{for } 0 < |f_d| < f_{\text{max}} \quad (\text{A-7})$$

It is worth noting that the generation of \mathbf{A} , \mathbf{Z} and the random seeds is done once only. The above method of generating the tap gains is flexible and defines clearly the fading model of the channel.

The contribution from each path to the i th received chip of the n th bit is $\tilde{r}_{i+m}(n) g_m(n)$ for $m=0, 1, \dots, M-1$. However, there might also interference due to the $(n-1)$ th bit of

$\tilde{r}_{i+m-N+1}(n-1)g_m(n)$ for $m=0, 1, \dots, M-1$. Therefore, it can be directly shown that the output of the fading channel of the i th chip at the n th symbol $\tilde{r}_i^f(n)$ is computed by:

$$\tilde{r}_i^f(n) = \sum_{m=0}^{M-1} \begin{cases} \tilde{r}_{i+m}(n)g_m(n) & \text{if}(i+m) \leq N-1 \\ \tilde{r}_{i+m-N+1}(n-1)g_m(n) & \text{if}(i+m) > N-1 \end{cases} \text{ for } i=0, 1, \dots, N-1 \quad (\text{A-8})$$

and the faded received vector will be $\mathbf{r}^f(n) = [\tilde{r}_0^f(n) \tilde{r}_1^f(n) \dots \tilde{r}_{N-1}^f(n)]^T$.

SOLUTION OF THE CONSTRAINED OPTIMIZATION PROBLEM

(Eqs. 5.26 & 5.27)

The exponentially windowed RLS algorithm selects the weights vector $\mathbf{z}_1(n)$ to minimize the sum of exponentially weighted output energy:

$$\text{minimize } \sum_{i=1}^n \lambda^{n-i} [\mathbf{z}_1^T(n) \mathbf{r}(i)]^2 \quad (\text{B-1})$$

$$\text{subject to } \mathbf{c}_1^T \mathbf{z}_1(n) = 1 \quad (\text{B-2})$$

where $0 < \lambda < 1$ is the forgetting factor ($1-\lambda \ll 1$), \mathbf{c}_1 is the spreading sequence of the desired user, and $\mathbf{r}(i)$ is the synchronous received vector given by:

$$\mathbf{r}(i) = d_1(i) \sqrt{P_1} \mathbf{c}_1 + \sum_{k=2}^K d_k \sqrt{P_k} \mathbf{c}_k + \sigma_n \boldsymbol{\eta} \quad (\text{B-3})$$

where $d_k(i)$ is the k th user data bit and P_k is its power, and $\boldsymbol{\eta}$ is additive white Gaussian noise vector of covariance matrix \mathbf{I} . Assuming a system with one user transmitting over AWGN channel, the linear MMSE detector has the form:

$$\hat{d}_1(n) = \text{sgn}[\mathbf{z}_1^T(n) \mathbf{r}(n)] \quad (\text{B-4})$$

where $\mathbf{z}_1(n)$ is chosen to minimize the mean square error (ξ) defined by:

$$\xi \stackrel{\Delta}{=} E[\{\mathbf{z}_1^T(n) \mathbf{r}(n) - d_1(n) \sqrt{P_1}\}^2] \quad (\text{B-5})$$

$$= E[\mathbf{z}_1^T(n) \mathbf{r}(n) \mathbf{r}^T(n) \mathbf{z}_1(n) - 2 d_1(n) \sqrt{P_1} \mathbf{z}_1^T(n) \mathbf{r}(n) + P_1]$$

Assuming that $d_1(n)$ and n are independent, the last equation can be written as:

$$\xi = \mathbf{z}_1^T(n) (\sigma_n^2 \mathbf{I} + P_1 \mathbf{c}_1 \mathbf{c}_1^T) \mathbf{z}_1(n) - 2P_1 \mathbf{z}_1^T(n) \mathbf{c}_1 + P_1 \quad (\text{B-6})$$

Taking the gradient of MSE with respect to $\mathbf{z}_1(n)$, and setting it to zero, we get

$$\nabla_{\mathbf{z}} \xi = 0 = 2 (\sigma_n^2 \mathbf{I} + P_1 \mathbf{c}_1 \mathbf{c}_1^T) \mathbf{z}_1(n) - 2P_1 \mathbf{c}_1$$

then the MMSE solution $\mathbf{z}^*(n)$ is given by [92]:

$$\mathbf{z}^*(n) = P_1 (\sigma_n^2 \mathbf{I} + P_1 \mathbf{c}_1 \mathbf{c}_1^T)^{-1} \mathbf{c}_1 \quad (\text{B-7})$$

The blind adaptive version of the MMSE detector is based on the decomposition of the linear detector as the sum of two orthogonal components. One component is equal to the spreading sequence \mathbf{c}_1 , which is known to be fixed, while the other \mathbf{x}_1 is an orthogonal and adaptive. The canonical representation for the MMSE detector is [92]:

$$\bar{\mathbf{z}}_1(n) = \mathbf{c}_1 + \mathbf{x}_1 \quad (\text{B-8})$$

where $\mathbf{c}_1^T \mathbf{x}_1 = 0$. Therefore, the MMSE detector minimizes the MSE subject to the constraint $\bar{\mathbf{z}}_1^T(n) \mathbf{c}_1 = \|\mathbf{c}_1\| = 1$. The canonical form $\bar{\mathbf{z}}_1(n)$ can be found by the method of Lagrange multipliers. Let

$$L(\mathbf{z}_1) = \xi - 2\gamma [\mathbf{c}_1^T \mathbf{z}_1(n) - 1] \quad (\text{B-9})$$

where γ is the Lagrange multiplier. Substituting Eq.(B-6) into Eq.(B-9) we get:

$$L(\mathbf{z}_1) = \mathbf{z}_1^T(n) [\sigma_n^2 \mathbf{I} + P_1 \mathbf{c}_1 \mathbf{c}_1^T] \mathbf{z}_1(n) - 2P_1 \mathbf{z}_1^T(n) \mathbf{c}_1 + P_1 - 2\gamma [\mathbf{c}_1^T \mathbf{z}_1(n) - 1] \quad (\text{B-10})$$

By setting the gradient $\nabla_{\mathbf{z}_1} L = 0$, we get:

$$2 (\sigma_n^2 \mathbf{I} + P_1 \mathbf{c}_1 \mathbf{c}_1^T) \mathbf{z}_1(n) - 2 P_1 \mathbf{c}_1 - 2\gamma \mathbf{c}_1 = 0.$$

$$\mathbf{z}_1(n) = (P_1 + \gamma) [\sigma_n^2 \mathbf{I} + P_1 \mathbf{c}_1 \mathbf{c}_1^T]^{-1} \mathbf{c}_1 \quad (\text{B-11})$$

On substituting this in the constraint $\mathbf{c}_1^T \mathbf{z}_1(n) = 1$, we get

$$(P_1 + \gamma) \mathbf{c}_1^T (\sigma_n^2 \mathbf{I} + P_1 \mathbf{c}_1 \mathbf{c}_1^T)^{-1} \mathbf{c}_1 = 1$$

$$\text{or } (P_1 + \gamma) = \frac{1}{\mathbf{c}_1^T (\sigma_n^2 \mathbf{I} + P_1 \mathbf{c}_1 \mathbf{c}_1^T)^{-1} \mathbf{c}_1} \quad (\text{B-12})$$

substituting (B-12) in (B-11) we get:

$$\bar{\mathbf{z}}_1 = \frac{1}{\mathbf{c}_1^T (\sigma_n^2 \mathbf{I} + P_1 \mathbf{c}_1 \mathbf{c}_1^T)^{-1} \mathbf{c}_1} \cdot (\sigma_n^2 \mathbf{I} + P_1 \mathbf{c}_1 \mathbf{c}_1^T)^{-1} \mathbf{c}_1 \quad (\text{B-13})$$

It may be noted that the autocorrelation matrix \mathbf{R} for a single user system is given by:

$$\mathbf{R} = E[\mathbf{r}(n)\mathbf{r}^T(n)] = P_1 \mathbf{c}_1 \mathbf{c}_1^T + \sigma_n^2 \mathbf{I} \quad (\text{B-14})$$

and the solution will be:

$$\bar{\mathbf{z}}_1 = \frac{1}{\mathbf{c}_1^T \mathbf{R}^{-1} \mathbf{c}_1} \mathbf{R}^{-1} \mathbf{c}_1 \quad (\text{B-15})$$

However, for a system of K synchronous users the autocorrelation matrix \mathbf{R} will be

$$\mathbf{R} = E[\mathbf{r}(n)\mathbf{r}^T(n)] = \sum_{k=1}^K P_k \mathbf{c}_k \mathbf{c}_k^T + \sigma_n^2 \mathbf{I} \quad (\text{B-16})$$

REFERENCES

- [1] B. Aazhang, B.P. Paris, and G. Orsak, "Neural networks for multi-user detection in CDMA communications," *IEEE Tans. Commun.*, vol. 40, no. 6, pp. 1212-1222, July 1992.
- [2] A. Abdulrahman, A.U. Sheikh, and D.D. Falconor, "Decision feedback equalization for CDMA in indoor wireless communications," *IEEE J. Select. Areas Commun.*, vol.12, no.4, pp. 698-706, May 1994.
- [3] T. Aboulnasr and K. Mayyas, "A robust variable step-size LMS-type algorithm: analysis and simulations," *IEEE Trans. Signal Process.*, vol.45, no.3, pp. 631-639, Mar. 1997.
- [4] S.T. Alexander and A.L. Ghirnkar, "A method for recursive least squares filtering based upon an inverse QR decomposition," *IEEE Trans. Signal Process.*, vol.41, no.1, pp. 20-30, Jan. 1993.
- [5] S.L. Ariyavisitakul, "Turbo space-time processing to improve wireless channel capacity," *IEEE Trans. Commun.* Vol.48, no.8, pp.1347-1359, Aug. 2000.
- [6] S. Bellini, *Bussgang techniques for blind deconvolution and equalization*, in *Blind Deconvolution*, S. Haykin Ed., Prentice-Hall, Inc., New Jersey, pp.8-59, 1994.
- [7] P.A. Bello, "Characterization of randomly time-variant linear channels," *IEEE Trans. Commun. Syst.*, vol. 11, pp.360-393, Nov. 1963.
- [8] S. Benedetto and E. Biglieri, "On linear receivers for digital transmission systems," *IEEE Trans. Commun.*, vol. 22, no.9, pp. 1205-1215, Sept. 1974.
- [9] S.E. Bensley and B. Aazhang, "Subspace-based channel estimation for code division multiple access communication systems," *IEEE Trans. Commun.*, vol. 44, no. 8, pp. 1009-1020, Aug. 1996.

- [10] S.E. Bensley and B. Aazhang, "Maximum-likelihood synchronization of a single user for code-division multiple-access communication systems," *IEEE Trans. Commun.*, vol. 46, no.3, pp. 392-399, March 1998.
- [11] A. Benveniste and M. Goursat, "Blind Equalizers," *IEEE Trans. Commun.*, vol. 32, pp. 871-883, Aug. 1984.
- [12] E. Biglieri, J Proakis and S. Shamai, "Fading Channels: Information-Theoretic and Communication Aspects," *IEEE Trans. Inform. Theory*, vol. 44, no. 6, pp. 2619-2692, Oct. 1998.
- [13] D. Boudreau and P. Kabal, "Joint time-delay estimation and adaptive recursive least squares filtering," *IEEE Trans. Signal Process.*, vol.41, no. 2, pp. 592-601, Feb. 1993.
- [14] J. Caffery and G.L. Stüber, "Nonlinear multiuser parameter estimation and tracking in CDMA systems," *IEEE Trans. Commun.*, vol. 48, no. 12, pp. 2053-2063, Dec. 2000.
- [15] Y. T. Chan, J.M.F Riley and J.B. Plant, " Modeling of time delay and its application to estimation of nonstationary delays," *IEEE trans. ASSP*, vol.29, no. 3, pp. 577-581, June 1981.
- [16] D.S. Chen and S. Roy, "An adaptive multiuser receiver for CDMA systems," *IEEE J. Select. Areas Commun.*, vol.12, no.5, pp. 808-816, June 1994.
- [17] G.A. Clark S.K. Mitra, and S.R. Parker, "Block Implementation of Adaptive Digital Filters," *IEEE Trans. on Acoust. Speech, and Signal Processing*, vol. ASSP-29, no.3, pp. 744-752, June 1981.
- [18] R. De Gaudenzi, F. Giannetti, and Luise, "Design of low-complexity adaptive interference-mitigating detector for DS/SS receiver in CDMA radio networks," *IEEE Trans. Commun.*, vol.46, no. 1, pp.125-134, Jan. 1998.

- [19] A. Duel-Hallen, "Decorrelating Decision-feedback multiuser detector for synchronous code-division multiple-access channel," IEEE Trans. Commun., vol.41, no.2, pp. 285-290, Feb. 1993.
- [20] A. Duel-Hallen, " A family of multiuser decision-feedback detectors for asynchronous code-division multiple-access channels," IEEE Trans. Commun., vol. 43, no.2/3/4, pp. 421-434, Feb.-Apr. 1995.
- [21] E. Eleftheriou and D.D. Falconer, "Tracking properties and steady-state performance of RLS adaptive filter algorithms," IEEE Trans. ASSP, vol. 34, no. 5, pp. 1097-1109, Oct. 1986.
- [22] H. Fathallah and L.A. Rusch, "A subspace approach to adaptive narrow-band interference suppression in DSSS," IEEE Trans. on Commun., vol. 45, no. 12, pp. 1575-1585, Dec. 1997.
- [23] V.K. Garg, K. Smolik, and J.E. Wilkes, *Applications of code-division multiple access (CDMA) in wireless/personal communications*, Upper Saddle River, NJ: Prentice-Hall, 1996.
- [24] W.M. Gentleman and H.T. Kung, "Matrix triangularization by systolic arrays," Proc. SPIE, vol. 298, Real-time signal processing IV, pp. 298-303, 1981.
- [25] M.S. Gerwal and A.P. Andrews, *Kalman filtering: Theory and practice*, Englewood Cliffs, NJ: Prentice-Hall, 1993.
- [26] R.D. Gitlin and F.R. Magee, Jr., "Self-orthogonalizing adaptive equalization algorithms," IEEE Trans. Commun, vol.25, no. 7, pp.666-672, July 1977.
- [27] D. Godard, "Channel equalization using a Kalman filter for fast data transmission," IBM J. Res. Develop., vol. 18, pp. 267-273, May, 1974.

- [28] D. N. Godard, "Self-recovering equalization and carrier tracking in two-dimensional data communication systems," *IEEE Trans. Commun.*, vol. 28, no.11, pp. 1867-1875, Nov. 1980.
- [29] R. Godfrey and F. Rocca, "Zero memory non-linear deconvolution," *Geophysical Prospecting*, vol.29, pp.189-228, 1981.
- [30] G.H. Golub and C. F. Van Loan, *Matrix Computations*, John Hopkins University Press, 1989.
- [31] F.D. Garber and M.B. Pursley, "Optimal phases of maximal length sequences for asynchronous spread-spectrum multiplexing," *IEE Electronics Letters*, vol.16, no.19, pp.756-757, Sept.1980.
- [32] K.W. Halford and M.B.-Pearce, "New-user identification in a CDMA system," *IEEE Trans. Commun.*, vol.46, no. 1, pp.144-155, Jan. 1998.
- [33] A.A. Hansson, "On antenna array receiver principles for space-time-selective Rayleigh fading channels," *IEEE Trans. Commun.*, vol.48, no.4, pp. 648-657, April 2000.
- [34] R. Harris et al, "A variable step-size (VSS) algorithm," *IEEE Trans. ASSP*, vol.34, no.6, pp. 499-510, June 1986.
- [35] S. Haykin *Adaptive Filter Theory*, Prentice-Hall, Englewood cliffs, NJ, first edition, 1986.
- [36] S. Haykin *Adaptive Filter Theory*, Prentice-Hall: Upper Saddle River, NJ, third edition, 1996.
- [37] P. Hoeher, "A statistical discrete time model for the WSSUS multipath channel," *IEEE Trans. on Veh. Tech.* vol. 41, pp. 461-468, Nov. 1992.
- [38] M. Honig, U. Madhow, and S. Verdu, "Blind adaptive multiuser detection," *IEEE Trans. Inform. Theory*, vol. 41, no.4, pp. 944-960, July 1995.

- [39] M. Honig and H.V. Poor, *Adaptive Interference Suppression*, in *Wireless Communication: Signal processing perspectives*, H.V. Poor, & G.W. Wornell, eds., Prentice-Hall Inc., Upper Saddle river, New Jersey 07458, pp.64-128, 1998.
- [40] M. Honig and M.K. Tsatsanis, "Adaptive techniques for multiuser CDMA receivers," *IEEE Signal Process. Magazine*, vol. 17, no. 3, pp. 49-61, May 2000.
- [41] A.L.C. Hui and K.B. Letaief, "Successive interference cancellation for multiuser asynchronous DS/CDMA detectors in multipath fading links," *IEEE Trans. Commun.*, vol.46, no. 3, pp. 384-391, Mar. 1998.
- [42] H.-C. Huang H.-C. and C.-H. Wei, "Blind adaptive algorithm for demodulation of DS/CDMA signals with mismatch," *IEE Proc.-Commun.*, vol. 146, No. 1, pp. 29-34, Feb. 1999.
- [43] R.A. Iltis, "An EKF-Based joint estimation for interference, multipath, and code delay in a DS spread-spectrum receiver," *IEEE Trans. Commun.*, vol. 42, no. 2/3/4, pp. 1288-1299, Feb/Mar./Apr. 1994.
- [44] R.A. Iltis and L. Mailaender, "An adaptive multiuser detector with joint amplitude and delay estimation," *IEEE JSAC*, vol. 12, No. 5, pp. 774-784, June 1994.
- [45] S.N. Jagdeesha, S.N. Sinha and D.K. Mehra, "A recursive modified Gram-Schmidt algorithm based adaptive beam former," *Signal Processing*, vol. 39, pp.69-78, 1994.
- [46] A. Kansal, "Adaptive maximum SINR RAKE filtering for DS-CDMA multipath fading channels," *IEEE JSAC*, vol. 16, no. 9, pp. 1765-1773, Dec. 1998.
- [47] A. Klein, G.K. Kaleh, and P.W. Baier, "zero forcing and minimum mean-square-error equalization for multiuser detection in code-division multiple-access channels," *IEEE Trans. Veh. Tech.*, vol. 45, no.2, pp.276-287, May 1996.

- [48] C. H. Knapp and G.C. Carter, "The generalized correlation method for estimation of time delay," IEEE Trans. ASSP, vol. 24, no. 4, pp. 320-327, Aug. 1976.
- [49] R. Kohno, H. Imai and M Haroti, "Cancellation techniques for co-channel interference in asynchronous spread spectrum multiple access systems," Electron. Commun. Jpn., vol. 66, no. 5, pp. 20-29, May 1983.
- [50] R. Kohno et al, "Combination of an adaptive array antenna and a canceller of interference for direct-sequence spread-spectrum multiple-access system," IEEE JSAC, vol. 8, no. 4, pp. 675-682, May 1990.
- [51] B.W. Kozminchuk and A. Sheikh, "A Kalman filter-based architecture for interference excision," IEEE Trans. Commun., vol. 43, no. 2/3/4, pp. 574-580, Feb./Mar./Apr. 1995.
- [52] V. Krishnamurthy, "Averaged stochastic gradient algorithms for adaptive blind multiuser detection in DS/CDMA systems," IEEE Trans. Commun., vol. 48, no. 1, pp. 125-134, Jan. 2000.
- [53] R.H. Kwong and E.W. Johnson, "A variable step size LMS algorithm," IEEE Trans. Signal Process., vol. 40, no.6, pp. 1633-1642, July 1992.
- [54] R.E. Lawrence and H. Kaufman, "The Kalman filter for the equalization of a digital communications channel," IEEE Trans Commun. Tech., vol. 19, no.6, pp. 1137-1141, Dec. 1971.
- [55] C.L. Lawson and R.J. Hanson *Solving Least Squares problems*, Prentice-Hall, Englewood cliffs, NJ, 1974.
- [56] J.C Lee, "Performance of transform-domain LMS adaptive digital filters," IEEE Trans. ASSP, vol. 34, no. 3, pp. 499-510, June 1986.

- [57] M-L. Leou, "A novel hybrid of adaptive array and equalizer for mobile communications," *IEEE Trans. On Vehicular Technology*, vol.49, no.1, pp. 1-10, Jan. 2000.
- [58] K.B. Letaief et al, "Fast simulation of DS/CDMA with and without coding in multipath fading channels," *IEEE JSAC*, vol. 15, no. 4, pp. 66-639, May 1997.
- [59] T.J. Lim and M.D. Macleod, "Adaptive algorithms for joint time delay estimation and IIR filtering," *IEEE Trans Signal Process.* vol. 43, no. 4, pp. 841-851, Apr. 1995.
- [60] T.J. Lim and L.K. Rasmussen, "Adaptive symbol and parameter estimation in asynchronous multiuser CDMA detector, " *IEEE Trans. Commun.*, vol. 45, no. 2, pp. 213-220, Feb. 1997.
- [61] T.J. Lim, "An asynchronous multiuser CDMA detector based on the Kalman filter," *IEEE JSAC*, vol. 10, no. 9, pp. 1711-1722, Dec. 1998.
- [62] T.J. Lim and Y. Ma, "The Kalman filter as the optimal linear minimum mean-squared error multiuser CDMA detector," *IEEE Inform. Theory*, vol. 46, no. 7, pp. 2561-2566, Nov.-2000.
- [63] F. Ling and D. Manolakis and J.G. Proakis, "A recursive modified Gram-Schmidt algorithm for least-squares estimation," *IEEE Trans. ASSP*, vol. 34, no.4, pp 829-836, Aug. 1986.
- [64] H. Liu and G. Xu, "A subspace method for signature waveform estimation in synchronous CDMA systems," *IEEE Trans. Commun.*, vol. 44, no. 10, pp. 1346-1354, Oct. 1996.
- [65] R. Lupas and S. Verdu, "Linear multiuser detectors for synchronous code-division multiple-access channels," *IEEE Trans. Inform. Theory*, vol. 35, no.1, pp. 123-136, Jan. 1989.

- [66] R. Lupas and S. Verdu, "Near-far resistance of multi-user detectors in asynchronous channels," *IEEE Trans. Commun.*, vol. 38, no.4, pp. 496-508, Apr. 1990.
- [67] U. Madhow, "Blind adaptive interference suppression for the near-far resistant acquisition and demodulation of direct-sequence CDMA signals," *IEEE Trans. Signal Processing*, vol. 45, no.1, pp. 124-136, Jan. 1997.
- [68] U. Madhow, "MMSE interference suppression for timing acquisition and demodulation in direct-sequence CDMA systems," *IEEE Trans. Commun.*, vol.46, no.8, pp.1065-1075, Aug. 1998.
- [69] U. Madhow, "Blind adaptive interference suppression for direct-sequence CDMA," *IEEE Proc.*, vol.86, no.10, pp.2049-2069, Oct. 1998.
- [70] U. Madhow and M.L. Honig, "MMSE interference suppression for direct-sequence spread-spectrum CDMA," *IEEE Trans. Commun.*, vol.42, no.12, pp. 3178-88, Dec. 1994.
- [71] D. Mansour and A.H. Gary, Jr., "Unconstrained frequency-domain adaptive filter," *IEEE Trans. ASSP*, vol. 30, no. 5, pp. 726-734, Oct. 1982.
- [72] V.J. Mathews and Z. Xie, "A stochastic gradient adaptive filter with gradient adaptive step size," *IEEE Trans. Signal Process.*, vol. 41, no.6, pp. 2075-2087, June 1993.
- [73] J. McWhirter, "Recursive least-squares minimization using a systolic array," *Proc. SPIE, Real-Time signal processing VI*, vol. 431, San-Diego, Calif., pp. 105-112, 1983.
- [74] S.L. Miller, "An adaptive direct-sequence CDMA receiver for multiuser interference rejection," *IEEE Trans. Commun.*, vol.43, no.2/3/4, pp.1746-1755, Feb./Mar./Apr.1995.
- [75] S.L. Miller, "Training analysis of adaptive interference suppression for direct-sequence code-division multiple-access systems," *IEEE Trans. Commun.*, vol. 44, no.4, pp. 488-495, Apr. 1996.

- [76] S. L. Miller, M. L. Honig and L. B. Milstein, "Performance analysis of MMSE receivers for DS-CDMA in frequency-selective fading channels," *IEEE Trans. Commun.*, vol. 48, no. 11, pp. 1919-1929, Nov. 2000.
- [77] L.B. Milstein, "Wideband code division multiple access," *IEEE JSAC*, vol. 18, no. 8, pp. 1344-1354, Aug. 2000.
- [78] U. Mitra and H.V. Poor, "Neural network techniques for adaptive multiuser demodulation," *IEEE JSAC*, vol. 12, No. 9, pp. 1460-1470, Dec. 1994.
- [79] U. Mitra and H.V. Poor, "Adaptive receiver algorithms for near-far resistant CDMA," *IEEE Trans. Commun.*, vol. 43, nos. 2-4, pp. 1713-1724, Feb.-Apr. 1995.
- [80] U. Mitra and H.V. Poor, "Analysis of an adaptive decorrelating detector for synchronous CDMA channels," *IEEE Trans. Commun.*, vol. 44, no. 2, pp. 257-268, Feb. 1996.
- [81] M. Montazeri and P. Duhamel, "A set of algorithms linking NLMS and block RLS algorithms," *IEEE Trans. Signal Process.*, vol. 43, no. 2, pp. 444-453, Feb. 1995.
- [82] M. Morf and T. Kailath, "Square-root algorithms for least-squares estimation," *IEEE Trans. Automatic Control*, vol. AC-20, no. 4, pp. 487-497, Aug. 1975.
- [83] S. Moshavi, "Multi-user detection for DS-CDMA communications," *IEEE Commun. Mag.*, vol. 34, pp. 124-136, Oct. 1996.
- [84] A.F. Naguib, N. Seshadri, and A.R. Calderbank, "Increasing data rate over wireless channels," *IEEE Signal Process. Magazine*, vol.17, no. 3, pp.76-92, May 2000.
- [85] S. Narayan and M. Peterson, "Frequency domain least-mean-square algorithm," *Proc. IEEE*, vol. 69, no.1, pp. 124-126, Jan. 1981.

- [86] M.J. Omid, P.G. Gulak, and S. Pasupathy, "Parallel structures for joint channel estimation and data detection over fading channels," IEEE JSAC, vol. 16, no. 9, pp. 1616-1629, Dec. 1998.
- [87] I. Oppermann and P.B. Rapajic, "Capacity of a band-limited CDMA MMSE receiver-based system when combined with trellis or convolutional coding," IEEE Trans. Commun., vol.48, no. 8, pp. 1328-1337, Aug. 2000.
- [88] H.C. Papadopoulos, *Equalization of Multiuser Channels*, in Wireless Communication: Signal processing perspectives, H.V. Poor, &G.W. Wornell, eds., Prentice-Hall Inc., Upper Saddle river, New Jersey 07458, pp. 129-178, 1998.
- [89] S. Parkvall, E.G. Strom, L.B. Milstein, and B.E. Otterson, "Asynchronous near-far resistant DS-SS receivers without a priori synchronization," IEEE Trans. Commun., vol. 47, no.1, pp. 78-88, Jan. 1999.
- [90] A.J. Paulraj and C.B. Papadias, "Space-time processing for wireless communications," IEEE Signal Process. Magazine, vol.14, no.6, pp. 49-83, Nov. 1997.
- [91] R.L. Pickholtz, D.L. Schilling, and L.B. Milstein, "Theory of spread spectrum communications- A tutorial," IEEE Trans. Commun., vol. 30, no. 5, pp. 855-884, May 1982.
- [92] H.V. Poor and X. Wang, "Code-aided interference suppression in DS/SS communications: Interference suppression capability" IEEE Trans. Commun. Vol. 45, no. 9, pp. 1101-1111, Sept. 1997.
- [93] H.V. Poor and X. Wang, "Code-aided interference suppression in DS/SS communications: Parallel blind adaptive implementations," IEEE Trans. Commun. Vol. 45, no. 9, pp. 1111-1122, Sept. 1997.
- [94] W. Press et al, *Numerical Recipes in C*, Cambridge press, 2nd edition, 1992.

- [95] J.G. Proakis, *Digital Communications*, New York: McGraw-Hill, 3rd edition, 1995.
- [96] P.B. Rapajic and D.K. Borah, "Adaptive MMSE maximum likelihood CDMA multiuser detection," *IEEE JSAC*, vol. 17, no. 12, pp. 2110-2122, Dec. 1999.
- [97] P.B. Rapajic and B.S. Vucetic, "Adaptive receiver structures for asynchronous CDMA systems," *IEEE J. Selected Areas Commun.*, vol. 12, no.4, pp. 685-697, May 1994.
- [98] G.G. Rayleigh and J.M., Cioffi, "Spatio-temporal coding for wireless communication," *IEEE Trans. Commun.*, vol.46, no.3, pp. 357-366, March 1998.
- [99] S. Roy, "Subspace blind adaptive detection for multiuser CDMA," *IEEE Trans. Commun.*, vol. 48, no.1, pp. 169-175, Jan-2000.
- [100] Y. Sato, "A method of self-recovering equalization for multilevel amplitude modulation," *IEEE Trans. Commun.*, vol. 23, no. 6, pp. 679-682, June 1975.
- [101] A.H. Sayed and T. Kailath, "A state-space approach to adaptive RLS filtering," *IEEE Signal Process. Magazine*, vol. 11, pp. 18-60, July 1994.
- [102] A.M.Sayeed, A. Sendonaris and B. Aazhang, "Multiuser detection in fast fading multipath environments," *IEEE JSAC*, vol. 16, no. 9, pp. 1691-1701, Dec. 1998.
- [103] A.M. Sayeed and B Aazhang, "Joint multipath-Doppler diversity in mobile wireless communications," *IEEE Trans. Commun.* vol.47, no.1, pp.123-132, Jan. 1999.
- [104] J.J. Shynk, "Frequency-domain and multirate adaptive filtering," *IEEE Signal Processing Mag.*, vol.9, pp.14-37, Jan. 1992.
- [105] R.F. Smith and S.L. Miller, "Acquisition performance of an adaptive receiver for DS-CDMA," *IEEE Trans. Commun.*, vol. 47, No. 9, pp. 1416-1424, Sept. 1999.
- [106] E.G. Strom, S. Parkvall, S. L. Miller, and B.E. Otterson, "Propagation delay estimation in asynchronous direct-sequence code-division multiple access systems," *IEEE Trans. Commun.*, vol. 44, no.1, pp. 84-93, Jan. 1996.

- [107] P.-A. Sung and K.-C. Chen, "A linear minimum mean square error multiuser receiver in Rayleigh-fading channels," *IEEE JSAC*, vol. 14, no. 8, pp. 1583-1594, Oct. 1996.
- [108] J.S. Thompson, P.M. Grant and B. Mulgrew, "Performance of antenna array receiver algorithms for CDMA," *Signal Process. Journal*, vol. 68, no. 1, pp. 23-41, July 1998.
- [109] J.R. Treichler and B.G. Agee, "A new approach to multipath correction of constant modulus signals," *IEEE Trans. ASSP*, vol. 31, no.2, pp. 349-377, April 1983.
- [110] J.R. Treichler and M.G. Larimore, "New processing techniques based on the constant modulus adaptive algorithm," *IEEE Trans. ASSP*, vol. 33, pp. 420-431, April 1985.
- [111] M.K. Tsatsanis, "Inverse filtering criteria for CDMA systems," *IEEE Trans. Signal Processing*, vol. 45, no.1, pp. 102-112, Jan. 1997.
- [112] S.Ulukus and R.D. Yates, "A blind adaptive decorrelating detector for CDMA systems," *IEEE JSAC*, vol. 16, no. 8, pp. 1530-1541, Oct. 1998.
- [113] M.K. Varanasi and B. Aazhang, "Optimally near-far resistant multiuser detection in differentially coherent synchronous channels," *IEEE Trans. Inform. Theory*, vol.37, no.4, pp.1006-018, July 1991.
- [114] M.K. Varanasi and B. Aazhang, "Multistage detection for asynchronous code-division multiple-access communications," *IEEE Trans. Commun.*, vol. 38, no.4, pp. 509-519, Apr. 1990.
- [115] M.K. Varanasi and B. Aazhang, "Near-optimum detection in synchronous code-division multiple-access systems," *IEEE Trans. Commun.*, vol. 39, no.5, pp. 725-736, May 1991.
- [116] S. Verdu, "Minimum probability of error for asynchronous Gaussian multiple-access channels" *IEEE Trans. Inform. Theory*, vol. 32, no. 1, pp.85-96, Jan. 1986.

- [117] S. Verdu, "Optimum multiuser asymptotic efficiency" IEEE Trans. Commun., vol. 34, no.9, pp.890-897, Sept. 1986.
- [118] S. Verdu, *Multiuser Detection*, in Advances in Statistical Signal Processing, Vol.2: *Signal Detection*, H.V. Poor and J.B. Thomas, Eds., Greenwich, CT: JAI Press, pp.369-409, 1993.
- [119] A.J. Viterbi, "Very low rate convolutional codes for maximum theoretical performance of spread spectrum multiple access channels," IEEE JSAC, vol. 8, no. 4, pp. 641-649, May 1990.
- [120] X. Wang and H.V. Poor, "Blind equalization and multiuser detection in dispersive CDMA channels," IEEE Trans. Commun., vol. 46, no. 1, pp. 91-103, Jan. 1998.
- [121] X. Wang and H.V. Poor, "Blind multiuser detection: A subspace approach," IEEE Trans. Inform. Theory, vol. 44, no. 2, pp. 677-690, Mar. 1998.
- [122] B.Widrow and S.D. Stearns, *Adaptive Signal Processing*, Prentice-Hall, Englewood Cliffs, NJ: 1985.
- [123] G. Woodward and B.S. Vucetic, "Adaptive detection for DS-CDMA", IEEE Proc., vol.86, no. 7, pp.1413-1434, July 1998.
- [124] Z. Xie, R.T. Short and C.K. Rushforth, "A family of suboptimum detectors for coherent multiuser communications," IEEE JSAC, vol. 8, no.4, pp.683-690, May1990.
- [125] G. Ye and G. Bi, "Code timing estimator for DS-CDMA signals in slow fading multipath channels," IEE Electronics Letters, vol.35, no.19, pp. 1604-1606, Sept. 1999.
- [126] K.W. Yip and T.S. NG, "Efficient simulation of digital transmission over WSSUS channels," IEEE Trans. Comm., vol. 43, no. 12, pp. 2907-2912, Dec. 1995.
- [127] D. Zheng, J. Li, S.L. Miller, and E.G. Strom, "An efficient code-timing estimator for DS-CDMA signals," IEEE Trans. Signal Processing, vol.45, no.1, pp. 82-89, Jan. 1997.

- [117] S. Verdu, "Optimum multiuser asymptotic efficiency" IEEE Trans. Commun., vol. 34, no.9, pp.890-897, Sept. 1986.
- [118] S. Verdu, *Multiuser Detection*, in Advances in Statistical Signal Processing, Vol.2: *Signal Detection*, H.V. Poor and J.B. Thomas, Eds., Greenwich, CT: JAI Press, pp.369-409, 1993.
- [119] A.J. Viterbi, "Very low rate convolutional codes for maximum theoretical performance of spread spectrum multiple access channels," IEEE JSAC, vol. 8, no. 4, pp. 641-649, May 1990.
- [120] X. Wang and H.V. Poor, "Blind equalization and multiuser detection in dispersive CDMA channels," IEEE Trans. Commun., vol. 46, no. 1, pp. 91-103, Jan. 1998.
- [121] X. Wang and H.V. Poor, "Blind multiuser detection: A subspace approach," IEEE Trans. Inform. Theory, vol. 44, no. 2, pp. 677-690, Mar. 1998.
- [122] B.Widrow and S.D. Stearns, *Adaptive Signal Processing*, Prentice-Hall, Englewood Cliffs, NJ: 1985.
- [123] G. Woodward and B.S. Vucetic, "Adaptive detection for DS-CDMA", IEEE Proc., vol.86, no. 7, pp.1413-1434, July 1998.
- [124] Z. Xie, R.T. Short and C.K. Rushforth, "A family of suboptimum detectors for coherent multiuser communications," IEEE JSAC, vol. 8, no.4, pp.683-690, May1990.
- [125] G. Ye and G. Bi, "Code timing estimator for DS-CDMA signals in slow fading multipath channels," IEE Electronics Letters, vol.35, no.19, pp. 1604-1606, Sept. 1999.
- [126] K.W. Yip and T.S. NG, "Efficient simulation of digital transmission over WSSUS channels," IEEE Trans. Comm., vol. 43, no. 12, pp. 2907-2912, Dec. 1995.
- [127] D. Zheng, J. Li, S.L. Miller, and E.G. Strom, "An efficient code-timing estimator for DS-CDMA signals," IEEE Trans. Signal Processing, vol.45, no.1, pp. 82-89, Jan. 1997.

- [128] Z. Zvonar and D. Brady, "Linear multipath-decorrelating receivers for CDMA frequency-selective fading channels," *IEEE Trans. Commun.*, vol. 44, no. 6, pp. 646-653, June 1996.

Errata

020

Page	Line	Existing form	Correction
28	7	Eqn.2.7	Eqn. 2.7 The term outside { } must be inside with respective integrals.
29	4&5 (Eq.2.9)	$\delta_k T_c$	δ_k
29	11	normalized	-----
29	12	$\eta(n)$	$\eta(n)$
30	12	error is by	error is given by
30	22	$\nabla(\xi) = \frac{\partial \xi}{\partial \mathbf{w}} = \left[\frac{\partial \xi}{\partial w_0} \quad \frac{\partial \xi}{\partial w_1} \quad \dots \quad \frac{\partial \xi}{\partial w_{N-1}} \right]^T$	$\nabla(\xi) = \frac{\partial \xi}{\partial \mathbf{w}} = \left[\frac{\partial \xi}{\partial w_0} \quad \frac{\partial \xi}{\partial w_1} \quad \dots \quad \frac{\partial \xi}{\partial w_{N-1}} \right]^T$
32	4	Eq.(2.22)	Eq.(2.25)
64	19	user	users
108	22	QRLS	QR-RLS
119	16	the weights, then using	the weights, using
138		Fig.4.9b	Fig.4.10b
139	16	error floor is at higher also higher	error floor is also higher
170	15	of the blind adaptive algorithms	of the TDE algorithms
221	3	(Eqs. 5.26 & 5.27)	(Eqs. 5.27 & 5.28)